Heterogeneity of food spoilage fungi

Maarten Punt

Heterogeneity of food spoilage fungi

Maarten Punt

Heterogeneity of food spoilage fungi

Heterogeniteit van voedselbedervende schimmels

(met een samenvatting in het Nederlands)

Proefschrift

ter verkrijging van de graad van doctor aan

de Universiteit Utrecht

op gezag van de

rector magnificus, prof. dr. H.R.B.M. Kummeling,

ingevolge het besluit van het college voor promoties

in het openbaar te verdedigen op

woensdag 2 februari 2022 des middags te 4.15 uur

door

Maarten Punt

geboren op 18 april 1993

te Pijnacker

Promotor:

Prof. dr. H.A.B. Wösten

Copromotoren:

Dr. R.A. Ohm

Dr. W.R. Teertstra

CONTENTS

1

General introduction

Maarten Punt

Introduction

The world population is estimated to reach between 9 and 11 billion within the second part of this century (Vollset et al., 2020). This will increase the demand for food. Use of more arable land is not an option, as it is projected to increase by only 5 % in 2050 compared to 2010 (Alexandratos, Nikos & Bruinsma, 2012). In addition, food production is often associated with deterioration of natural ecosystems. Up to 80 % of worldwide deforestation is due to agricultural expansion, primarily in the tropics (Hosonuma et al., 2012). For example, tropical forests are being burned down and replaced by cattle ranches or oil palm plantations. These practices increase carbon emissions and will accelerate global climate change. Genetically modified crops can increase food production on existing arable land by preventing losses caused by pests and weeds. Indeed, a global 13 % increase in yield has been obtained between 1996 and 2015 after the introduction of genetically modified corn (Brookes & Barfoot, 2020). Yet, despite these technological improvements the world population is predicted to increase more rapidly than the food production (Llewellyn, 2018). A change to a more plant-based diet would increase food availability because livestock requires more land for less food: 77 % of all agricultural land is used for livestock and generates about 18 % of the global calorie supply (Ritchie & Roser, 2013). Food scarcity can also be limited by reducing food loss. A third of the food produced for human consumption is lost or wasted every year (Gustavsson et al., 2010). In fact, the Chinese government now campaigns to encourage citizens to 'finish their plates' instead of leaving left-overs (Vervaeke, 2020).

Food loss refers to the total decrease of food post-harvest, while food waste specifically refers to losses caused at the end of the supply chain where food suitable for human consumption is discarded. Food loss in low-income countries primarily occurs early in the food supply chain, while in medium to high income countries more than 40 % of food loss occurs at the end of the food chain at the retail or consumer level. The main cause of food loss is food spoilage, which can be of physical, chemical, or microbiological origin. Fungi, bacteria, and parasites are the main agents causing microbiological food spoilage (Garnier et al., 2017). Spoilage due to these micro-organisms causes deterioration of food and affects the taste, odour, colour, or nutritional value of the product (Pitt & Hocking , 2009). Micro-organisms do not only spoil food, but their presence can even lead to foodborne diseases.

Friends and foes

Basidiomycota and Ascomycota are the two main phyla within the fungal kingdom. Basidiomycota represents most mushroom-forming fungi, while most yeast- and mould-like fungi belong to the Ascomycota. Fungi from both phyla have been used as a food source and in food production for thousands of years. Mushrooms are an obvious example of Basidiomycota that have a long history as a food source. For ascomycetes, the food applications are more diverse. In the eighties of last century Quorn was introduced as a meat replacement (Trinci, 1994). Quorn products are made from the vegetative mycelium of *Fusarium venenatum* (previously known as *Fusarium graminearum*) that is grown in bioreactors. The use of baker's yeast (*Saccharomyces cerevisiae*) in beer brewing, *Rhizopus oligosporus* to ferment soybeans into Tempeh and *Penicillium roqueforti* in the production of blue-veined cheeses (e.g. Roquefort cheese) have a much longer history in food production. Use of fungi in food fermentation can improve the nutritional value, taste, and shelf life. On the other hand, fungi can also spoil food, rendering them unsuitable for consumption. Up to the first half of last century, fungal food spoilage received little attention as it was only perceived as an aesthetic issue (Pitt & Hocking, 2009). Yet, fungal spoilage, for instance by *Aspergillus*, *Penicillium* or *Cladosporium* species, is a significant economic problem. Pitt & Hocking (2009) estimated that 5 - 10 % of all produced food is lost due to fungal spoilage. For example, *Claviceps purpurea* growing on cereal plants like rye and wheat causes ergotism, which can result in gangrene of limbs, convulsions and even death. Toxin-containing sclerotia of *C. purpurea,* known as ergots, are produced in the ears of the grain. These survival structures end up in the flour that is used to make bread; intoxicating the consumers of the flour. Fungal food spoilage has been around for centuries. First reports of ergot date back to around 600 BC on an Assyrian cuneiform tablet where it is described as 'noxious pustule in the ear of grain' (van Dongen & de Groot, 1995). In the Middle Ages, ergotism was known as Saint Anthony's Fire and led to the death of thousands of people (Shephard, 2008). Some of its victims are thought to be depicted by Pieter Bruegel in one of his last works (Figure 1).

Figure 1. De Kreupelen (The Cripples) by Pieter Bruegel the Elder. The central characters in the painting are believed to suffer from ergotism, 1568.

In the last 60 years numerous secondary metabolites, known as mycotoxins, have been discovered. Since then, food producers, consumers and health inspectors take fungal spoilage far more serious, as mycotoxins affect human and animal health (Pitt & Hocking, 2009; Shephard, 2008). For example, PR toxin produced by *P. roqueforti* in silage impacts intestinal, neurological, and immune functions in animals (Dubey et al., 2018; Gillot et al., 2017), while aflatoxins produced by *Aspergillus flavus* in corn or peanuts are carcinogenic and can cause liver damage in humans and feed refusal and infertility in animals (Filtenborg et al., 1996; Hussein & Brasel, 2001; Osweiler, 2000; Williams et al., 2004). The toxicity of aflatoxin was the reason for Iraq to produce this mycotoxin in their bioweapon program in the nineteen-eighties (Klassen-Fischer, 2006). These examples show that the mechanisms underlying toxicity of fungal secondary metabolites is very diverse, ranging from being carcinogenic to immune suppressive and can result in renal failure or fetal malformations (Fung & Clark, 2004).

The fungal spore

When fungal spores germinate, they form hyphae that grow at their apices and that branch sub-apically. As a result, a mycelium, also known as a colony, is formed that consists of a network of interconnected hyphae. This vegetative body of the fungus can produce asexual spores directly from its hyphae. In addition, it can form sexual and / or asexual spore producing reproductive structures. The low or even absent metabolic activity of spores enables a long survival time in nature (Wyatt et al., 2013). One could consider the fungal spore as a time capsule, waiting for suitable conditions to start germinating.

Part of the ascomycetes are known to produce sexual spores. These spores are formed in structures known as ascomata. The ascospores produced by species of the *Eurotiales*, e.g., *Penicillium* and *Aspergillus*, are formed in closed fruiting bodies called cleistothecia (Dijksterhuis, 2017). Ascospore-formation is slow, as it can take up to four months before cleistothecia arise in *Penicillium* (Ropars et al., 2014; Samson et al., 2010). Ascospores can be very stress resistant. For example, ascospores of some *Trichocomaceae* can survive temperature shocks of more than 10 minutes at 70 °C (Dijksterhuis, 2017; Wyatt et al., 2013, 2015), or even 85 °C in the case of *Talaromyces macrosporus* (Beuchat, 1986; Dijksterhuis & Teunissen, 2004; Houbraken et al., 2006; Wyatt et al., 2015). In fact, ascospores often need rigorous environmental triggers such as a heat shock or extreme pressure to break their dormancy and to start germination (Dijksterhuis et al., 2018). Since ascospores are embedded in the fruiting body they are assumed not to be easily dispersed by vectors like wind, water, and insects. In contrast, the asexual conidia that are produced on conidiophores are easily dispersed by these vectors (Teertstra et al., 2017). A cubic meter of air can contain several hundred conidia, but much higher numbers are possible too, for instance close to composting plant waste (Aimanianda et al., 2009). The high number of conidia in the air is caused by the enormous number of these spores that can be produced by a single fungal colony. Colonies of *Aspergillus niger* and *P. roqueforti* produce a few billion conidia in a few days when grown on agar media in a 9 cm wide Petri dish. The conidia are not only dispersed by wind, but also by water (including aerosols) and other vectors. As a consequence, they can easily reach food sources. In fact, conidia are likely the main source of contamination of food products.

Conidia possess several traits that make them particularly resistant to post-harvest food processing treatments (Dijksterhuis, 2017). Their thick, often pigmented, cell wall and

accumulated compatible solutes protect them against high or low temperatures and UV radiation (Dijksterhuis, 2019). For example, *A. fumigatus* conidia survive UV irradiation treatments of 1 minute and 1 year old conidia kept on a dried-out agar slant show similar viability as 1-day old conidia, even their transcriptomes are highly similar (Hagiwara et al., 2017; Lamarre et al., 2008). In contrast, melanin-deficient *P. roqueforti*, *A. niger* and *Paecilomyces variotii* strains show increased sensitivity to UV radiation (Seekles et al., 2021). Resistance to high temperature was shown for *Pae. variotii* conidia, which survive treatments up to 20 minutes at 60 °C (van den Brule et al., 2020a). The higher stress resistance of conidia compared to vegetative hyphae has been mainly attributed to the accumulation of the polyols mannitol, arabitol, erythritol and glycerol and the saccharide trehalose (Wyatt et al., 2013). The kosmotropic properties of trehalose and mannitol have a stabilizing effect on bio-macromolecules such as proteins, protecting them against damaging conditions (Cray et al., 2013). This protective effect is derived from their high affinity to form hydrogen bonds (Collins, 1997; Washabaugh & Collins, 1986). A correlation between heat resistance and trehalose content has been found in conidia of *Aspergillus nidulans* and *Aspergillus oryzae*, where reduced trehalose concentrations increased sensitivity to thermal stress (Fillinger et al., 2001; Sakamoto et al., 2008). Likewise, a *Pae. variotii* strain producing more trehalose in its spores has an increased resistance to heat (van den Brule et al., 2020a). It should be noted that compatible solutes could also provide a source of energy upon germination. Indeed, conidia of *Cladosporium halotolerans* and *P. rubens* germinate in pure water (Segers et al., 2017), illustrating the need for an internal carbon source.

Proteins are also involved in stress resistance of fungal spores. This was demonstrated for hydrophilins of *Neosartorya fischeri*. A putative late embryogenesis abundant protein (LeaA) and two heat-shock proteins (Hsp12A and Hsp12B) were shown to increase resistance to desiccation, salt and osmotic stress and high temperatures in ascospores (van Leeuwen et al., 2016). Hsp12 is an unfolded protein in solution, however in the dry state it can form amphipathic α-helices, which stabilize phospholipids and membranes (Popova et al., 2011; Sales et al., 2000; Welker et al., 2010). Interestingly, Hsp12 acts synergistically with trehalose in response to desiccation stress (Kim et al., 2018). Other molecules may also function in stress resistance. For instance, glycine betaine, which is a small, water-soluble molecule, protects plants, animals, and bacteria against abiotic stress (Lambou et al., 2013). The choline

oxidase gene is one of the two genes involved in the conversion of choline to glycine betaine. It is highly up-regulated in the initial stages of conidial germination of *A. fumigatus* (Lamarre et al., 2008). Yet, glycine betaine-deficient mutants of *A. fumigatus* do not show increased sensitivity to heat shock, hydrogen peroxide treatment or desiccation (Lambou et al., 2013). This may depend on the environmental conditions during which the spores are formed.

Combatting fungal spoilage

Fresh food often provides a favourable environment for fungi to grow and thrive because of their physico-chemical properties such as pH, water activity (a_w) and redox potential (Garnier et al., 2017). Fungi capable to reach a food source, potentially spoil it. This is counteracted by processing food, which introduces adverse conditions, known as hurdles, which limit fungal growth. Such processing techniques are not new. In fact, drying, fermentation, and curing are examples of processing techniques that have been used already for over 5000 years (Joardder & Masud, 2019). Today, industrial food producers apply both preventive methods and various processing techniques in their fight against spoilage. Preventive measures aim to avoid contamination during processing by limiting the exposure of the product to potential spoilage sources. Examples are the use of air filtration systems, packaging in aseptic conditions, the application of good hygienic practices and a Hazard Analysis and Critical Control Points (HACCP) system (Solberg, 1991). Processing methods aim to slow down fungal growth, for instance packaging under modified atmosphere, the addition of chemical preservatives or storage under refrigeration temperatures (Garnier et al., 2017). Pasteurization or even sterilization, high-pressure or pulsed electric field treatments can even totally inactivate fungi (Timmermans et al., 2016). The efficacy of these methods can be enhanced when applied after triggering germination as germinating spores are more sensitive to stress than dormant conidia (Wyatt et al., 2015). The disadvantage of these techniques is the high use of energy and / or the reduction of food quality.

Weak-acid preservatives

A commonly applied procedure to slow down microbial growth is the addition of chemical preservatives such as sorbic and benzoic acid. While the effect of these weak acids has been studied in many fungi, their mode-of-action is not completely understood. According to the 'classic weak-acid theory' there is an equilibrium between the undissociated and dissociated

forms of the weak acids in an aqueous solution. The undissociated form is favoured at low pH, whereas at neutral pH the dissociated form is more abundant. The undissociated weak acids are lipid-soluble and can diffuse over the plasma membrane into the cytoplasm. The more neutral pH in the cells causes dissociation of the weak acids hampering the molecule to diffuse out of the cell (Novodvorska et al., 2016; Plumridge et al., 2004; Stratford et al., 2013). The protons released during the weak-acid dissociation cause cytoplasmic acidification in yeast and moulds (Krebs et al., 1983; Plumridge et al., 2004) and inhibit enzyme activity (Plumridge et al., 2008). Next to the classical weak-acid theory it is hypothesized that the inhibitory effect of some weak acids is due to their lipophilicity. For example, the partition coefficient of sorbic acid suggests that it accumulates in significant levels in membranes where they interact with the hydrophobic parts of amino acid transporters (Melin et al., 2008; Stratford et al., 2009).

Some fungi degrade weak acids. For example, sorbic and cinnamic acid are decarboxylated in *A. niger* by the activity of phenylacrylic acid decarboxylase (*padA*), 4-hydroxybenzoate decarboxylase (*cdcA*) and a sorbic acid decarboxylase regulator (SdrA) (Lubbers et al., 2019; Plumridge et al., 2010; Stratford et al., 2012). Together, they catalyse the non-oxidative decarboxylation of sorbic acid to the volatile 1,3-pentadiene, which has a kerosene like odour (Stratford et al., 2012). On the other hand, benzoic acid is converted to *p*-hydroxybenzoic acid by 4-monooxygenase A (BhpA) (van den Brink et al., 2000; van Gorcom et al., 1990). Transcriptomic studies revealed that its encoding gene is highly up-regulated by benzoic acid in the medium (Lubbers et al., 2019).

Impact of heterogeneity in food spoilage

The highly variable physico-chemical properties of food often select one to three fungal species that can spoil a given product (Filtenborg et al., 1996). It is virtually impossible to prevent contamination of raw ingredients by these fungi as their conidia are ubiquitous in the environment. Hence, inactivation protocols such as pasteurization are commonly applied to prevent spoilage. However, treatments are not always effective. This is caused by the heterogeneity of conidia. Despite its impact, heterogeneity is an under-appreciated aspect of food spoiling fungi. The genetic background, environmental growth conditions, differentiation stage, and heterogeneous composition of conidia cause heterogeneity in

spore populations of a given species. Intra-species variation has already been demonstrated between isolates of the insect pathogen *Metarhizium anisopliae.* Conidia from two out of 16 isolates show > 80 % survival after an 8 h treatment at 45 °C, while for half of the isolates over 50 % of the conidia is inactivated after a 2 h treatment at this temperature (Rangel et al., 2005). A similar phenomenon is observed for *Pae. variotii*, a common spoilage fungus in soft drinks. The decimal reduction times (*D* value; minutes needed to inactive 90 % of the spores at a set temperature) of a resistant and sensitive isolate were 22.9 and 3.7 min at 60 °C, respectively (van den Brule, et al., 2020a).

The impact of environmental growth conditions on heterogeneity of spore resistance has been demonstrated in the case of *A. fumigatus* and *P. roqueforti*. Conidia that have been produced at a higher temperature are more heat-resistant (Hagiwara et al., 2017; Chapter 3). In the case of *P. roqueforti* it requires up to 4 times longer treatment at 56 °C to reach similar inactivation when conidia have been produced at 15 °C compared to 30 °C. Heterogeneity can even be observed within a spore population originating from a single colony. These populations show 'phenotypic heterogeneity' as their response to a stressor differs despite their uniform genetic makeup (Hewitt et al., 2016). Phenotypic heterogeneity has been described for *Zygosaccharomyces bailii* that spoils various products including soft drinks, syrups, wine, and cider (Stratford et al., 2013). A small subpopulation of vegetative cells shows extreme resistance to weak-acid preservatives. This is attributed to their lower intracellular pH compared to the sensitive bulk population (Stratford et al., 2013). Likewise, phenotypic heterogeneity has been described in *A. niger* conidia, where a resistant subpopulation survives thermal treatment (Fujikawa & Itoh, 1996). Yet, in this case the resistant subpopulation consisted of spores that had not been fully exposed to the heat treatment by adherence to a dry part of the container during the treatment rather than being submerged (Fujikawa et al., 2000). However, resistant subpopulations do exist in *A. niger.* Part of this heterogeneity can be attributed to differences in maturation of conidia (Teertstra et al., 2017). The conidiophores in the centre of the colony are older than those at the periphery. This and the fact that only part of the conidia is released during a dispersion event makes that the conidia that are released at a given moment differ in age and maturation. Their phenotypic heterogeneity is exemplified by the fact that a higher percentage of younger spores germinate when compared to older spores (Teertstra et al., 2017). Subpopulations of

conidia have also been observed in *Pae. variotii*. A single colony was shown to produce a subpopulation of conidia that is discernibly larger than the main population (van den Brule et al., 2020a). Notably, a correlation was found between the average conidia size and heat resistance (van den Brule et al., 2020b). Therefore, it is tempting to speculate that the subpopulation of large spores is more heat-resistant than the smaller spores within the same population.

Quantification of heterogeneity

Knowledge on the variability in resistance of a fungal species can aid in risk assessment studies. Figure 2 shows *D*-values for *P. roqueforti* (Blank et al., 1998; Blaszyk et al., 1998; Bröker et al., 1987a, 1987b; Kunz, 1981; Shearer et al., 2002). The included studies used different strains and growth conditions (such as media and growth temperature) showing the variability the *D*-value of a species can have. Using the *D*-values, the Z-value (the temperature needed to lower $\log_{10} D$-value by 1) can be estimated. For *P. roqueforti* the Z-value is 7.998 °C, which is similar to that of *A. niger*. Similar differences are observed for the prediction interval, in the case of *P. roqueforti* it covers an average of 1.766 $\log_{10}$ minutes while for *A. niger* this bandwidth has an average of 2.040 $\log_{10}$ minutes.
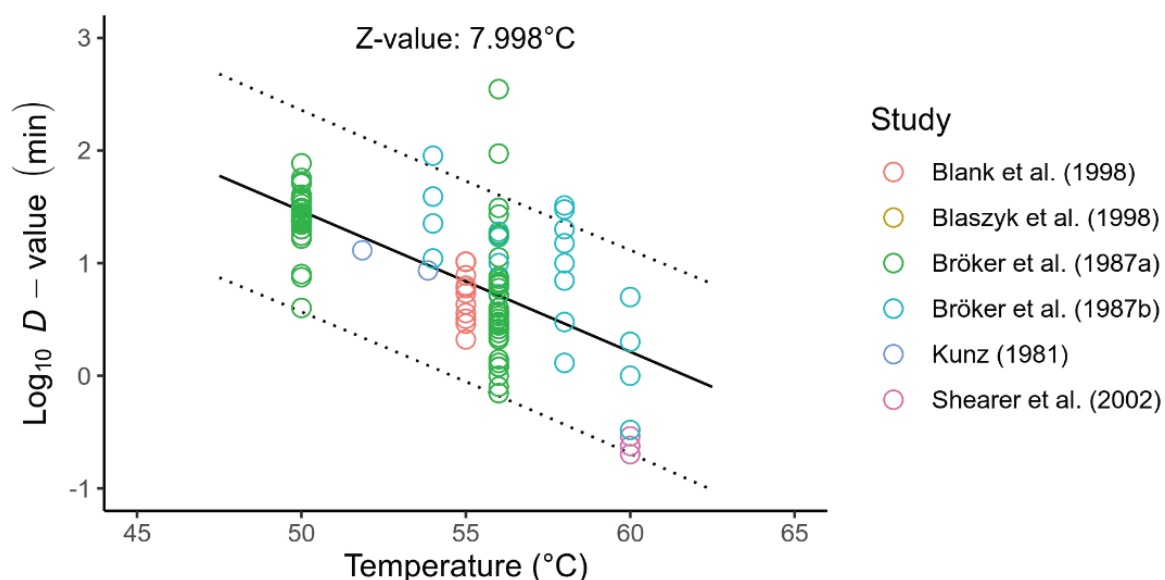

Figure 2. Heat inactivation data collected from literature for *Penicillium roqueforti*. The solid line depicts the estimated Z-value and the dotted lines outline the 95 % prediction interval of the Z-value.

Spore germination

Dormant conidia are more resistant to external stressors than vegetative cells (see above). Hence, it is of interest to understand why and how conidia leave their resting state as it would render them more vunerable to potential treatments. Rapid germination has a selective advantage, as the forming colony could be the first to colonize a substrate. However, when nutrients are lacking rapid germination could lead to death. Conidial germination is characterized by two distinct morphological phases (van Leeuwen et al., 2013). In the first phase a conidium grows isotropically as result of water uptake, which is accompanied by a decrease in the viscosity of the cytoplasm (van Leeuwen et al., 2010). Transcriptomic studies in *A. fumigatus* suggest that during this swelling phase the cell wall is restructered in preparation for the next phase (Baltussen et al., 2018). This phase is characterized by polarized growth and the formation of a germ tube.

Germination of *A. niger* is triggered by sugars including glucose, mannose and xylose (Hayer et al., 2013) or organic nitrogen compounds such as amino acids including proline and alanine (Hayer et al., 2014; Ijadpanahsaravi et al., 2020; Chapter 2). For *A. niger* conidia, Hayer and others (2013) demonstrated that isotropic growth and polarized growth can be disconnected. For instance, D-tagatose, D-lyxose and 2-deoxy-D-glucose trigger swelling but do not support outgrowth, while D-galactose only supports polarized growth. Likewise, inorganic nitrogen compounds, urea and several amino acids are unable to induce swelling, but they can promote outgrowth (Hayer et al., 2014).

***Penicillium roqueforti* and *Aspergillus niger* as model species**

Despite the specificity often observed for spoilage fungi, some fungi are common spoilers. *P. roqueforti* is one of those species, as it capable to spoil a wide range of food. These include mostly dairy and grain products such as yoghurt, rye bread and margarine. *P. roqueforti* strains may produce mycotoxins like PR-toxin and Roquefortine C. As these unwanted mycotoxins pose health risks in humans, secondary metabolite production of *P. roqueforti* has been extensively studied (Dubey et al., 2018; Fernández-Bodega et al., 2009; Gallo et al., 2015). The prevalence of *P. roqueforti* as spoilage agent has been attributed to several aspects. It is relatively well adapted to low temperature as it grows between 5 °C and 33 °C with an optimum at 27 °C (Kalai et al., 2017). Furthermore, this fungus is among the few fungal

species that are identified as preservative-resistant moulds; it is remarkably resistant to weak-acid preservatives such as sorbic, propionic and benzoic acid (Rico-Munoz et al., 2019; Samson et al., 2004). *P. roqueforti* strains typically grow at concentrations ranging from 4 to 21 mM undissociated sorbic acid (Chapter 5) and 9000 ppm (± 60 mM, pH 5.5) is the maximum sorbic acid amount at which growth has been reported (Liewen & Marth, 1984). These values are high since a maximum of 300 to 2000 ppm (= mg kg^{-1}) sorbic acid is allowed in food products according to EU regulations, depending on the product category (Garnier et al., 2017). Resistance to propionic acid is even more pronounced as *P. roqueforti* grows at 0.5 M of this compound at pH 5.6 (Kalai et al., 2017). However, the mechanisms underlying weak-acid resistance have not been studied in *P. roqueforti* thus far.

Another common spoilage mould is *A. niger*, which can cause post-harvest decay of fruit, nuts, cereals, meat and cheese (Pitt & Hocking, 1997). The optimal growth temperature of *A. niger* is 30 °C, with minimum and maximum growth temperatures of 10 °C and 43 °C, respectively (Gougouli & Koutsoumanis, 2010). *A. niger* is less resistant to weak acids when compared to *P. roqueforti*. For example, one of the highest reported minimal inhibitory concentration of sorbic acid for *A .niger* is 49.1 mM at pH 6.0 (Huang et al., 2010). While the effect of weak acids has been studied more extensively in *A. niger* compared to *P. roqueforti* their mode-of-action is not completely understood.

Thesis outline

The aim of this thesis was to study heterogeneity in stress resistance and germination of conidia of *P. roqueforti* and *A. niger*. This could lead to new mild food preservation strategies to prevent fungal food spoilage.

Chapter 2 describes the minimal nutrients required for germination of *A. niger* conidia. A method was developed to quantify germination in time. Swelling and germ tube formation were analysed using an asymmetric model. The maximum number of spores (P_{max}) that were activated to swell and to form germ tubes was < 1 % in water or 50 mM glucose. Combining 50 mM glucose with either $NaNO_3$, KH_2PO_4, or $MgSO_4$ increased P_{max} of swelling and germination, while combining glucose with two of these inorganic components further

increased P_{max} values of swelling and germ tube formation up to 26 % and 11 %, respectively. In addition, it was shown that amino acids have different capacity to induce germination. High (e.g. proline), intermediate, and low (e.g. cysteine) inducing amino acids were distinguished. Together, a combination of an inducing carbon source with either inorganic phosphate, inorganic nitrogen or magnesium sulphate is the minimum requirement for *A. niger* conidia to germinate.

Similarly, germination of *P. roqueforti* conidia is analysed and quantified in **Chapter 3**. Spore germination was assessed in a defined medium consisting of $NaNO_3$, Na_2HPO_4/NaH_2PO_4, $MgSO_4$ and KCl with 10 mM glucose or 10 mM of one out of the 20 proteogenic amino acids. Remarkably, these conditions resulted in germ tube formation without pronounced swelling. The maximum number of spores that formed a germ tube in 72 h in glucose-containing medium was approximately 13 %, with a germination time of 14 h. Most conditions did not reach more than > 5 % germination in 72 h, however low amounts of conidia (< 1 %) were found to have germinated in all tested conditions after seven days. With germination rates of 21 % and 13 %, respectively, arginine and alanine were the most inductive amino acids.

Chapter 4 describes how temperature and incubation time affect thermal resistance, compatible solute content, spore size distribution and the transcriptome profile of *P. roqueforti* conidia. Conidia cultured for seven days at 15 °C and 30 °C showed D_{56}-values of 1.12 ± 0.05 min and 4.19 ± 0.11 min, respectively. A correlation was found between heat resistance of conidia and levels of trehalose and arabitol, while this was not found for glycerol, mannitol and erythritol. RNA-sequencing showed that the expression profiles of conidia of three- to ten-day-old cultures that had been grown at 25 °C were distinct from conidia that had been formed at 15 °C and 30 °C after seven days. Apart from trehalose and arabitol, products encoded by the up-regulated genes during conditions resulting in the most heat-resistant conidia may form the core of heat resistance of *P. roqueforti* conidia.

The variability in thermal resistance of *P. roqueforti* conidia from 20 different strains is described in **Chapter 5**. The most heat-resistant strain (DTO013F5) showed an 8.6 higher D_{56}-value when compared to the most heat-sensitive strain (DTO130C1). A correlation analysis revealed that heat resistance, compatible solute content, and spore size of the 20 strains do

not correlate. Finally, a meta-analysis is performed with data obtained from literature and this Chapter, showing that up to 43 % of the total heterogeneity in heat resistance can be attributed to strain variability, while experimental and biological variability have a lower impact. These findings are similar compared to other microbes.

The variability in weak-acid resistance, in particular to sorbic acid, of 34 *P. roqueforti* strains is described in **Chapter 6**. We demonstrate that the minimum inhibitory concentration of undissociated sorbic acid (MIC_u) ranges from 4.2 to 21.2 mM among 34 *P. roqueforti* strains, of which six strains are distinctly more resistant than the other strains. When both resistant and sensitive strains were assessed on yoghurt supplemented with sorbic acid, it was shown that sorbic acid resistance persisted on a food-type matrix. A genome-wide association study of these strains revealed a gene cluster (SORBUS) containing 70 genes, of which 51 genes are unique for the resistant strains. Whole genome transcriptomic analysis was used to identify genes with similar expression patterns in resistant and sensitive strains. With CRISPR/Cas9 a partial SORBUS mutant was made and the transformant was shown to have reduced sorbic acid resistance.

Results are summarized and discussed in **Chapter 7**.

2

Minimal nutrient requirements for induction of germination of *Aspergillus niger* conidia

Maarten Punt[1,2], Maryam Ijadpanahsaravi[1], Han A. B. Wösten[1,2], Wieke R. Teertstra[1,2]

[1]Microbiology, Department of Biology, Utrecht University, Padualaan 8, 3584 CH Utrecht, The Netherlands;

[2]TiFN, P.O. Box 557, 6700 AN, Wageningen, The Netherlands.

Abstract

Aspergillus niger reproduces asexually by forming conidia. Here, we studied the minimal nutrient requirements that activate germination of *A. niger* conidia. To this end, germination of conidia was monitored in time using an oCelloScope imager. An asymmetric model was used to describe the process of swelling and germ tube formation. The estimated maximum number of spores (P_{max}) that were activated to swell and to form germ tubes was 32.5 % and 20.5 %, respectively, in minimal medium with 50 mM glucose. In contrast, P_{max} of germ tube formation was < 1 % in water or in 50 mM glucose. Combining 50 mM glucose with either $NaNO_3$, KH_2PO4, or MgSO4 increased incidence of swelling and germination with a P_{max} between 9.3 and 15.3 % and between 1.9 and 5.4 %, respectively. Combining glucose with two of these inorganic components further increased incidence of swelling and germ tube formation with a P_{max} between 23.5 -25.9 % and 3.8 -11 %. In the next set of experiments 10 mM amino acid was combined with a sodium phosphate buffer and $MgSO_4$. High inducing, intermediate inducing and low inducing amino acids were distinguished. Proline and alanine belonged to the former class, proline being a better inducer than glucose with a P_{max} of 97 % for swelling and 55 % for germ tube formation. In contrast, the effect of cysteine was low or even non-existing with a P_{max} of swelling and germ tube formation ≤ 1 %. Together, a combination of an inducing carbon source with either inorganic phosphate, inorganic nitrogen or magnesium sulphate is the minimum requirement for *A. niger* conidia to germinate.

Introduction

The genus *Aspergillus* (Galagan et al., 2005; Hawksworth, 2011) includes species that are among the most abundant fungi worldwide. *Aspergilli* can grow as saprotrophs on a wide variety of dead organic material, can be pathogens of plants, animals and human, and can act as endophytes (Bennett, 2010; Krijgsheld et al., 2013). *Aspergilli* also grow in a wide range of abiotic conditions (Bennett, 2010; Krijgsheld et al., 2013). For instance, *Aspergillus penicillioides* can grow at a water activity as low as 0.585 (Stevenson et al., 2017), while *A. niger* grows at a pH as low as 1.5 (Krijgsheld et al., 2013). The production and dispersion of enormous numbers of conidia also explains the abundance of *Aspergilli* (Taha et al., 2005; Teertstra et al., 2017). Their asexual spores are among the most dominant fungal structures in the air (Bennett, 2010; Hameed et al., 2004). For instance, more than ten *A. fumigatus*

conidia were found per cubic meter air (Mullins et al., 1984), implying that humans inhale hundreds of these spores each day.

Conidia are formed on conidiophores after a period of vegetative growth. The conidiophores of *A. niger* are formed one to two days after inoculation on minimal medium at 30 °C, while conidia are formed up to four days after inoculation (Teertstra et al., 2017). A single conidiophore produces about ten thousand conidia. Consequently, a colony in a Petri dish can easily form more than a billion of these spores. Prolonged incubation results in maturation of the conidia on the conidiophores. The conidia of ten-day-old colonies are still metabolically active (Novodvorska et al., 2016; Teertstra et al., 2017). Yet, these matured conidia germinate slower than young conidia. In addition, dispersal efficiency of the matured conidia by water is lower than that of young immature conidia, while dispersal by wind and a hydrophobic object is not affected (Teertstra et al., 2017). Data also showed that a minor fraction of the spores of an *A. niger* colony is released by a single exposure to a vector. From these data and reporter studies (Bleichrodt et al.,2013) it was concluded that a colony of *A. niger* releases a population of conidia that is heterogeneous in age, composition and germination ability. This heterogeneity was proposed to provide a selective advantage in environments with rapidly changing conditions such as availability of water (Teertstra et al., 2017).

Conidia have to decide when to germinate. Resting conidia are relative stress resistant, while germlings can colonize a substrate and prevent competitors to take this niche. Immediate germination, i.e. without sensing the environmental conditions, will have a selective advantage by allowing the fungus to rapidly colonize a substrate. However, the germling will die when nutrients are scarce. Unravelling the signals that initiate germination will help us to understand how conidia cope with the dilemma when to give up the stress resistant state of dormancy. The signals that induce germination also impact the ecological niche of fungi and partly explain why certain fungi spoil certain food sources or infect certain hosts.

Activation of germination of conidia results in swelling by water uptake. The swollen conidia form germ tubes by switching from isotropic to polarized growth. When sufficient nutrients are available these germ tubes grow out into hyphae that grow at their apices and that branch sub-apically. Sugars that trigger germination and outgrowth of *A. niger* conidia include

glucose, mannose, and xylose (Hayer et al., 2013). On the other hand, tagatose, lyxose, and 2-deoxy-glucose activate the conidia to swell but do not support subsequent outgrowth. Galactose and arabinose are among the non-triggering sugars but the former does support outgrowth when a triggering sugar is also present. Together, particular sugars activate germination and / or support outgrowth. Hayer et al. (2014) studied N-sources that trigger germination and / or support outgrowth. To this end, a non-triggering sugar was also added in the medium to support outgrowth of the hyphae. A total of 14 out of 20 proteinogenic L-amino acids triggered germination and supported outgrowth. Inorganic nitrogen compounds, urea, alanine, arginine, glycine, histidine, lysine, and methionine did not activate spores but did support outgrowth. It was shown that both the triggering sugars and amino acids are initially not taken up by the conidia, implying that the nutrient sensors reside in the plasma membrane (Hayer et al., 2013; 2014).

Here, we studied the minimum nutrient requirements that activate swelling and germ tube formation of *A. niger* conidia. To this end, oCelloScope imaging was performed enabling high throughput analysis of conidia germination. Data show that the presence of an inducing carbon source combined with either inorganic phosphate, inorganic nitrogen or magnesium sulphate is sufficient to trigger germination for > 5 % of the conidia.

Material and Methods

Strains and culture conditions

A. niger strain N402 (Bos et al., 1988) was routinely grown at 30 °C on minimal medium (MM; 1 % glucose, 70.6 mM $NaNO_3$, 11 mM KH_2PO_4, 6.7 mM KCl, 2 mM $MgSO_4.7H_2O$, trace elements according to Vishniac & Santer (1957)) supplemented or not with 1.5 % agar. Plates (20 mL MM) were inoculated by spreading 10^7 conidia over the agar surface and five-day-old conidia were harvested with water after colonies had grown for seven days. Miracloth (Millipore, www.merckmillipore.com) was used to filter the conidia and the spores were washed twice with water with intermittent centrifugation for 10 min at 4 °C and 1700 *g*.

Germination analysis

Swelling of conidia and germ tube formation was monitored in MMG or (mixtures of) its components (Table 1). In the latter case, concentrations of these components were used that

are present in MM, unless stated otherwise. Moreover, the impact of replacing KH_2PO_4 for K_2HPO_4, NaH_2PO_4, or Na_2HPO_4 was assessed (Table 2) as well as the effect of using amino acids as carbon source (Table 3). Conidia were used directly after harvesting. As a control, conidia were used that had been heat-inactivated by exposure to 85 °C for 15 min. Wells of a 24-wells suspension culture plate (Greiner Bio-One, Cellstar 662102, www.gbo.com) were seeded with $5 \cdot 10^4$ conidia contained in 750 µL MM or solutions containing one or more of its components. Alternatively, $4 \cdot 10^4$ conidia were seeded in 96-wells suspension culture plates (Greiner Bio-One, Cellstar 655185) in 150 µL medium. These different densities allowed imaging of at least 200 spores per well, while 683-5325 spores were analysed per experimental condition (i.e adding up the spores of the biological replicates) (see Table 1-3). Germination of conidia was monitored on line at 30 °C using an oCelloScope imager (Biosense Solutions, www.biosensesolutions.dk) (Fredborg et al., 2013) with UniExplorer software version 8.1.0.7682-RL2. Measurements (using at least biological triplicates) were started after 1 h of incubation, enabling settling of the conidia at the bottom of the well. Objects were scanned every hour during the first 10 h and every 2 h during the next 14 h. The scan area length was set at 405 (96-wells plates) or 2205 (24-wells plate) µm, the object area (min-max) at 70-700 pixels, and the maximum number of objects at 1200. Individual objects were followed over time using oCelloScope XY coordinates and a custom R script. Conidial aggregates and non-conidial objects at t = 1 h were manually removed from the data set. Conidia were followed in time based on their X and Y coordinates using the fast k-nearest neighbor (KNN) searching algorithm from the R package 'FNN' (Beygelzimer et al., 2019). This was done from t = x to t = x+1 and vice versa. In addition, neighbor distance of an object was not allowed to exceed 27.5 µm (i.e. 50 pixels) between 2 adjacent time points. The lineage was discontinued if these conditions were no longer met. The objects were classified into four groups based on surface area and circularity (Teertstra et al., 2017). Resting conidia had a surface area ≤ 39 µm^2 and a circularity > 0.97, swollen conidia had a surface area > 39 µm^2 and a circularity > 0.97; conidia with germ tubes had a surface area > 39 µm^2 and a circularity > 0.75 and ≤ 0.97, while hyphae had a surface area > 39 µm^2 and a circularity ≤ 0.75. The latter circularity equals a length of the germ tube/hypha ≥ the length of the swollen spore.

Modelling of germination kinetics

The asymmetric model (Dantigny et al., 2011) was used to describe swelling and germ tube formation (P) as a function of time, τ (h) (Eq. 1).

$$P = P_{max} \left(1 - \frac{1}{1 + \left(\frac{t}{\tau}\right)^d} \right)$$

(1)

P_{max} is the maximal percentage of swollen conidia or spores that had formed a germ tube (the asymptotic value of P at t →+∝), τ (h) is the time at which P = 0.5 P_{max} and d is a shape parameter that can be correlated to heterogeneity of the population. A low d reflects a population where conidia have more variable individual germination times. To estimate the model parameters, the biological triplicates were fitted per tested condition with the R package GrowthRates (Petzoldt, 2019) using the Levenberg-Marquardt algorithm. Parameters were limited to P ≥ 0 and ≤ 120 %, τ ≥ 1 and ≤ 18, d ≥ 1 and ≤ 30 when fitting the model. Confidence intervals (95 %) were determined using the standard error of the parameter estimates, were Y represents the estimated P, τ or d value; SEy is the standard error obtained for P, τ or d; α is 0.05; df is the degrees of freedom; *qt* represents the Students T distribution function (Eq. 2).

$$CI_y = SE_y \pm qt(1 - \frac{\alpha}{2}, df)$$

(2)

Objects that had an object area > 300 pixels (90 μm^2) and that decreased in size were excluded from the data set. Missing objects represent resting spores (R) that are lost during the analysis without moving to the swelling (S) or germination (G) stage. Size and circularity data of all objects were used for the parameter estimation until a time point when hyphal growth had obscured resting spores.

Results

Minimal medium with glucose (MMG) is routinely used to grow *A. niger.* It consists of glucose (G), KCl (K), NaNO$_3$ (N), KH$_2$PO$_4$ (P), MgSO$_4$ (S) and Vishniac trace elements (V) (for concentrations see Material and Methods). Here, it was assessed which components of MM are required to activate swelling and germ tube formation of conidia. In addition, it was assessed whether mono- or di-potassium phosphate salts or mono- or di-sodium phosphate salts impact activation of germination and which amino acids can replace glucose.

Effect of glucose and inorganic salts on germination

Swelling and germ tube formation of five-day-old conidia was monitored for 24 h with an oCelloScope imager after inoculation in liquid minimal medium with 50 mM glucose (MMG_{50}). Monitoring of swelling and germ tube formation started after 1 h to enable conidia to settle at the bottom of the 24 wells plate. After 1 h incubation, ≥ 99 % of the spores were still in the resting stage (Figure 1AD), while after 8 h both resting and swollen spores were observed as well as germ tubes and hyphae (Figure 1BD). More conidia had germinated after 16 h and germ tubes and short hyphae had extended into long filaments (Figure 1CD). The asymmetric model (Dantigny et al., 2011) was used with P_{max}, τ and d as outcome to describe the process of swelling and germ tube formation. The former is the maximal percentage of swollen spores or conidia that had formed a germ tube, τ is the time when $P = 0.5$ P_{max} and d is a shape parameter showing the heterogeneity within the spore population. After 14 h, too many objects had formed long hyphae that could not be traced back to one of the objects or that obscured other objects. Therefore, data of 14 h were also used in the modelling for time points 16-24 h. Visual inspection confirmed that no additional spores germinated after 14 h, thereby legitimizing this approach. P_{max} of swelling and germ tube formation was 32.5 % and 20.5 %, respectively, while τ was 5.03 h and 7.26 h (Figure 2A; Table 1).
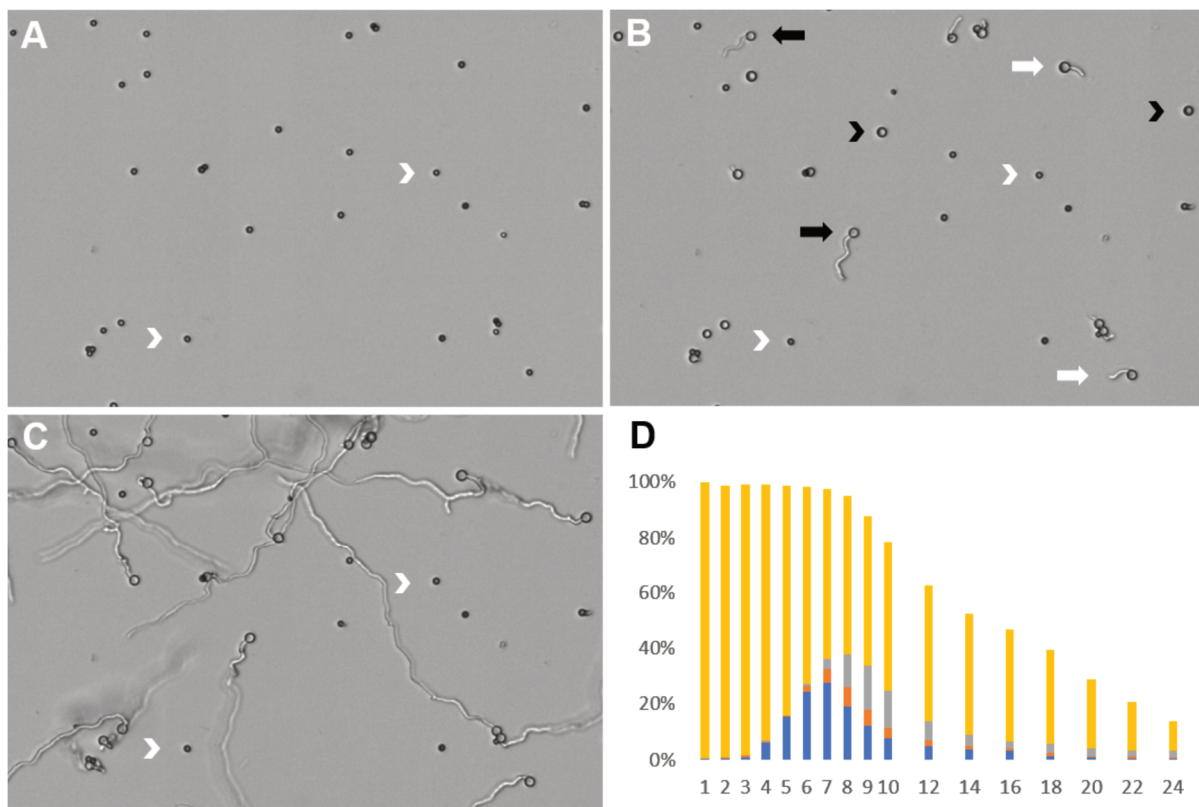
Figure 1. Germination of *A. niger* conidia in MMG_{50} monitored by oCelloScope. Imaging started after 1 h of settling (t=1). Selected area of oCelloScope images after 1 (A), 8 (B) and 16 (C) hours. Resting and swollen conidia and germ tubes are indicated by white arrowheads, black arrowheads, and white arrows, respectively, while hyphae are indicated by black arrows. Circularity and surface area were used to classify 489 objects in time as resting (yellow) and swollen (blue) spores and as spores forming germ tubes (orange) and hyphae (grey) (D). Resting conidia had a surface area $\leq$ 39 μm^2 and a circularity > 0.97, swollen conidia had a surface area > 39 μm^2 and a circularity > 0.97; conidia with germ tubes had a surface area > 39 μm^2 and a circularity > 0.75 and $\leq$ 0.97, while hyphae had a surface area > 39 μm^2 and a circularity $\leq$ 0.75. After 7 h, part of the objects are no longer included in the analysis because the object was obscured by hyphae of other objects or the hypha of the object itself had become too long to be able to trace it back to the original object by the oCelloScope. This explains the decrease in total percentage of the objects.

Table 1. Parameter estimates of the asymmetrical model used to describe swelling and germ tube formation of spores in MMG_{50} and components thereof. MMG_{50} consists of 50 mM glucose (G_{50}), KCl (K), $NaNO_3$ (N), KH_2PO_4 (P), $MgSO_4$ (S) and Vishniac trace elements (V). Confidence intervals are indicated between brackets, N represents the number of objects at t=1 h, while M represents the number of objects that were no longer detected between 2 and 14 h because the hypha had become too long or the object was obscured by hyphae of other objects. RMSE represents the root mean square error of the modelled data and is a measure for the goodness of fit (Dantigny et al., 2011; Ratkowsky, 2004).

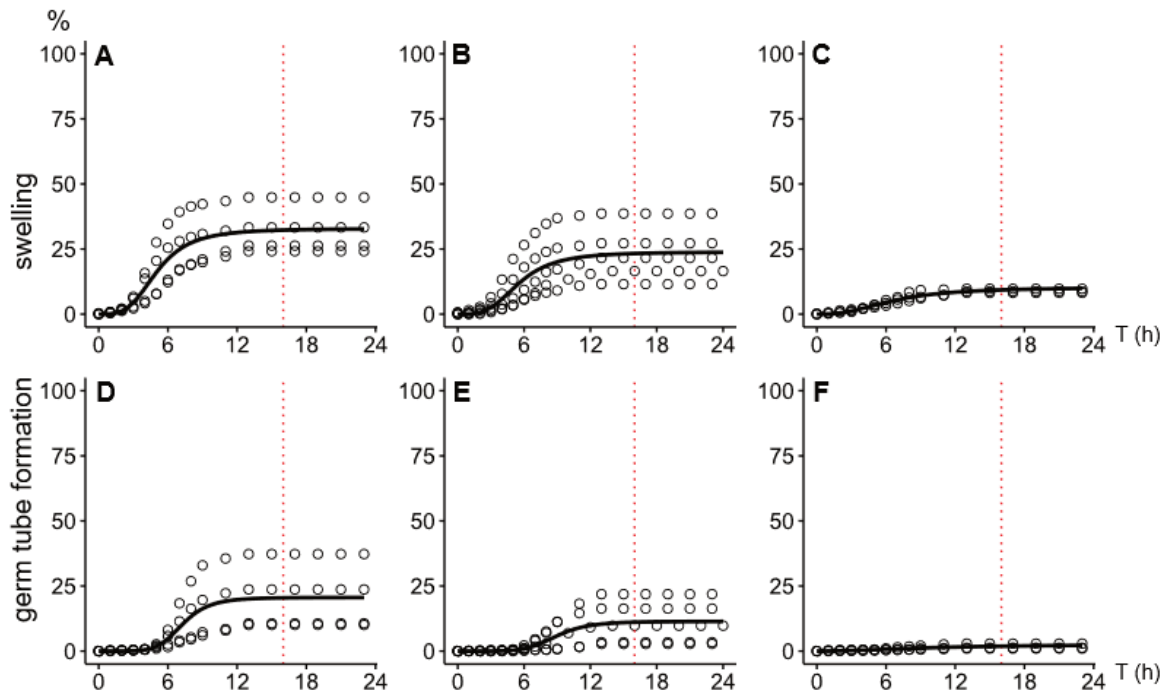|	Parameter estimates						Objects	
	P_{max} (%)		τ (h)		d (-)		RMSE	N	M
Component				**Swelling**					
MMG_{50}	32.54	[29.08;36.01]	5.03	[4.25;5.82]	3.59	[1.69;5.49]	0.90	3822	293
MMG_{50}-KV	46.56	[43.76;49.36]	4.82	[4.38;5.26]	3.94	[2.63;5.24]	0.80	2312	284
$G_{50}PS$	25.85	[22.17;29.54]	4.67	[3.62;5.73]	3.13	[1.01;5.25]	0.92	4389	100
$G_{50}NS$	23.47	[20.03;26.92]	5.50	[4.39;6.61]	3.59	[1.09;6.09]	0.86	3970	130
$G_{50}NP$	25.50	[21.40;29.60]	5.12	[3.90;6.35]	2.85	[0.96;4.73]	0.88	3863	557
$G_{50}N$	12.86	[6.19;19.52]	5.12	[1.14;9.11]	2.32	[-1.73;6.37]	1.09	3051	19
$G_{50}P$	15.25	[12.64;17.85]	5.87	[4.53;7.21]	2.84	[1.07;4.62]	0.48	3289	22
$G_{50}S$	9.34	[8.72;9.97]	6.07	[5.54;6.60]	2.93	[2.21;3.65]	0.12	5325	47
				Germ tube formation					
MMG_{50}	20.51	[16.92;24.10]	7.26	[6.03;8.49]	6.28	[-0.03;12.59]	1.01	3822	293
MMG_{50}-KV	29.33	[25.61;33.04]	7.21	[6.35;8.08]	7.07	[1.47;12.67]	1.10	2312	284
$G_{50}PS$	5.02	[3.90;6.14]	7.58	[5.79;9.38]	4.46	[0.05;8.87]	0.25	4389	100
$G_{50}NS$	10.99	[8.83;13.14]	8.75	[7.18;10.33]	6.59	[-0.26;13.43]	0.54	3970	130
$G_{50}NP$	3.78	[3.10;4.46]	5.58	[4.19;6.97]	3.01	[0.81;5.22]	0.14	3863	557
$G_{50}N$	2.08	[1.57;2.60]	7.18	[5.16;9.20]	3.34	[0.43;6.25]	0.09	3051	19
$G_{50}P$	5.40	[1.88;8.91]	7.48	[0.36;14.60]	1.81	[-0.34;3.95]	0.25	3289	22
$G_{50}S$	1.90	[1.23;2.57]	7.27	[4.14;10.39]	2.64	[0.07;5.22]	0.09	5325	47

Figure 2. Parameter estimates of the asymmetrical model used to describe swelling (A-C) and germ tube formation (D-F) of spores in MMG$_{50}$ (A, D), NSG$_{50}$ (B, E) and SG$_{50}$ (C, F). MM consists of NaNO$_3$ (N), MgSO$_4$ (S), KH$_2$PO$_4$ (P), KCl (K), and Vishniac trace elements (V). NSG medium contains glucose, NaNO$_3$ and MgSO$_4$, while SG medium contains glucose and MgSO$_4$. Open dots represent data points of individual measurements. Experimental data of 16-24 h were not used in the modelling. Instead, those of 14 h were used (for explanation see Results section). Dotted line indicates this time limit for data used in the model.

To assess which constituents of MMG$_{50}$ determine germination of conidia, five-day-old spores were inoculated in solutions containing one or more of these components. P$_{max}$ of swelling and germ tube formation was < 1.5 % when glucose was excluded from MM (Table S1). This low percentage is indicative of the absence of germination since heat-killed spores showed a similar P$_{max}$ (Table S1). In contrast, P$_{max}$ of swelling and germination was 46.6 % and 29.3 %, respectively, while τ was 4.82 and 7.21 h (Table S1) when both K and V were excluded from MMG$_{50}$. Thus, external K and V are not needed to induce germination of conidia. Therefore, these components were not included in further analysis.

Spores did not settle at the bottom of the well plates in water or water containing G$_{50}$ only, disabling automated monitoring of germination with the oCelloScope. Mathematical analysis was also not possible when spores were directly dry-tipped from plates onto siliconized glass cover slides (Teertstra et al., 2017). Although these spores remained attached to the slide in water or water containing G$_{50}$ only, focusing was impaired due to slight drifting of the slides.

Visual inspection showed that spores did not swell and did not show outgrowth during 24 h (data not shown). Spores did settle in the presence of only N, P, or S, thus allowing oCelloScope analysis. Presence of N, P or S showed a P_{max} and τ of swelling $\leq$ 1.45 % and $\geq$ 1.00 h, respectively (see rows G_0N, G_0P and G_0S in Table S1). These values were $\leq$ 0.88 % and $\geq$ 1,00 h for germ tube formation. Together, presence of a single medium component hardly, if at all, induces swelling and germination of spores.

In the next set of experiments G_{50} was combined with N, P or S. P_{max} of swelling and germination of these two-component media were between 9.34 and 15.25 % and 1.90 and 5.40 %, respectively, while τ was between 5.12 and 6.07 h and 7.18 and 7.48 h (Table 1; Figure 2C, F). Next, swelling and germination in $G_{50}NP$, $G_{50}NS$ and $G_{50}PS$ were analysed. P_{max} of swelling and germination of these three-component media were between 23.47 and 25.85 % and 3.78 % and 10.99 %, respectively, while τ was between 4.67 and 5.50 h and 5.58 and 8.75 (Table 1; Figure 2B, E). These data imply that swelling and germination incidence is increased about two-fold in the three-component media when compared to the two-component media. Moreover, τ of swelling is reached at least 30 min earlier.

The effect of glucose concentration was assessed by growing spores in MM, MM-KV and in the single, double and triple component media (see above) in the presence of 10 or 50 mM glucose. P_{max} and τ of swelling were 11.74 and 32.54 % and 6.00 and 5.03 h, respectively, for MMG_{10} and MMG_{50} (Table S1, Table 1). These values were 5.11 and 20.51 % and 8.21 and 7.26 h for germination. Thus, reducing the glucose concentration slows down and reduces the number of spores that swell and form germ tubes. Similar results were obtained in MM-KV, and the double and triple media (Table S1).

The effect of sodium and potassium phosphate on germination
The effect of KH_2PO_4, K_2HPO_4, NaH_2PO_4 or Na_2HPO_4 on germination was assessed by combining either the phosphate source with 2 mM $MgSO_4$ and either 10 mM glucose or proline. The pH of the K_2HPO_4 and Na_2HPO_4 solutions ranged between 8.0 and 8.5, while the pH of the solutions containing KH_2PO_4 and NaH_2PO_4 was 4.5 (Table 2). P_{max} of swelling in the presence of glucose was between 20.12 and 36.23 %, while τ was between 4.82 and 7.31 h. The values for germ tube formation were 3.94 – 15.21 % and 9.99 – 15.00 h (Table 2). No

significant differences were observed in swelling and germ tube formation between the different phosphate salts.

Table 2. Parameter estimates of the asymmetrical model used to describe swelling and germ tube formation of spores in 11 mM KH_2PO_4 (K), K_2HPO_4 (K$_2$), NaH_2PO_4 (Na), Na_2HPO_4 (Na$_2$), 2 mM $MgSO_4$ (S) and 10 mM glucose (Glu) as carbon source (C) or 10 mM proline (Pro) as carbon and nitrogen source (C-N). Confidence intervals are indicated between brackets, N represents the number of objects at t=1 h, while M represents the number of objects that were no longer detected between 2 and 16 h because the hypha had become too long or the object was obscured by hyphae of other objects. RMSE represents the root mean square error of the modelled data and is a measure for the goodness of fit (Dantigny et al., 2011, Ratkowsky, 2004).

			Parameter estimates						Objects	
			P_{max} (%)		τ (h)		d (-)		RMSE	N	M
Salts	C/C-N	pH			Swelling						
KS	Glu	4.5	22.79	[14.4;31.2]	5.50	[2.5;8.5]	2.00	[0.0;4.0]	0.44	729	51
K$_2$S	Glu	8.5	20.12	[13.7;26.5]	6.86	[3.8;9.9]	2.00	[0.6;3.4]	4.10	745	2
NaS	Glu	4.5	36.23	[28.3;44.1]	4.82	[3.1;6.5]	2.00	[0.7;3.3]	1.17	722	121
Na$_2$S	Glu	8.5	27.04	[17.0;37.0]	7.31	[3.5;11.1]	2.00	[0.5;3.5]	0.51	753	12
KS	Pro	4.5	81.87	[79.4;84.4]	3.74	[3.5;4.0]	2.83	[2.4;3.3]	0.73	725	23
K$_2$S	Pro	8.5	53.13	[50.1;56.1]	7.50	[7.1;7.9]	4.84	[3.6;6.1]	13.04	811	9
NaS	Pro	4.5	91.04	[89.4;92.7]	4.01	[3.9;4.1]	3.56	[3.2;3.9]	2.02	692	26
Na$_2$S	Pro	8.0	54.85	[47.8;61.9]	7.65	[6.6;8.7]	3.87	[1.9;5.8]	0.85	786	5
					Germ tube formation						
KS	Glu	4.5	10.84	[5.1;16.6]	9.99	[4.5;15.5]	2.84	[-0.1;5.8]	6.64	729	51
K$_2$S	Glu	8.5	3.94	[-2.2;10.1]	15.00	[-8.4;38.4]	2.31	[-0.9;5.5]	5.91	745	2
NaS	Glu	4.5	15.21	[8.2;22.2]	10.89	[5.2;16.6]	2.33	[0.8;3.9]	4.15	722	121
Na$_2$S	Glu	8.5	4.58	[1.0;8.2]	15.00	[4.4;25.6]	2.60	[0.7;4.5]	0.34	753	12
KS	Pro	4.5	17.53	[10.2;24.9]	14.98	[12.1;17.9]	7.8	[-1.8;17.5]	1.12	725	23
K$_2$S	Pro	8.5	0.63	[0.4;0.8]	7.39	[5.2;9.6]	5.54	[-3.5;14.4]	7.79	811	9
NaS	Pro	4.5	47.61	[36.7;59.2]	15.00	[13.2;16.8]	6.30	[2.8;9.8]	0.58	692	26
Na$_2$S	Pro	8.0	4.87	[2.0;7.2]	15.00	[7.2;22.6]	2.64	[1.2;4.1]	5.47	786	5

Incidence of swelling was higher when proline was used as a carbon source instead of glucose, either combined with KH_2PO_4, K_2HPO_4, NaH_2PO_4 or Na_2HPO_4. In contrast, incidence of germ tube formation was only significantly higher in the case of proline compared to glucose when combined with NaH_2PO_4. P_{max} of swelling in the presence of proline was between 53.13 and 91.04 %, while τ was between 3.74 and 7.65 h (Table 2). These values were between 0.63 % and 47.61 % and 7.39 h and 15.00 h for germ tube formation. P_{max} of swelling and germ tube

formation were significantly different between KH_2PO_4 and K_2HPO_4 and between NaH_2PO_4 and Na_2HPO_4. In both cases the $H_2PO_4^-$ salts were superior in promoting swelling and germ tube formation when compared to the HPO_4^{2-} salts, probably explained by the pH difference of these solutions (Table 2). Notably, P_{max} of swelling and germ tube formation were significantly higher in the case of NaH_2PO_4 when compared to KH_2PO_4, (Table 2). Moreover, no significant difference in τ of swelling was detected while using glucose, but τ of swelling with proline was significantly lower with the $H_2PO_4^-$ salts compared to the HPO_4^{2-} salts. Together, NaH_2PO_4 and KH_2PO_4 show highest germination incidence in the case of proline, while germination is not affected by the phosphate salt in the case of glucose.

The effect of amino acids on germination

Conidia were exposed to 10 mM of one of the proteogenic amino acids (as C- and N-source) in Na-phosphate buffer (pH 6) containing $MgSO_4$. The pH of all media was 6 at the start and after 24 h of incubation, except for incubations with L-tyrosine where the pH at the start and the end of the incubation was between 1 and 2. High, intermediate, and low inducing amino acids were distinguished that had a P_{max} of swelling < 5 %, ≥ 5 % - < 25 %, and ≥ 25 %, respectively (Figure 3; Table 3). Alanine and proline highly induced swelling with a P_{max} of swelling of 84 % and 97 %, respectively, and a τ of 5.57 h and 3.18 h. P_{max} of germ tube formation of these amino acids was 37 % and 55 %, while τ was 12.05 and 11.25 h respectively. Cysteine, glutamine, histidine, leucine, lysine, methionine, threonine, tyrosine and valine were classified as low inducing amino acids with a P_{max} of swelling between 0.5 % and 3.7 %, while τ was between 2.46 and 15.00 h (modeling only allowed a maximum for τ of 15 h, see Material and Methods, therefore 15 h means ≥ 15 h). Their P_{max} of germ tube formation was between 0.17 and 2.02 %, and 4.31 and 15.00 h respectively.
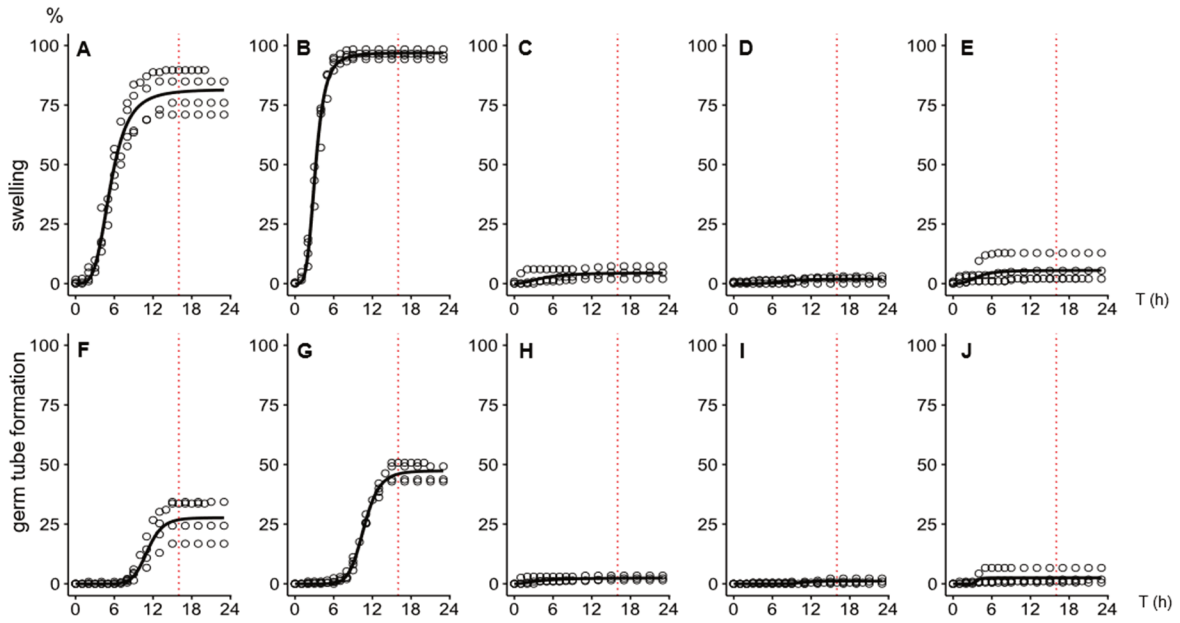
Figure 3. Parameter estimates of the asymmetrical model used to describe swelling (A-E) and germ tube formation (F-J) of spores in Na-phosphate buffer containing $MgSO_4$ and 10 mM of the nonpolar amino acids alanine (A, F) and proline (B, G), the negatively charged amino acid glutamate (C, H), the positively charged amino acid histidine (D, I), and phenylalanine that has an aromatic side chain (E, J). Open dots represent data points of individual measurements. Experimental data of 16-24 h were not used in the modelling. Instead, those of 14 h were used (for explanation see Results section). Dotted line indicates this time limit for data used in the model.

Table 3. Asymmetric modelling of swelling and germination of spores in 25 mM NaPO$_4$ buffer pH 6.0 (NaP), 2 mM MgSO$_4$ (S), and 10 mM L-amino acid (AA), the latter described by their three letter code (IUPAC). The pH was 6 throughout the experiment, except for tyrosine that had a pH between 1 and 2. Confidence intervals are indicated between brackets, N represents the number of objects at t=1 h, while M represents the number of objects that were no longer detected between 2 and 16 h because the hypha had become too long or the object was obscured by hyphae of other objects. RMSE represents the root mean square error of the modelled data and is a measure for the goodness of fit (Dantigny et al., 2011, Ratkowsky, 2004). Grey shading indicates amino acids that are highly inducing in swelling or germ tube formation, while light grey and no shading indicates amino acids that are intermediate or lowly inducing.

		Parameter estimates						Objects	
		P$_{max}$ (%)		τ (h)		d (-)		RMSE	N	M
Salts	AA				Swelling					
NaPS	Ala	83.84	[80.74;86.94]	5.57	[5.28;5.87]	3.85	[3.11;4.58]	1.44	683	88
NaPS	Arg	20.71	[14.44;26.97]	11.89	[8.83;14.95]	3.23	[1.61;4.86]	0.20	786	75
NaPS	Asn	5.46	[-3.52;14.43]	15.00	[-8.89;38.89]	2.32	[-1.02;5.67]	1.03	840	49
NaPS	Asp	7.78	[-1.70;17.27]	15.00	[-4.82;34.82]	2.03	[0.01;4.05]	0.19	832	83
NaPS	Cys	0.55	[0.33;0.76]	2.46	[-0.08;5.01]	2.00	[-2.21;6.21]	1.72	940	5
NaPS	Gln	3.65	[1.49;5.80]	9.48	[2.39;16.56]	2.00	[0.22;3.78]	0.23	909	42
NaPS	Glu	8.11	[2.50;13.73]	9.11	[0.84;17.37]	2.00	[-0.22;4.22]	0.26	956	13
NaPS	Gly	6.79	[0.26;13.33]	15.00	[0.82;29.18]	2.28	[0.38;4.19]	1.41	945	29
NaPS	His	2.48	[1.08;3.88]	8.20	[2.11;14.29]	2.00	[-0.03;4.03]	1.38	856	11
NaPS	Ile	5.52	[1.00; 10.03]	12.28	[0.47;24.10]	2.00	[0.24;3.76]	0.30	842	8
NaPS	Leu	1.65	[1.24;2.07]	3.02	[1.33;4.72]	2.00	[-0.30;4.30]	1.83	855	14
NaPS	Lys	1.97	[1.13;2.82]	6.86	[2.79;10.94]	2.00	[0.12;3.88]	0.93	946	10
NaPS	Met	3.15	[-3.58;9.89]	15.00	[-20.2;50.2]	2.00	[-1.47;5.47]	0.41	874	6
NaPS	Phe	6.26	[3.76;8.75]	3.25	[0.50;6.00]	2.00	[-1.47;5.47]	0.46	818	79
NaPS	Pro	96.95	[95.90;98.01]	3.18	[3.10;3.26]	4.14	[3.76;4.51]	0.35	934	28
NaPS	Ser	7.61	[4.77;10.46]	8.83	[5.66;12.01]	3.76	[-0.59;8.11]	0.61	810	32
NaPS	Thr	1.76	[1.01;2.50]	7.76	[3.36;12.16]	2.00	[0.37;3.63]	1.44	1016	14
NaPS	Trp	8.82	[3.04;14.60]	15.00	[4.58;25.42]	2.08	[0.96;3.21]	0.36	972	10
NaPS	Tyr	2.95	[1.46;4.44]	8.96	[3.23;14.7]	2.02	[0.36;3.69]	1.26	737	9
NaPS	Val	3.31	[1.68;4.93]	5.18	[1.23;9.12]	2.00	[-0.87;4.87]	0.52	750	9
NaPS	no	1,66	[1.43;1.90]	1.26	[0.37;2.14]	2.00	[0.75;4.75]	0.54	706	7
					Germ tube formation					
NaPS	Ala	37.21	[33.99;40.44]	12.05	[11.38;12.71]	6.3	[4.52;8.07]	0.19	683	88
NaPS	Arg	15.27	[11.04;19.49]	14.84	[12.19;17.49]	3.96	[2.50;5.42]	0.48	786	75
NaPS	Asn	2.82	[-0.13;5.77]	15.00	[4.73;25.27]	3.84	[-1.24;8.92]	0.24	840	49
NaPS	Asp	3.92	[1.65;6.19]	11.35	[5.70;17.00]	3.33	[-0.22;6.88]	0.64	832	83
NaPS	Cys	0.17	[0.01;0.33]	4.31	[-2.89;11.50]	2.00	[-4.66;8.66]	1.25	940	5

NaPS	Gln	2.02	[-0.25;4.29]	13.22	[-3.83;30.27]	2.00	[-0.18;4.18]	0.59	909	42
NaPS	Glu	7.30	[-1.66;16.25]	15.00	[-5.61;35.61]	2.00	[-0.01;4.01]	1.37	956	13
NaPS	Gly	2.75	[1.55;3.95]	15.00	[11.49;18.51]	5.12	[1.39;8.85]	0.54	945	29
NaPS	His	1.65	[-0.24;3.54]	15.00	[0.70;29.30]	2.80	[-0.35;5.95]	3.44	856	11
NaPS	Ile	1.64	[0.70;2.57]	11.49	[6.05;16.93]	3.50	[-0.29;7.30]	0.45	842	8
NaPS	Leu	0.17	[0.00;0.34]	4.37	[-3.15;11.89]	2.00	[-4.84;8.84]	3.88	855	14
NaPS	Lys	0.83	[-0.24;1.91]	13.46	[-6.33;33.25]	2.00	[-0.44;4.44]	0.21	946	10
NaPS	Met	0.68	[0.33;1.04]	15.00	[11.26;18.74]	6.28	[-0.53;13.09]	0.20	874	6
NaPS	Phe	2.53	[1.87;3.20]	3.66	[1.94;5.38]	6.90	[-12.9;26.7]	1.58	818	79
NaPS	Pro	54.95	[52.75;57.14]	11.25	[10.95;11.56]	7.24	[6.04;8.43]	1.24	934	28
NaPS	Ser	3.37	[1.97;4.77]	11.21	[7.89;14.53]	5.87	[-2.33;14.07]	0.28	810	32
NaPS	Thr	0.69	[-0.11;1.49]	15.00	[0.05;29.95]	2.71	[-0.32;5.74]	0.44	1016	14
NaPS	Trp	2.80	[0.71;4.89]	15.00	[5.99;24.01]	2.93	[0.71;5.16]	0.56	972	10
NaPS	Tyr	1.33	[0.40;2.26]	8.52	[0.81;16.22]	2.00	[-0.40;4.40]	0.23	737	9
NaPS	Val	0.97	[0.62;1.32]	1.06	[-1.09;3.21]	2.00	[-6.08;10.08]	2.15	750	9
NaPS	no	1.02	[0.71;3.11]	15.00	[-10.96;40.96]	2.01	[-0.59;4.62]	0.50	706	7

Discussion

Conidia are dispersed by wind, water or other vectors such as insects. At a certain moment, these spores will settle in an environment of unknown composition. The main decision for a conidium to make is when to germinate. Presence of water is the main prerequisite to sustain germination and outgrowth of spores. Conidia of *Cladosporium halotolerans* and *Penicillium rubens* germinate in pure water (Segers et al., 2017). However, germination of conidia of most other fungi, including *A. niger,* are only triggered in the presence of water and certain nutrients. We here assessed the minimal nutrient requirements that activate swelling and / or germ tube formation of *A. niger* conidia. A combination of an inducing carbon source with either inorganic phosphate, inorganic nitrogen or magnesium sulphate was sufficient to activate germination up to 6 % of the conidia. This shows that a fraction of the conidia germinate in environments that do not support full outgrowth into a colony. Apparently, conidia, at least a fraction of them, take a chance by germinating without signalling the presence of all nutrients needed to sustain establishment of a colony. Minimal sensing of the environment would allow fast colonization of a substrate in the case all these nutrients are present and would thus give a competitive advantage. The fact that the time needed to reach half P_{max} was similar in nutrient poor and nutrient rich media supports this hypothesis.

Initiation of germination without scanning the presence of all nutrients that are needed to sustain growth can be a successful strategy considering the enormous numbers of conidia that are released from colonies of *A. niger.* The opposite is also observed; even when all nutrients were present did only a fraction of the conidia germinate within 24 h. Only 20 % of the conidia produced germ tubes in a minimal medium with 50 mM glucose. Thus, the majority of the conidia remained in their resting state despite the presence of a medium that can fully support establishment of a colony. Activation of germination is probably a bet hedging strategy to prevent that all individuals die when environmental conditions become unfavourable. For instance, temperature may exceed the cardinal temperature of 47 °C during daytime (Krijgsheld et al., 2013), which would kill the germlings but not the conidia. An important question to address is what makes conidia heterogeneous with respect to their activation. Previously, we showed that conidia are heterogeneous in composition of proteins and RNA (Bleichrodt et al., 2013; Teertstra et al., 2017). Possibly, conidia differ with respect

to the number of sensors in or near their plasma membrane such as G- or Ras-proteins (Fortwendel et al., 2004; Lafon et al., 2005).

Particular carbon and nitrogen sources can either activate or support outgrowth of conidia, while others can do neither or both (Hayer et al., 2013; 2014). Inorganic nitrogen compounds, urea, alanine, arginine, glycine, histidine, lysine, and methionine did not activate spores to germinate but could support outgrowth (Hayer et al., 2014). In our case alanine, arginine, glycine were classified as highly or intermediate inducing amino acids, while cysteine, glutamic acid, leucine, threonine, tyrosine and valine lowly induced germination. What could explain the differences between our study and that of Hayer et al. (2014)? Our study did not include alternative organic compounds or an alternative nitrogen source. In contrast, Hayer et al. included the non-inducing sugar galactose as well as nitrate. In addition, Hayer et al. determined swelling after 1 h incubation in a liquid shaken culture. In our set up, swelling and outgrowth were monitored on line for 24 h. Up to 20.71 % of the conidia were activated to swell by the group of nine intermediate inducing amino acids. The time needed to reach half P_{max} could be as high as 15 h explaining why part of these amino acids were considered non-activating by Hayer et al. (2014). Our study also used a different analysis system but this does not seem to play a role since we obtained similar results as Hayer et al. (2014) when we tested their medium composition with the oCelloScope imager (our unpublished data).

Proline and alanine were classified as highly inducing by activating > 80 % of the conidia to swell. In contrast, P_{max} of germ tube formation was only about 50 % and 35 %, respectively. Notably, 80 % of the conidia form germ tubes within 24 h when they are incubated in a mixture of amino acids and even 100 % in the combined presence with glucose (data not shown). This implies that spores have different sensors that each contribute to the activation of germination of spores. Why certain amino acids are stronger inducers than others remains unknown. Our study does not indicate that certain classes of amino acids are strictly low inducing amino acids. Further research is required to reveal why proline and alanine are such strong activators of germination. It is tempting to speculate that *A. niger* senses these amino acids because they accumulate in plants exposed to stress (Meena et al., 2019; Ricoult et al., 2005). For instance, proline accumulates during drought, in saline conditions, and at high temperatures, while alanine accumulates in plants that experience hypoxia. Such plants may

be weaker to prevent fungal colonization (Chojak-Koźniewska et al., 2018) and would thereby be an easy target for *A. niger.* Onions are known to be infected by this fungus and this plant indeed accumulates proline under salt and drought stress and during cold storage (Hanci & Cebeci, 2015; Romo-Pérez et al., 2020).

Supplementary material

Table S1. Asymmetric model on swelling and germination of spores in MMG_0, MMG_{10} and MMG_{50}, and components thereof. https://bit.ly/3lmq3B8

3

Penicillium roqueforti conidia induced by L-amino acids can germinate without detectable swelling

Maarten Punt[1,2], Wieke R. Teertstra[1,2], Han A. B. Wösten[1,2*]

[1]TiFN, P.O. Box 557, 6700 AN, Wageningen, The Netherlands;

[2]Microbiology, Department of Biology, Utrecht University, Padualaan 8, 3584 CH Utrecht, The Netherlands.

Abstract

Penicillium roqueforti is used for the production of blue-veined cheeses but is a spoilage fungus as well. It reproduces asexually by forming conidia. Here, we studied nutrient requirements that activate *P. roqueforti* conidia to germinate. To this end, germination of > 300 conidia per condition were monitored in time using an oCelloScope imager and an asymmetric model was used to describe the germination process. Spores were incubated for 72 h in $NaNO_3$, Na_2HPO_4/NaH_2PO_4, $MgSO_4$ and KCl with 10 mM glucose or 10 mM of 1 out of the 20 proteogenic amino acids. In the case of glucose, the maximum number of spores (P_{max}) that had formed germ tubes was 12.7 %, while time needed to reach 0.5 P_{max} (τ) was about 14 h. Arginine and alanine were the most inducing amino acids with a P_{max} of germ tube formation of 21 % and 13 %, respectively, and a τ of up to 33.5 h. Contrary to the typical stages of germination of fungal conidia, data show that *P. roqueforti* conidia can start forming germ tubes without a detectable swelling stage.

Introduction

Penicillium roqueforti is well known for its use in production of blue-veined cheeses. On the other hand, it is known as a food spoilage fungus of, for instance, rye bread and dairy products. In nature, it is also known to be a saprophytic fungus degrading dead organic material (Coton et al., 2020; Samson et al., 2010). The ability of *P. roqueforti* to grow at high CO_2 concentrations (up to 84.8 %), low O_2 levels (as low as 0.3 %), and at low temperature (as low as 0 °C) distinguishes this species from other filamentous fungi (Kalai et al., 2017; Nguyen Van Long, et al., 2017b). After a period of vegetative growth, *P. roqueforti* forms conidia that are distributed via the air. These asexual reproductive structures are produced in enormous quantities and are capable to survive prolonged periods in a resting state that is characterized by low metabolic activity and stress resistance (Dijksterhuis, 2017; Wyatt et al., 2013).

Germination of fungal conidia is characterized by three stages; activation, swelling and germ tube formation (d'Enfert, 1997). Activation of dormant conidia results in swelling of the spores. This period of isotropic growth is followed by polarized growth resulting in the production of a germ tube that will grow out into a hypha. Conidia of *Cladosporium halotolerans* and *Penicillium rubens* germinate in pure water (Segers et al., 2017), while most other conidia, including those of *Aspergillus niger* (Ijadpanahsaravi et al., 2020; Chapter 2)

also require certain nutrients. Until now, the nutrient requirements of *P. roqueforti* conidia are not known. Yet, the impact of water activity (a_w), temperature and pH on germination of these spores has been studied (Kalai et al. 2017). Modelling shows that *P. roqueforti* conidia germinate at temperatures between -0.2 and 33 °C with an optimum at 26.9 °C. The optimum pH is close to 5.6 and ranges between 2.84 and 13.8, while the lower limit of water activity (a_w) is 0.83 with an optimum of 0.98. Germination starts after 10 h when exposed to optimal conditions. Germination of conidia is also impacted by conditions during the production of the conidia. For instance, a low temperature and low a_w, but not pH, during sporulation significantly reduces the germination time (Nguyen Van Long et al., 2017a).

Here, we studied medium requirements for germination of conidia of *P. roqueforti.* Data show that glucose, alanine and arginine activate 12 - 21 % of the conidia to germinate. Other amino acids are much less, if at all, effective in inducing germination. In all cases, swelling of conidia was minimal or even undetectable before germ tube formation.

Material and Methods

Strains and culture conditions

P. roqueforti strain DTO377G3 was routinely grown at 25 °C on malt extract agar (MEA; Oxoid, Hampshire, UK). Plates (20 mL MEA) were inoculated by spreading 10^7 conidia over the agar surface and conidia were harvested with ACES buffer (10 mM N(2-acetamido)-2-aminoethanesulfonic acid, 0.02 % Tween 80, pH 6.8) after seven days of growth. The spores were filtered using sterilized glass wool and washed twice with ACES buffer with intermittent centrifugation for 5 min at 4 °C and 1700 *g*. Conidia concentration was determined using a Bürker-Türk haemocytometer.

Germination analysis

Conidia were used directly after harvesting. A total number of 6 10^3 spores was seeded per well of a 96 wells suspension culture plate (Greiner Bio-One, Cellstar 655185, www.gbo.com) in 150 μL NPS (70.6 mM NaNO$_3$, 11 mM Na$_2$HPO$_4$/NaH$_2$PO$_4$ (pH 6.0), 2 mM MgSO$_4$) either or not containing 6.71 mM KCl and / or 10 mM carbon source (i.e. glucose or 1 of the 20 proteogenic L-amino acids). Milli-Q was used as a control. Germination of conidia was monitored on line at 25 °C using an oCelloScope (Biosense Solutions,

www.biosensesolutions.dk) (Fredborg et al., 2013) with UniExplorer software version 8.1.0.7682-RL2. Measurements (using biological triplicates and technical duplicates) started after 1 h of incubation, enabling settling of the conidia at the bottom of the well. Objects were scanned every hour during the first 24 h and every 2 h during the next 48 h. The scan area length was set at 405, the object area (min-max) at 70-1500 pixels, and the maximum number of objects at 1500. Individual objects were followed over time using oCelloScope XY coordinates and a custom R script. Conidial aggregates, and non-conidial objects at t = 1 h were manually removed from the data set. Conidia were followed in time based on their X and Y coordinates using the fast k-nearest neighbour (KNN) searching algorithm from the R package 'FNN' (Beygelzimer et al., 2019). This was done from t = x to t = x+1 and vice versa. In addition, neighbour distance of an object was not allowed to exceed 27.5 µm (i.e. 50 pixels) between 2 adjacent time points. The lineage was discontinued if these conditions were no longer met. The objects were classified as resting, swelling or germinating conidia. At t = 1 h, resting conidia had a surface area of < 68 µm^2 (225 pixels) and circularity ≥ 0.83, swollen conidia were defined as objects with a ≥ twofold increased surface area when compared to t = 1 h with a circularity ≥ 0.83. Conidia with germ tubes had a circularity < 0.83 and had a ≥ 2-fold increased surface area when compared to t = 1 h. Conidia that met the parameter settings of germ tube formation but that had not been classified as swollen conidia in preceding time points were nonetheless classified as swollen at the moment germ tube formation had started.

Modelling of germination kinetics

The asymmetric model (Dantigny et al., 2011) was used to describe swelling and germ tube formation (P) and germination time τ (h) as a function of time (Eq. 1).

$$P = P_{max}\left(1 - \frac{1}{1+\left(\frac{t}{\tau}\right)^d}\right) \tag{1}$$

P_{max} is the maximal percentage of swollen conidia or spores that form a germ tube (the asymptotic value of P at t →+∝). Germination time τ (h) is the time at which P = 0.5 · P_{max}, while d is a shape parameter that can be correlated to the heterogeneity of the population. A low d reflects a population where conidia have more variable individual germination times. Confidence intervals (95 %) were determined using the standard error of the parameter estimates, were Y represents the estimated P, τ or d value; SEy is the standard error obtained

for P, τ or d; α is 0.05; df is the degrees of freedom; *qt* represents the Students T distribution function (Eq. 2).

$$CI_y = SE_y \pm qt(1 - \frac{\alpha}{2}, df)$$ (2)

To estimate the model parameters of the asymmetric model, three biological replicates (≥ 300 conidia per condition) were fitted together with the R package GrowthRates (Petzoldt, 2019) using the Levenberg-Marquardt algorithm. Parameters were limited to P ≥ 0 and ≤ 120 %, τ ≥ 1 and ≤ 60, d ≥ 1 and ≤ 30 when fitting the model. Objects that had an object area > 300 pixels and that had decreased in size were excluded from the data set. Missing objects represent resting spores (R) that are lost during the analysis (i.e. that were no longer detected at t ≥ 2 h because the object had moved or was obscured for instance by germlings of other spores) before they reached the swelling (S) or germination (G) stage. Size and circularity data of all objects were used for the parameter estimation until the time point when hyphal growth started to obscure resting spores.

Results

The effect of L-amino acids on germination

P. roqueforti conidia were incubated in Milli-Q or NPS medium (containing NaNO₃, Na₂HPO₄/NaH₂PO₄, and MgSO₄) either or not containing KCl (KNPS medium) and / or L-amino acids or glucose. Swelling and germ tube formation were monitored for 72 h with an oCelloScope imager. The asymmetric model (Dantigny et al., 2011) was used with P_{max}, τ and d as outcome to describe the process of swelling and germ tube formation (see Ijadpanahsaravi et al., 2020; Chapter 2). Monitoring of the germination process started after 1 h, allowing conidia to settle at the bottom of the 96-wells plate. P_{max} of swelling and germ tube formation in Milli-Q was 0.66 % (Table 1) and 0.41 % (Figure 1A; Table 2), respectively. Microscopy revealed no swelling and germination under this condition and therefore, these values are considered to represent the base line of swelling and germ tube formation. Similar results were obtained with NPS (data not shown) or KNPS (Tables 1,2). The addition of KCl to NPS medium, however, did increase P_{max} of swelling and germ tube formation in the presence of alanine or arginine (± threefold) (data not shown). The same was observed when NaNO₃, or Na₂HPO₄/NaH₂PO₄ was replaced for either KNO₃ or K₂HPO₄/KH₂PO₄, showing that potassium facilitates *P. roqueforti* germination (data not shown).

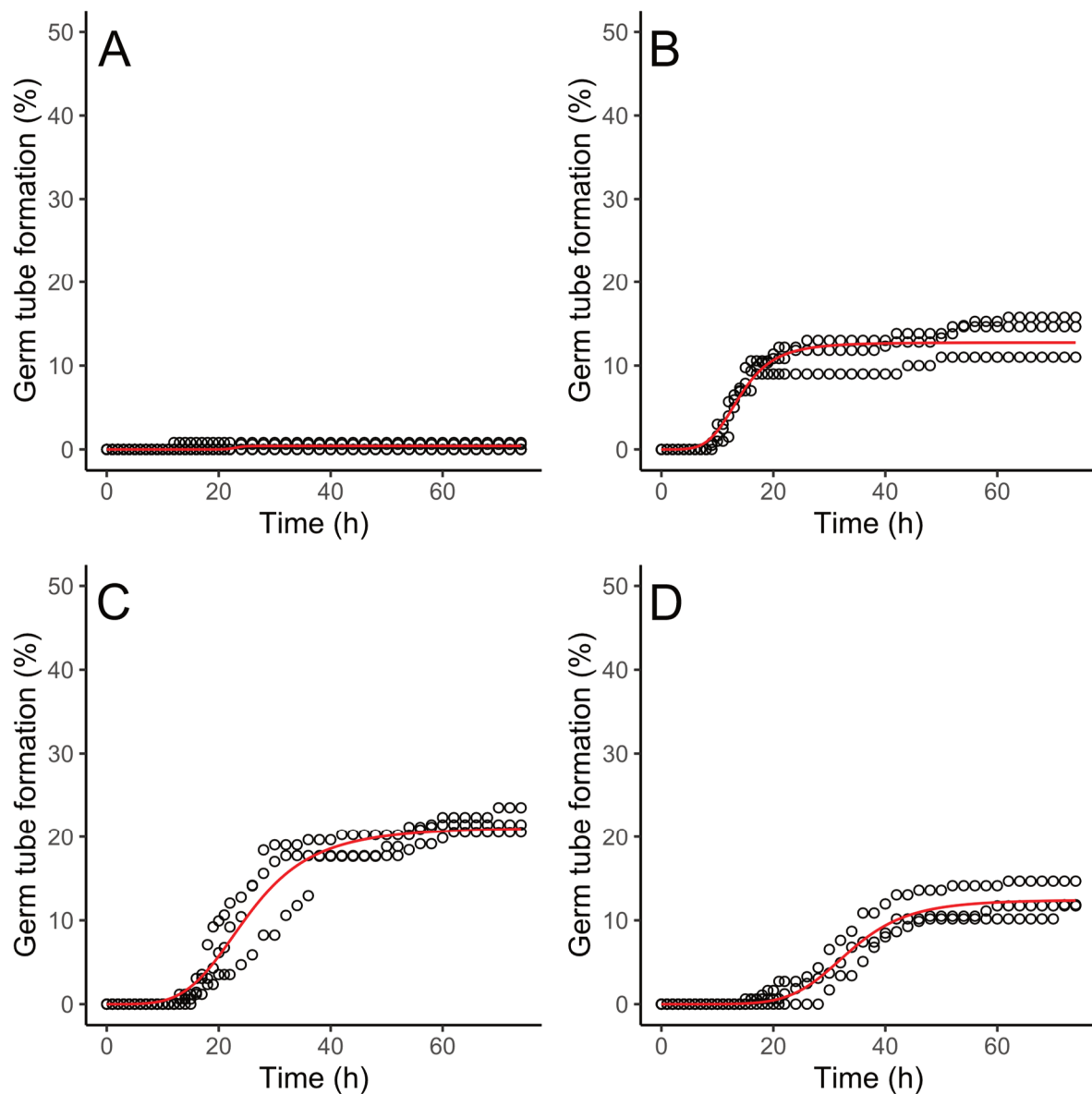**Figure 1**. The asymmetrical model used to describe germ tube formation by *P. roqueforti* conidia in Milli-Q (A) or KNPS (6.71mM KCl, 70.6 mM NaNO$_3$, 11mM Na$_2$HPO$_4$/NaH$_2$PO$_4$ (pH 6.0), 2 mM MgSO$_4$) supplemented with 10 mM glucose (B), arginine (C) or alanine (D). Open dots represent the average of two technical replicates.

Table 1. Parameter estimates of the asymmetrical model used to describe swelling of spores in the presence of 10 mM glucose (G) or 10 mM of one of the 20 proteinogenic amino acids (AA). Spores were seeded in KNPS (6.71mM KCl, 70.6 mM NaNO3, 11mM Na2HPO4/NaH2PO4 (pH 6.0), 2 mM MgSO4) or Milli-Q. Confidence intervals are indicated between brackets, N represents the number of objects at t=1 h, while M represents the number of objects that were no longer detected at t ≥ 2 h because the object had moved or the object was obscured. RMSE represents the root mean square error of the modelled data and is a measure for the goodness of fit (Dantigny et al., 2011, Ratkowsky, 2004).

AA	G	medium	P_{max} (%)		τ (h)		d (-)		RMSE	N	M
Ala	0	KNPS	13.11	[12.47; 13.74]	30.94	[29.6; 32.27]	6.16	[4.78; 7.55]	0.14	405	290
Arg	0	KNPS	21.3	[20.53; 22.06]	25.01	[23.98; 26.03]	4.41	[3.75; 5.06]	0.16	389	263
Asn	0	KNPS	0.2	[0.15; 0.26]	53.07	[49.3; 56.84]	30	[-25.74; 85.74]	0.01	402	34
Asp	0	KNPS	2.68	[-1.31; 6.67]	60	[-29.65; 149.65]	2.02	[0.28; 3.76]	0.05	362	70
Cys	0	KNPS	3.02	[0.94; 5.1]	60	[42.32; 77.68]	5.44	[1.86; 9.02]	0.05	427	41
Gln	0	KNPS	0.55	[0.35; 0.75]	18.89	[9.54; 28.25]	3.49	[-2.22; 9.2]	0.05	451	83
Glu	0	KNPS	5.58	[-2.57; 13.73]	60	[-104.99; 224.99]	1.05	[0.21; 1.88]	0.08	305	69
Gly	0	KNPS	1.6	[1.41; 1.8]	24.83	[21.54; 28.13]	6.39	[2; 10.77]	0.05	393	59
His	0	KNPS	0.6	[0.5; 0.71]	31.55	[27.23; 35.87]	10.39	[-2.59; 23.36]	0.03	389	12
Ile	0	KNPS	1.85	[-2.88; 6.58]	60	[-150.81; 270.81]	1.45	[-0.57; 3.47]	0.05	414	46
Leu	0	KNPS	3.48	[2.99; 3.96]	33.04	[29.04; 37.04]	4.34	[2.56; 6.11]	0.07	462	104
Lys	0	KNPS	1.85	[1.47; 2.23]	30.81	[25.02; 36.59]	5.37	[0.9; 9.84]	0.07	421	57
Met	0	KNPS	0.83	[-0.76; 2.42]	60	[-19.22; 139.22]	3.07	[-0.96; 7.09]	0.02	466	50
Phe	0	KNPS	1.43	[-1.42; 4.28]	49.98	[-51.93; 151.89]	2.16	[-1.23; 5.55]	0.06	449	88
Pro	0	KNPS	0.97	[0.56; 1.39]	38.22	[25.54; 50.9]	3.95	[0.35; 7.56]	0.04	434	133
Ser	0	KNPS	2.26	[1.92; 2.61]	25.46	[21.06; 29.86]	4.29	[1.7; 6.89]	0.07	421	74
Thr	0	KNPS	1.37	[0.95; 1.8]	37.08	[29.47; 44.69]	8.7	[-5.12; 22.53]	0.09	459	71
Trp	0	KNPS	1.2	[0.97; 1.42]	20.83	[16.5; 25.16]	6.83	[-2.07; 15.73]	0.07	376	41
Tyr	0	KNPS	0.57	[0.26; 0.89]	29.87	[10.75; 49]	2.41	[0.11; 4.7]	0.02	348	33

Val	0	KNPS	1.79	[1.42; 2.16]	43.92	[38.56; 49.27]	5.15	[2.81; 7.48]	0.03	422	54
-	0	Milli-Q	0.66	[0.59; 0.74]	7.78	[5.43; 10.14]	2.25	[0.75; 3.74]	0.02	342	339
-	0	KNPS	0.2	[0.15; 0.25]	23.01	[19.26; 26.76]	30	[-68.57; 128.57]	0.02	375	50
-	10	KNPS	12.72	[12.32; 13.13]	13.89	[13.21; 14.57]	4.73	[3.72; 5.74]	0.14	426	302

Table 2. Parameter estimates of the asymmetrical model used to describe germ tube formation of spores in the presence of 10 mM glucose (G) or 10 mM of one of the 20 proteogenic amino acids (AA). Spores were seeded in KNPS (6.71mM KCl, 70.6 mM NaNO3, 11mM Na2HPO4/NaH2PO4 (pH 6.0), 2 mM MgSO4) or Milli-Q. Confidence intervals are indicated between brackets, N represents the number of objects at t=1 h, while M represents the number of objects that were no longer detected at t ≥2 h because the object had moved or the object was obscured. RMSE represents the root mean square error of the modelled data and is a measure for the goodness of fit (Dantigny et al., 2011, Ratkowsky, 2004).

AA	G	medium	P_{max} (%)		τ (h)		d (-)		RMSE	N	M
Ala	0	KNPS	12,45	[11,89; 13,01]	33,5	[32,28; 34,72]	6,3	[5,05; 7,54]	0,11	405	290
Arg	0	KNPS	21,18	[20,4; 21,97]	25,24	[24,18; 26,3]	4,27	[3,65; 4,9]	0,16	389	263
Asn	0	KNPS	0,2	[0,15; 0,26]	53,07	[49,3; 56,84]	30	[-25,74; 85,74]	0,01	402	34
Asp	0	KNPS	2,68	[-1,31; 6,67]	60	[-29,65; 149,65]	2,02	[0,28; 3,76]	0,05	362	70
Cys	0	KNPS	2,25	[1,28; 3,23]	60	[53; 67]	10,38	[2,83; 17,93]	0,05	427	41
Gln	0	KNPS	0,55	[0,34; 0,76]	19,62	[9,79; 29,45]	3,46	[-2,13; 9,06]	0,05	451	83
Glu	0	KNPS	5,58	[-2,57; 13,73]	60	[-104,99; 224,99]	1,05	[0,21; 1,88]	0,08	305	69
Gly	0	KNPS	1,6	[1,4; 1,8]	24,97	[21,54; 28,41]	6,11	[1,94; 10,27]	0,05	393	59
His	0	KNPS	0,6	[0,5; 0,71]	31,55	[27,23; 35,87]	10,39	[-2,59; 23,36]	0,03	389	12
Ile	0	KNPS	1,85	[-2,88; 6,58]	60	[-150,81; 270,81]	1,45	[-0,57; 3,47]	0,05	414	46
Leu	0	KNPS	3,51	[3; 4,01]	33,76	[29,61; 37,9]	4,33	[2,54; 6,12]	0,07	462	104
Lys	0	KNPS	1,83	[1,48; 2,19]	30,93	[25,51; 36,36]	5,79	[0,86; 10,72]	0,07	421	57
Met	0	KNPS	0,83	[-0,76; 2,42]	60	[-19,22; 139,22]	3,07	[-0,96; 7,09]	0,02	466	50

Phe	0	KNPS	1,57	[-2,29; 5,43]	55,53	[-85,81; 196,87]	2,03	[-1,24; 5,3]	0,06	449	88
Pro	0	KNPS	1,06	[0,44; 1,68]	41,79	[22,7; 60,87]	3,44	[0,31; 6,57]	0,04	434	133
Ser	0	KNPS	2,22	[1,92; 2,53]	25,69	[21,83; 29,55]	5,06	[1,93; 8,2]	0,07	421	74
Thr	0	KNPS	1,31	[0,89; 1,73]	36,89	[28,87; 44,92]	8,55	[-5,61; 22,71]	0,09	459	71
Trp	0	KNPS	1,2	[0,97; 1,42]	20,83	[16,5; 25,16]	6,83	[-2,07; 15,73]	0,07	376	41
Tyr	0	KNPS	0,57	[0,26; 0,89]	29,87	[10,75; 49]	2,41	[0,11; 4,7]	0,02	348	33
Val	0	KNPS	2,01	[1,36; 2,67]	48,83	[39,52; 58,13]	4,48	[2,32; 6,65]	0,03	422	54
-	0	Milli-Q	0,41	[0,33; 0,5]	11,49	[9,49; 13,49]	30	[-83,7; 143,7]	0,04	342	339
-	0	KNPS	0,2	[0,15; 0,25]	23,01	[19,26; 26,76]	30	[-68,57; 128,57]	0,02	375	50
-	10	KNPS	12,75	[12,34; 13,16]	14,05	[13,36; 14,74]	4,6	[3,63; 5,57]	0,13	426	302

Penicillium roqueforti conidia induced by L-amino acids can germinate without detectable swelling

Next, swelling and germ tube formation were monitored in KNPS in the presence of glucose or one of the proteogenic amino acids. P_{max} of swelling and germ tube formation was 12.72 % (Table 1) and 12.75 % (Figure 1B; Table 2) in the case of glucose, while τ was 13.89 h for swelling and 14.05 h for germ tube formation. In the case of the proteogenic L-amino acids, P_{max} of swelling ranged between 0.2 % and 21.3 % (Table 1). P_{max} of swelling in the presence of arginine or alanine was 21.3 % and 13.11 %, respectively, with a τ of 25.01 h and 30.94 h (Table 1). P_{max} of germ tube formation of these two L-amino acids was 21.18 % and 12.45 %, while τ was 25.24 h and 33.5 h respectively (Table 2; Figure 1CD). In the case of the other amino acids, P_{max} ranged between 0.2 % and 5.8 % and, as a consequence, the predicted model parameters were often inaccurate (e.g. represented by a > 20 h variance in τ) despite the low (< 0.1) RMSE values. Together, glucose, arginine and alanine induce germination of *P. roqueforti* conidia, while other amino acids hardly, if at all, induce germination within the 72 h period. Yet, some hyphal growth was observed by microscopy in every condition (including Milli-Q) after seven days. This shows that a small part of the *P. roqueforti* conidia do germinate in absence of nutrients added to the medium.

P_{max} and τ of swelling and germ tube were distinct in the case of *A. niger* (Chapter 2; Ijadpanahsaravi et al., 2020), showing that these stages are separated in time. Notably, these parameters were similar in the case of swelling and germination of *P. roqueforti* conidia. Detailed analysis of the arginine, alanine and glucose data showed that the surface area of most *P. roqueforti* conidia had not increased from t = 1 h onwards at the moment germ tubes had formed (Figure 1; Figure S2).

Discussion

Here, we assessed germination of *P. roqueforti* conidia in water or defined medium consisting of $NaNO_3$, Na_2HPO_4/NaH_2PO_4, $MgSO_4$ and KCl (KNPS) either or not supplemented with glucose or one of the 20 proteogenic amino acids. Out of these carbon sources only glucose, arginine and alanine induced germination > 10 % during a 72 h period according to the asymmetrical model. In all cases, but in particular in the presence of arginine and alanine, spores could form germ tubes without detectable swelling.

Potassium salts were shown to increase germination of *P. roqueforti* conidia about threefold, while up to 100 % germination was observed in their absence in the case of *A. niger* conidia (Ijadpanahsaravi et al., 2020; Chapter 2). Potassium salts are considered essential for cellular development, implying that *A niger* spores have an internal storage. This suggests that this fungus has a selective advantage in K-depleted substrates such as soil (Benito et al., 2004) when compared to *P. roqueforti*. An inducing effect of potassium on germination has also been reported for the nematophagous fungus *Hirsutella rhossiliensis.* Addition of 0.4 M KCl increased germination of this fungus from 66 % to 86 % in a 24 h period (Eayre et al., 1990). In contrast, germination of *Penicillium frequentans* and *Septoria tritici* was reduced by 70 % as result of the addition of 0.5 and 0.75 M KCl, respectively (Guijarro et al., 2007; Mann et al., 2004).

Arginine and alanine were the strongest inducers of germination for *P. roqueforti* conidia, while proline and alanine were the strongest inducing amino acids in the case of *A. niger*. The response of *P. roqueforti* and *A. niger* conidia to arginine was similar (± 20 % germination) but alanine-induced germination was significantly reduced in *P. roqueforti* compared to *A. niger* conidia (Ijadpanahsaravi et al., 2020; Chapter 2). It should be noted that L-alanine and L-arginine were previously reported to be non-inducing amino-acids for *A. niger* conidia (Hayer et al., 2014; see discussion Chapter 2)*. Germination time (τ) of *P. roqueforti* conidia was almost 10 h lower in glucose when compared to the amino acids but percentage of germinating conidia were similar. This implies that glucose is not a stronger inducer of conidial germination but does enable germinating conidia to quickly form germ tubes.

Although germination was hardly, if at all, observed in most of the culturing conditions during the first 72 h, growth was observed in most cases after seven days of growth, even in pure water. Germination of *P. rubens* has also been observed in pure water (Segers et al., 2017). Possibly, conidia do not need an external trigger to start germination but triggers simply speed up the process. We can also not exclude that nutrients are released due to lysis of some of the conidia in the wells.

Conidia diameter increases more than two-fold during swelling of several *Aspergilli* (Baltussen et al., 2018; Ijadpanahsaravi et al., 2020; van Leeuwen et al., 2010; Chapter 2). In contrast,

swelling of *P. roqueforti* conidia was quite limited or even absent in germinating spores in our defined medium. Yet, preliminary data show that these *P. roqueforti* spores do show pronounced swelling in malt extract broth (Figure S3). Possibly, swelling in defined medium may be limited by nutrient availability. For instance, *Fusarium culmorum* conidia show minimal swelling in the absence of a nitrogen source (Marchant & White, 1966). Under such conditions, conidia may consume their internal compatible solute content at a higher rate, leading to a lower osmotic pressure. This would reduce the water uptake and as a consequence the swelling of the spores.

Understanding conidial germination of spoilage fungi such as *P. roqueforti* is relevant for the food industry, as fungal spores are abundantly present throughout the food supply chain. The heterogeneity in the response of spores to inducers of germination and the fact that nutrient availability, environmental conditions and history of the spores also affects germination makes it unlikely that spore germination can be controlled with a one-size fits all approach.
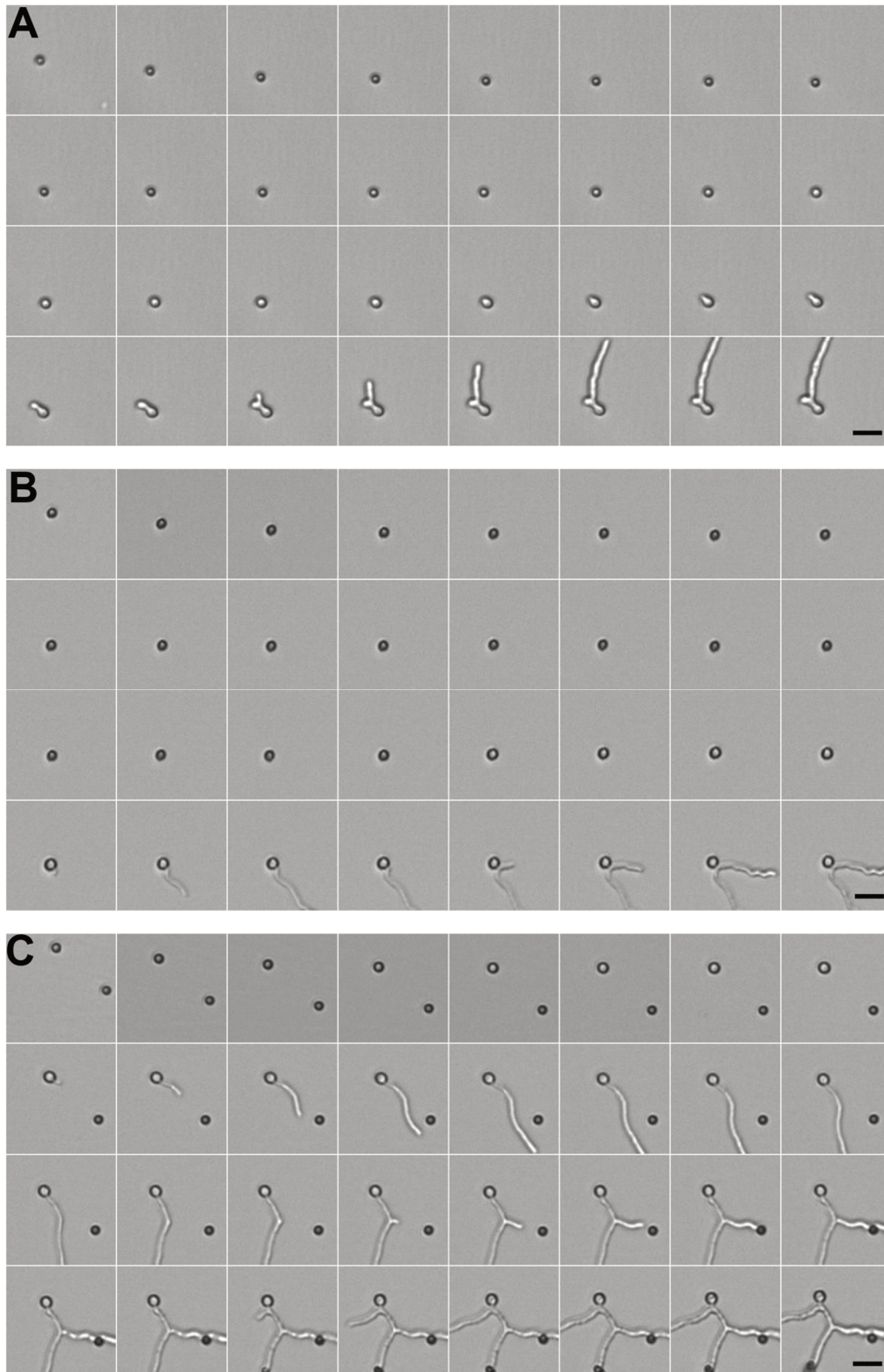
Supplementary material

Figure S1. Germination of a single conidium of *P. roqueforti* in KNPS + alanine (A), arginine (B) and glucose (C) monitored by oCelloScope (scale bars, 15 µm). Imaging started after 1 h of settling swith 1 h (1 - 23 h) and 2 h (23 - 41 h) intervals.
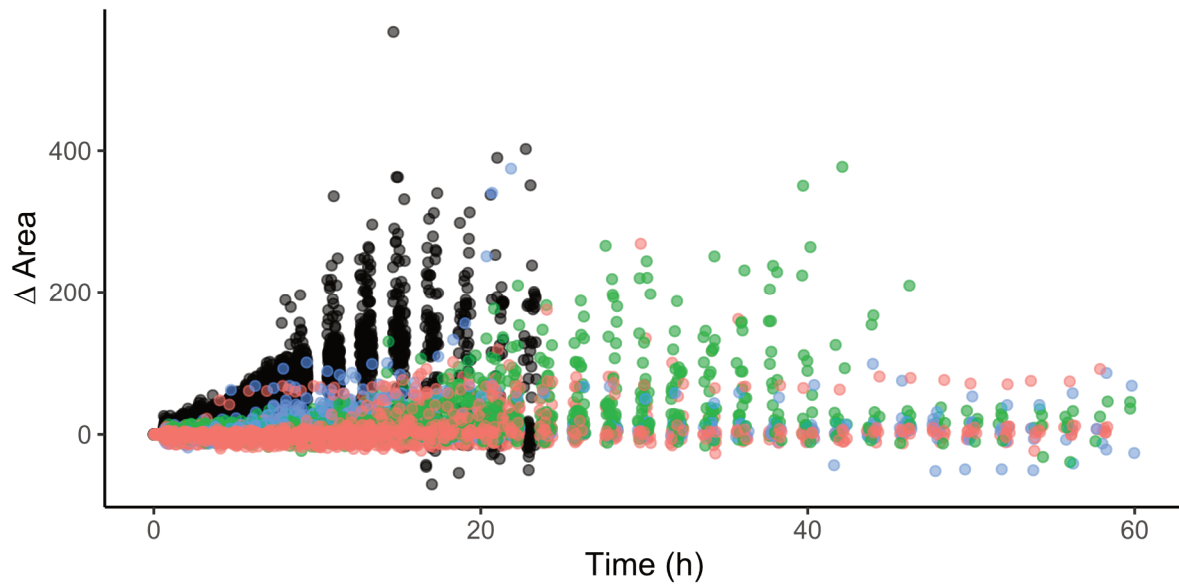
Figure S2. ΔArea (Area$_{t=x}$-Area$_{t=1}$) in pixels of germinating conidia of *P. roqueforti* incubated in KNPS + arginine (red), alanine (green) or glucose (blue) over time. Black dots show germinating *A. niger* conidia in NPS + alanine (see Chapter 2). Only objects with > 0.83 circularity are shown.
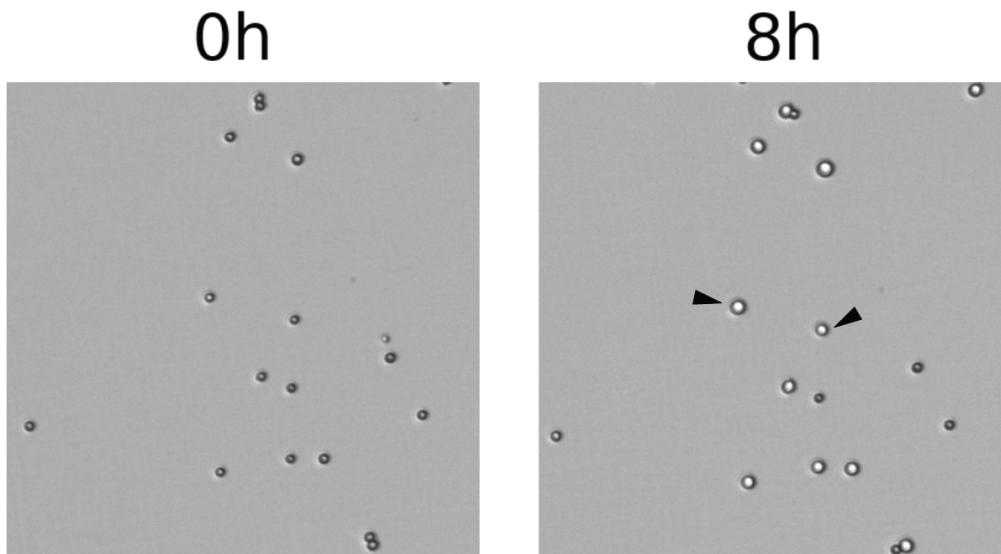
Figure S3. Conidia swelling of *P. roqueforti* in malt extract broth. Arrows indicate swollen conidia.

4

Impact of maturation and growth temperature on cell-size distribution, heat resistance, compatible solute composition and transcription profiles of *Penicillium roqueforti* conidia

Maarten Punt[1,2], Tom van den Brule[1,3], Wieke R. Teertstra[1,2], Jan Dijksterhuis[1,3], Heidy M. W. den Besten[1,4], Robin A. Ohm[1,2], Han A. B. Wösten[1,2]

[1]TiFN, P.O. Box 557, 6700 AN, Wageningen, The Netherlands;

[2]Microbiology, Utrecht University, Padualaan 8, 3584 CH, Utrecht, The Netherlands;

[3]Westerdijk Fungal Biodiversity Institute, Uppsalalaan 8, 3584 CT, Utrecht, The Netherlands;

[4]Food Microbiology, Wageningen University, Bornse Weilanden 9, 6708 WG, Wageningen, The Netherlands.

Abstract

Penicillium roqueforti is a major cause of fungal food spoilage. Its conidia are the main dispersal structures of this fungus and therefore the main cause of food contamination. These stress resistant asexual spores can be killed by preservation methods such as heat treatment. Here, the effects of cultivation time and temperature on thermal resistance of *P. roqueforti* conidia were studied. To this end, cultures were grown for three, five, seven and ten days at 25 °C or for seven days at 15, 25 and 30 °C. Conidia of three- and ten-day-old cultures that had been grown at 25 °C had D_{56}-values of 1.99 ± 0.15 min and 5.31 ± 1.04 min, respectively. The effect of cultivation temperature was most pronounced between *P. roqueforti* conidia cultured for seven days at 15 °C and 30 °C, where D_{56}-values of 1.12 ± 0.05 min and 4.19 ± 0.11 min were found, respectively. Notably, D_{56}-values were not higher when increasing both cultivation time and temperature by growing for ten days at 30 °C. A correlation was found between heat resistance of conidia and levels of trehalose and arabitol, while this was not found for glycerol, mannitol and erythritol. RNA-sequencing showed that the expression profiles of conidia from three- to ten-day-old cultures grown at 25 °C were distinct from conidia that had been formed by seven-day-old cultures at 15 °C and 30 °C. Only 33 genes were up-regulated at both prolonged incubation time and increased growth temperature. Their encoded proteins as well as trehalose and arabitol may form the core of heat resistance of *P. roqueforti* conidia.

Introduction

Food deterioration can have chemical, physical or microbiological causes. It results in a product with changed sensory properties such as visible appearance and the presence of off-odors and off-flavours. Furthermore, food spoilage can be associated with the introduction of toxic compounds. The impact of spoilage on food security is significant. Microbes alone have been estimated to spoil 25 % of the global food supply (Bondi et al., 2014).

Fungal conidia are ubiquitously present in the environment. These asexual spores are produced in overwhelming quantities and are effectively dispersed by wind, water, or animals like insects (Dijksterhuis, 2019). Fungal growth in food products can be precluded by preventing spores from entering the product and by food preservation processes such as heat

treatment, storage at low temperature, and addition of food preservatives (Dijksterhuis, 2017). As a single spore can cause spoilage, inactivating the most resistant spore is crucial from a food preservation perspective.

Most conidia will be killed by thermal food processing, but a resistant sub-population of cells may survive. Heterogeneity in a spore population occurs due to differences in genetic background, the developmental state of spores, and environmental growth conditions (Fujikawa & Itoh, 1996; Hallsworth & Magan, 1995, 1996; Nanguy et al., 2010). Heterogeneity is also observed between spores from a single colony (Bleichrodt et al., 2013; Hewitt et al., 2016; Krijgsheld et al., 2013; van den Brule et al., 2020a, 2020b). This may not only be caused by differences in developmental state or local differences in environmental growth conditions but also by stochastic gene expression. It should be noted that survival of a small subpopulation of conidia can also be introduced by the experimental procedure allowing small numbers of spores to escape the maximal heat exposure.

Cultivation temperature is an example of an environmental condition that affects stress resistance of conidia. For example, *Aspergillus fumigatus* conidia produced at elevated temperature are more resistant to oxidative stress and heat treatment (Hagiwara et al., 2017). This was associated with higher trehalose and mannitol levels as was observed in other *Aspergilli* (Fillinger et al., 2001; Ruijter et al., 2003; Wolschek & Kubicek, 1997). A similar increase in compatible solutes was found for *P. expansum* and *P. roqueforti* (Nguyen Van Long et al., 2017a), however, the heat resistance of the *Penicillium* sp. conidia was not assessed. Apart from compatible solutes, heat-shock proteins and hydrophilins have been implicated in heat resistance (Wyatt, Wösten, & Dijksterhuis, 2013). Transcripts of their encoding genes were found to accumulate in dormant conidia of *Aspergillus niger* (van Leeuwen et al., 2013).

The genus *Penicillium* consists of hundreds of species that are relevant in food spoilage and post-harvest damage (Samson et al., 2019). This is in part explained by the fact that conidia of *Penicillium* are among the most abundant spores in air samples and the fact that members of this genus can grow at low temperature. *P. roqueforti* is used in cheese making but is a food spoiler as well (Samson et al., 2010). For instance, it spoils grain, rye bread, and dairy products including cheese (Aran & Eke, 1987; Lund, Filtenborg, & Frisvad, 1995; Lund, Westall, & Frisvad, 1996; Nielsen & Rios, 2000; Samson et al., 2019; Taniwaki et al., 2001). *P. roqueforti*

changes the sensory properties of the product and it can also produce mycotoxins like PR toxin, roquefortine C and mycophenolic acid (Gillot et al., 2017). *P. roqueforti* is one of the fastest growing *Penicillium* species reaching 40-77 mm in seven days at 25 °C (Samson et al., 2019) and can grow at temperatures below 0 °C and up to 33 °C at a pH between 2.8 and 13.8 (Kalai et al., 2017). Furthermore, it survives atmospheres containing up to 70 % CO_2 (Taniwaki et al., 2001) or having a partial O_2 pressure as low as 0.1 % (Magan & Lacey, 1984; Yanai et al., 1980). In addition, *P. roqueforti* is one of few fungi that is classified as a preservative-resistant mould. It can spoil products containing weak organic acids such as sorbic, benzoic or propionic acid (Samson et al., 2004). In the case of sorbic acid this is due to degradation of the preservative by the fungus (Marth et al., 1966).

Here, the impact of cultivation time and temperature on thermal resistance of *P. roqueforti* conidia was studied and related to spore size, compatible solute concentrations, and transcriptomes. To this end, cultures were grown for three to ten days at 25 °C or at 15-30 °C for seven days. The D_{56}-value of *P. roqueforti* conidia was up to 4-fold higher at longer cultivation time and when formed at increased temperature. Compatible solute analysis suggests that trehalose and arabitol accumulation is important for conidial heat resistance, while RNA sequencing indicates a role for hydrophilins and heat-shock proteins.

Material and methods

Strain and cultivation conditions

Strain *P. roqueforti* DTO377G3 (LCP 97 4111, Muséum National d'Histoire Naturelle, France) was used in this study. Conidia were stored at -80 °C in 30 % glycerol and spot inoculated on malt extract agar (MEA ,Oxoid, Hampshire, UK). Conidia were harvested with a cotton bud from seven-day old cultures that had been incubated at 25 °C. The spores were suspended in 1 mL 10 mM N(2-acetamido)-2-aminoethanesulfonic acid, 0.02 % Tween 80, pH 6.8 (called ACES buffer from now on) and 100 µL of this suspension was spread on a MEA plate and incubated for three, five, seven or ten days at 15, 25 or 30 °C depending on the experiment. Conidia were harvested, taken up in 10 mL ice-cold ACES buffer, and washed twice with ACES buffer (van den Brule et al., 2020a). The conidia suspension was diluted 100 times, after which conidia concentration was determined using a haemocytometer.

Heat inactivation of conidia

Heat inactivation was performed with conidia of three- to ten-day-old cultures grown at 25 °C and with conidia of seven-day-old cultures grown at 15 °C and 30 °C. ACES buffer (19.8 ml) was pre-heated in a 100 mL Erlenmeyer in a water bath at 56 °C and 100 rpm. 200 µL spore suspension (containing $2 \cdot 10^8$ mL^{-1} conidia) was added to the Erlenmeyer and 1 mL samples were taken after 2-45 min followed by immediate cooling on ice. As a control, the untreated spore suspension was used. Decimal dilutions were made of each sample in ACES buffer and 100 µL was spread on a MEA plate and incubated at 25 °C. Colony forming units were quantified after 3-7 days depending on the lag time after the heat treatment. Experiments were done in triplicate, i.e. each experiment was performed with conidia derived from a biologically independent culture.

D-value determination

Inactivation curves were obtained by plotting log$_{10}$ surviving counts against the time of the thermal treatment using the modified Weibull model (Metselaar et al., 2013) that allows fitting of concave and convex inactivation curves:

$$\log N_t = \log N_0 - 5 \left(\frac{t}{t_{5D}} \right)^{\beta} \tag{1}$$

Log N_t represents the log$_{10}$ number of surviving spores (log$_{10}$ CFU mL^{-1}) at time t, log N_0 the log$_{10}$ initial number of spores (log$_{10}$ CFU mL^{-1}), t time in minutes, 5D time to reach 5 log$_{10}$ reduction in minutes, and β the shape parameters where $\beta > 1$ is concave and $\beta < 1$ is convex. Based on the experimental range a decimal reduction of 5D was selected. Each replicate was fitted with the R package GrowthRates (Hall et al., 2014) using the Levenberg-Marquardt algorithm. When β was significantly different from 1, the D_{56}-value was estimated as t_{5D} / 5. If not, the -1/ slope of a linear model was used to estimate the D_{56}-value. ANOVA followed by Tukey's Post Hoc test was applied to compare the D_{56}-values between the different experimental conditions.

Microscopy

Conidia chain length of *P. roqueforti* colonies that had been grown for 3-7 days at 15-30 °C was monitored with a Nikon Zoom AZ-100 stereomicroscope linked to a Nikon DS-Ri2 camera (Nikon Instruments, Amsterdam, the Netherlands).

Compatible solute concentration assessment

Compatible solute extraction and quantification was performed as described (van den Brule et al., 2020a) using conidia that had been harvested from three- to ten-day-old cultures that had been cultivated at 15 °C, 25 °C or 30 °C. In short, 10^8 conidia were pelleted for 1 min at 4 °C and 21.000 *g* and flash-frozen in liquid nitrogen after discarding the supernatant. Conidia were crushed with stainless steel beads in pre-cooled adapters (-80 °C) using a Tissuelyzer (2 min, 25 Hz) (QIAGEN, Hilden, Germany). After adding 1 mL Milli-Q and heating for 30 min at 95 °C, samples were centrifuged at 4 °C for 30 min at 20.000 *g* and filtered using an Acrodisc nylon syringe filter (0.2 µm, Pall Life Science, Mijdrecht, The Netherlands). Compatible solutes were determined in a sample volume of 20 µL with HPLC as described (van den Brule et al., 2020a). Shortly, the sample was injected in a mobile phase consisting of 0.1 mMol Ca EDTA in ultrapure water and were followed for 30 min. To quantify the concentration of compatible solutes in conidia, their size was measured using a Coulter counter Multisizer3 equipped with a 70 µm aperture tube with a measuring range of 1.4 - 42 µm (Beckman, Fichtenhain, Germany). To this end, conidial suspensions (described above) were diluted to $1 \cdot 10^5$ mL^{-1} in ISOTON II solution (Beckman Coulter) and 100 µL was used to measure spore size. At least 10^3 data points per sample were used to determine the mean conidia diameter and volume. ANOVA followed by Tukey's Post Hoc test was applied to compare the spore diameter between the different experimental conditions.

DNA extraction, genome sequencing, assembly and annotation

P. roqueforti was incubated for 48 h at 25 °C and 200 rpm in an Erlenmeyer flask containing 25 mL complete medium with 1 % glucose (w/v). Mycelium was harvested by filtering the culture through miracloth. DNA was extracted using the PowerPlant DNeasy kit (Qiagen) from lyophilized mycelium that was ground in a mortar and sequenced with Illumina NextSeq500 150 bp paired-end technology (Utrecht Sequencing Facility, useq.nl). The sequence reads were assembled using SPAdes v3.11.1 (Bankevich et al., 2012). The RNA sequencing reads

(see below) were used for gene prediction. Reads were pooled and aligned to the assembly using HISAT version 2.1.0, (Kim et al., 2015) using settings --min-intronlen 20 --max-intronlen 250 --no-unal. BRAKER version 2.1.2 (Hoff et al., 2016) was used to train the *ab initio* gene predictor Augustus version 3.0.3 (Stanke et al., 2006), which was subsequently used to generate gene predictions. Functional annotation of the predicted genes was performed essentially as described (de Bekker et al., 2017), with the exception that PFAM version 32 was used (El-Gebali et al., 2019). This whole genome shotgun project has been deposited at DDBJ/ENA/GenBank under the accession JABCSE000000000. The version described in this paper is version JABCSE010000000.

RNA extraction and sequencing

A genome-wide transcriptome analysis was performed on *P. roqueforti* conidia from biological triplicates of cultures grown for seven days at 15, 25 and 30 °C and cultures grown for three, five, seven and ten days at 25 °C. Conidia were harvested in 10 mL ACES buffer and filtered through sterile glass wool in a 10 mL syringe. After centrifugation for 5 min at 1120 *g*, the pellet was suspended in 100 µL RNA-*later* (ThermoFisher, Waltham, MA, USA), frozen in liquid nitrogen and lysed with metal beads in a Tissuelyzer (1 min, 25 Hz) (see above). Total RNA was isolated with the RNeasy Plant Mini Kit (Qiagen) and purified by on-column DNase digestion according to the manufacturer's protocol. RNA was sequenced with Illumina NextSeq500 75 bp single-end technology (Utrecht Sequencing Facility). Transcripts were mapped to the assembled genome using HISAT v2.1.0 (Kim et al., 2015) with the following input settings: --min-intronlen 20 --max-intronlen 1000 --no-unal –dta-cufflinks. Cuffdiff (which is part of the Cufflinks suite (version 2.2.1; Trapnell et al., 2013)) was used to determine the expression levels of each gene, normalized to the number of reads per kilobase of transcript per million reads (RPKM). Cuffdiff was also used to identify differentially expressed genes between conditions. Heatmaps were generated in R with the pheatmap and ComplexHeatmap packages (Gu, Eils, & Schlesner, 2016). The RNA-Sequencing expression data are available from the NCBI GEO database under accession GSE149235.

Results

Spore formation and thermal inactivation curves

Cultures of *P. roqueforti* were grown for three, five, seven and ten days at 15 °C, 25 °C and 30 °C. These temperatures were selected based on the cardinal temperatures of strain FM163 (Kalai et al., 2017). The selected temperature of 25 °C is close to the optimal growth temperature of this fungus, while growth rate at the suboptimal temperature 15 °C is similar to that at 30 °C (Kalai et al., 2017). At 15 °C, 1000 times less spores were harvested from three-day-old cultures when compared to seven-day-old cultures; 90 % of the spores were formed between five and ten days (Table 1). The conidia chain length was observed to increase over time at 15 °C (Figure 1) thus explaining, at least in part, the increase in spore formation over time. In contrast, spore numbers had reached their maximum values already after three days when cultures had grown at 25 °C and 30 °C.
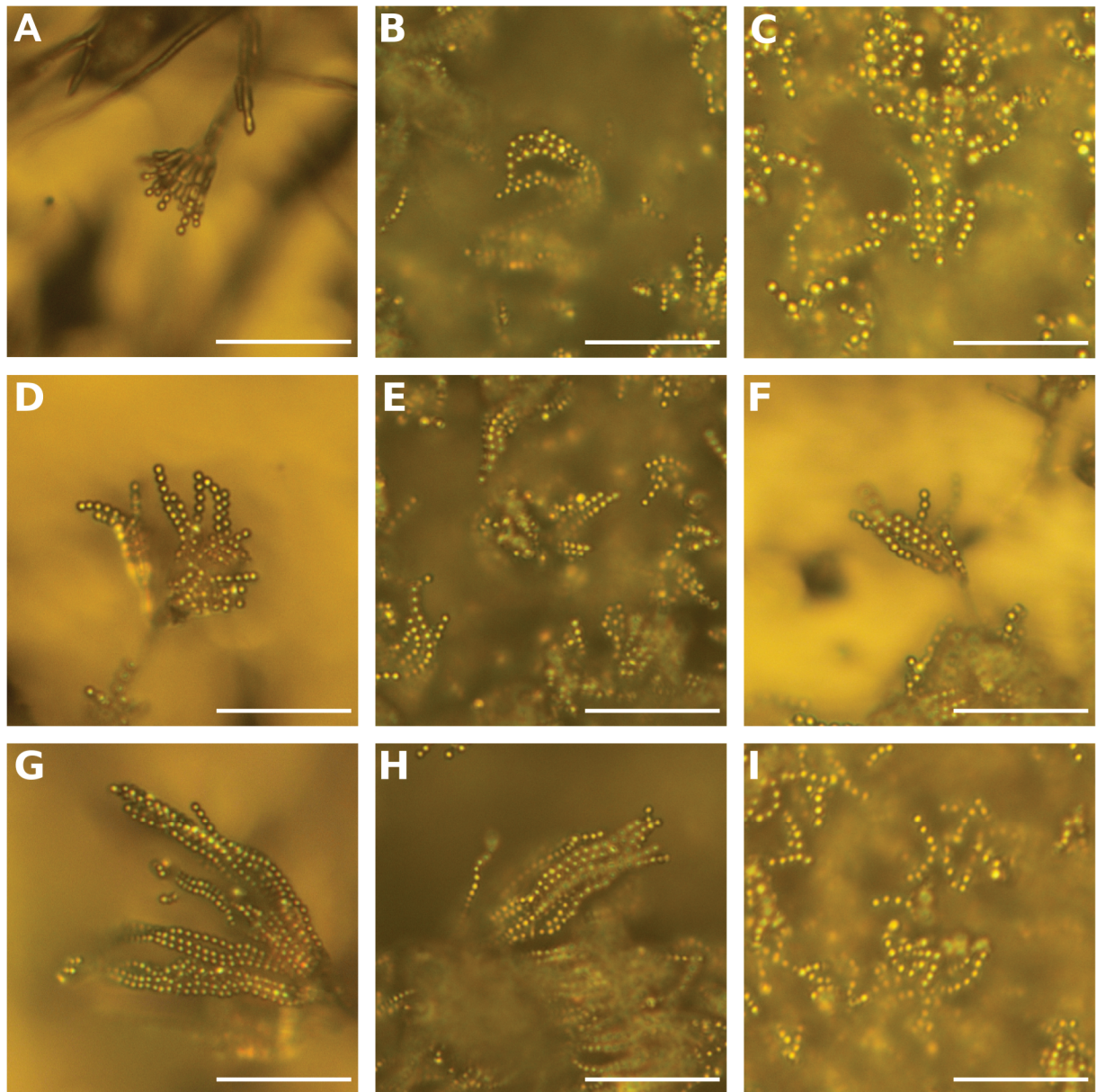
Figure 1. Light microscopy images of chains of *P. roqueforti* conidia of three- (A-C), five- (D-F) and seven- (G-I) day-old cultures that had been grown at 15 °C (A,D,G), 25 °C (B,E,H) and 30 °C (C,F,I). Bar indicates 50 μm

The effect of cultivation time and cultivation temperature on heat resistance of conidia was determined by treatment of spores at 56 °C (Figure 2). The inactivation curves were fitted with the modified Weibull model and a linear model. In the case β (the shape parameter) was significantly different from 1 the modified Weibull model was used to estimate the D_{56}-value, the linear model was used if β was not significantly different from 1 (Table S1). The time needed to inactivate conidia increased with increasing cultivation time at 25 °C (Figure 2A). Conidia of three- and ten-day-old cultures grown at 25 °C had estimated D_{56}-values of 1.99 ±

0.15 min and 5.31 ± 1.04 min, respectively. No significant difference in D_{56}-values was found between five-day-old (3.46 ± 0.08 min) and seven-day-old (3.41 ± 0.09 min) cultures. Remarkably, conidia formed at a temperature of 30 °C, showed a clear shoulder in the (concave) inactivation curve. This indicates that a longer heat treatment results in an accelerated killing of conidia. An almost fourfold increase in D_{56}-value was found when conidia of seven-day-old cultures had been formed at 30 °C (4.19 ± 0.11 min) when compared to 15 °C (1.12 ± 0.05 min) (Figure 2B). Notably, no further increase in thermal resistance was found when conidia were tested of cultures grown at 30 °C for ten days (D_{56}-value 3.97 ± 0.11 min) (Figure 2B). This demonstrates that thermal resistance of the conidia was maximal after seven days of cultivation at 30 °C. Together, these results show that D_{56}-values of *P. roqueforti* conidia differ fourfold within the tested cultivation time and temperature range.
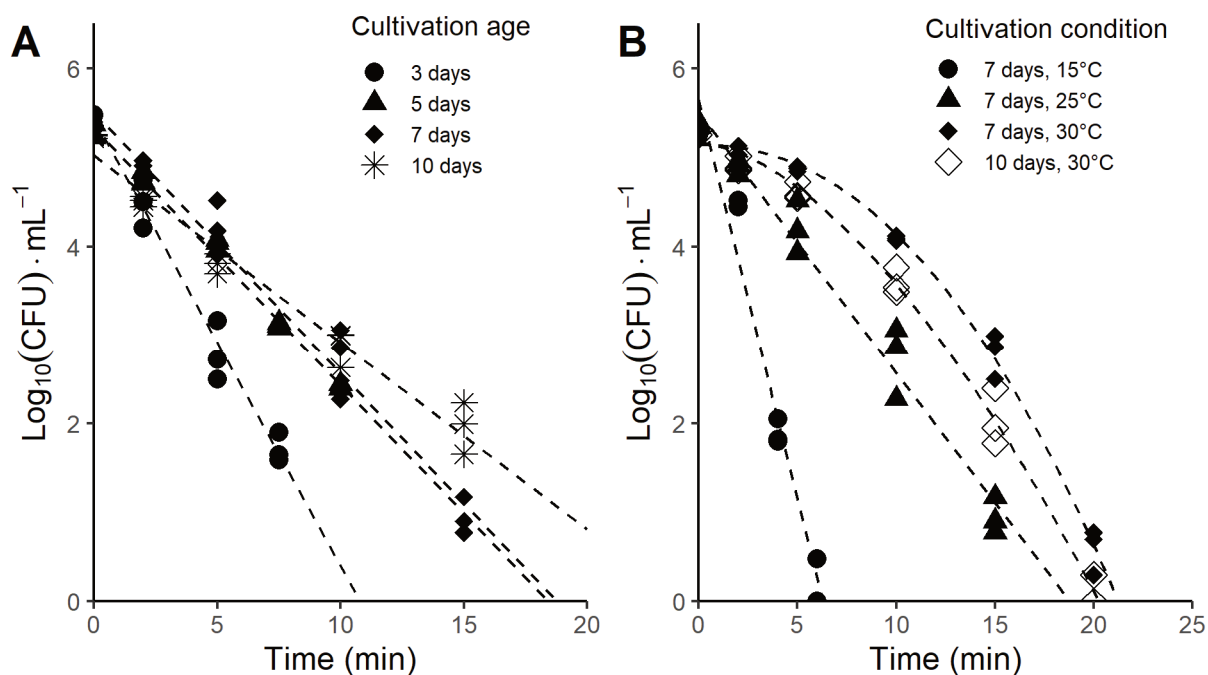

Figure 2. Thermal inactivation curves at 56 °C of *P. roqueforti* conidia obtained from three- (●), five- (▲), seven- (◆) and ten-day-old (*) cultures that had been incubated at 25 °C (A) or seven-day-old cultures that had been grown at 15 °C (●), 25 °C (▲) or 30 °C (◆) (B). Open diamonds (◇) indicate the inactivation curve for conidia produced at 30 °C harvested after ten days. Dashed line depicts average inactivation curve.

Conidia size and compatible solute content

The average diameter of conidia and their size distribution were determined with a Coulter counter using a population of ≥ 1000 conidia (Table 1). The average diameter of the conidia that had been produced at 15, 25 and 30 °C by 7-day-old cultures was 3.97 ± 0.03 μm, 3.94 ± 0.02 μm and 4.14 ± 0.02 μm, respectively (Figure 3). These data show a significant difference in cell size with conidia formed at 30 °C being on average 12-14 % bigger compared to those formed at lower temperatures.

The compatible solute content of conidia was determined with HPLC. Mean conidial volume was determined with a Coulter counter (Table 1) and used to estimate the intracellular concentration of trehalose, glycerol, mannitol, arabitol and erythritol (Figure 4A-E). Combined accumulation of the measured compatible solutes was fastest in the case of conidia that had been formed at 25 °C, reaching 1.36 M after 3 days. In contrast, conidia of cultures grown at 30 °C or 15 °C reached > 1.2 M total polyol content after five and seven days, respectively (Figure 4F). The highest total compatible solute levels were observed in conidia of five-day-old cultures grown at 25 °C. This was mainly due to the glycerol and arabitol levels.

Table 1. Effect of cultivation time and temperature on size and number of conidia of *P. roqueforti* as measured by Coulter counter and total spore count per colony. Mean spore diameter (in μm) and spore count ($\log_{10}$ total spores / plate) are shown ± SE. Asterisk indicates statistical significant differences of the diameter of conidia compared to conidia formed at 15 °C with the same cultivation time (Tukey's HSD, p < 0.01). Different letters indicate statistical significant differences of diameter of conidia within each temperature group (Tukey's HSD, p < 0.01)

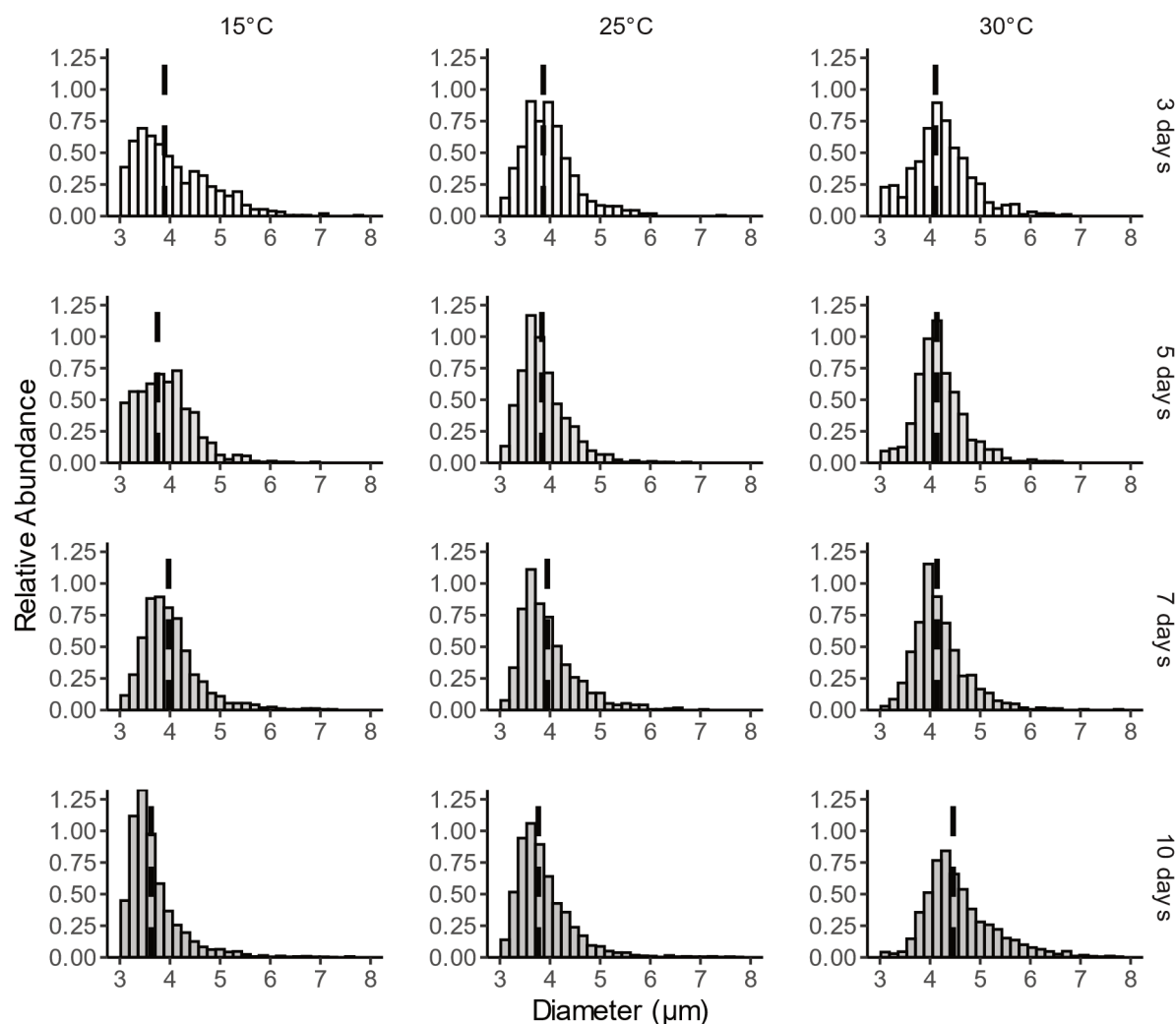| Culture age	15 °C		25 °C		30 °C	
	Diameter	Spore count	Diameter	Spore count	Diameter	Spore count
3 days	3.89 ± 0.03[a]	6.07 ± 0.14	3.87 ± 0.02[ab]	9.06 ± 0.06	4.11 ± 0.02[a*]	8.99 ± 0.07
5 days	3.75 ± 0.02[b]	8.43 ± 0.14	3.84 ± 0.02[ac]	9.07 ± 0.03	4.13 ± 0.02[a*]	8.69 ± 0.07
7 days	3.97 ± 0.03[a]	9.23 ± 0.05	3.94 ± 0.02[b]	9.13 ± 0.02	4.14 ± 0.02[a*]	8.91 ± 0.05
10 days	3.62 ± 0.01[c]	9.40 ± 0.02	3.77 ± 0.01[c*]	9.11 ± 0.02	4.46 ± 0.02[b*]	9.15 ± 0.1

Figure 3. Size distribution of conidia harvested from three- to ten-day-old cultures grown at 15, 25 or 30 °C. Number of bins is equal between conditions. Dashed line highlights mean conidia diameter. Particles < 3 µm are not conidia but cellular debris.

Trehalose concentration increased significantly with increasing culture age at all incubation temperatures. The highest trehalose concentration (0.102 M) was found in conidia of ten-day-old cultures that had been grown at 30 °C. Similar maximal levels of erythritol were found at 30 °C but in this case they were reached at day three and had declined at day ten. Glycerol, arabitol and mannitol were the most abundant compatible solutes. Glycerol reached the highest levels in conidia of three-day-old cultures when grown at 25 and 30 °C and in conidia of seven-day-old cultures that had been grown at 15 °C. In fact, the highest concentration of glycerol (0.63 M) was observed in the latter condition. Arabitol levels were generally highest at day seven and ten and reached maximum levels of 0.62 M in conidia of ten-day-old cultures that had been grown at 25 °C. Heat resistance correlated with arabitol (R^2 = 0.57; p-value = 0.051) and trehalose (R^2 = 0.48; p-value = 0.084) levels, while a negative correlation (R^2 = 0.88;

p-value = 0.0017) was observed in the case of glycerol (Figure 4G-I). No strong correlation (p-value > 0.1) was found between heat resistance and erythritol, mannitol or total compatible solute content (Figure S1).
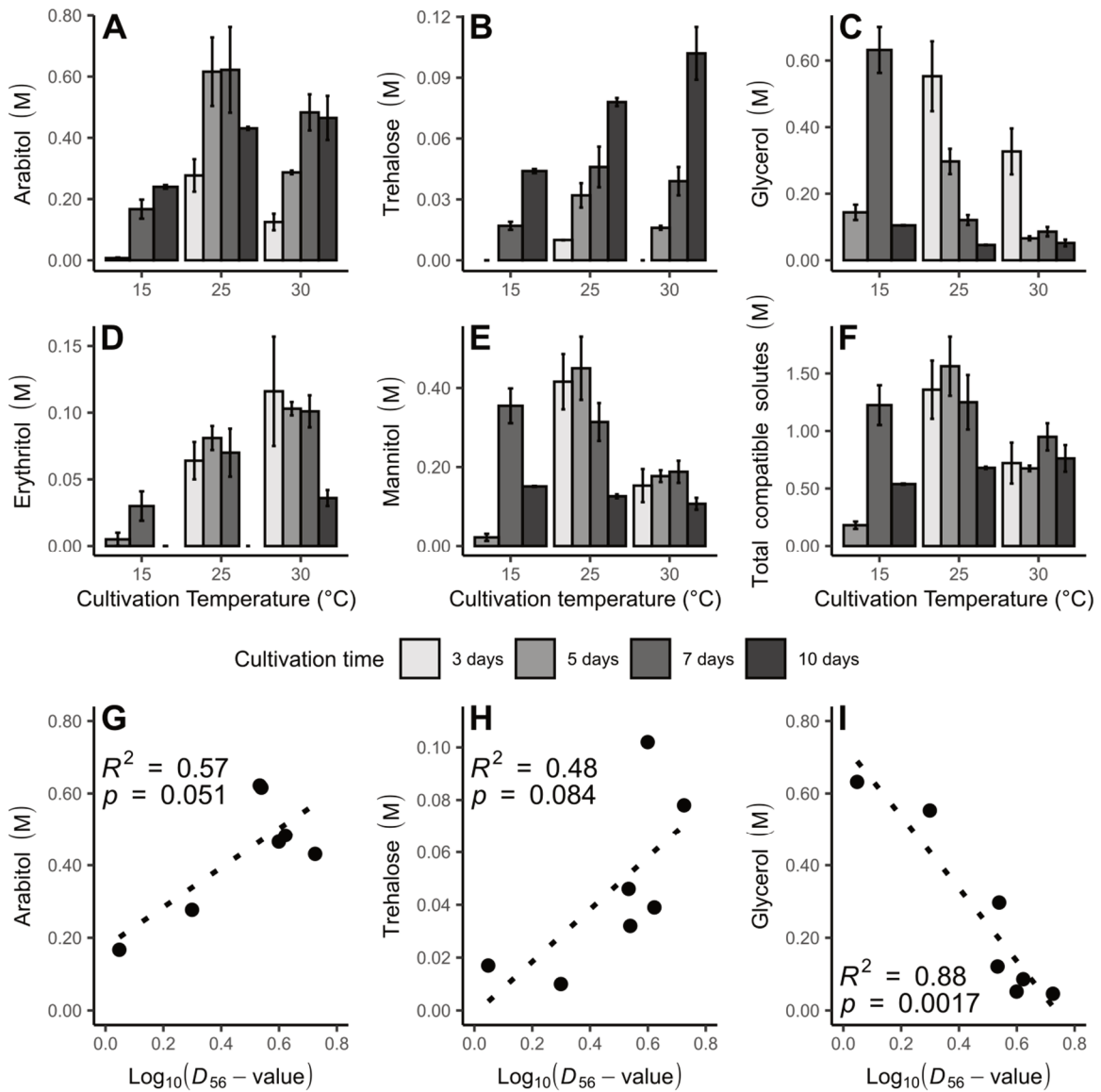

Figure 4. Arabitol (A), trehalose (B), glycerol (C), erythritol (D), mannitol (E), and total compatible solute concentration (F) of conidia harvested from three- to ten-day-old cultures grown at 15, 25 or 30 °C (± standard deviation). Each bar graph represents biological triplicates. Note that three-day-old cultures grown at 15 °C did not yield sufficient number of conidia to quantify polyol content. Relationship between $\log_{10}$ (D_{56}-value) and arabitol (G), trehalose (H) or glycerol (I) concentration across all samples for which a D_{56}-value has been determined.

Transcriptome analysis

The genome of *P. roqueforti* strain DTO377G3 was sequenced as a reference for a genome-wide transcriptome analysis. Sequencing was performed with approximately 126 x coverage. Genome assembly and gene prediction resulted in a 26.97 Mbp assembly and 9762 predicted

genes (Table S2). RNA was isolated from dormant *P. roqueforti* conidia harvested from cultures that had been grown for seven days at 15, 25 and 30 °C and grown for three, five, seven and ten days at 25 °C. RNA-sequencing produced at least 18.5 million 75 bp reads per biological replicate of which > 98 % mapped to the reference genome. Transcripts of 9723 genes were detected in the conidia that had been formed at these various conditions (Table S3). The expression profiles of all 9723 genes are visualized in a heatmap (Figure 5A), which shows that gene expression changed over time as well as at increasing temperatures. Overall, cultivation time and temperature have distinct effects on gene expression. This is further illustrated by a multi-dimensional scaling (MDS) plot of the expression data (Figure 5B), which shows that samples from increasing cultivation times aligned along the M1 axis in order of increasing temperature. A similar trend was observed along the M2 axis for the samples differing in cultivation temperature.

Gene expression data was filtered to identify differentially expressed genes with similar expression profiles in time as well as increased cultivation temperature. First, genes were selected that were significantly differentially expressed ($\alpha < 0.05$) in any of the conditions (6047 genes). This selection was used to compare expression levels between conidia that had been formed by cultures that had been grown at different temperatures or cultivation times. Next, genes were selected with an expression value of > 50 RPKM in at least one condition (3247 genes, Table S3). Among these 3247 genes, 85 (Table S4) and 274 genes (Table S5) were at least fourfold up-regulated in conidia from seven-day-old cultures produced at 30 °C compared to 15 °C and from three-day-old cultures compared to ten-day-old cultures produced at 25 °C, respectively. Only 33 genes were shared in these two gene sets (Figure 5C). These genes included 17 unknown genes, the hydrophilin genes *con-6* and *con-10*, the conidial pigmentation biosynthesis oxidase gene *laccase-1* and the predicted aflatoxin biosynthesis regulatory gene *aflR* (Table 2) (Note that it is unlikely that aflatoxin is produced in *P. roqueforti;* Fontaine et al., 2015)*.*
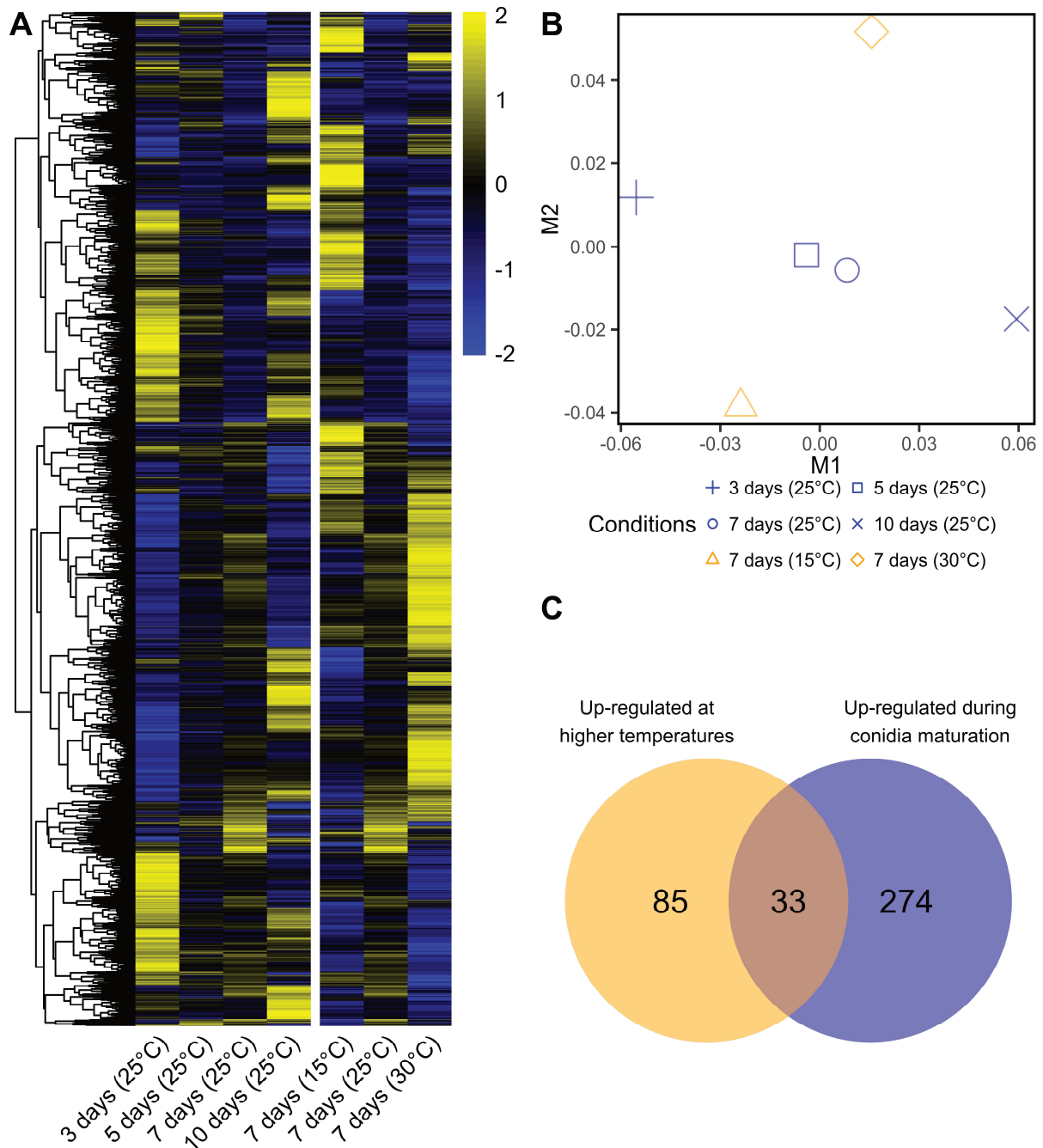
Figure 5. (A) Heatmap depicting hierarchically clustered expression data of 9723 genes expressed in conidia formed by three-, five-,seven- and ten-day-old 25 °C grown cultures and formed by seven-day-old cultures that had been grown at 15, 25 or 30 °C. Values represent mean RPKM values transformed into Z-scores. Yellow and blue shading represents higher and lower expression, respectively. (B) Multi-dimensional scaling plot of RNA-seq samples used in this study. (C) Venn-diagram with number of genes ≥ fourfold differentially expressed in conidia from ten-day-old cultures compared to three-day-old cultures (blue circle) or ≥ fourfold differentially expressed genes in conidia from seven-day-old cultures grown at 30 °C compared to 15 °C (orange circle).

Table 2. Genes that were at least fourfold up-regulated both in conidia formed at higher cultivation temperature (30 °C versus 15 °C) and cultivation time (three versus ten days of culturing). Each gene had RPKM levels > 50 in one or more conditions.

Gene ID	Temperature: 25 °C				Culture age: 7 days		Ratio		Functional annotation	Gene name
	3 days	5 days	7 days	10 days	15 °C	30 °C	10 d : 3 d	30 °C : 15 °C		
2891	0.9	49.4	200.9	715.5	0.8	362.7	775.0	443.4	Conidiation-specific protein	con-10
3236	19.7	146.4	415.9	1270.0	17.8	149.2	64.4	8.4	Aegerolysin	
8873	4.0	29.0	66.5	173.7	17.2	82.6	43.3	4.8	Conidiation-specific protein	con-6
1335	37.8	241.0	510.3	1333.8	30.1	357.1	35.3	11.9	hypothetical protein	
8393	5.9	49.2	72.0	189.1	13.7	82.5	32.1	6.0	hypothetical protein	
2892	2.4	11.6	30.5	59.5	4.5	27.2	25.1	6.1	Hemerythrin HHE cation binding domain	
4038	4.3	18.4	45.9	104.4	8.8	43.5	24.1	5.0	hypothetical protein	
3817	101.5	763.9	888.5	2296.0	61.8	1089.1	22.6	17.6	hypothetical protein	
8946	17.1	104.0	158.2	361.0	25.8	117.1	21.1	4.5	Arylsulfotransferase (ASST)	
263	303.0	1482.7	2633.4	6381.2	666.9	2781.3	21.1	4.2	hypothetical protein	
8700	7.1	38.3	57.8	144.5	7.5	65.0	20.4	8.6	hypothetical protein	
3247	20.0	52.6	112.5	393.5	17.9	79.8	19.7	4.5	Zinc-regulated transporter	
8125	4.6	23.3	47.3	90.3	0.8	51.9	19.5	63.2	hypothetical protein	
3238	54.2	227.2	298.4	961.9	58.6	241.1	17.8	4.1	hypothetical protein	
9274	8.0	33.2	61.9	139.2	9.5	69.8	17.5	7.3	hypothetical protein	
3532	3.5	17.2	21.1	54.2	9.7	73.1	15.7	7.5	Ankyrin repeat-containing domain	
1797	29.9	104.7	180.4	393.1	30.4	151.5	13.2	5.0	hypothetical protein	
71	44.4	161.5	226.0	579.3	39.4	352.4	13.1	8.9	hypothetical protein	
3818	9.1	37.1	46.4	117.8	6.5	113.5	12.9	17.6	Fungal Zn(2)-Cys(6) binuclear cluster domain	
3096	6.3	21.8	39.4	76.5	7.1	46.0	12.2	6.5	Aflatoxin biosynthesis regulatory protein	aflR
5339	10.9	38.7	52.7	100.2	6.7	59.9	9.2	8.9	hypothetical protein	

4209	17.8	38.7	70.5	145.2	14.8	59.9	8.1	4.1	hypothetical protein	
2064	1575.6	4650.9	5570.8	11916.9	890.5	7382.7	7.6	8.3	hypothetical protein	
6013	11.5	36.1	38.3	81.9	13.9	62.5	7.1	4.5	Pyridoxal phosphate-dependent decarboxylase	
4965	36.4	105.3	139.5	232.0	67.5	276.7	6.4	4.1	Beta-1,3-glucanase	
5161	15.3	42.2	54.5	97.5	19.3	89.5	6.4	4.6	Platelet-activating factor acetylhydrolase	
3533	22.8	75.2	69.3	142.4	48.4	206.7	6.3	4.3	hypothetical protein	
6552	2.7	3.4	6.4	15.0	0.2	58.2	5.6	258.5	hypothetical protein	
4451	33.7	64.9	84.4	181.5	17.6	93.0	5.4	5.3	Extradiol ring-cleavage dioxygenase	
6680	26.9	49.6	61.2	140.1	8.3	76.6	5.2	9.2	Glutathione S-transferase, N-terminal domain	
3246	39.6	63.7	82.1	194.7	21.1	87.8	4.9	4.2	Conidial pigment biosynthesis oxidase	Laccase-1
7290	27.1	47.7	56.1	109.6	13.1	95.5	4.0	7.3	hypothetical protein	
1023	13.6	27.1	32.1	55.0	4.9	72.0	4.0	14.6	Acetolactate synthase	

In an all-versus-all comparison, the largest number of differentially expressed genes was found when comparing conidia from three-day-old and ten-day-old cultures grown at 25 °C (2062 up / 2051 down) (Table S6). The smallest number of differentially expressed genes (87 up / 55 down) was found when conidia from five-day-old and seven-day-old 25 °C-cultures were compared (Table S6). The top 40 genes showing the highest RPKM ratio between conidia of ten-day-old and three-day-old cultures grown at 25 °C were analysed (Table 3). This set contained 20 genes that are also part of the 33 differentially expressed genes shared between the sets of ≥ fourfold up-regulated genes found at increased cultivation time and cultivation temperature. Notably, the hydrophilin genes were among the four genes with highest ten-day:three-day ratio. Next, the top 40 genes were analysed that were at least fourfold up-regulated between 15 °C and 30 °C of seven day old-cultures (Table 4). In this selection, *con-10* was the gene with the highest 30 °C:15 °C RPKM ratio. In addition, this gene set contained two genes encoding heat-shock proteins, a gene encoding a GPI-anchored cell wall protein and a gene encoding a protein with a NLPC/P60 domain. 16 genes of this gene set were also part of the 33 differentially expressed genes that were shared between the sets of ≥ fourfold up-regulated genes found at increased cultivation time and cultivation temperature.

Table 3. Top 40 of genes with the highest RPKM ratios between ten- and three-day-old cultures grown at 25 °C. Each gene had RPKM levels > 50 in one or more conditions. Grey shading indicates genes that are part of the 33 genes that are fourfold up-regulated at increased cultivation time as well as at increased cultivation temperature (see Table S5).

| Gene ID | Temperature: 25 °C | | | | Culture age: 7 days | | Ratio | Functional annotation |
	3 days	5 days	7 days	10 days	15 °C	30 °C	10 d : 3 d	
2891	0.9	49.4	200.9	715.5	0.8	362.7	775.0	Conidiation-specific protein
3236	19.7	146.4	415.9	1270.0	17.8	149.2	64.4	Aegerolysin
3235	11.9	58.9	147.3	575.6	22.8	79.6	48.5	Multicopper oxidase
8873	4.0	29.0	66.5	173.7	17.2	82.6	43.3	Conidiation protein 6
1335	37.8	241.0	510.3	1333.8	30.1	357.1	35.3	hypothetical protein
8393	5.9	49.2	72.0	189.1	13.7	82.5	32.1	hypothetical protein
2892	2.4	11.6	30.5	59.5	4.5	27.2	25.1	Hemerythrin HHE cation binding domain
4038	4.3	18.4	45.9	104.4	8.8	43.5	24.1	hypothetical protein
3817	101.5	763.9	888.5	2296.0	61.8	1089.1	22.6	hypothetical protein
3259	3.2	19.1	26.4	69.8	7.6	21.9	22.2	Major Facilitator Superfamily
4035	802.8	3559.3	7076.0	17536.5	10914.6	4379.8	21.8	hypothetical protein
8946	17.1	104.0	158.2	361.0	25.8	117.1	21.1	Arylsulfotransferase (ASST)

263	303.0	1482.7	2633.4	6381.2	666.9	2781.3	21.1	hypothetical protein
3613	4.0	20.2	37.4	82.7	14.1	17.1	20.8	hypothetical protein
8700	7.1	38.3	57.8	144.5	7.5	65.0	20.4	hypothetical protein
3247	20.0	52.6	112.5	393.5	17.9	79.8	19.7	ZIP Zinc transporter
8125	4.6	23.3	47.3	90.3	0.8	51.9	19.5	hypothetical protein
4008	103.9	510.3	976.6	1895.6	361.5	549.5	18.2	CVNH domain
3238	54.2	227.2	298.4	961.9	58.6	241.1	17.8	hypothetical protein
9274	8.0	33.2	61.9	139.2	9.5	69.8	17.5	hypothetical protein
4036	143.5	818.2	1101.3	2501.4	499.1	1177.2	17.4	hypothetical protein
9209	78.1	436.1	634.4	1334.5	272.7	384.1	17.1	hypothetical protein
3532	3.5	17.2	21.1	54.2	9.7	73.1	15.7	Ankyrin repeat-containing domain
8439	6.1	26.5	60.3	90.1	11.3	28.0	14.7	Membrane dipeptidase (Peptidase family M19)
7080	77.8	354.7	461.7	1091.5	207.0	440.2	14.0	Phenazine biosynthesis-like protein
4034	21.2	66.8	125.4	296.8	507.6	121.4	14.0	hypothetical protein
4123	24.8	131.4	164.4	329.9	163.0	153.1	13.3	hypothetical protein
1797	29.9	104.7	180.4	393.1	30.4	151.5	13.2	hypothetical protein
71	44.4	161.5	226.0	579.3	39.4	352.4	13.1	hypothetical protein
85	42.7	171.1	272.1	553.9	100.2	183.6	13.0	non-haem dioxygenase in morphine synthesis N-terminal
3818	9.1	37.1	46.4	117.8	6.5	113.5	12.9	Fungal Zn(2)-Cys(6) binuclear cluster domain
4021	406.2	1841.9	3089.7	5166.2	600.9	2401.5	12.7	hypothetical protein
704	21.4	77.5	127.7	264.3	79.6	83.2	12.3	hypothetical protein
8036	24.1	105.3	149.7	294.8	60.5	125.8	12.2	hypothetical protein
3096	6.3	21.8	39.4	76.5	7.1	46.0	12.2	Fungal Zn(2)-Cys(6) binuclear cluster domain
3993	579.1	2228.8	3120.2	6939.2	861.9	3026.8	12.0	Membrane transport protein
7452	248.8	967.6	1341.9	2957.6	299.5	977.4	11.9	hypothetical protein
454	2019.0	7702.0	10383.1	23272.9	5435.4	9066.7	11.5	Steryl acetyl hydrolase
959	8.0	24.9	43.8	91.5	32.4	43.5	11.5	MULE transposase domain
6230	89.9	368.5	474.2	1023.4	200.9	341.6	11.4	hypothetical protein

Table 4. Top 40 of genes with the highest RPKM ratios between seven-day-old cultures produced at 30 °C compared to seven-day-old cultures produced at 15 °C. Each gene had RPKM levels > 50 in one or more conditions. Grey shading indicates genes that are part of the 33 genes that are both fourfold up-regulated at increased cultivation time and increased cultivation temperature (see Table S4).

Gene ID	Temperature: 25 °C				Culture age: 7 days		Ratio	Functional annotation
	3 days	5 days	7 days	10 days	15 °C	30 °C	10 d : 3 d	
2891	0.9	49.4	200.9	715.5	0.8	362.7	443.4	Conidiation-specific protein
6552	2.7	3.4	6.4	15.0	0.2	58.2	258.5	hypothetical protein
5882	245.8	88.4	19.8	20.8	6.7	1026.5	152.1	NlpC/P60 family
8119	96.7	45.4	11.2	5.4	1.2	102.8	82.3	Major Facilitator Superfamily
8125	4.6	23.3	47.3	90.3	0.8	51.9	63.2	hypothetical protein
3417	21.5	15.8	50.9	23.9	6.6	171.4	26.0	hypothetical protein
8792	2.8	1.9	2.3	3.0	4.8	111.8	23.2	Sugar (and other) transporter
8545	29.4	11.4	7.4	16.1	10.5	241.4	22.9	hypothetical protein
152	37.6	22.4	25.0	33.1	45.4	899.7	19.8	hypothetical protein
3817	101.5	763.9	888.5	2296.0	61.8	1089.1	17.6	hypothetical protein
5090	16.4	13.9	5.3	15.1	4.7	83.0	17.6	Putative peptidase family
3818	9.1	37.1	46.4	117.8	6.5	113.5	17.6	Fungal Zn(2)-Cys(6) binuclear cluster domain
8798	46.1	60.0	61.8	70.6	7.9	123.7	15.8	Hsp70 protein
2807	61.2	26.5	41.5	31.8	4.3	67.8	15.6	hypothetical protein
9099	46.4	43.8	42.0	37.1	12.8	196.8	15.4	HSP20-like domain found in ArsA
7966	48.1	67.1	51.9	72.8	112.9	1683.1	14.9	hypothetical protein
1023	13.6	27.1	32.1	55.0	4.9	72.0	14.6	Thiamine pyrophosphate enzyme
4065	31.3	50.1	73.4	95.1	8.0	104.3	13.0	hypothetical protein
8031	19.5	38.1	45.1	55.4	2.4	28.9	11.9	hypothetical protein
1335	37.8	241.0	510.3	1333.8	30.1	357.1	11.9	hypothetical protein
8064	306.6	258.8	243.2	426.2	80.0	939.8	11.7	hypothetical protein
770	8.3	19.9	20.5	31.0	10.7	117.6	10.9	Sugar (and other) transporter
1081	63.5	88.3	93.6	213.0	23.3	235.2	10.1	glycosyl-phosphatidyl-inositol-anchored membrane family
1351	14.1	8.0	7.5	8.0	6.3	61.9	9.8	hypothetical protein
6680	26.9	49.6	61.2	140.1	8.3	76.6	9.2	Glutathione S-transferase, N-terminal domain
6473	26.4	26.0	26.5	20.3	23.3	212.5	9.1	Tryptophan dimethylallyltransferase
71	44.4	161.5	226.0	579.3	39.4	352.4	8.9	hypothetical protein
5339	10.9	38.7	52.7	100.2	6.7	59.9	8.9	hypothetical protein
3287	34.5	37.9	50.6	32.7	28.2	246.1	8.7	hypothetical protein
8700	7.1	38.3	57.8	144.5	7.5	65.0	8.6	hypothetical protein
3236	19.7	146.4	415.9	1270.0	17.8	149.2	8.4	Aegerolysin
2064	1575.6	4650.9	5570.8	11916.9	890.5	7382.7	8.3	hypothetical protein

8469	33.3	31.1	33.9	69.9	12.4	102.4	8.3	RNA recognition motif
8882	15.9	18.2	27.2	10.9	9.8	80.1	8.1	O-methyltransferase domain
3532	3.5	17.2	21.1	54.2	9.7	73.1	7.5	Ankyrin repeats (3 copies)
7509	11.1	11.8	9.9	11.7	16.8	123.7	7.4	hypothetical protein
9274	8.0	33.2	61.9	139.2	9.5	69.8	7.3	hypothetical protein
7290	27.1	47.7	56.1	109.6	13.1	95.5	7.3	hypothetical protein
4272	11.6	14.4	13.3	20.4	7.6	53.7	7.1	hypothetical protein
4248	37.4	24.3	26.3	34.9	9.7	65.7	6.8	hypothetical protein

Expression profiles of genes involved in polyol biosynthesis and genes encoding heat-shock proteins and hydrophilins were assessed. To this end, orthologs were identified in *P. roqueforti* of genes characterized in *Aspergilli* (polyol biosynthesis and heat-shock proteins) and *Neurospora crassa* (hydrophilins) (Table S7). A heatmap was generated from the Z-scores of the expression patterns of stress- and polyol-related genes (Figure 6). Only genes that were significantly differentially expressed and showed > 50 RPKM in at least one condition were included. Trehalose-6-phosphate synthase (*tpsB* & *tpsC*) and α,α-trehalose glucohydrolase (*treA*) showed increased expression levels in older conidia compared to conidia derived from three- or five-day-old cultures. This coincided with an increased trehalose content in these conidia (Figure 4A). Conversely, expression of *tpsC* and *tppB* decreased in conidia formed at 30 °C compared to conidia of the same age produced at 15 or 25 °C. Yet, trehalose content was not lower under these conditions. No clear correlation between the expression profiles of erythrose reductases (*err1*) and erythritol content was observed. Expression levels of the hydrophilins *lea*, *con-6* and *con-10* were higher in older cultures at 25 °C. At 25 °C and 30 °C, expression levels of *con-6* and *con-10* also were higher when compared to 15 °C, but this was not the case for *lea*.

In total 17 predicted heat-shock proteins (HSP's) were identified in the transcriptome, of which only two showed a ≥ fourfold change in expression levels between ten- and three-day-old cultures grown at 25 °C or seven-day-old cultures grown at 30 °C or 15 °C (Table 4). Among this set of 17 HSPs, *hsp12* has been previously described to play a role in the protection against heat stress in *Aspergillus fischeri* (van Leeuwen et al., 2016) but the *P. roqueforti* homolog of *hsp12* did not show a significant change in expression.

In addition to changes in expression patterns, the 20 most highly expressed genes in each condition were analyzed, yielding 37 different genes of which the four most highly expressed genes were shared among all conditions (Table S8). Notably these included two glucose-repressible proteins (*grg1* & *grg2*), hydrophobins 1 (*hpb1*) and 2 (*hpb2*), an extracellular membrane protein (CFEM) and a 30 kDa heat-shock protein (*hsp30*).
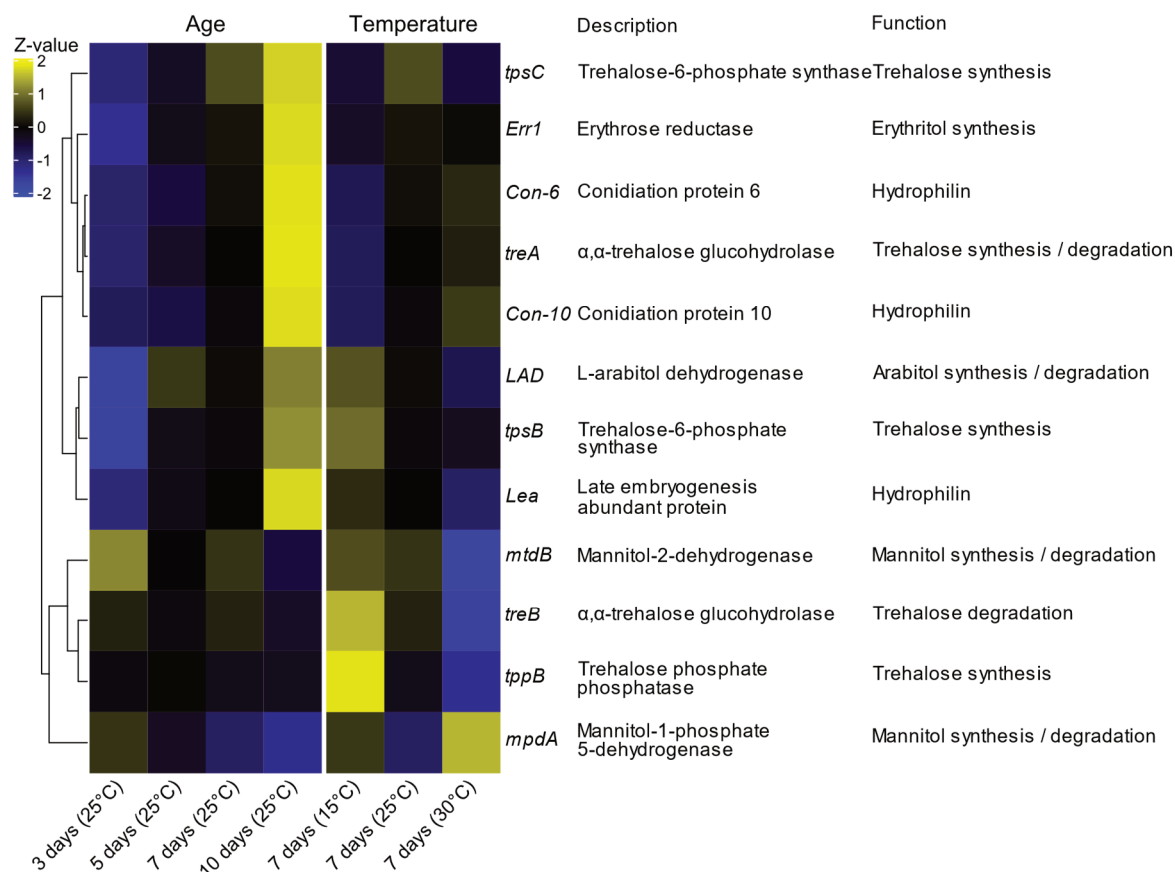

Figure 6. Heatmap depicting hierarchically clustered expression data of 12 *P.* roqueforti genes that are orthologous to genes related to compatible solute biosynthesis and heat-shock proteins in other fungi. Values represent mean RPKM values transformed into Z-scores. Profiles for conidia obtained from three-, five-, seven- and ten-day-old cultures incubated at 25 °C and for seven-day old cultures produced at 15 °C, 25 °C or 30 °C are shown. Yellow and blue shading represent higher and lower expression, respectively**.**

Discussion

P. roqueforti conidia that are present in air at a certain location and time will not all have matured for the same time on the conidiophores before they had been released and will not have been formed under the same environmental conditions. Here we showed that both incubation temperature and culture age affect heat resistance (D_{56}-values) of *P. roqueforti* conidia and that this correlates with compatible solute composition and RNA profiles. Our data imply that airborne *P. roqueforti* conidia are heterogeneous with respect to their

maturation, and as a consequence, to their heat resistance and their composition. This is expected to be a more general phenomenon. For instance, survival of *A. fumigatus* conidia to a heat shock increases when they are formed at a higher temperature (Hagiwara et al., 2017). In contrast to our findings with *P. roqueforti*, no increase in heat resistance was found between conidia obtained from *A. fumigatus* cultures with different age (3-14 days). It should be noted that heat resistance is not only the result of the composition of conidia but also of the environmental conditions during stress exposure. For example, *P. roqueforti* conidia are less sensitive to heat treatment when they are exposed to a matrix with low water activity such as bread (Bröker et al., 1987a; Garcia et al., 2019; Raynaud & Lelieveld, 1997).

P. roqueforti conidia cultivated at 30 °C showed a 12-14 % increased volume compared to conidia cultivated at 15 °C and 25 °C. Conversely, Nguyen Van Long et al. (2017a) demonstrated that cultivation at 5 °C increases spore diameter by about 25 % compared to *P. roqueforti* conidia produced at 20 °C and 27 °C. Combined with our results this suggest that conidia size increases under suboptimal conditions as both 30 °C and 5 °C are close to the growth boundaries of *P. roqueforti* (Kalai et al., 2017). Significant differences in conidia size distributions have been observed within a single *Paecilomyces variotii* colony and it has been postulated that the larger conidia are more heat-resistant (van den Brule et al., 2020a). Maturation time also impacted the average size of the conidia. Size reduced when conidia matured at 15 °C and 25 °C, while it increased at a growth temperature of 30 °C. The former can be explained by evaporation of water from the spores, the explanation for increased spore size is not yet clear.

Trehalose has been associated with heat resistance of fungal conidia (van den Brule et al., 2020a; Hagiwara et al., 2017; Nguyen Van Long et al., 2017a; Ruijter et al., 2003; Sakamoto et al., 2009; Wyatt et al., 2015). Indeed, trehalose concentration increased in older conidia of *P. roqueforti* and in conidia that had been grown at higher temperature. Similar results have been found for *Aspergillus fischeri* ascospores and conidia of *A. niger, Beauveria bassiana, Cordyceps farinose* (formerly described as *Paecilomyces farinosus*) and *Metarhizium anisopliae* (Hallsworth & Magan, 1996; Teertstra et al., 2017; Wyatt et al., 2015). It should be noted that the conditions that yielded conidia with the highest trehalose concentration (ten days, 30 °C) did not result in the most heat-resistant conidia. This suggests that trehalose has

other functions and, indeed, trehalose serves as a carbon storage molecule in fungi (Perfect et al., 2017). Notably, *P. roqueforti* conidia produced at 27 °C contain more trehalose and have an extended germination time compared to conidia produced at 5 °C (Nguyen Van Long et al., 2017a*). Possibly, the high levels of trehalose under these conditions delay the germination time, as intracellular trehalose is shown to reduce germination speed in *B. bassiana*, *M. anisopliae* and *C. farinosus* (Hallsworth & Magan, 1995). Delaying the germination time may be a strategy to prevent premature germination; i.e. at the site where the spores are produced. The fact that conidia with the highest trehalose concentration are not the most heat-resistant also implies that other factors, in particular arabitol, contribute to heat resistance of *P. roqueforti* conidia. No clear relation was found between heat resistance and mannitol or erythritol concentration, while a negative correlation was observed for heat resistance and glycerol levels. The neutral effect of mannitol contrasts other studies that link concentration of this compatible solute with heat resistance of fungal conidia (Dijksterhuis & de Vries, 2006; Wyatt et al., 2013). The effect of glycerol was in line with other studies. This compatible solute as well as erythritol has been related with desiccation resistance (Beever & Laracy, 1986; Hallsworth & Magan, 1995).

Gene expression profiles of spores were analyzed to identify genes that are potentially involved in heat resistance. Overall, cultivation time and temperature had distinct effects on gene expression. Notably, only 33 genes were ≥ fourfold up-regulated both in the most heat-resistant spores resulting from different incubation temperature and from different incubation time. This set included 17 predicted proteins with unknown function as well as the hydrophilins con-6 and con-10. The hydrophilins have been implicated in heat resistance (see below) and are therefore expected to fulfil such a role in *P. roqueforti* conidia as well. Expression profiles of significant differentially expressed genes involved in polyol biosynthesis were compared between conditions leading to higher thermal resistance (ten-day-old conidia vs. three-day old conidia, conidia produced at 30 °C vs at 15 °C). For cultivation time these included *treA*, *tpsB* and *tpsC* (involved in trehalose synthesis), *lad* (arabitol synthesis) and *err1* (erythritol synthase), whereas for cultivation temperature these included *mtdB* and *mpdA* (mannitol synthesis and degradation). Thus, some of the genes involved in production of trehalose, erythritol, and mannitol are up-regulated in conidia that are more heat-resistant.

Hydrophilins have been linked to increased resistance of conidia against heat, desiccation and osmostic stress in *A. fischeri* (van Leeuwen et al., 2016). Absence of *con-6* and *con-10* promotes accumulation of the desiccation-related compatible solutes glycerol and erythritol in *Aspergillus nidulans* conidia (Suzuki et al., 2013). Interestingly, we observe a similar effect; decreased glycerol and erythritol concentrations correlate with increased *con-6* and *con-10* expression levels.

Together, the unknown up-regulated genes, the hydrophilins, trehalose, arabitol and increased spore size may contribute to heat resistance of *P. roqueforti* conidia. The roles of hydrophilins, trehalose, arabitol as well as the products of the up-regulated genes still need to be assessed in more detail. Apart from the fundamental point of view, our results also have implications for industry. Industry should screen various conidiation conditions for their thermal inactivation protocols since optimal growth conditions might not result in the most stress-resistant spores.

Supplementary material

Figure S1. Correlation between $\log_{10}(D_{56}$-value) and erythritol, mannitol or total compatible solutes. https://bit.ly/3EfRUvp

Table S1. Fitted model parameters for linear and modified Weibull model of each replicate. https://bit.ly/3z5db7u

Table S2. Assembly and gene model statistics of *P. roqueforti* strain DTO377G3. https://bit.ly/2XcQxgD

Table S3. RPKM list of 9762 genes of *P. roqueforti* strain DTO377G3 that are expressed during at least one of the conditions. https://bit.ly/3A34fAJ

Table S4. RPKM list of the 85 genes of *P. roqueforti* strain DTO377G3 that were more than fourfold higher expressed in seven-day-old cultures cultivated at 30°C compared to seven-day-old cultures cultivated at 15°C. https://bit.ly/390DYav

Table S5. RPKM list of the 274 genes of *P. roqueforti* strain DTO377G3 that were over fourfold higher expressed in three-day-old cultures cultivated at 25°C compared to ten-day-old cultures cultivated at 25°C. https://bit.ly/3lh6hXP

Table S6. Number of differentially expressed genes in spores of *P. roqueforti* strain DTO377G3 formed at different cultivation temperatures and cultivation times. https://bit.ly/2VBIgBU

Table S7. Best bidirectional hits were identified by BLAST for polyol- and stress-related genes used in the expression analysis of *P. roqueforti* strain DTO377G3. https://bit.ly/3lh0fXi

Table S8. RPKM expression levels of the 20 most highly expressed transcripts of *P. roqueforti* strain DTO377G3. https://bit.ly/3ld2Fpy

5

Inter-strain heterogeneity of *Penicillium roqueforti* conidia

Maarten Punt[1,2], Tom van den Brule[1,3], Sjoerd J. Seekles[1,4], Erna Jónsdóttir[5], Jos Houbraken[1,3], Arthur F.J. Ram[1,4], Han A.B. Wösten[1,2], Jan Dijksterhuis[1,3], Marcel H. Zwietering[1,5], Heidy M.W. den Besten[1,5]

[1]TiFN, P.O. Box 557, 6700 AN Wageningen, the Netherlands

[2]Utrecht University, Department of Biology, Microbiology, Padualaan 8, 3584 CH Utrecht, the Netherlands;

[3]Westerdijk Fungal Biodiversity Institute, Applied & Industrial Mycology, Uppsalalaan 8, 3584 CT Utrecht, the Netherlands;

[4]Department Molecular Microbiology and Biotechnology, Institute of Biology, Leiden University, Sylviusweg 72, 2333 BE Leiden, the Netherlands;

[5]Wageningen University, Food Microbiology, Bornse Weilanden 9, 6708 WG Wageningen, the Netherlands.

Abstract

Inter-strain variability of size, compatible solute content and heat resistance of conidia of 20 strains of the food-spoilage fungus *Penicillium roqueforti* was quantified. Mean spore diameter ranged from 3.47 μm to 4.22 μm. Arabitol and mannitol were the most abundant compatible solutes in the strains with concentrations ranging from 82 to 535 mM and 130 to 304 mM, respectively. Total compatible solute content varied between 413 and 919 mM. Differences in spore size or compatible solute content did not correlate with heat resistance of strains even though the latter also varied considerably with D_{56}-values ranging between 1.6 and 13.6 minutes. A meta-analysis demonstrated that heat resistance of conidia can even differ up to 2-log. Strain variability accounts for up to 43 % of the total variation in heat resistance that has been described in literature. Together, these results demonstrate that industry should take inter-strain heterogeneity in heat resistance into account when developing food processing strategies.

Introduction

Diversity of microbial species is key to adapt to environmental changes and to thrive in different niches. Intra-specific variability includes all variation within a species, including genotypic and phenotypic differences. Strain variability describes differences between two or more genetically different isolates that results in differences in phenotypic traits. Intra-specific variability also occurs within strains, i.e. in populations of cells that are genetically identical. This phenotypic heterogeneity has been widely studied in the past two decades (Ackermann, 2015). Genotypic variability is now also gaining more attention, especially in the fields of clinical and food microbiology (den Besten et al., 2018; Lianou et al., 2020; Lianou & Koutsoumanis, 2013; Sanchez & Martinez, 2019).

As microbial species are inherently variable, strains of the same species or cells of the same strain may differ in their response to environmental stress. Indeed, large differences in heat resistance can be found within species. Therefore, heat resistance is a pronounced trait to quantify intra-species variability. Besides strain variability (σ_s), biological variability (σ_b) and experimental variability (σ_e) are important sources of variability when traits are quantified. Here, σ_e is defined as differences between technical replicates of the same culture, while σ_b is defined as the variation between biologically independent cultures of the same strain.

These levels of variability have been quantified for multiple bacterial species (Aryani et al., 2015, 2016; den Besten et al., 2017; den Besten et al., 2018; Wells-Bennik et al., 2019). Notably, each time σ_s is the largest source of variability, followed by σ_b and σ_e and values of each level of variability has the same order of magnitude among the different species.

Spores are an integral part of the fungal life cycle to overcome periods of unfavourable environmental conditions and for dispersion by air, wind or other vectors. Stress resistance of fungal spores varies strongly. It ranges from spores that display stress resistance similar to that of vegetative cells to that of the most stress-resistant cells in nature like that of bacterial spores (Beuchat, 1986; van Leeuwen et al., 2010; Wyatt et al., 2013). Asexual fungal spores called conidia are resistant to various environmental stresses including UV radiation, desiccation, and cold and heat stress (Wyatt et al., 2013). Conidial resistance has been associated with presence of compatible solutes. For instance, *Aspergillus fumigatus* conidia that are produced at elevated temperatures contain more mannitol and trehalose and are less sensitive to heat stress (Hagiwara et al., 2017). Similar observations have been reported for other *Aspergilli* (Fillinger et al., 2001; Ruijter et al., 2003; Wolschek & Kubicek, 1997), while arabitol and trehalose correlate with heat resistance of *P. roqueforti* conidia (Chapter 3). Spore shape and size have also been implicated in heat resistance of conidia. Various strains of *Paecilomyces variotii* produce distinct spore populations that differ both in size and shape and that positively correlate to increased heat resistance of its conidia (van den Brule et al., 2020a, 2020b).

In this study, heterogeneity in size, compatible solute content and heat resistance of conidia was assessed of 20 strains of the food spoilage fungus *P. roqueforti*. Conidial diameter ranged between 3.47 - 4.22 µm, while arabitol and mannitol were the most abundant compatible solutes with concentrations ranging from 82 to 535 mM and 130 to 304 mM, respectively. D_{56}-values that ranged between 1.6 and 13.6 minutes did not correlate with size or compatible solute content and was shown to be mainly explained by strain variability encompassing up to 43 % of the total variability.

Table 1. *Penicillium roqueforti* strains used in this study

Strain No.	Other collections	Substrate	Location	Genbank accession number[A]	Reference
DTO003H1	CBS 147308	Environment dairy factory	the Netherlands	MW148162	
DTO012A2	CBS 147309	Tortilla (flour)	California, USA	MW148163	
DTO012A6	CBS 147310	Tortilla (corn)	California, USA	MW148164	
DTO013F5	CBS 147311	Margarine	the Netherlands	MW148165	
DTO070G2	CBS 147317	Wood	Unknown	MW148166	
DTO081F9	CBS 147318	Air in cheese warehouse	the Netherlands	MW148167	
DTO101D6	CBS 147325	Cheese surface	the Netherlands	MW148168	
DTO102I9	CBS 147326	Drink	the Netherlands	MW148169	
DTO126G2	CBS 147330	Air in bakery	USA	MW148170	
DTO127F7	CBS 147331	Chicory root extract	the Netherlands	MW148171	
DTO127F9	CBS 147332	Chicory root extract	the Netherlands	MW148172	
DTO130C1	CBS 147333	Air of cheese factory	the Netherlands	MW148173	
DTO163C3	CBS 147337	Single ascospore isolate of DTO006G1 and DTO027I6	the Netherlands	MW148174	
DTO163F5	CBS 147338	Cheese, Garstang Blue	UK	MW148175	
DTO163G4	CBS 147339	Barley	Denmark	MW148176	
DTO265D5	CBS 147372	Edge of brine bath	the Netherlands	MW148177	
DTO369A1	CBS 147354	From mayonnaise, containing K-sorbate	the Netherlands	MW148178	
DTO375B1	CBS 147355	Cheese	Mexico	MW148179	
DTO377G2	LCP 96.3914	Stewed fruit	France	MW148180	Ropars *et al.* (2012)
DTO377G3	LCP 97.4111	Wood	France	MW148181	Ropars *et al.* (2012)

[A]Genbank accession numbers of partial *benA* gene sequences.

Material and Methods

Strain selection and identification

P. roqueforti strains were obtained from the CBS-KNAW culture collection and the working collection of the Applied and Industrial Mycology (DTO) group of the Westerdijk Fungal Biodiversity Institute (Table 1). Strains included the previously studied strain DTO377G3 (LCP 97 4111, Chapter 3), while the other 19 strains used in this study had been taken randomly from a set of 176 strains. Identity of strains was confirmed by sequencing part of the β-tubulin gene *benA* of *P. roqueforti* as described (Samson et al., 2009; Varga et al., 2011; Visagie et al., 2014). After alignment using MUSCLE, a maximum likelihood tree of each species was computed with 1000 bootstrap replications using MEGA (Kumar et al., 2016). Reference sequences of closely related species and the type strain were included in the phylograms (Houbraken et al., 2020). The Jukes-Cantor model was used during tree building as it was the model with the lowest Bayesian Information Criterion score.

Growth conditions and harvesting conidia

Growth conditions and harvesting of conidia were done as described (van den Brule et al., 2020b). In short, fungal strains that had been stored in 30 % glycerol at -20 °C were spot-inoculated on malt extract agar (MEA, Oxoid, Hampshire, UK) and incubated for seven days at 25 °C. Freshly harvested spores were used to spread-inoculate a new MEA plate. After seven days of growth at 25 °C, conidia were harvested with ACES buffer (10 mM N(2-acetamido)-2-aminoethanesulfonic acid, 0.02 % Tween 80, pH 6.8) and filtered using glass wool. Subsequently, the conidia were washed two times in ACES buffer and diluted to $2 \cdot 10^8$ conidia mL^{-1} after counting the spores with a Bürker-Türk heamocytometer (VWR, Amsterdam, The Netherlands).

Spore size distributions

Spore size distributions were essentially determined as described (van den Brule et al., 2020a). To this end, conidial suspensions (see above) were diluted to $1 \cdot 10^5$ mL^{-1} in ISOTON II solution (Beckman Coulter) and 100 μL was measured using a Coulter counter Multisizer3 (Beckman, Fichtenhain, Germany) equipped with a 70 μm aperture tube with a measuring range of 1.4 - 42 μm. At least 10^3 data points were used to determine conidia diameter and upper and lower quantiles.

Compatible solute concentration assessment

Fresh conidia suspensions were diluted to 10^8 conidia and spun down for 1 min at 4 °C and 21.000 g. After discarding the supernatant, the pellet was flash-frozen in liquid nitrogen. Conidia were subsequently crushed with stainless steel beads in pre-cooled adapters (-80 °C) using a Tissuelyzer (2 min, 25 Hz) (QIAGEN, Hilden, Germany). After adding 1 mL Milli-Q and heating for 30 min at 95 °C, samples were centrifuged at 4 °C for 30 min at 20.000 g and filtered using an Acrodisc nylon syringe filter (0.2 µm, Pall Life Science, Mijdrecht, The Netherlands). Compatible solutes were determined with HPLC as described (van den Brule et al., 2020a). In short, 20 µL samples were injected in a mobile phase consisting of 0.1 mMol Ca EDTA in ultrapure water and followed for 30 min. The mean volume of the conidia measured by the Coulter Counter (see above) was used to calculate the concentration of compatible solutes (± standard deviation).

Quantification of heat resistance

200 µL spore suspension was added to pre-heated 19.8 mL ACES buffer in 100 mL Erlenmeyer flasks in a water bath. Conidia were treated at 56 °C using biological triplicates and technical duplicates. After 2, 5, 7.5, 10, 15, 20, 30 and 45 min, 1 mL samples were taken and 100 µL 10-fold diluted sample was surface-inoculated on a MEA plate and incubated at 25 °C. Non-heated spore suspension was used to determine the viable number of spores at t=0 min. The colony forming units (CFU) were determined after seven days. The logCFU mL^{-1} was calculated for each sampling time point. The re-parameterized Weibull model (Eq. 1) (Metselaar et al., 2013) was fitted to each heat inactivation curve with the R package Growthrates using the Levenberg-Marquardt algorithm (Hall et al., 2014). The Weibull model (Eq. 1) allows fitting linear, concave, and convex inactivation curves and was able to fit the different thermal inactivation curves of the strains.

$$Log_{10}(N_t) = Log_{10}(N_0) - \Delta \cdot \left(\frac{t}{t_{\Delta D}}\right)^{\beta} \tag{1}$$

where N_0 is the initial concentration of conidia (CFU mL^{-1}), N_t is the number of surviving conidia (CFU mL^{-1}) at time point t, Δ is the number of decimal reductions, $t_{\Delta D}$ represents the time needed to reduce the initial number of conidia with Δ decimals and β the shape parameter where $\beta > 1$ is concave and $\beta < 1$ is convex. Due to differences between strains in thermal reduction during the observed measuring time, Δ was set independently for each

experiment with a range between two and five. If β was significantly different from 1, the average *D*-value was estimated as $\frac{t_{\Delta D}}{\Delta}$. If not, the negative reciprocal of the linear regression slope, $\frac{-1}{slope}$, was used to estimate the *D*-value as described before (van den Brule et al., 2020a).

Quantification of variability

Experimental, biological and strain variability was quantified using the Aryani method (Aryani et al., 2015). Experimental variability (σ_e) was expressed by the root mean square error (RMSE, $\sqrt{MSE}$) of Eq. 2

$$MSE = \frac{RSS}{DF} = \frac{\sum_{S=1}^{N}\sum_{B=1}^{3}\sum_{E=1}^{2}(X_{EBS}-X_{BS})^2}{n-p} \tag{2}$$

where MSE represents the mean square error, RSS the Residual Sum of Squares and DF the Degrees of Freedom. represents the log$_{10}$*D*-value of each experiment with *E* indicating the experimental replicates of biological replicate *B* of strain *S*. X_{BS} is the average of the log$_{10}$*D*-value of the experimental duplicates (of each biological replicate *B* of strain *S*), *N* is the number of strains used (20) and DF is the number of data points ($n = 2 * 3 * N$) minus the number of parameters ($p = 3 * N$).

Biological variability (σ_b) was expressed by $\sqrt{MSE}$ of Eq. 3

$$MSE = \frac{RSS}{DF} = \frac{\sum_{S=1}^{N}\sum_{B=1}^{3}(X_{BS}-X_S)^2}{n-p} \tag{3}$$

where X_S is the average of X_{BS} from the biological triplicates of strain *S* and DF is the number of data points ($n = 3 * N$) minus the number of parameters ($p = 1 * N$).

Strain variability (σ_s) was expressed by $\sqrt{MSE}$ of Eq. 4

$$MSE = \frac{RSS}{DF} = \frac{\sum_{S=1}^{N}(X_S-X)^2}{n-p} \tag{4}$$

where *X* is the average of X_S of all *N* strains and DF is the number of data points ($n = N$) minus the number of parameters ($p = 1$).

The 95 % confidence intervals of σ_e, σ_b and σ_s were calculated according to Eq. 5

$$\sqrt{\frac{RSS}{\chi^2_{DF; \alpha/2}}} \leq \sigma \leq \sqrt{\frac{RSS}{\chi^2_{DF; 1-\alpha/2}}} \tag{5}$$

where χ^2 is the critical Chi-square value at $\alpha/2$ and $1 - \alpha/2$ with $\alpha = 0.05$, using the same RSS and DF definitions as in Eq. 2-4.

Meta-analysis

Data of inactivation kinetics of *P. roqueforti* conidia were collected from the literature. The obtained *D*-values were $\log_{10}$ transformed and the mean $\log_{10}D$-value of each strain presented in this study was added to the data resulting in a total of 148 data points. After applying a linear regression on the $\log_{10}D$-values versus the temperature, the *Z*-value was determined by the negative reciprocal of the slope, $\frac{-1}{slope}$. Subsequently, a 95 % prediction interval of the linear regression was calculated using Eq. 6.

$$Log_{10}D_{ref} \pm t_{DF;\, 1-0.5\alpha}\sqrt{\frac{RSS}{DF}} \qquad (6)$$

Where D is the reference $\log_{10}D$-value of the *Z*-value regression at a given temperature, t is Student t-value with DF degrees of freedom $n - 2$ and $\alpha = 0.05$, RSS is the residual sum of squares calculated from the deviation of the data to the linear regression line. The total variability (σ_t) found in the meta-analysis, was defined as the last product of Eq. 6.

Results

Verification of strain identity

Strain identity was verified by sequencing the partial coding sequence of *benA.* All 20 strains grouped with type strain CBS 221.30 and segregated from the closely related *Penicillium mediterraneum* (Fig. 1), demonstrating they belong to *P. roqueforti*.
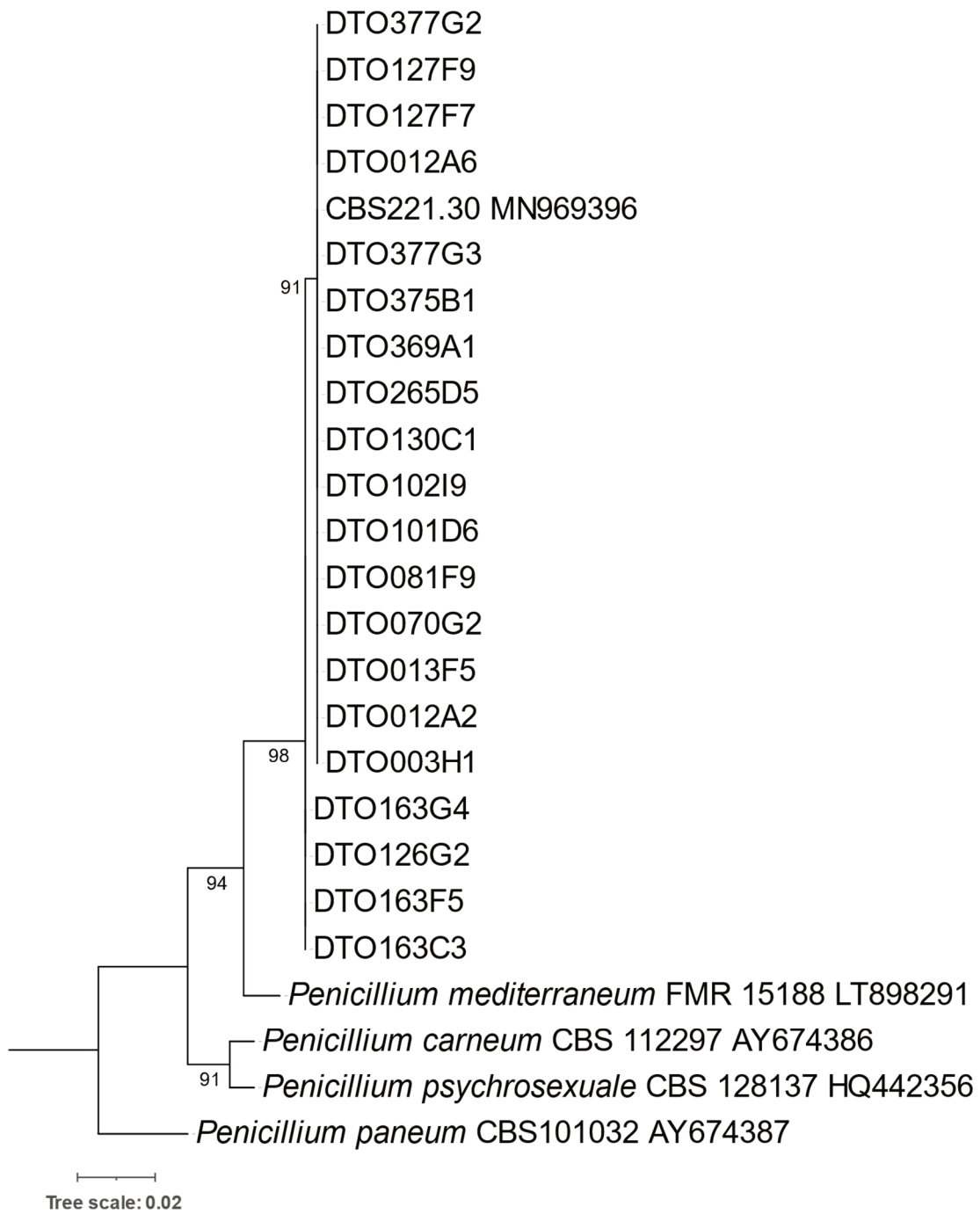
Figure 1. Phylogram of partial *benA* sequences *of P. roqueforti* strains, including type strain CBS 221.30 and other closely related *Penicillium* species with *Penicillium paneum* as outgroup.
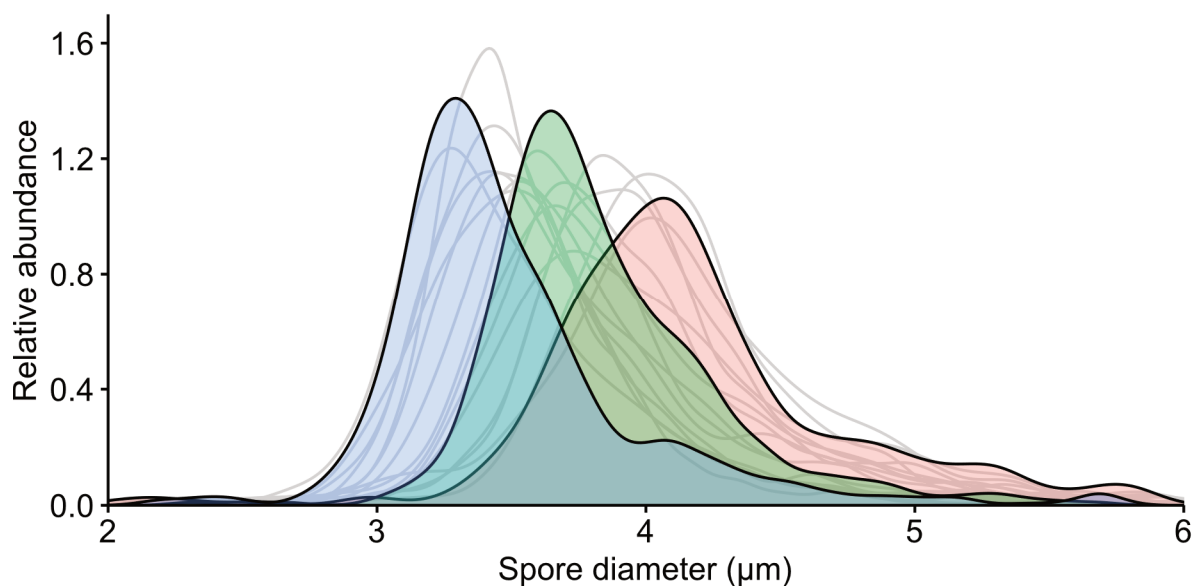
Figure 2. Spore diameter distribution of 18 *P. roqueforti* strains as measured by Coulter Counter. Distributions of DTO127F9, DTO126G2 and DTO013F5 are highlighted in blue, green and red, respectively.

Size and compatible solute concentration of Penicillium roqueforti conidia

Conidia diameter of 18 *P. roqueforti* strains was measured with the Coulter Counter (Table 2). Two strains were not analysed because of the limited spore yield. Figure 2 depicts the relative abundance of conidia diameter for each strain and shows that for most strains conidia diameter is slightly left skewed. Strains DTO127F9, DTO126G2 and DTO013F5 are highlighted as they produce conidia with a relatively small (3.47 [3.21 - 3.64]), average (3.83 [3.57 - 4.03]) and large (4.22 [3.84 - 4.42]) diameter, respectively. Next, the concentration of the compatible solutes arabitol, erythritol, glycerol, mannitol and trehalose were determined in the conidia of the 18 strains (Figure 3; Table 2). Arabitol and mannitol were the most abundant in all strains with concentrations ranging from 82 to 535 mM and 130 to 304 mM, respectively. Erythritol concentration ranged from 3 to 37 mM, glycerol from 6 to 67 mM, trehalose from 35 to 120 mM. The total amount of compatible solute concentration ranged from 413 to 919 mM within the 18 strains.

Table 2. Conidia diameter and compatible solute content of 18 *P. roqueforti strains.* The average spore diameter is indicated (in μm), including upper and lower quantiles, for the compatible solute the values are in mM ± standard deviation.

| Strain No.	Spore diameter	Arabitol	Erythritol	Glycerol	Mannitol	Trehalose	Total amount
DTO003H1	4.01 [3.72; 4.23]	409 ± 135	41 ± 32	16 ± 25	248 ± 73	58 ± 25	786 ± 309
DTO012A2	3.6 [3.32; 3.76]	179 ± 40	21 ± 5	20 ± 19	269 ± 31	72 ± 16	561 ± 94
DTO012A6	4.07 [3.65; 4.35]	136 ± 20	26 ± 4	41 ± 11	304 ± 60	73 ± 6	589 ± 110
DTO013F5	4.22 [3.84; 4.42]	251 ± 37	11 ± 2	9 ± 4	107 ± 16	32 ± 6	413 ± 64
DTO070G2	3.79 [3.45; 4.01]	396 ± 8	16 ± 2	11 ± 20	170 ± 22	49 ± 2	650 ± 37
DTO081F9	3.94 [3.57; 4.19]	232 ± 4	8 ± 7	11 ± 12	132 ± 9	31 ± 3	414 ± 30
DTO101D6	3.99 [3.72; 4.18]	312 ± 37	18 ± 6	9 ± 8	157 ± 9	39 ± 6	539 ± 43
DTO102I9	3.53 [3.32; 3.69]	399 ± 25	39 ± 5	22 ± 5	168 ± 6	48 ± 5	675 ± 35
DTO126G2	3.83 [3.57; 4.03]	313 ± 21	29 ± 5	16 ± 1	130 ± 4	38 ± 2	525 ± 32
DTO127F7	3.54 [3.22; 3.74]	369 ± 81	28 ± 3	32 ± 20	172 ± 24	77 ± 17	684 ± 132
DTO127F9	3.47 [3.21; 3.64]	535 ± 39	31 ± 9	11 ± 13	208 ± 1	103 ± 9	919 ± 85
DTO130C1	-	-	-	-	-	-	
DTO163C3	-	-	-	-	-	-	
DTO163F5	4.14 [3.85; 4.33]	82 ± 7	23 ± 4	34 ± 4	298 ± 21	58 ± 5	496 ± 22
DTO163G4	4.14 [3.83; 4.43]	247 ± 11	3 ± 5	21 ± 9	135 ± 24	31 ± 1	437 ± 39
DTO265D5	3.57 [3.29; 3.78]	337 ± 92	18 ± 7	5 ± 9	177 ± 50	46 ± 2	607 ± 182
DTO369A1	3.84 [3.53; 4.01]	203 ± 31	14 ± 3	31 ± 8	142 ± 27	43 ± 3	432 ± 71
DTO375B1	3.91 [3.59; 4.11]	356 ± 53	21 ± 5	18 ± 2	135 ± 23	52 ± 5	582 ± 76
DTO377G2	3.63 [3.31; 3.85]	94 ± 21	15 ± 2	58 ± 40	201 ± 12	49 ± 2	428 ± 44
DTO377G3	3.71 [3.39; 3.95]	351 ± 25	17 ± 5	27 ± 3	171 ± 1	52 ± 8	618 ± 27
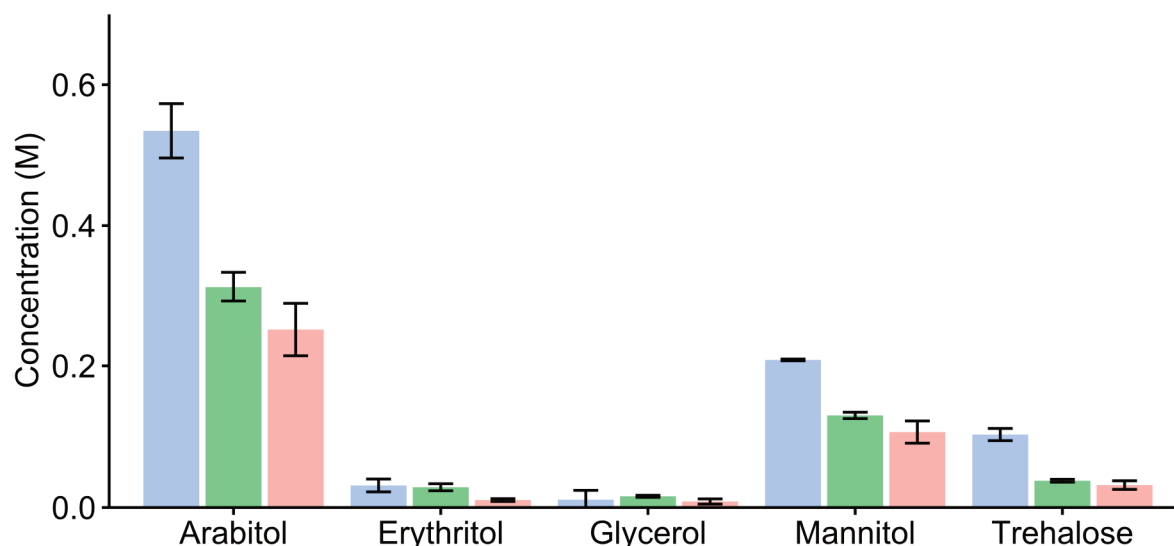
Figure 3. Arabitol, erythritol, glycerol, mannitol, trehalose, and total compatible solute concentration of conidia of DTO127F9 (blue), DTO126G2 (green), DTO013F5 (red) are depicted (M ± standard deviation). Each bar graph represents biological triplicates.

Quantification and variability of heat resistance

Conidia of the 20 *Penicillium roqueforti* strains were heat treated. Differences between the technical duplicates were rather small (Figure 4A) compared to those between the biological triplicates (Figure 4B). Variety in both technical and biological differences were lower than the differences between strains (Figure 4C). Most inactivation kinetics could be described without tailing or a shoulder, and, therefore, a linear model was used to calculate the *D*-value (Table S1).
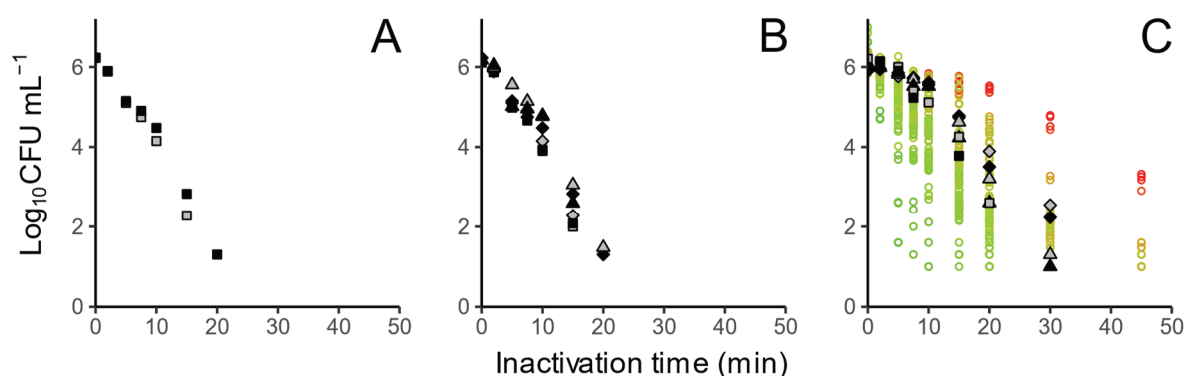
Figure 4. Experimental variability (A), biological variability (B) and strain variability (C) is depicted by the logCFU counts of each experiment. *P. roqueforti* DTO126G2 is highlighted showing three biological replicates (□, ◇ and △) and two experimental replicates (dark fill, light fill). All other strains (○; C) are coloured using a gradient from green (heat-sensitive) to red (heat-resistant) based on the mean *D*-values presented in Table S1.

The most heat-resistant *P. roqueforti* strain was DTO013F5, while the most heat-sensitive strain was DTO130C1 with D_{56}-values of 13.6 ± 3.01 and 1.6 ± 0.38 min, respectively. To illustrate this difference, an eight-fold difference in *D*-value means that the same heat treatment leads to one out of ten survivors in the resistant strain and one out of 10^8 cells in the heat-sensitive strain. Experimental, biological and strain variability of *P. roqueforti* were compared using the standard deviation of $\log_{10}D$-values, quantitatively expressed in RMSE (Figure 5). Experimental variability had the lowest variability, followed by the biological and strain variability with values of 0.044, 0.096 and 0.179 for σ_e, σ_b and σ_s, respectively.
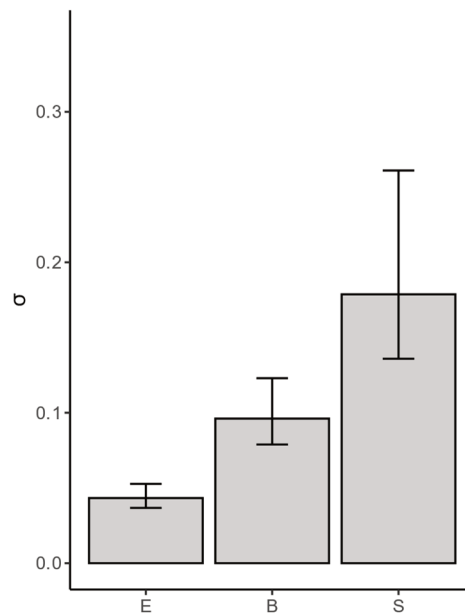
Figure 5. Experimental (E), biological (B) and strain (S) variability of *P. roqueforti*. Error bars represent the 95 % confidence interval of the RMSE values.

Correlation of heat resistance, size and compatible solute content of conidia

Pearson correlations were made to assess whether heat resistance correlated with spore diameter, and / or arabitol, erythritol, glycerol, mannitol, trehalose or total compatible solute concentration (Figure 6). A negative correlation was found between spore size and trehalose (-0.51) and arabitol concentration (-0.42) but no significant correlation was found between $\log_{10}D$-value and spore size or $\log_{10}D$-value and the concentration of any of the compatible solutes. Among the polyols, mannitol correlated significantly with glycerol (0.43), trehalose (0.61) and erythritol (0.43). Erythritol also correlated with trehalose (0.55) and arabitol (0.45), while a negative correlation was found between glycerol and arabitol (-0.61). Mannitol, unlike

the other polyols that were measured, did not correlate significantly with the total amount of compatible solutes.
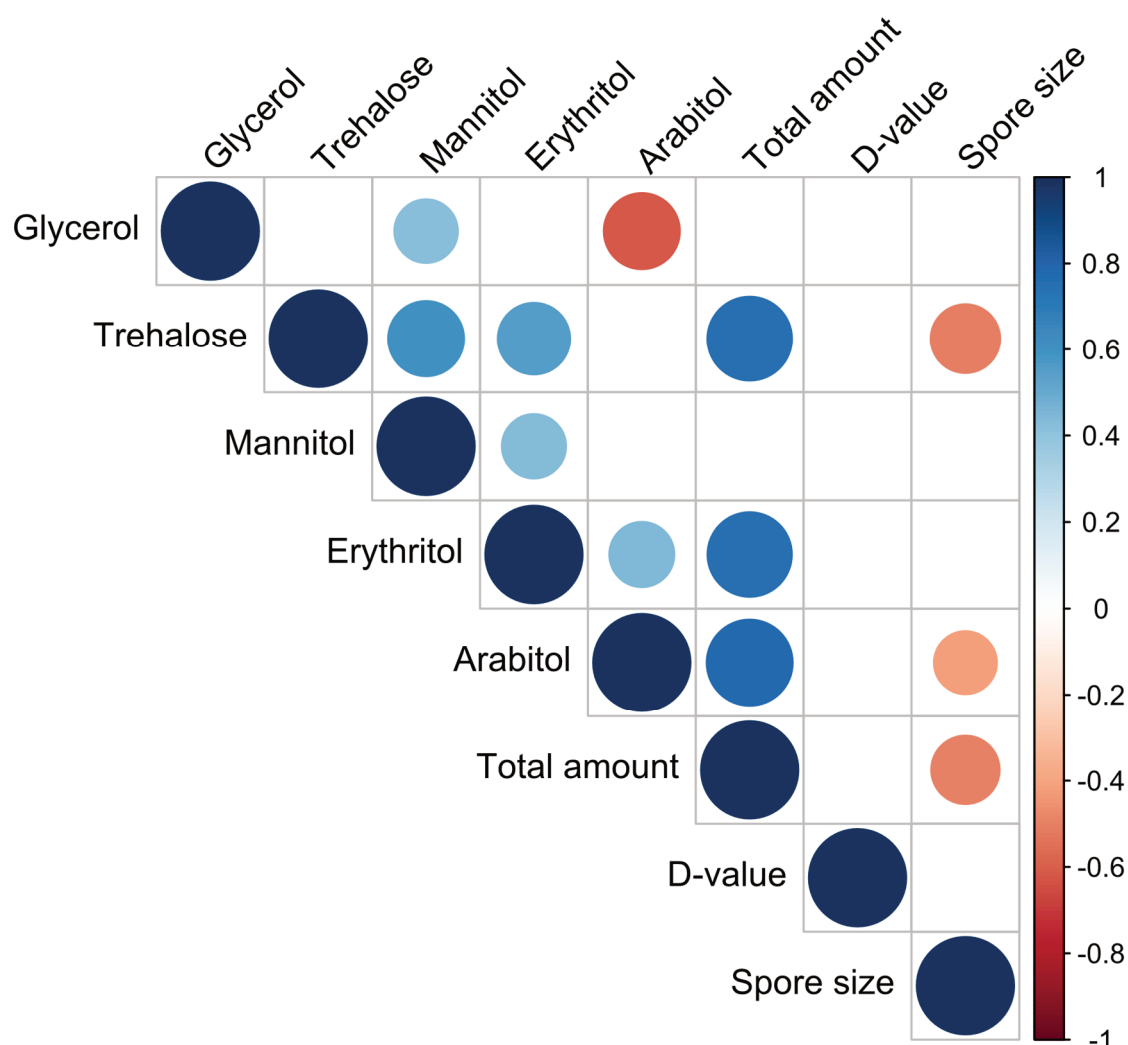

Figure 6. Correlation between concentration of compatible solutes (glycerol, trehalose, mannitol, erythritol, arabitol, and total compatible solutes) in conidia, average spore diameter and $\log_{10}D$-values of 18 *P. roqueforti* conidia are shown. A coloured gradient from red (negative correlation) to blue (positive correlation) is used. Insignificant correlations (p > 0.05) are not shown.

Meta-analysis

The conidial heat resistance of *P. roqueforti* strains presented in this study was compared with data from the literature (Figure 7). This allowed us to compare the strain variability σ_s with the total variability σ_t that for instance also includes environmental pre-culture conditions, heating menstrua, inactivation methods, lab equipment and personnel. Furthermore, data were used that resulted from different temperatures used for inactivation treatment. The latter gives the possibility to estimate the Z-values of *P. roqueforti* conidia, which expresses the temperature increase needed to cause a one $\log_{10}$ reduction in D-value. The deviation of

each data point to the linear regression between $\log_{10}D$-value and temperature was used to determine the total variability found in the meta-analysis. From literature, 128 data points on *P. roqueforti* heat resistance were collected (Blank et al., 1998; Bröker et al., 1987a, 1987b; Kunz, 1981; Punt et al., 2020; Shearer et al., 2002) (Table S2). For the linear regression, the mean $\log_{10}D$-values of each strain presented in this study were included in the analysis, resulting in 148 data points (Figure 5). Based on these data the Z-value of *P. roqueforti* conidia was estimated to be 7.8 °C and a total variability σ_t of this dataset was 0.415. Together with the experimentally determined $\log_{10}D$-values, the meta-analysis demonstrates that strain variability accounts for 43 % of the σ_t of *P. roqueforti* conidia.
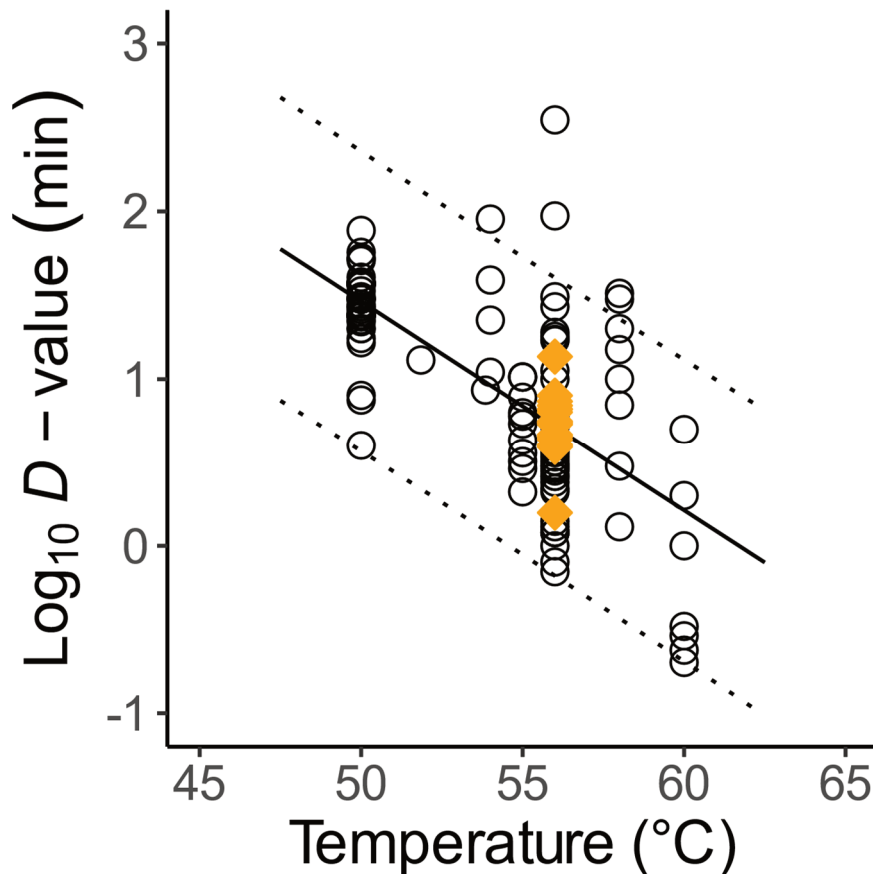
Figure 7. $\log_{10}D$-values from literature (○) and mean $\log_{10}D$-values per strain presented in this study (◇) were used in a meta-analysis to determine *Z*-values and total variability for *P. roqueforti*. The 95 % prediction intervals of the *Z*-value analysis are depicted as dashed lines. All data from literature is summarized in Table S2

Discussion

Here, heterogeneity in size, compatible solute content and heat resistance of conidia of 18-20 strains of *P. roqueforti* was studied. An 8.6-fold difference in $\log_{10}$ *D*-value between the most heat-resistant and heat-sensitive strain was found, which is similar to that found in other fungal and bacterial species (van den Brule et al., 2021). This is remarkable considering the different mechanisms that are involved in heat resistance. For instance, arabitol and the hydrophillins con-6 and con-10 have been implicated in heat resistance of *P. roqueforti* conidia (Punt et al., 2020), while conidia of *A. niger* contain large amounts of Hsp70 transcripts (van Leeuwen et al., 2013) and mannitol (Ruijter et al., 2003) . On the other hand, *Pae. variotii* conidia predominantly contain trehalose as compatible solute (van den Brule et al., 2020a) which could, at least in part, explain its remarkable high tolerance for heat stress compared to other fungal species.

The biological and strain variability are embedded within a total variability. For example, environmental conditions impact heat resistance. Growing cultures at higher temperature significantly enhance heat resistance of *A. fumigatus* (Hagiwara et al., 2017) and *P. roqueforti* (Punt et al., 2020) conidia. Similarly, conidia of the insect-pathogenic fungus *Metarhizium robertsii* formed at pH 8 are more heat-resistant than those formed at pH 4.6 (Rangel et al., 2015). The maturation of conidia also plays a role in the development of heat resistance as conidia from older colonies of *A. niger* and *P. roqueforti* show higher robustness to heat treatment (Punt et al., 2020; Teertstra et al., 2017).

Strain heterogeneity is also observed in spore size. For example, the spore diameter of a *P. roqueforti* strain can differ up to 12-25 % compared to standard cultivation temperatures under suboptimal growth conditions (Nguyen Van Long et al., 2017a; Punt et al., 2020). Interestingly, this intra-strain variability correlated with heat resistance (Chapter 3). Here, it was shown that average spore diameter varied between 3.47 µm to 4.22 µm between the 20 strains. Yet, neither spore size nor compatible solute content of the different strains correlated with heat resistance. In contrast, a correlation between heat resistance and conidia size was observed between strains of *Pae. variotii* (van den Brule et al., 2020b). Taken together, these data suggest that average spore size and compatible solute concentration are not the limiting factors contributing to the total heat resistance of *P. roqueforti* conidia.

It is well known that heat resistance of bacterial spores and vegetative cells differ enormously among species, and consequently the *D*-values of these cells are very different when determined at the same temperature. Interestingly, the intra-species variability of these cell types are in the same magnitude when the spore forming bacteria *Bacillus subtilis*, *Bacillus cereus*, *Geobacillus stearothermophilus* and the non-spore forming bacteria *Listeria monocytogenes* and *Lactobacillus plantarum* are compared (den Besten et al., 2018). The σ_s, σ_b and σ_e of heat resistance of these bacteria ranges from 0.2 to 0.4, 0.05 to 0.2 and 0.02 to 0.08, respectively. These values are similar for conidia of *P. roqueforti*, *A. niger* and *Pae. variotii.* The experimental variability for these fungi ranged from 0.033 to 0.045, the biological variability from 0.084 to 0.096, and the strain variability from 0.179 to 0. Future studies should address whether intra-species variability is also high for other stresses than heat stress and whether strain variability is also the main contributor in total variation in these cases.

Supplementary material

Table S1. D-values of experimental and biological replicates of all strains used in this study.

https://bit.ly/3nwrTCa

Table S2. Heat resistance data obtained from literature for *Penicillium roqueforti*.

https://bit.ly/3ljaR7S

6

High sorbic acid resistance of *Penicillium roqueforti* is mediated by the SORBUS gene cluster

Maarten Punt[1,2], Sjoerd J. Seekles[1,3], Jisca L. van Dam[3], Connor de Adelhart Toorop[2], Raithel R Martina[2], Jos Houbraken,[1,4], Heidy M. W. den Besten[1,5], Arthur F. J. Ram[1,3], Han A. B. Wösten[1,2], Robin A. Ohm[1,2]

[1]TiFN, P.O. Box 557, 6700 AN, Wageningen, The Netherlands;

[2]Microbiology, Department of Biology, Utrecht University, Padualaan 8, 3584 CH, Utrecht, The Netherlands;

[3]Department Molecular Microbiology and Biotechnology, Institute of Biology, Leiden University, Sylviusweg 72, 2333 BE Leiden, the Netherlands;

[4]Westerdijk Fungal Biodiversity Institute, Uppsalalaan 8, 3584 CT Utrecht, The Netherlands;

[5]Wageningen University, Food Microbiology, Bornse Weilanden 9, 6708 WG Wageningen, The Netherlands.

Abstract

Penicillium roqueforti is a major food-spoilage fungus known for its high resistance to the food preservative sorbic acid. Here, we demonstrate that the minimum inhibitory concentration of undissociated sorbic acid (MIC_u) ranges between 4.2 and 21.2 mM when 34 *P. roqueforti* strains were grown on malt extract broth. Six and 28 of these strains were resistant and sensitive to sorbic acid, respectively, which was also found when yoghurt was used as growth medium. A genome-wide association study revealed that the six resistant strains contained the 180 kb gene cluster SORBUS, which was absent in the sensitive strains. In addition, a SNP analysis revealed five genes outside the SORBUS cluster that may also be linked to sorbic acid resistance. A partial SORBUS knock-out in a resistant strain reduced their sorbic acid resistance to similar levels as observed in the sensitive strains. Whole genome transcriptome analysis revealed a small set of genes in a resistant and a sensitive *P. roqueforti* strain that were differentially expressed in the presence of the weak acid. These genes could explain why *P. roqueforti* is more resistant to sorbic acid when compared to other fungi, even in the absence of the SORBUS cluster. Together, the MIC_u of 21.2 mM makes *P. roqueforti* among the most sorbic acid-resistant fungi, if not the most resistant fungus. This resistance is mediated by the SORBUS gene cluster.

Introduction

Fungi are responsible for 5–10 % of all food spoilage (Pitt & Hocking, 2009) resulting in the production of off-flavors, discoloration and acidification (Filtenborg et al., 1996; Pitt & Hocking, 2009). Some species also produce mycotoxins, such as PR toxin and roquefortine C in the case of *Penicillium roqueforti* (Gillot et al., 2017). Toxins partially contribute to the high incidence of food-borne diseases affecting up to 30 % of the people in industrialized countries every year (Bondi et al., 2014).

Food spoilage by filamentous fungi is believed to be mainly caused by spores that are spread through the air, water or other vectors like insects (Dijksterhuis, 2019). Preservation techniques such as pasteurization, fermentation, cooling or the addition of preservatives are used to reduce spoilage (Kaczmarek et al., 2019). Some of the most applied preservatives are weak organic acids such as benzoic, propionic and sorbic acid. *Paecilomyces variotii, Penicillium paneum, Penicillium carneum* and *P. roqueforti* are among the few filamentous

fungi capable of spoiling products containing weak acids, and are therefore called preservative-resistant moulds (Rico-Munoz et al., 2019). Weak-acid preservatives inhibit microbial growth, but their mode-of-action is not completely understood. According to the classical 'weak-acid preservative theory' the antimicrobial activity of weak acids is derived from their undissociated form that can pass the plasma membrane. These weak acids dissociate in the cytosol due to its neutral pH, and inhibit growth through acidification of the cytoplasm (Stratford & Anslow, 1998). The inhibitory activity of sorbic acid at pH 6.5 and the correlation of sorbic acid resistance with ethanol tolerance in *Saccharomyces cerevisiae* suggest that this weak acid can also act as a membrane-active compound (Stratford & Anslow, 1998).

In *A. niger*, sorbic acid resistance is mediated by the phenylacrylic acid decarboxylase gene *padA*, and the putative 4-hydroxybenzoate decarboxylase gene, known as the cinnamic acid decarboxylase (*cdcA*) gene (Lubbers et al., 2019; Plumridge et al., 2010). These genes encode proteins that catalyze the conversion of sorbic acid into 1,3-pentadiene. Genes *padA* and *cdcA* are regulated by the sorbic acid decarboxylase regulator (SdrA), which is a Zn2Cys6-finger transcription factor (Plumridge et al., 2010). These three genes are present on the same genetic locus in *A. niger* with *sdrA* being flanked by *cdcA* and *padA*. Orthologs of *cdcA* and *padA* are also clustered in *S. cerevisiae*, but this is not the case for the *sdrA* homologue (Mukai et al., 2010; Plumridge et al., 2010). Inactivation of *cdcA, padA* or *sdrA* results in reduced growth of *A. niger* on sorbic acid and cinnamic acid (Lubbers et al., 2019). The fact that growth is not abolished and the fact that *padA* transcript levels are less affected than that of *cdcA* on sorbic acid upon deletion of *sdrA* suggests that an additional regulator is involved (Lubbers et al., 2019). For example, a weak-acid regulator A (warA), which has been recently identified in *A. niger* and is involved in sorbic acid resistance as well as a range of other weak acids such as propionic and benzoic acid (Geoghegan et al., 2020).

Weak-acid resistance in fungi is subject to intra- and inter-strain heterogeneity. Intra-strain heterogeneity has been observed in *Zygosaccharomyces bailii* with the existence of a small sub-population of cells that are more than two times more resistant (MIC = 7.6 mM) to sorbic acid than the sensitive population (MIC = 3 mM) (Stratford et al., 2013), while inter-strain resistance has been observed in *P. roqueforti* with the existence of sorbic acid-resistant and

sorbic acid-sensitive strains (Liewen & Marth, 1985). Genome analysis of *P. roqueforti* strains have yielded clues about adaptive divergence in this species. Genomic islands with high identity are present in distant *Penicillium* species, while they are absent in closely related species, supporting the hypothesis of recent horizontal gene transfer events (Ropars et al., 2014, 2015). For instance, the presence of two large genomic regions, *Wallaby* and *CheesyTer* correlates with faster growth and functions relevant in a cheese matrix, respectively (Cheeseman et al., 2014; Ropars et al., 2015). Noteworthy, the *CheesyTer* and *Wallaby* regions are only present in cheese isolates other than Roquefort, indicating that the Roquefort isolate population is potentially more closely related to the 'ancestral' *P. roqueforti* populations (Dumas et al., 2020).

In this study, sorbic resistance of 34 *P. roqueforti* strains was assessed, of which 28 strains were sensitive and six strains were resistant to this weak acid. A genome-wide association analysis revealed the presence of the 180 kb gene cluster SORBUS in the resistant strains. A partial SORBUS knockout in such a strain showed a reduced sorbic acid resistance similar to that of the sensitive *P. roqueforti* strains.

Methods

Strain and cultivation conditions

All fungal strains (Table S1; for their description see Chapters 3 and 4) were provided by the Westerdijk Fungal Biodiversity Institute. Conidia were harvested with a cotton swab after seven days of growth at 25 °C on malt extract agar (MEA, Oxoid, Hampshire, UK) and suspended in 10 mL ice-cold ACES buffer (10 mM N(2-acetamido)-2-aminoethanesulfonic acid, 0.02 % Tween 80, pH 6.8). The conidia suspension was passed through a syringe containing sterilized glass wool and washed twice with ACES buffer after centrifugation at 4 °C for 5 min at 2,500 *g*. The spore suspension was set to $2 \cdot 10^8$ spores mL^{-1} using a Bürker-Türk haemocytometer (VWR, Amsterdam, The Netherlands) and kept on ice until further use.

Weak acid growth assay

Conidia suspension (5 μL) was inoculated in the centre of MEA plates containing 5 mM potassium sorbate, benzoic acid, or sodium propionate (all from Sigma). Medium was set at pH 4.0 using HCl, which corresponds to undissociated concentrations of 4.26, 3.07 and 4.42

mM of these acids, respectively. The absence of preservative was used as a control. Cultures were photographed after 5 days and colony surface area was measured using a manual threshold in ImageJ.

Sorbic acid resistance

Conidial suspensions of 34 *P. roqueforti* strains were diluted to 10^7 spores mL^{-1} and mixed in a 1:99 ratio with MEB pH 4.0 with and without 25 mM potassium sorbate. 300 µL of the resulting mixture was added in a well of a 96 wells plate (Greiner Bio-One, Cellstar 650180, www.gbo.com). Serial dilutions were made by mixing 225 µL MEB with potassium sorbate and 75 µL MEB without potassium sorbate, resulting in wells with potassium sorbate concentrations of 25, 18.75, 14.06, 10.55, 7.91, 5.93, 4.45 and 0 mM. This corresponded to undissociated sorbic acid concentrations of 21.22, 15.92, 11.94, 8.95, 6.72, 5.04, 3.78 and 0 mM. The undissociated sorbic acid concentrations were determined using the Henderson-Hasselbach equation.

The 96-wells plates were sealed with parafilm and incubated for 28 days at 25 °C using biologically independent replicates. After 28 days, growth was assessed for each strain and the undissociated minimal inhibitory concentration (MIC$_u$) was determined per strain. The MIC$_u$ was defined as the lowest undissociated concentration in which no hyphal growth was observed. An one-way ANOVA followed by a Tukey's HSD test was used to test for significant differences in MIC$_u$ ($P < 0.05$).

Yoghurt challenge test

Sterilized 2 M potassium sorbate was mixed with 500 mL yoghurt (DuPont, Brabrand, Denmark) using a sterile kitchen mixer resulting in a final concentration of 3, 6, 9, 12, and 15 mM sorbic acid. As a control, both mixed and unmixed yoghurt without added potassium sorbate were included and the pH of the yoghurt mixtures was measured. The different sorbic acid concentrations altered the pH of the yoghurt from 4.27 to 4.32, 4.39, 4.44, 4.50 or 4.55, respectively. These concentrations correspond to 0, 2.18, 4.18, 6.02, 7.66 and 9.17 mM undissociated sorbic acid. Conidia suspension (10 µl, $2 \cdot 10^3$ spores / mL) was seeded on top of 4 mL yoghurt in 12-wells cell culture plates (Greiner Bio-One, Cellstar 665182, www.gbo.com) and incubated at 8 °C for 45 days and monitored daily for growth and conidia formation. In

total, three biologically independent replicates with each six technical replicates were used. Growth probability in a biological replicate was computed by dividing the number of wells showing growth by the total number of technical replicates (e.g. growth in 2 out 6 technical replicates is a probability of 0.33). A model to describe the probability of growth on yoghurt was used, where time, potassium sorbate concentration (undissociated) and *P. roqueforti* strain were the explanatory variables. *P. roqueforti* strain DTO377G3 grown on yoghurt without sorbic acid was used as control. The following logistic regression model was used to describe the data (Eq. 1).

$$ln\left(\frac{p}{1-p}\right) = b_0 + b_1 * strain + b_2 * conc + b_3 * time \qquad (1)$$

The parameters (i.e. $b_0, …, b3$) were estimated with strain, conc (undissociated concentration of potassium sorbate in mM) and time (in days) as the variables. The model was fitted in R and a stepwise procedure was employed removing insignificant ($p > 0.01$) parameters. The performance of the model was evaluated with the Nagelkerke R^2 and receiver operating curve (ROC-curve) c-value statistics (dos Santos et al., 2018).

DNA extraction, genome sequencing, assembly and annotation

DNA extraction was performed as described (Punt et al., 2020) and Illumina NextSeq500 150 bp paired-end technology was used for sequencing (Utrecht Sequencing Facility, useq.nl). The sequence reads were trimmed on both ends when quality was lower than 15 using bbduk from the BBMap tool suite (BBmap version 37.88; https://sourceforge.net/projects/bbmap/). The trimmed reads were assembled with SPAdes v3.11.1 applying kmer lengths of 21, 33, 55, 77, 99 and 127 and the –careful setting was used to reduce the number of indels and mismatches (Bankevich et al., 2012). Genes were predicted with Augustus version 3.0.3 (Stanke et al., 2006) using the parameter set that was previously generated for *P. roqueforti* (Punt et al., 2020). Functional annotation of the predicted genes was performed as described (de Bekker et al., 2017). Repetitive sequences in the assembly were masked using RepeatMaker (Smit, 2010), RepBase library (Bao et al., 2015) and RepeatScout (Price et al., 2005). The genomes, gene predictions and functional annotations can be accessed interactively at https://fungalgenomics.science.uu.nl.

Genomic phylogeny and analysis

Single-copy orthologous groups were identified and aligned using OrthoFinder v2.5.2 (Emms & Kelly, 2019). A maximum likelihood (ML) inference was performed using RAxML (Stamatakis, 2014) under the PROTGAMMAAUTO model. The number of bootstraps used was 200 (Average WRF = 0.43 %) and *Penicillium rubens* Wisconsin 54-1255 (van den Berg et al., 2008) was used to root the tree. The phylogenetic tree was visualized using iTOL v5 (Letunic & Bork, 2021).

Genome-wide association study

A genome-wide association study (GWAS) was performed based on the sorbic acid resistance screening and the whole-genome sequences. First, *P. roqueforti* strains were grouped into a resistant (R-type) or sensitive (S-type) group. DTO006G7 was selected from the R-group as reference for the analysis, because the assembly of this strain was the least fragmented in this group. Next, MUMmer (http://mummer.sourceforge.net/, version 4.0) was used to perform whole-genome alignment. Each genome was aligned to the reference and with the BEDtools package regions and genes unique for the R-type isolates were identified. The genome alignment was visualized with pyGenomeTracks (Lopez-Delisle et al., 2021). A gene was considered absent when 90 % or more of its sequence was not found in the genome of a strain. The best practices recommended by GATK (Genome Analysis Toolkit) were used to obtain single nucleotide polymorphisms (SNPs) for each strain. In short, the sequence reads were aligned to the reference genome (DTO006G7) using Bowtie2 (version 2.2.9) and PCR duplicates were removed with Picard tools (MarkDuplicates; version 2.9.2). For variant calling, the HaplotypeCaller (GATK, version 3.7) was used with the following parameters: -stand_call_conf 30, -ploidy 1 and -ERC. The single-sample variant files (GVCFs) were joined into a GenomicsDB before joint genotyping. The variants were annotated using SNPeff (version 4.3) based on their predicted biological effect, such as the introduction of an early stop-codon or a synonymous annotation. The number of SNPs and their putative impact ('low', 'moderate' or 'high', as defined by SNPeff) was listed for each gene per genome. The SNPs were then correlated to sorbic acid resistance using PLINK v1.9 (Purcell et al., 2007) with parameters '–maf 0.5 –allow-extra-chr'. The resulting association files were analysed and visualized using R.

RNA extraction and sequencing

A genome-wide transcriptome analysis was performed on the sorbic acid sensitive *P. roqueforti* strain DTO377G3 and the sorbic acid-resistant *P. roqueforti* strain DTO006G7. Erlenmeyer flasks containing 50 mL MEB (pH 4.0) were inoculated with 100 µl ACES containing 10^7 conidia and incubated for 48 h at 25 °C and 200 rpm. Mycelium was harvested using a sterilized miracloth filter and equally divided in Erlenmeyer flasks with 50 mL MEB (pH 4.0) or 50 mL MEB containing 3 mM potassium sorbate (pH 4.0). Growth was continued for another four hours, after which the mycelium was harvested using a sterilized Miracloth filter and frozen in liquid nitrogen. Total RNA was isolated with the RNeasy Plant Mini Kit (Qiagen) and purified by on-column DNase digestion according to the manufacturer's protocol. RNA was sequenced with Illumina NextSeq2000 2x50 bp paired-end technology (Utrecht Sequencing Facility; useq.nl). The transfer experiment and subsequent RNA-sequencing was performed in biological triplicates. The transcript lengths, counts per gene and read mapping were determined using Salmon v1.5.2 with --validateMappings (Patro et al., 2017). The transcript abundance of reads was quantified using custom constructed indices for DTO006G7 and DTO377G3.

DESeq2 (Love et al., 2014) was used for pairwise comparisons of the samples and the identification of differentially expressed genes. Genes with low read counts (<10) were excluded from the analysis and a gene was considered differentially expressed when the adjusted p-value was < 0.05. In addition, genes were considered up- or down-regulated when they had a $\log_2$ fold change of > 2 or < -2, respectively. A Fisher Exact test as implemented in PyRanges (Stovner & Sætrom, 2020) was employed to identify over- and under-representation of functional annotation terms in sets of genes. To correct for multiple testing the False Discovery Rate method was used, with a P-value < 0.05 as cut off.

Plasmid construction and generation knockout strain

To facilitate genome-editing, a *ku70* deficient DTO0013F2 strain was constructed as described (Seekles et al., 2021). CRISPR/Cas9 technology was employed to remove a 93 kb region (from 84 to 177 kb) of the SORBUS cluster in DTO013F2 Δ*ku70*. Two single-guide RNAs (sgRNAs) were designed to perform a simultaneous double restriction in the 93 kb SORBUS region. Transformation procedures were performed as described, with some modifications (van

Leeuwe et al., 2019). In short, plasmid pFC332 (Nødvig et al., 2015) was used as a vector to express the sgRNA, *cas9* and a hygromycin selection marker (for primer sequences used in this study see Table S2). The 5' and 3' flanking regions of sgRNA were amplified using plasmids pTLL108.1 and pTLL109.2 as template (van Leeuwe et al., 2019). The amplified products were fused and introduced into pFC332 using Gibson assembly (NEBuilder HiFi DNA Assembly Master Mix, New England Biolabs, MA, USA). The vectors containing the sgRNA were then transformed into competent *Escherichia coli* TOP10 cells for multiplication overnight. Plasmids were recovered using Quick Plasmid Miniprep Kit (ThermoFisher, Waltham, MA, USA) and digested using SacII to verify the presence of the sgRNA. In addition, the correct integration of the sgRNA was confirmed with sequencing. To construct donor DNA, two 1 kb homologous regions located at scaffold 43 at nucleotide position 83573 to 84629 and 177760 to 178854 were amplified and fused using a unique 23 nucleotide sequence GGAGTGGTACCAATATAAGCCGG with a PAM site for further genetic engineering.

Transformation was performed as described with adjustments (Arentshorst et al., 2012). In short, *P. roqueforti* conidia were incubated 48 h at 25 °C in 100 mL potato dextrose broth at 200 rpm. The mycelium was washed in SMC and incubated for 4 h at 37 °C in lysing enzymes from *Trichoderma harzianum* (Sigma) dissolved in SMC. Protoplasts were resuspended in 1 mL STC and kept on ice after centrifuging for 5 min at 3000 g. To 100 µL of protoplasts, 2 µg donor DNA, 2 µg of each pFC332 vector containing sgRNA and 1.025 mL of freshly made PEG solution was added (see Table S3 for the vectors used in this study). After 5 min, STC was added and the protoplasts were mixed with 20 mL liquid MMS containing 0.3 % agar and 200 µg hygromycin mL^{-1} (InvivoGen, San Diego, CA, USA). The mixture was poured on MMS containing 0.6 % agar and 200 µg hygromycin mL^{-1}. Transformants were grown for 7-10 days at 25 °C and then single streaked on MM containing 100 µg mL^{-1} hygromycin until sporulating colonies appeared. Next, the plasmid was removed by a single streak on MM plates without antibiotic. Finally, transformants were single streaked on MM, MM containing 100 µg hygromycin mL^{-1} and MEA plates to confirm that transformants lost the plasmids.

Results

Weak-acid screening

Weak-acid sensitivity of 34 *P. roqueforti* wild-type strains was assessed on MEA plates supplemented with 5 mM propionic, sorbic or benzoic acid, which corresponds to 4.42, 4.25 and 3.07 mM undissociated acid, respectively. Three strains had been isolated from blue-veined cheeses such as Roquefort and the other 31 strains had been isolated from non-cheese environments (mostly related to spoiled food) (Table S1). The colony surface area was determined after five days of growth (Figure 1). The inhibitory effect of propionic acid at the tested concentration was limited for most strains, since 26 out of 34 strains grew to > 80 % of the colony surface area reached under control conditions. Strains DTO012A1 and DTO012A8 even showed an increased colony size (up to 120 %) when compared to the control. The inhibitory effects of sorbic and benzoic acid were more pronounced. MEA supplemented with potassium sorbate reduced colony area for all 34 *P. roqueforti* strains. The surface area under sorbic acid stress ranged from 0 to 80 % of the surface area reached under control conditions. Strains DTO006G1, DTO006G7, DTO013E5 and DTO013F2 showed the highest sorbic acid resistance, followed by DTO046C5. Benzoic acid was the most inhibitory compound, resulting in a maximum colony surface area between 0 and 20 % of the control. The most benzoic acid-resistant strains were DTO013F2 and DTO013E5. As these strains were also among the most sorbic acid-resistant strains, similar resistance mechanisms may be involved to cope with benzoic and sorbic acid stress.
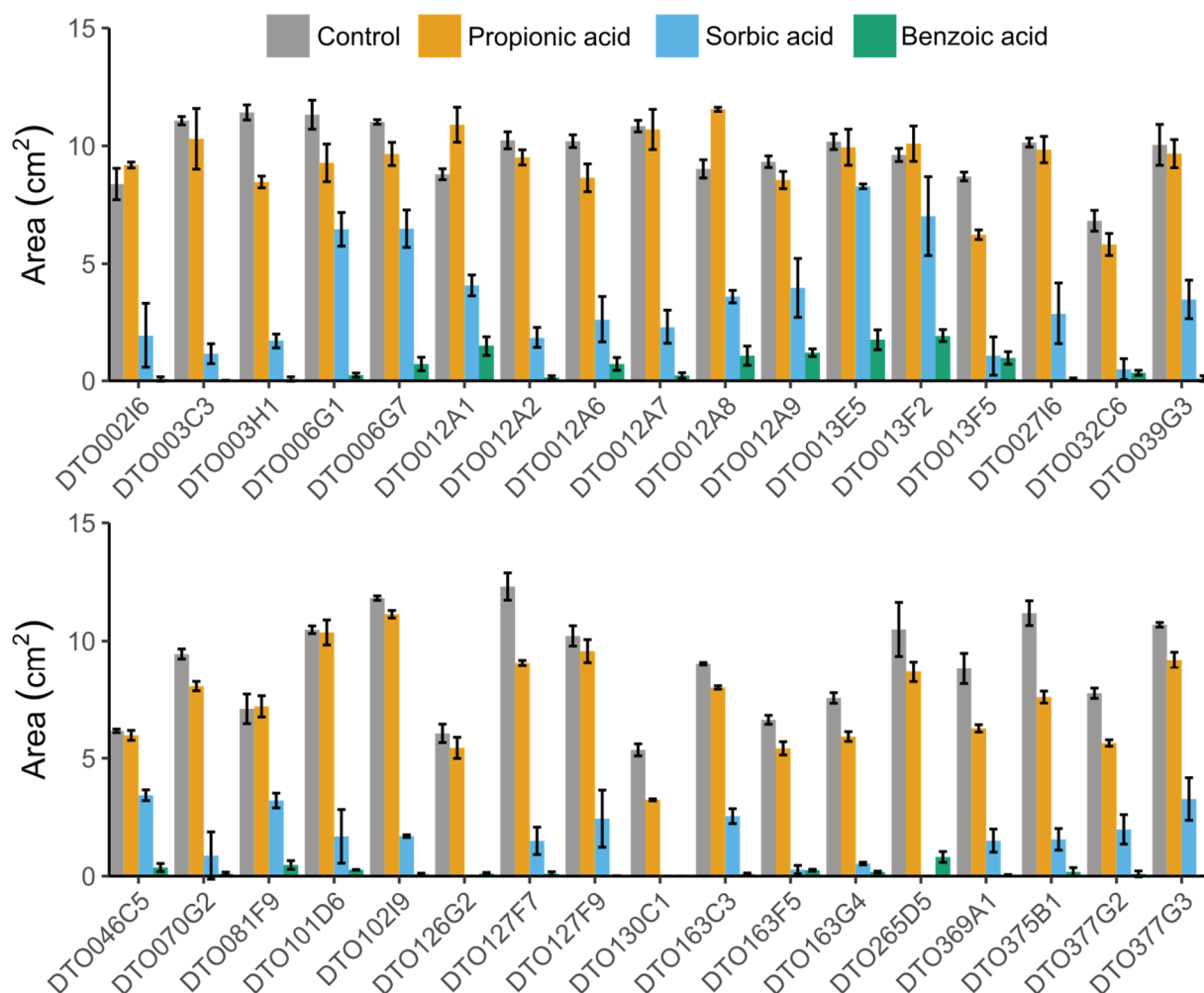
Figure 1. Average colony size (cm^2) of 34 *P. roqueforti* strains after five days of growth on MEA (pH 4.0) (grey) or MEA (pH 4.0 supplemented with 5 mM propionic acid (orange), sorbic acid (blue) or benzoic acid (green)). Strains DTO006G1, DTO006G7, DTO013E5 and DTO013F2 are relatively resistant to sorbic acid. Error bars indicate standard deviation of biologically independent replicates.

Sorbic acid resistance was further analyzed and MIC$_u$ values of sorbic acid were determined for the 34 *P. roqueforti* strains. The four strains with the highest sorbic acid resistance on MEA (Figure 1), were also among the strains (DTO006G1, DTO006G7, DTO012A1, DTO012A8, DTO013E5 and DTO013F2) which showed the highest MIC$_u$ (Figure 2). DTO013E5 and DTO013F2 were the most resistant to potassium sorbate even showing growth at the highest tested undissociated sorbate concentration of 21.2 mM, indicating a MIC$_u$ > 21.2 mM. The other strains showed a distinctly lower MIC$_u$, ranging between 4.2 mM and 9.95 mM. Only strain DTO012A9 showed an intermediate resistance to sorbic acid with an average MIC$_u$ of 13.72 mM undissociated sorbic acid.
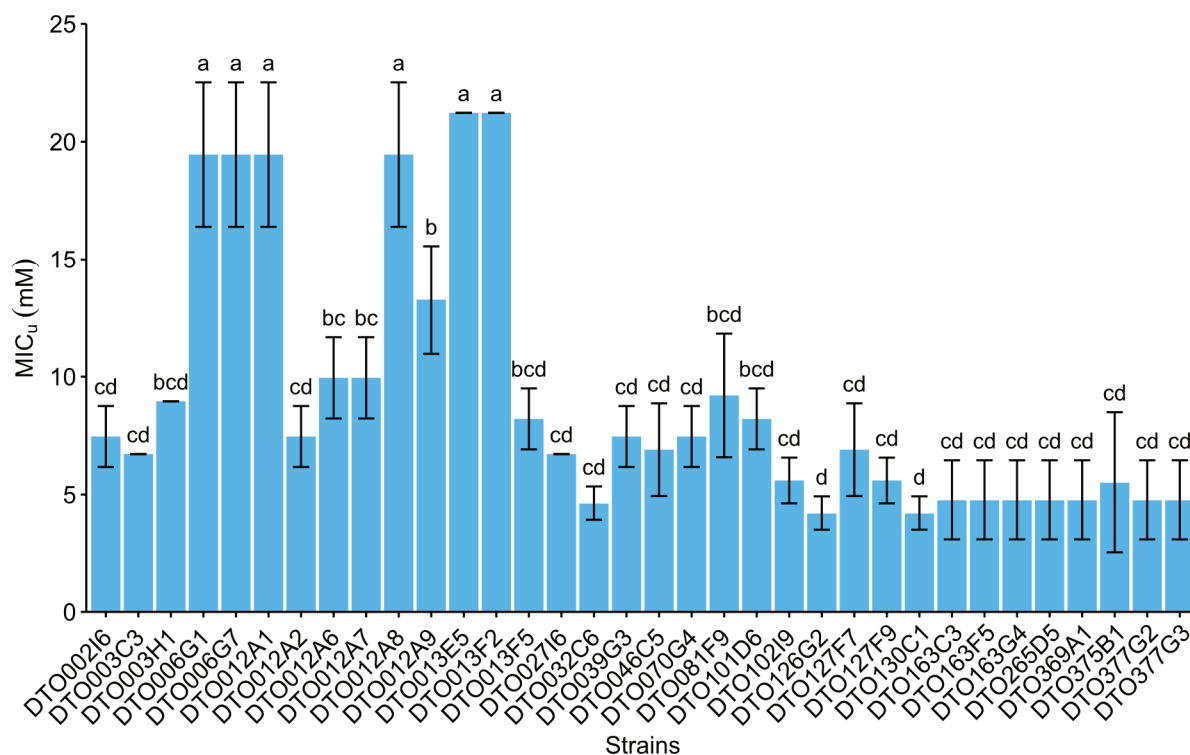
Figure 2. Average undissociated MIC_u values of sorbic acid of 34 *P. roqueforti* strains (mM ± standard deviation). Each bar graph represents biological triplicates. Error bars indicate standard deviation and letters indicate significant difference in MIC_u ($p < 0.05$).

Modelling growth on yoghurt

A logistic regression model was developed to describe the probability of growth for *P. roqueforti* on yoghurt. The pH of each yoghurt sample was measured and when the pH was included in the model its effect was significant. However, we excluded the pH in the final model because its variations were dependent on the sorbic acid concentration. Furthermore, pH has been described to only have a slight effect on fungal growth within the range of 3 – 8 (Dantigny, 2016). We found similar results when employing a linear model compared to a logistic one, but the goodness-of-fit statistics were lower for the linear model (Table S4). For the logistic model, the estimated parameters (± standard deviations) and goodness-of-fit statistics are listed in Table S5. The statistics show the model can predict the data accurately (Nagelkerke R^2 = 0.995). Among the tested variables, undissociated potassium sorbate concentration exerted the largest effect on growth of *P. roqueforti*. The other variables (strain and time) were shown to have a significant, but smaller, impact on growth. For the five tested strains, growth was observed after 10-11 days in yoghurt without sorbic acid (Figure 3). We demonstrate that the maximum sorbic acid concentration at which growth was observed in yoghurt is 6 mM. Furthermore, we found that growth was delayed significantly at 3 mM sorbic

acid for strain DTO377G3 and DTO013F5 (it took 21-28 days before growth was observed), whereas only a slight delay compared to the control was observed for strain DTO013F2 and DTO006G1 (11-15 days until growth was observed). In addition, strain DTO126G2 was shown to be markedly more sensitive to potassium sorbate concentration as it did not grow at all at 3 mM sorbic acid (Figure 3).
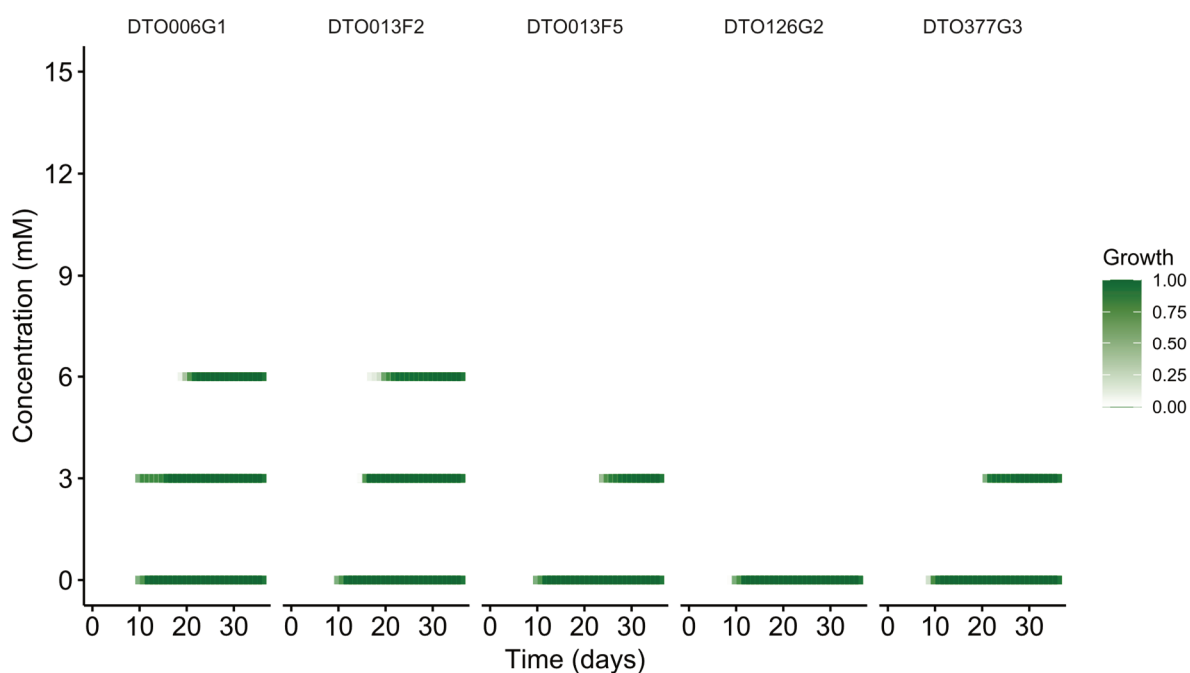

Figure 3. Graphical representation of fungal growth on yoghurt. Figure depicts *in-vitro* growth development of five *P. roqueforti* strains (R :DTO006G1 and DTO013F2; S: DTO013F5, DTO126G2 and DTO377G3) on yoghurt medium supplemented with 3, 6, 9, 12 or 15 mM potassium sorbate. The cultures were incubated at 8 °C. Growth is depicted as the average of all replicates per strain (n=3) with darker shading indicating a higher fraction growing at a certain day (i.e growth in six out of 18 wells would be 0.33).

Genome statistics and phylogeny
The genomes of the 34 *P. roqueforti* strains were sequenced. Scaffold count varied between 45 and 1358, assembly length between 26.53 and 31.74 Mb and GC content between 46.85 and 48.44 % (Table 1). The number of predicted genes varied between 9633 and 10644, the number of genes with PFAM domains between 73.11 and 75.38 %, and the number of secondary metabolism gene clusters between 32 and 36. All strains had a BUSCO completeness of >99 %, indicating high quality assembly and gene predictions, except for DTO012A8 with a completeness of 94.83 %. This and the high scaffold count of the DTO012A8 assembly (1358 scaffolds) indicates that its genome assembly is not complete. The strain was kept in the downstream analysis as most other metrics (Table 1) did not differ much compared

to the other strains. Figure 4 presents a phylogenetic tree of the 34 *P. roqueforti* strains based on 6923 single-copy orthologous genes. Four of the six sorbic acid-resistant strains (DTO012A2, DTO013F2, DTO013E5 and DTO012A8) are located in one clade, the two other resistant strains are not closely related to this clade.
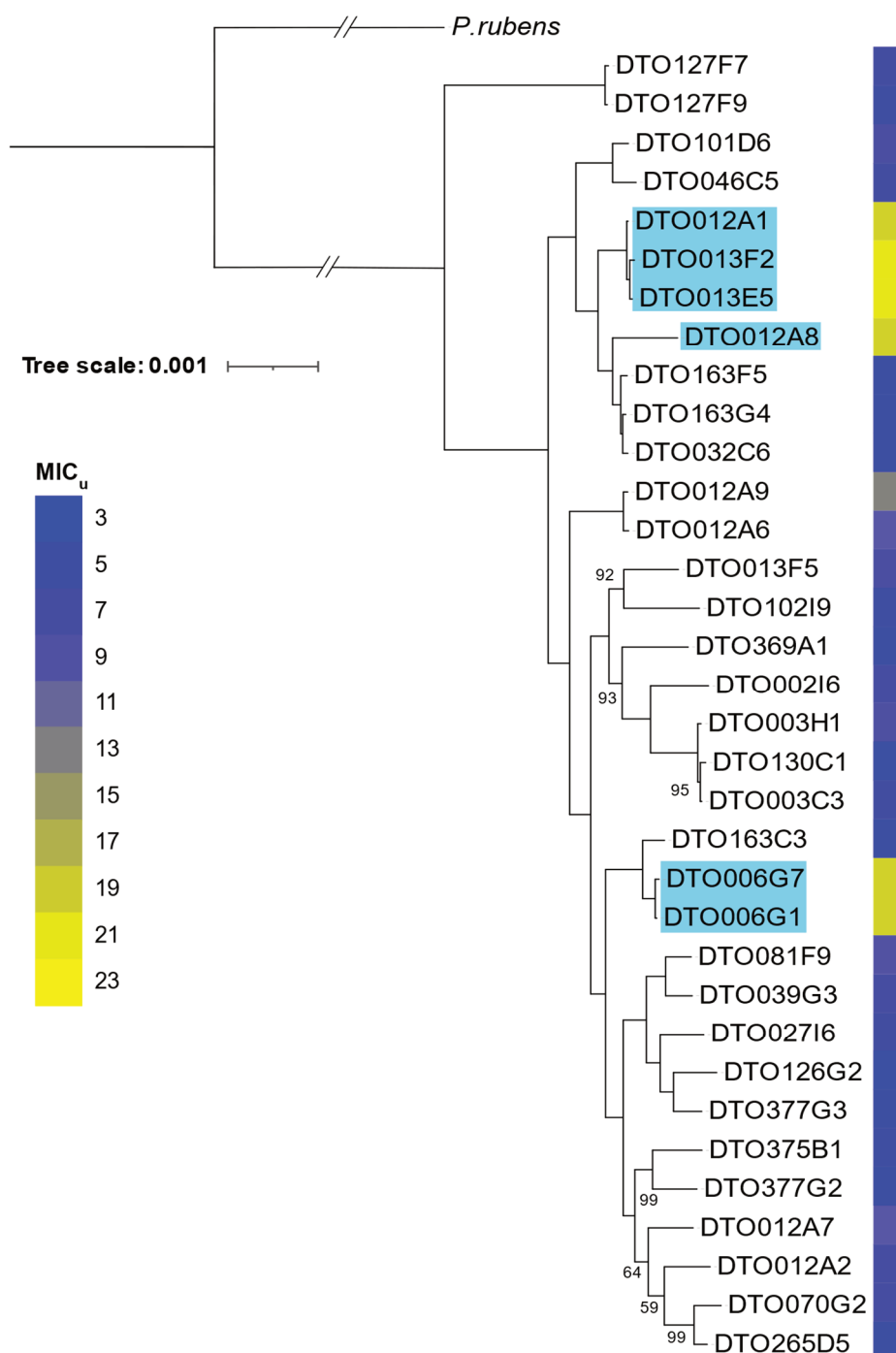

Figure 4. Phylogenetic tree of the 34 *P. roqueforti* strains used in this study. The sorbic acid resistance (MIC$_u$) is indicated in blue-yellow shading. The tree is based on 6923 single-copy orthologous genes and was constructed using RAxML. *P. rubens* (van den Berg et al., 2008) was used as outgroup. Bootstrap values <100 are indicated. Strains containing the SORBUS cluster are highlighted in blue.

Table 1. Genome assembly and annotation statistics. The number of scaffolds, assembly length, GC content and genes of the 34 sequenced *P. roqueforti* strains are listed. In addition, the number of genes with a PFAM domain, the number of secondary metabolism gene clusters and the BUSCO completeness are listed. The type column indicates if the strain is sorbic acid-resistant (R) or sorbic acid-sensitive (S).

Assembly				Annotation			Annotation quality	Type
Strain	Scaffolds	Total assembly length (Mbp)	Assembly GC content (%)	Genes	Genes with PFAM (total, %)	Secondary metabolism gene cluster	BUSCO2 completeness (%)	R/S
DTO002I6	134	29.48	47.75	10135	7539 (74.39%)	33	99.66%	S
DTO003C3	353	30.28	47.82	10362	7612 (73.46%)	36	99.66%	S
DTO003H1	382	30.29	47.82	10349	7607 (73.5%)	36	99.66%	S
DTO006G1	109	27.97	48.18	9975	7468 (74.87%)	33	99.66%	R
DTO006G7	100	27.97	48.18	9982	7471 (74.84%)	33	99.66%	R
DTO012A1	158	29.37	48.11	10280	7557 (73.51%)	33	100%	R
DTO012A2	73	27.07	48.26	9786	7362 (75.23%)	33	99.66%	S
DTO012A6	93	27.29	48.32	9817	7376 (75.13%)	33	99.66%	S
DTO012A7	62	27.33	48.07	9748	7335 (75.25%)	34	99.66%	S
DTO012A8	1358	29.6	47.88	10253	7483 (72.98%)	32	94.83%	R
DTO012A9	581	29.84	47.89	10341	7613 (73.62%)	34	99.31%	S
DTO013E5	165	29.27	48.11	10252	7537 (73.52%)	33	100%	R
DTO013F2	657	31.74	47.49	10644	7739 (72.71%)	33	100%	R
DTO013F5	304	29.56	48.04	10313	7591 (73.61%)	35	99.66%	S
DTO027I6	177	29.3	48.12	10325	7560 (73.22%)	32	99.66%	S
DTO032C6	141	28.45	48.13	10008	7441 (74.35%)	33	100%	S

DTO039G3	45	27.22	48.14	9764	7352 (75.3%)	32	99.66%	S
DTO046C5	143	28.8	48.15	10098	7488 (74.15%)	33	99.66%	S
DTO070G2	60	26.75	48.39	9724	7324 (75.32%)	33	100%	S
DTO081F9	47	27.24	48.13	9760	7349 (75.3%)	32	99.66%	S
DTO101D6	141	28.96	48.07	10109	7497 (74.16%)	33	99.31%	S
DTO102I9	186	28.53	47.92	9978	7439 (74.55%)	32	99.66%	S
DTO126G2	174	28.06	48.02	9939	7431 (74.77%)	33	99.31%	S
DTO127F7	59	26.54	48.43	9639	7315 (75.89%)	35	99.66%	S
DTO127F9	54	26.53	48.44	9633	7311 (75.9%)	36	99.66%	S
DTO130C1	537	30.48	47.79	10375	7612 (73.37%)	36	99.66%	S
DTO163C3	239	30	48.16	10485	7653 (72.99%)	33	99.66%	S
DTO163F5	284	30.9	46.85	10010	7441 (74.34%)	33	100%	S
DTO163G4	104	28.45	48.12	10006	7441 (74.37%)	33	100%	S
DTO265D5	66	26.76	48.44	9751	7350 (75.38%)	33	100%	S
DTO369A1	156	28.29	47.97	9945	7437 (74.78%)	32	99.66%	S
DTO375B1	62	27.2	48.2	9804	7378 (75.25%)	33	99.31%	S
DTO377G2	101	28.07	48.14	9962	7444 (74.72%)	33	99.31%	S
DTO377G3	84	26.97	48.24	9762	7335 (75.14%)	33	99.66%	S

Average	217.32	28.55	48.05	10038.65
Min	45	26.53	46.85	9633
Max	1358	31.74	48.44	10644

Sorbic acid resistance correlates with a genomic cluster containing genes regulating sorbic acid decarboxylation

The 34 *P. roqueforti* strains were divided into two groups based on their sorbic acid resistance, a group of six resistant (R-type) strains ('a', Figure 2) and a group of 28 sensitive (S-type) strains ('b-d', Figure 2). Whole genome comparison methods are often based on differences in variants (SNPs), however these methods do no reveal larger missing regions or genes between strains. Hence, a GWAS method was developed to compare whole-genome assemblies based on the MUMmer software. With this method 57 genes unique for the R-type group were identified, of which 51 were present on scaffold 43 of DTO006G7 (Table 2). In addition to the 51 unique genes in this scaffold, it contains 19 genes which are also found completely or in part in some of the S-type strains. Genomic alignment of all isolates shows the genes present on scaffold 43 for the R-type strains (Figure 5). The first 80 kb (g12000-g12029) mainly contains hypothetical proteins without predicted function, while the following region between 80-180 kb (g12030 – g12069) contains multiple regions homologous to genes previously reported as related to weak-acid resistance in *A. niger*. Predicted genes orthologous to *padA*, *cdcA* and *sdrA* of *A. niger* were found alongside each other (g12064-g12066) with respective identities (based on BLAST) of 87 %, 83 % and 53 %. Additional orthologs of *cdcA*, named *cdcB* (g12056) and *cdcC* (g12040) were identified on the same gene cluster as well, with identities of 72 % and 71%, respectively, when compared to *cdcA* of *A. niger*. Another locus (g2591) outside of this cluster also contains a protein homologous to *cdcA* (82 % identity), even in the S-type strains. Similarly, two *padA* orthologs with high BLAST similarities to *padA* of *A. niger* (63 % and 58 %) were identified on the R-type specific cluster and named *padB* (g12032) and *padC* (g12057). In contrast, no homologs of *A. niger sdrA* and *padA* were found outside of the cluster. In addition, a transcription factor (g2820 in DTO006G7) orthologous to *warA* was identified outside of the cluster in the genomes of all strains. Together these results indicate that the R-type *P. roqueforti* strains contain a gene cluster similar to the sorbic acid resistance gene cluster described in *A. niger*, but considerably expanded (Lubbers et al., 2019; Plumridge et al., 2010). For further reference, we name this cluster SORBUS after the tree *Sorbus aucuparia* as sorbic acid has been first isolated from its berries by August Hoffman (Naidu, 2000; Nielsen & Rios, 2000). While SORBUS as a whole is only present in the R-type strains (DTO006G1, DTO006G7, DTO012A2, DTO012A8, DTO013F2, DTO013E5), some S-type strains share up to 5 kB parts of

the sequence, especially in the first 80 kB of the cluster (Figure 5). It should be noted that the R-type strains were all isolated from non-cheese environments. Based on alignments of the sequencing reads to DTO006G7 we confirmed that out of 35 previously sequenced *P. roqueforti* strains (Dumas et al., 2020), none of the 17 cheese strains contained the SORBUS cluster, while two out of the 18 non-cheese strains contained the SORBUS cluster (Table S1).

Table 2. Genes (DTO006G7) located on the SORBUS cluster. The fold change (log₂FC) of the sorbic acid samples compared to the control is given. Numbers in bold are significantly differently expressed (adjusted p-value < 0.05) and the mean expression (FPKM) of three biological replicates is given per condition (control and sorbic acid). Rows highlighted in grey indicate genes that are not unique for the R-type strains.

GeneId	Name	Functional annotation (PFAM or description)	Expression (FPKM)		log₂FC	p-value (Adj.)
			Control	Sorbic acid		
12000		FAM167	4	8	0.69	0.66
12001		hypothetical protein	16	86	**2.18**	**0.00**
12002		NEMP	2	2	-0.27	0.89
12003		BTB/POZ domain	16	23	0.48	0.35
12004		hypothetical protein	59	40	-0.56	0.16
12005		hypothetical protein	0	0	1.05	0.59
12006		Reverse transcriptase	0	0	-	-
12007		DUF3723	0	0	-	-
12008		hypothetical protein	0	0	-	-
12009		Hly-III related protein	0	0	-	-
12010		Cyclin like F-box	1	1	0.72	0.32
12011		Cyclin like F-box	17	24	0.47	0.25
12012		Reverse transcriptase	3	7	**1.02**	**0.03**
12013		Endonuclease/Exonuclease/phosphatase family	1	4	**1.40**	**0.00**
12014		Probable transposable element	1	3	0.83	0.51
12015		Aldo/keto reductase family	463	365	-0.34	0.36
12016		Reverse transcriptase	26	20	-0.35	0.57
12017		Telomere-associated recq-like helicase	13	15	0.23	0.57
12018		Cyclin like F-box	29	25	-0.23	0.41
12019		hypothetical protein	0	0	-1.04	0.83
12020		hypothetical protein	1	1	0.22	0.96

12021		Centrosomin N-terminal motif 1	0	0	2.51	0.24
12022		hypothetical protein	3	7	1.02	0.09
12023		Cyctochrome C mitochondrial import factor	1	0	-0.84	0.73
12024		hypothetical protein	8	10	0.21	0.86
12025		hypothetical protein	5	6	0.25	0.60
12026		Winged helix-turn helix	0	0	-	-
12027		hypothetical protein	15	10	-0.57	0.23
12028		Pronucleotidyl transferase	0	0	-0.14	0.95
12029		Pronucleotidyl transferase	1	0	-0.83	0.64
12030		hypothetical protein	11	15	0.42	0.58
12031		hypothetical protein	0	0	-	-
12032	*padB*	Flavoprotein	450	288	-0.62	0.15
12033		PHF5-like protein	3	3	0.11	0.91
12034		Pyridoxamine 5'-phosphate oxidase	370	287	-0.36	0.48
12035		Mitochondrial carrier protein	11	12	0.06	0.96
12036		Mitochondrial carrier protein	12	17	0.42	0.65
12037		GTP cyclohydrolase II	10	2	**-1.86**	**0.01**
12038		Potassium channel tetramerisation domain	26	30	0.18	0.82
12039		hypothetical protein	17	10	-0.58	0.58
12040	*cdcC*	UbiD	134	65	**-1.02**	**0.01**
12041		Pyridoxamine 5'-phosphate oxidase	2	1	-0.54	0.90
12042		hypothetical protein	9	11	0.27	0.76
12043		GTP cyclohydrolase II	5	1	**-1.63**	**0.03**
12044		GPR1/FUN34/yaaH family	47	9	**-2.05**	**0.00**
12045		Mitochondrial carrier protein	1	1	-0.61	0.73
12046		hypothetical protein	12	12	-0.03	0.97
12047		Helix-turn-helix domain/endonuclease	8	8	0.03	0.95
12048		Flavonol reductase/cinnamoyl-CoA reductase	53	56	0.07	0.93
12049		Flavonol reductase/cinnamoyl-CoA reductase	9	8	-0.26	0.63
12050		Tannase	427	352	-0.27	0.55

12051		hypothetical protein	0	1	1.76	
12052		Transposase-like protein	6	7	0.13	0.84
12053		Reverse transcriptase	0	0	0.31	0.89
12054		Zinc finger transcription factor	26	13	-0.98	0.07
12055		Transposase-like protein	0	0	1.64	
12056	*cdcB*	UbiD	211	142	-0.51	0.65
12057	*padC*	Flavoprotein	78	75	-0.07	0.90
12058		Pyridoxamine 5'-phosphate oxidase like	348	504	0.50	0.28
12059		GTP cyclohydrolase II	25	24	-0.04	0.96
12060		GPR1/FUN34/yaaH family	3	3	-0.39	0.67
12061		Flavin reductase like domain	2028	1532	-0.40	0.42
12062		hypothetical protein	272	295	0.08	0.86
12063		3, 4-dihydroxy-2-butanone 4-phosphate synthase	65	34	-0.85	0.25
12064	*padA*	Flavoprotein	92	45	-0.97	0.08
12065	*cdcA*	UbiD	65	22	**-1.53**	**0.00**
12066	*sdrA*	Hypothetical transcription factor	2	1	-0.76	0.71
12067		hypothetical protein	0	0		
12068		NACHT domain	4	8	0.85	0.09
12069		Histone H3	3	6	**0.95**	**0.00**
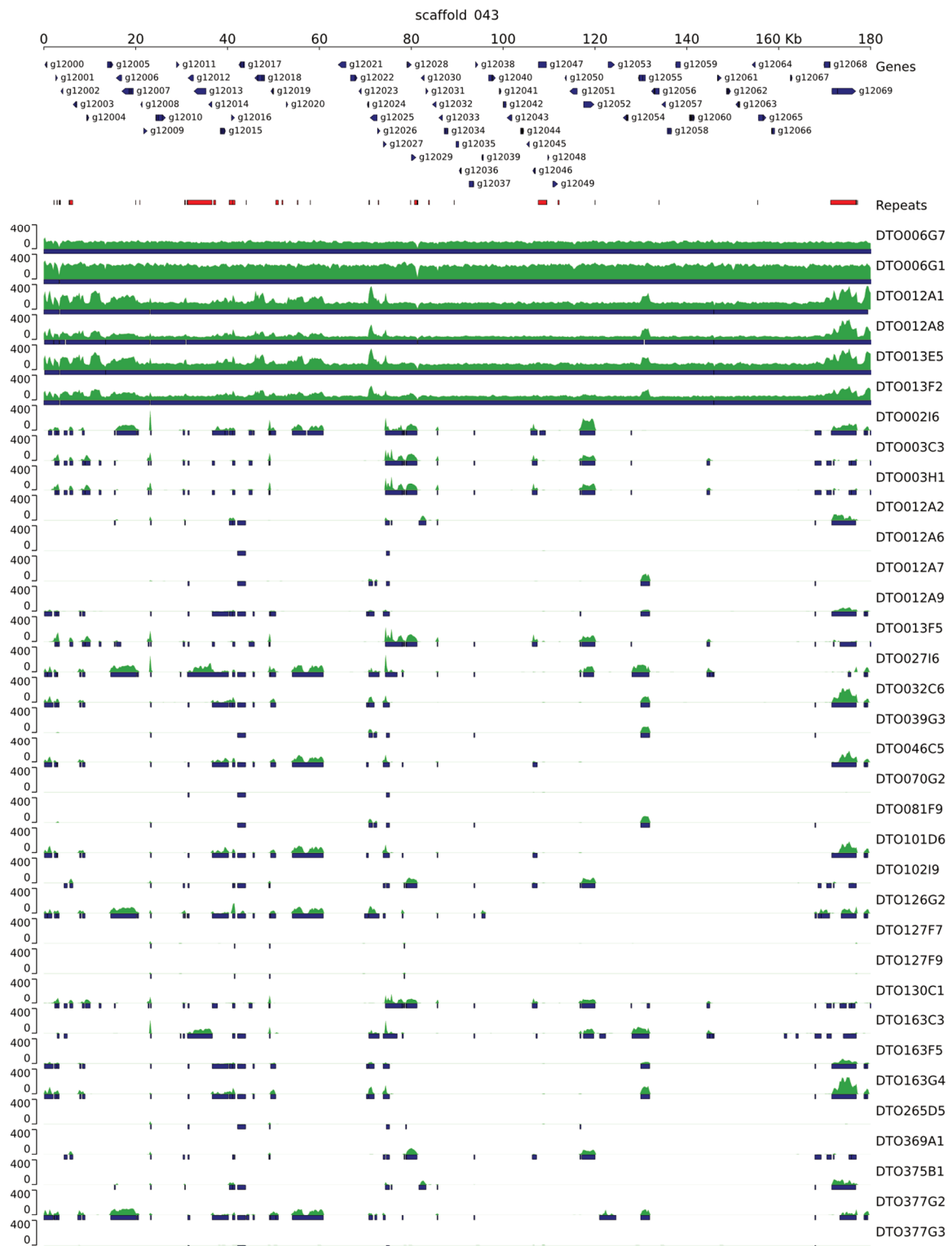
Figure 5. Genomic alignment of 33 *P. roqueforti* strains to the SORBUS cluster (scaffold 43 of DTO006G7). Predicted genes are indicated with arrows, repetitive DNA is indicated in red, the sequence read coverage is indicated in the green tracks, and blue bars indicate (partial) overlap with DTO006G7. The complete SORBUS cluster is only present in the R-type strains (DTO006G1, DTO006G7, DTO012A2, DTO012A8, DTO013F2 and DTO013E5).

In another approach, PLINK (Purcell et al., 2007) was used to identify which SNPs correlate to sorbic acid resistance of the fungal strains. This method allowed for the quantitative use of $\log_{10}(MIC_u)$ values as input for analysis, as opposed to the approach described above. The SNPs are visualized in a Manhattan plot (Figure 6). SNPs located on genes with a $-\log_{10}(P) > 5$ and either a high or moderate impact (SNPeff) were selected (Table 3). This resulted in 338 SNPs in 41 genes. Out of these SNPs, 29 had a 'high' impact according to SNPeff and were located in 17 genes. Only six out of these 17 genes with high impact variants (g7017, g8100, g8106, g9942, g9943, g9976) were not located in the SORBUS cluster, the other 11 genes were either among the non-unique genes present on SORBUS, or genes of which less than 90 % of the sequence was found in S-type strains. With a BLAST analysis (protein-protein) and PFAM annotations the functions of the predicted proteins were assessed. This revealed that gene g8100 contains an ankyrin-repeat containing domain and gene g9943 is homologous to a zinc finger C3H1-type domain-containing protein, the putative function of the other three genes could not be assessed (hypothetical proteins). In all cases, the five genes showed high homology (> 99 %) to other *Penicillium* species. The PLINK analysis also revealed SNPs in two genes encoding proteins with a putative transmembrane transporter (g216) or cation transporter (g296) function.

Table 3. Genes (DTO006G7) containing SNPs associated with sorbic acid resistance. Only SNPs with a $-\log_{10}$(p-value) > 5 and a moderate or high impact as determined by SNPeff are listed. Grey shading indicates overlap with sequence repeats.

| GeneID | SNP impact | | Effect | PFAM annotation |
	Moderate	High		
g103	1	0		hypothetical protein
g216	1	0		ABC transporter transmembrane region
g235	1	0		STAG domain
g296	5	0		Cation transporter/ATPase, N-terminus
g312	1	0		Probable molybdopterin binding domain
g313	1	0		DDHD domain
g314	1	0		hypothetical protein
g315	1	0		FAD binding domain
g7015	1	1	Stop lost & splice region variant	hypothetical protein
g8100	0	1	Stop gained	Ankyrin repeats (3 copies)
g8101	3	0		DDE superfamily endonuclease

g8104	7	0		hypothetical protein
g8105	10	0		hypothetical protein
g8106	3	1	Stop gained	hypothetical protein
g8107	26	0		Ankyrin repeats (3 copies)
g12002	2	0		NEMP
g12005	9	1	Frameshift variant	hypothetical protein
g12006	42	2	Frameshift variant & Stop gained	Reverse transcriptase
g12007	8	0		Protein of unknown function (DUF3723)
g12013	48	3	Frameshift variants	Endonuclease/Exonuclease/phosphatase family
g12014	8	1	Stop lost & splice region variant	Probable transposable element
g12016	2	0		Reverse transcriptase
g12019	11	0		hypothetical protein
g12025	9	1	Stop gained	hypothetical protein
g12028	18	1	Stop lost & splice region variant	Pronucleotidyl transferase
g12029	26	6	Stop gained, Stop lost & splice variant	Pronucleotidyl transferase
g12030	16	2	Frameshift variant & Stop lost	hypothetical protein
g12046	1	0		hypothetical protein
g12052	4	1	Stop gained	Transposase-like protein
g12053	1	0		Reverse transcriptase
g12054	4	0		hypothetical protein
g12055	6	2	Frameshift variant & Stop lost	Transposase-like protein
g12069	7	1	Frameshift variant	Histone H3
g9749	7	0		hypothetical protein
g9942	1	2	Stop gained	hypothetical protein
g9943	2	2	Stop gained	AAA domain
g9944	8	0		hypothetical protein
g9945	4	0		ATPase family associated with various cellular activities (AAA)
g9961	1	0		hypothetical protein
g9966	2	0		Endonuclease-reverse transcriptase
g9976	0	1	Start lost	hypothetical protein
TOTAL	309	29		

Two genes with homology to transposase-like proteins (g912052 and g12055) and several reverse-transcriptase domains were identified in in the SORBUS cluster. To investigate the evolutionary origin of this cluster, presence of five PFAM domains (from g12060, g12061 and g12063-g12065) that are present on the SORBUS cluster was analysed in 32 Aspergilli and Penicillia as well as the 34 *P. roqueforti* strains (Table 4). These PFAM domains encode a putative GPR1/FUN34/yaaH family (g12060), a flavin reductase like domain (g12061), 3, 4-dihydroxy-2-butanone 4-phosphate synthase (g12063), a flavoprotein (g12064, *padA*) and a UbiD domain (g12065, *cdcA*). These domains are selected as they are clustered and because of their predicted role. The first domain has been associated with acetic acid sensitivity in *S. cerevisiae* (Paiva et al., 2004), while the latter four domains are part of the gene cluster described in *A. niger* (Lubbers et al., 2019).
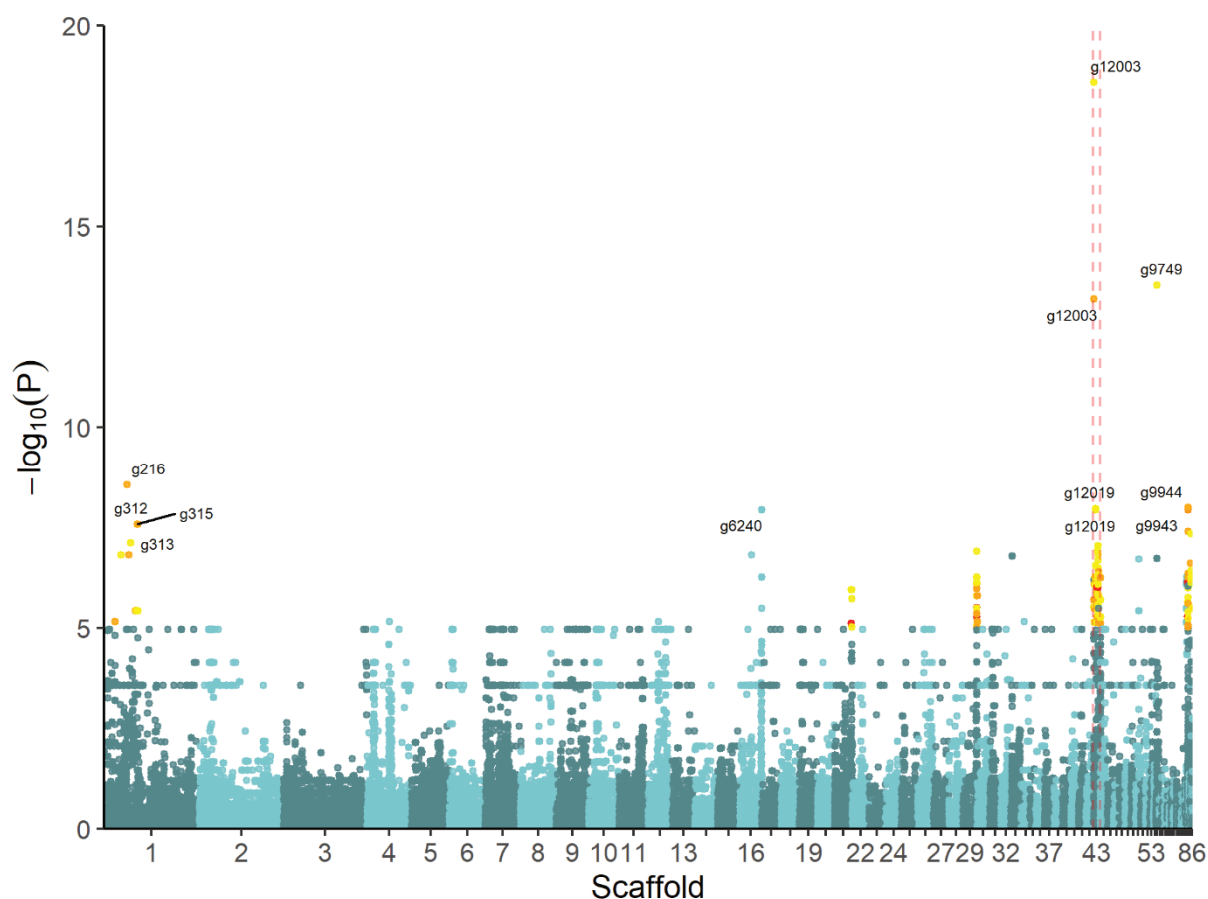
Figure 6. Manhattan plot of SNPs associated with sorbic acid resistance in $\log_{10}(MIC_u)$ in 33 *P. roqueforti* strains with DTO006G7 as reference. The scaffold is listed on the x-axis and the y-axis displays the significance of the association, $-\log_{10}$(p-value). Yellow, orange and red dots indicate 'low', 'moderate' or 'high' impact SNPs as determined by SNPeff, respectively. The GeneIDs associated with the SNPs with a $-\log_{10}$(p-value) > 7.5 are indicated. The SORBUS cluster is located between the dashed lines.

Genes containing these domains were aligned using MAFFT and alignments were used to construct a phylogenetic tree per domain. Based on these phylogenetic trees the relatedness of the five genes of the SORBUS cluster was assessed. This revealed that the SORBUS genes g12061, g12064 and g12065 cluster more closely with several *Aspergillus* species (Table 4), whereas the PFAM domains from g12060 and g12063 did not cluster with any of the species included. In addition, the PFAMs present in the core genome (present both in S- and R-type strains) aligned more closely to *P. digitatum* or *P. oxalicum*. The homology of some domains to *Aspergilli* and the presence of the transposase-like proteins suggests that SORBUS has been obtained from an *Aspergillius* species by horizontal gene transfer.

Table 4. Number of genes containing PFAM domains corresponding to g12060, g12061 and g12063-g12065 (PF01184, PF01613, PF00926, PF02441, PF01977) based on phylogenetic trees constructed with their respective PFAM domains. Top six strains are R-type *P. roqueforti* strains containing the SORBUS cluster. C (CORE) indicates if the domains aligned closely to the PFAMs not unique for the SORBUS cluster or did not align to *P. roqueforti*, S (SORBUS) indicates the number of PFAM domains which aligned closely to PFAMs originated from SORBUS.

Strain	g12060 PF01184		g12061 PF01613		g12063 PF00926		g12064 PF02441 (*padA*)		g12065 PF01977 (*cdcA*)	
	C	S	C	S	C	S	C	S	C	S
DTO013F2	7	1	4	1	1	1	5	3	2	3
DTO013E5	7	1	3	1	1	1	5	3	2	3
DTO012A8	7	1	3	1	1	1	5	3	2	3
DTO012A1	7	1	3	1	1	1	5	3	2	3
DTO006G7	7	1	4	1	1	1	5	3	2	3
DTO006G1	7	1	4	1	1	1	5	3	2	3
DTO377G3	7	0	4	0	1	0	5	0	2	0
DTO377G2	7	0	4	0	1	0	5	0	2	0
DTO375B1	7	0	3	0	1	0	5	0	2	0
DTO369A1	7	0	4	0	1	0	5	0	2	0
DTO265D5	7	0	3	0	1	0	5	0	2	0
DTO163G4	7	0	3	0	1	0	5	0	2	0
DTO163F5	7	0	3	0	1	0	5	0	2	0
DTO163C3	7	0	4	0	1	0	5	0	2	0
DTO130C1	7	0	3	0	1	0	5	0	2	0
DTO127F9	7	0	3	0	1	0	5	0	2	0
DTO127F7	7	0	3	0	1	0	5	0	2	0

DTO126G2	7	0	4	0	1	0	5	0	2	0
DTO102I9	7	0	4	0	1	0	5	0	2	0
DTO101D6	7	0	3	0	1	0	5	0	2	0
DTO081F9	7	0	4	0	1	0	5	0	2	0
DTO070G2	7	0	3	0	1	0	5	0	2	0
DTO046C5	7	0	3	0	1	0	5	0	2	0
DTO039G3	7	0	4	0	1	0	5	0	2	0
DTO032C6	7	0	3	0	1	0	5	0	2	0
DTO027I6	7	0	4	0	1	0	5	0	2	0
DTO013F5	7	0	4	0	1	0	5	0	2	0
DTO012A9	7	0	3	0	1	0	5	0	2	0
DTO012A7	7	0	3	0	1	0	5	0	2	0
DTO012A6	7	0	3	0	1	0	5	0	2	0
DTO012A2	7	0	3	0	1	0	5	0	2	0
DTO003H1	7	0	3	0	1	0	5	0	2	0
DTO003C3	7	0	3	0	1	0	5	0	2	0
DTO002I6	7	0	3	0	1	0	5	0	2	0
Penicillium roqueforti FM164	8	0	3	0	1	0	5	0	2	0
Penicillium oxalicum	4	0	2	0	1	0	2	0	0	0
Penicillium digitatum	1	0	2	0	1	0	4	0	1	0
Paecilomyces variotii	8	0	6	0	1	0	4	1	2	0
Paecilomyces variotii DTO217A2	7	0	7	0	1	0	5	1	3	0
Paecilomyces niveus	9	0	8	0	1	0	5	1	2	0
Aspergillus wentii	4	0	5	0	1	0	4	1	2	0
Aspergillus violaceofuscus	4	0	5	1	1	0	4	0	2	0
Aspergillus vadensis	3	0	5	0	1	0	4	1	2	1
Aspergillus uvarum	4	0	5	1	1	0	3	0	2	0
Aspergillus tubingensis	3	0	6	0	1	0	4	0	2	1
Aspergillus sclerotiicarbonarius	3	0	5	1	1	0	4	1	2	0
Aspergillus sclerotioniger	3	0	4	1	1	0	3	0	1	0
Aspergillus piperis	3	0	5	0	1	0	4	1	2	0
Aspergillus aureofulgens	3	0	5	0	1	0	4	1	2	0
Aspergillus niger N402	3	0	7	0	1	0	5	1	3	0
Aspergillus niger ATCC 1015	3	0	7	0	1	0	5	1	3	0
Aspergillus neoniger	4	0	5	0	1	0	4	1	2	1
Aspergillus niger (lacticoffeatus)	3	0	5	0	1	0	4	1	2	0
Aspergillus japonicus	4	0	5	1	1	0	4	0	3	0
Aspergillus indologenus	4	0	5	1	1	0	4	0	2	0

Aspergillus ibericus	3	0	5	1	1	0	4	1	1	0
Aspergillus heteromorphus	3	0	5	0	1	0	3	1	2	0
Aspergillus fumigatus	3	0	3	0	1	0	2	0	0	0
Aspergillus flavus	5	0	4	0	1	0	4	0	2	0
Aspergillus fijiensis	4	0	5	1	1	0	4	1	4	0
Aspergillus eucalypticola	3	0	5	0	1	0	4	1	2	1
Aspergillus ellipticus	3	0	5	0	1	0	6	2	7	0
Aspergillus costaricaensis	4	0	5	0	1	0	4	0	2	1
Aspergillus brunneovolaceus	4	0	6	1	1	0	4	1	4	0
Aspergillus aculeatinus	4	0	5	1	1	0	4	0	3	0
Arthroderma benhamiae	2	0	1	0	0	1	2	0	0	0

Genome-wide expression profiles of a sorbic acid-sensitive and sorbic acid-resistant strain

A genome-wide expression profile was performed on a sorbic acid-sensitive strain (DTO377G3) and a sorbic acid-resistant strain (DTO006G7) grown on MEB in the presence or absence of 3 mM sorbic acid. The sequence reads were aligned to the assemblies of these two *P. roqueforti* strains. Gene expression values were calculated and differentially expressed genes were identified (Table S6). The expression profiles of the biological replicates were similar, demonstrated by their clustering in the PCA plot (Figure 7). Combined, PC1 and PC2 explain 90 % of the variation observed. The samples treated with sorbic acid separate from the control samples on Y-axis while the differences between the strains are separated by on the X-axis.
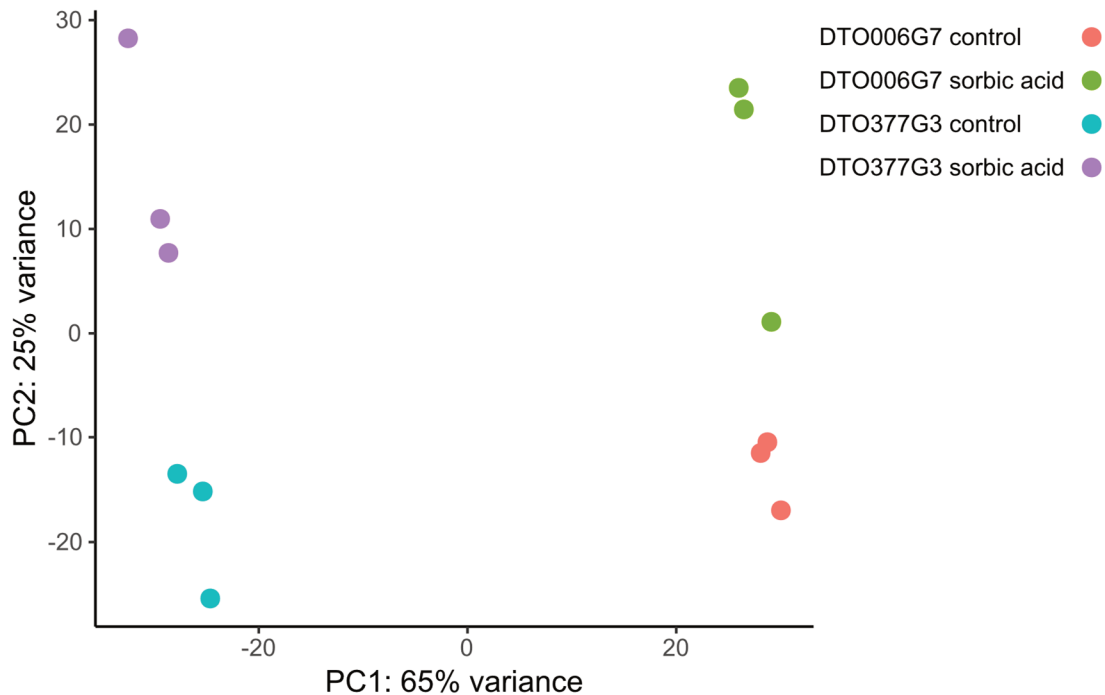
Figure 7. Principle component analysis of gene expression levels for the RNA-sequencing samples described in this study. Each dot represents a biological replicate. PC1 and PC2 together describe 90% of the variation. The sample grown on sorbic acid separate on the Y-axis and the two strains are separated on the X-axis.

Genes that are either up- or down-regulated in both the R-type and S-type strain when exposed to sorbic acid might be involved in a general response to sorbic acid stress in *P. roqueforti*. Venn diagrams were constructed revealing that 33 genes were significantly up-regulated in both the S-type and R-type strain (Figure 8A). An enrichment analysis revealed that the functional annotation terms 'secretion signal' and 'small secreted protein' are over-represented in these genes. Among the 21 shared down-regulated genes (Figure 8B) the NmrA-like family and NAD(P)H-binding domains were over-represented. Table S7 lists all genes present in both shared pools. The expression of the SORBUS genes (g12000-g12069) was analysed. This revealed that nine out of the 70 genes were significantly differentially expressed (Table 2), including two out of the three genes homologous to *cdcA* that were lower expressed ($\log_2$FC = -1.5) in the presence of sorbic acid. On the SORBUS cluster g12061 (with a flavin-reductase like domain) was the highest expressed gene, reaching 2000 FPKM in the control condition.
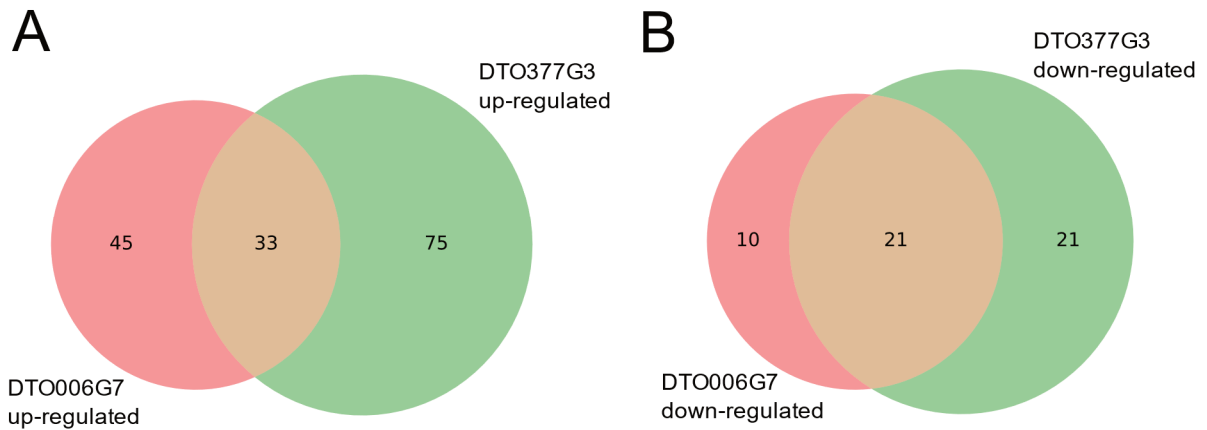
Figure 8. Venn diagram of differentially expressed genes in the presence of sorbic acid when compared to its absence. Up- (A) or down-regulated (B) in R-type DTO006G7 and S-type DTO377G3 when exposed to sorbic acid compared to the control in the absence of this weak acid. Genes were considered up- or down-regulated when the $\log_2$FC > 2, p-value < 0.05 and FPKM >10.

93 Kbp gene cluster knock-out confirms role of SORBUS in sorbic acid resistance

Strains *P. roqueforti* DTO013F2Δ*ku70* SC1 and SC2 were obtained lacking 93 kb of the SORBUS cluster. Multiple primers were designed (JD1-JD10, see Table S2) to investigate if blocks of approximately 1000 bps across the cluster were present in these two transformants (Figure 9; all diagnostic PCRs leading to this overview can be found in Figure S1). It was confirmed that most of the 93 kbp was not present in the knockout strains SC1 and SC2. Both these strains had a reduced resistance to sorbic acid when compared to DTO013F2 and DTO013F2 Δ*ku70* with a MIC$_u$ similar to the S strain DTO377G3 (Figure 10). This shows that the 93 kb part of the SORBUS cluster is involved in sorbic acid stress mitigation.
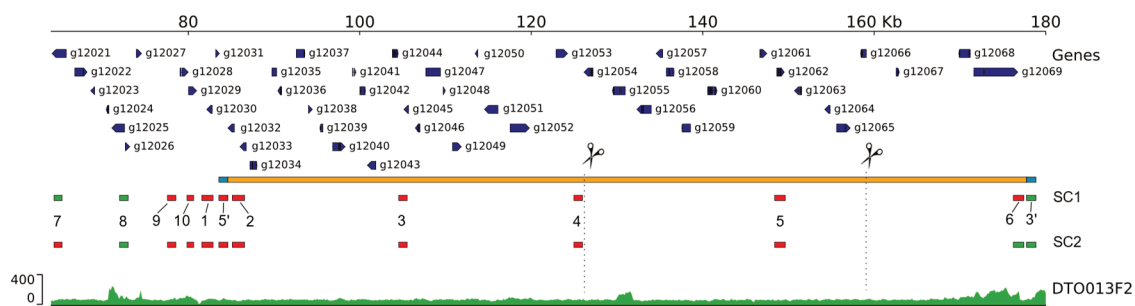
Figure 9. Schematic overview of the diagnostic PCRs performed on knock-out strains SC1 and SC2. The orange bar indicates the targeted knock-out region, flanked by the 5' and 3' ends (in blue). Dotted lines and scissors indicate the loci targeted by the sgRNAs. The green bars indicate the location of correctly amplified fragments and red blocks indicate regions that were not amplified correctly (See Figure S1). The numbers correspond to the primer pairs listed in Table S2 (JD1-JD10) to amplify these parts.
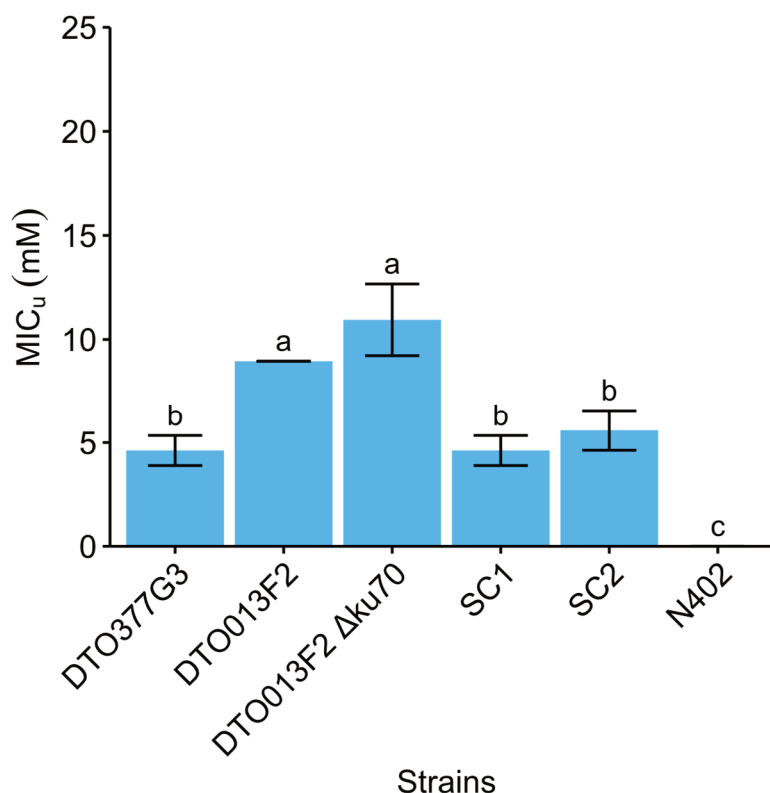
Figure 10. Average MIC_u values of sorbic acid for five *P. roqueforti* strains and *A. niger* N402 (mM ± standard deviation). Each bar graph represents average value of biological independent triplicates. Error bars indicate standard deviation and letters indicate significant difference in MIC_u ($p < 0.05$)

Discussion

P. roqueforti is often encountered as a spoiling contaminant in food. This can partly be attributed to its ability to grow at refrigeration temperatures (Kalai et al., 2017), low O_2 levels (Nguyen Van Long et al., 2017b) and its resistance to preservatives, such as sorbic acid (Quattrini et al., 2019). The inhibitory effect of propionic, benzoic and sorbic acid on *P. roqueforti* growth was assessed and benzoic acid was found to have the strongest inhibitory effect on 34 *P. roqueforti* strains. Previous studies report that *P. roqueforti* is resistant to benzoic acid. Growth was observed up to levels of 3000 ppm sodium benzoate (Blaszyk et al., 1998; Suhr & Nielsen, 2004), while we observed growth at 610 ppm (5 mM). Propionic acid hardly affected the growth of *P. roqueforti*, which is not surprising since it had already been reported that this fungus germinates on potato dextrose agar containing 0.5 M propionic acid (pH 5.6) with an estimated MIC of 0.79 M (Kalai et al., 2017). The sorbic acid resistance of *P. roqueforti* has also been assessed previously (Blaszyk et al., 1998; Bullerman, 1985; Huang et al., 2010; Liewen & Marth, 1985; Quattrini et al., 2019; Razavi-Rohani & Griffiths, 1999; Suhr & Nielsen, 2004), reporting MIC values ranging from 0 – 40 mM sorbic acid (i.e. a MIC_u = 0 –

20 mM). This is similar to the range (MIC_u = 4.2 – 21.3 mM) found in this study. In fact, a resistant and sensitive group (R- and S-types) consisting of six and 28 strains, respectively, were found in this study. S-type and R-type strains showed a resistance up to 11.9 mM and 21.2 mM undissociated sorbic acid, respectively. The same classification of strains was found when they were challenged in yoghurt supplemented with sorbic acid. However, the strains were unable to grow at more than 9 mM sorbic acid in yoghurt. This may be explained by the composition of the yoghurt. During fermentation of milk various organic acids, such as lactic and acetic acid, are produced and these could inhibit fungal growth. Also, the lower temperature that was used during incubation in yoghurt may affect sorbic acid resistance as a lower temperature has an inhibitory effect on the growth rate of *P. roqueforti* (Kalai et al., 2017).

The R-type but not the S-type strains were found to contain a gene cluster (SORBUS) containing 70 genes, of which 51 genes are unique for the R-type strains. Even though the R-type strain DTO006G7 was used with the least fragmented assembly, the limits of the SORBUS cluster could not be established, as none of the S-type strains was sufficiently homologous at the flanks of scaffold 43. Likely, SORBUS is flanked by highly repetitive regions due to which the assembler breaks the scaffold at these regions. The higher than average coverage found on both edges for most of the strains points to this as well. Long-read sequencing techniques may resolve the genomic location of SORBUS. Genes homologous to sorbic acid degradation-associated genes in *A. niger* (*sdrA*, *cdcA*, *padA*, *warA*) were identified in the *P. roqueforti* genome (Geoghegan et al., 2020; Lubbers et al., 2019). A total of 1, 4, 3 and 1 orthologs were found, respectively, and only *warA* and one *cdcA* ortholog were not located on the SORBUS cluster. Two genes with putative transmembrane transport (g216) or cation transporter (g296) function were identified in the PLINK analysis. The encoded proteins might be also be involved in sorbic acid stress mediation alongside the SORBUS cluster, because in addition to decarboxylation, sorbic acid stress could be mediated by an efflux pump or through removal of protons from the plasma membrane by H^+-ATPase (Geoghegan et al., 2020; Lambert & Stratford, 1999).

As mentioned only six out of the 34 strains assessed in this study were found to contain the SORBUS cluster. This might be explained by the prevalence of *P. roqueforti* on silage. A

traditional approach to prevent spoilage in silage is to treat it with lactic acid bacteria. These bacteria produce a range of small organic acids such as lactic, formic and acetic acid (Broberg et al., 2007). The elevated levels of weak acids might act as selection pressure to maintain SORBUS in *P. roqueforti* strains which grow in this niche environment. In contrast, this selection pressure is not present in cheese which might explain that none of *P. roqueforti* strains in the 'cheese' population contain the SORBUS cluster (Dumas et al., 2020). It should be noted that the S-type sequence fragments that aligned with SORBUS mostly consists of proteins annotated as transposase-like proteins or reverse transcriptase, which might explain why these fragments are found in the S-type strains and it suggests that SORBUS may have been obtained via horizontal gene transfer. This is supported by the phylogenetic analysis on PFAM domains of five SORBUS genes, as the results show that three out of the five SORBUS specific genes are more closely aligned to *Aspergillus* species than *Penicillium* species. Gene cluster SORBUS was also present in two of 35 previously sequenced *P. roqueforti* strains (Dumas et al., 2020) and their sorbic acid resistance could be determined to validate the role of SORBUS in sorbic acid resistance.

Transcriptome analysis of the R-type *P. roqueforti* strain DTO006G7 revealed that two of the three *cdcA* paralogs (*cdcA* and *cdcC*) are significantly down-regulated during growth in the presence of sorbic acid. This is in contrast with the results described by Lubbers et al. (2019), where the authors found a fold change of more than 500 for *cdcA* when *A. niger* was cultivated on sorbic acid. This difference might be caused by the difference in medium type, because Lubbers et al. (2019) used sorbic acid as the sole carbon source, whereas in our experiments sorbic acid was used as a stressor in a nutrient-rich medium. This indicates that the sorbic acid content in the medium does not increase gene expression of the loci leading to increased resistance, suggesting that either these genes are constitutively expressed or expression is induced based on a different compound present in MEB.

A partial SORBUS knockout strain in the DTO013F2 Δ*ku70* R strain showed reduced sorbic acid resistance to a level similar to that of the S-type strains. Despite the absence of a full SORBUS cluster in the S-type strains and the deletion strain, their MIC is still relatively high when compared to other fungal species such as *A. niger* (as shown in Figure 10) or *A. fumigatus* (Geoghegan et al., 2020). This suggests that along with the genes on the SORBUS cluster,

other proteins are involved in sorbic acid stress mitigation. Our transcriptomics analysis revealed 21 down-regulated and 33 up-regulated genes that were similarly expressed both in a S-type and a R-type strain when exposed to sorbic acid. One of these up-regulated genes is the cation transporter (g1689, Table S6) which could have H$^+$ ATPase activity in the plasma membrane to counteract the acidification caused by the undissociated sorbic acid in the cytosol (Lambert & Stratford, 1999).

In conclusion, the results presented in this study demonstrate that weak-acid resistance varies between *P. roqueforti* strains and the SORBUS cluster contributes to a high sorbic acid resistance. Yet, even in the absence of this cluster the resistance is still relatively high, implying that other mechanisms are also involved in resistance to this weak acid.

Supplementary material
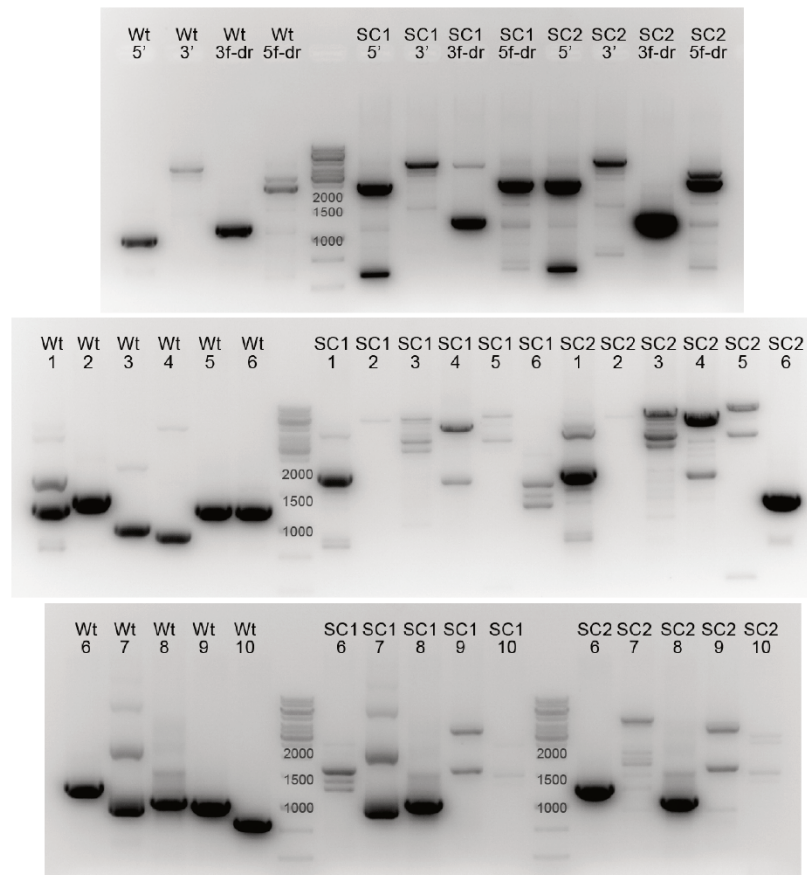
Figure S1. Overview of diagnostic PCRs of SORBUS cluster transformants. Corresponding gels for the amplification of the fragments (see Supplementary Table 1 for the primers used) on genomic DNA from Wt: parental "wildtype" strain DTO013F2 Δ*ku70*, DTO013F2 Δ*ku70* ΔSC1 (SC1) and DTO013F2 Δ*ku70* ΔSC2 (SC2). Amplified bands for Wt (except 3'), correspond with correct size. Gels were run on 1% agarose gel with the Generuler 1 kb DNA ladder.

Table S1. *Penicillium* spp. used in this study. https://bit.ly/3EdeKUA

Table S2. Primers used for plasmid and donor DNA construction and diagnostic PCR.

Name	Sequence (5' - 3')	Product
gTE_FWD	GTTTCCGCTGAGGGTTTAATACTCCGCCGAACGTACTG	CRISPR gRNA
gTE_REV	CTGTCTCGGCTGAGGTCTTAAAAAGCAAAAAAGGAAGGTACAAAAAAGC	CRISPR gRNA
MP1_ku70	CTATATTCTTAAATGGGCGGGTTTTAGAGCTAGAAATAGCAAG	CRISPR gRNA
MP2_ku70	CCGCCCCATTTAAGAATATAGGACGAGCTTACTCGTTTCG	CRISPR gRNA
Ku70_p7F	GGGAATCAAATCACCGTCAGCC	Repair template *ku70*
Ku70_p8R	CCCCCATTACCCTGTTATCCCTATATCATCGAGACGCGCTCTCTG	Repair template *ku70*
Ku70_p9F	TAGGGATAACAGGGTAATGGGGGATCTTGGTGGGATCCAGGGTTG	Repair template *ku70*
Ku70_p10R	GGAGAGGGTGGCAGTTTGGATA	Repair template *ku70*
MP5_sdrA	CTTTGAAATCGACCTCCTTCGTTTTAGAGCTAGAAATAGCAAG	CRISPR gRNA
MP6_sdra	GAAGGAGGTCGATTTCAAAGGACGAGCTTACTCGTTTCG	CRISPR gRNA
MP7_warB	TTGGGTGCGGATTAGAGATTGTTTTAGAGCTAGAAATAGCAAG	CRISPR gRNA
MP8_warB	AATCTCTAATCCGCACCCAAGACGAGCTTACTCGTTTCG	CRISPR gRNA
SC_p1f	CTTGACTCGGACGCCGCCAT	SC 5' flank, 5f primer
SC_p1r	GGAGTGGTACCAATATAAGCCGGGCCACGCTGCACTTCTCCGA	SC 5' flank, 5r primer
SC_p2f	CCGGCTTATATTGGTACCACTCCCGTCCCTGCTCAGCCGTGTT	SC 3' flank, 3f primer
SC_p2r	CACCCAGGCTGTCGCACGAA	SC 3' flank, 3r primer
JD_del_f	TCCTTCCACTACTGCAAGGGGG	Diagnostic PCR SC deletion
JD_del_r	ACTGTTCTATAGTTCGTAGGAACCTT	Diagnostic PCR SC deletion
JD_nodel_f	GCTCTGGGCTGAAGCAGTCG	Diagnostic PCR no deletion
JD_nodel_r	CTGCAGTGGCTTCCGCTCCT	Diagnostic PCR no deletion
JD1f	TCCTTTGGATGGCCGCCAGC	Diagnostic PCR fragment 1
JD1r	TCGACCTTGGGGAGCTGCCA	Diagnostic PCR fragment 1
JD2f	GGCCGGGCAGGGAAGTTGTT	Diagnostic PCR fragment 2
JD2r	GCGCGACCGGGACACTCTTT	Diagnostic PCR fragment 2
JD3f	GGAGCTACTGGCGGCTGCAT	Diagnostic PCR fragment 3
JD3r	ATGTTCGGCGTCGTCCACGG	Diagnostic PCR fragment 3
JD4f	TCGGACACTCGCAGCTGCAC	Diagnostic PCR fragment 4
JD4r	CGCGCTGAGCCGACCTTGAT	Diagnostic PCR fragment 4
JD5f	CAAGGCCACCCTTTCCCGCA	Diagnostic PCR fragment 5
JD5r	ACCCCCATCGCGCTTTTGGG	Diagnostic PCR fragment 5
JD6f	ATCCTTTCCGGCCGCTGCTG	Diagnostic PCR fragment 6
JD6r	GGGAAGCCAGCAAGCTACTCGC	Diagnostic PCR fragment 6

JD7f	TTGCTCTGACCGGTGGGGCT	Diagnostic PCR fragment 7
JD7r	AGGAAGACGGGGCCGCTCAT	Diagnostic PCR fragment 7
JD8f	TCCGTGCCGAGCTGCTGAAC	Diagnostic PCR fragment 8
JD8r	ACGGCGCGAGGTATACCGGA	Diagnostic PCR fragment 8
JD9f	CGACCGAGCCACGAACAGCT	Diagnostic PCR fragment 9
JD9r	CAGGAACCAAGCCGCACCGT	Diagnostic PCR fragment 9
JD10f	TGCATGGCCAGCAGGAGCAG	Diagnostic PCR fragment 10
JD10r	CGTCTGTCGGTTGCAAGCGC	Diagnostic PCR fragment 10

Table S3. Plasmids used in this study.

Plasmid name	Parental plasmid	Gene number of target gene	Gene name	Target Sequence	Reference
pFC332	-	-	-	-	(Nødvig et al., 2015)
pTF	pFC332	Pro_DTO013F2_2|g10054.t1	*TF*	TTGGGTGCGGATTAGAGATT	This study
pSdrA	pFC332	Pro_DTO013F2_2|g10066.t1	*sdrA*	CTTTGAAATCGACCTCCTTC	This study
pKU	pFC332	Pro_DTO013F2_2|g2981.t1	*ku70*	CTATATTCTTAAATGGGCGG	This study

Table S4. The model factors with the estimates (± standard deviations) and goodness-of-fit statistics obtained from a linear regression model of *P. roqueforti* growth on yoghurt. conc = undissociated potassium sorbate concentration. Not significant estimates are listed as n.s.

Factor	Estimate	T-value	p-value
DTO006G1	0.12 ± 0.01	8.95	0.000
DTO013F2	0.11 ± 0.01	7.73	0.000
DTO013F5	n.s.	n.s.	n.s.
DTO126G2	-0.09 ± 0.01	-6.31	0.000
conc	-0.09 ± 0	-62.37	0.000
Time	0.01 ± 0	29.70	0.000
constant	0.42 ± 0.01	29.81	0.000
Statistics			
Nagelkerke R^2	0.798		
c-value (ROC-curve)	0.986		

Table S5. *P. roqueforti* grown on yoghurt. The model factors with the estimates (± standard deviations) and goodness-of-fit statistics obtained from a logistic regression model of *P. roqueforti* growth on yoghurt (see Eq. 1). conc = undissociated potassium sorbate concentration.

Factor	Estimate	T-value	p-value
DTO006G1	2.88 ± 0.11	27.00	0.000
DTO013F2	2.5 ± 0.1	24.06	0.000
DTO013F5	-0.41± 0.1	-4.13	0.000
DTO126G2	-2.46 ± 0.11	-21.83	0.000
conc	-1.86 ± 0.03	-38.35	0.000
Time	0.23 ± 0.005	45.36	0.000
constant	-2.32 ± 0.1	-16.21	0.000
Statistics			
Nagelkerke R^2	0.995		
c-value (ROC-curve)	0.987		

Table S6. FPKM list as determined by DESeq2 of 9993 genes of *P. roqueforti* strain DTO377G3 and DTO006G7. https://bit.ly/3C4w5NC

Table S7. Significantly differentially expressed genes between *P. roqueforti* strain DTO377G3 and DTO006G7. https://bit.ly/2XcrMki

Summary and general discussion

Maarten Punt

Introduction and scope

The world population is projected to reach up to 11 billion inhabitants this century (Vollset et al., 2020). As a consequence, the demand for food will rise up to 70 % in 2050 (Alexandratos, Nikos & Bruinsma, 2012). One of the methods to meet this demand is by limiting the amount of food wasted each year, which is currently about one third of all food produced (Gustavsson et al., 2010). Food loss occurs throughout the food supply chain, either during production, transportation and storage of the products or even in the consumers' home. In high- and medium-income countries more than 40 % of the food loss happens at retail or consumer level. The main cause for this loss is food spoilage, which can have a physical, chemical or microbiological origin. Microorganisms such as fungi cause microbiological spoilage (Garnier et al., 2017) and fungal deterioration changes edible food into unappetizing products. In some cases, fungal spoilage even leads to food-borne disease. Fungal spoilage is predominantly caused by mould or yeast-like fungi that belong to the Ascomycota. The moulds grow by means of vegetative hyphae, that extend at their apices and that branch sub-apically and that form an interconnected network called mycelium. After a period of vegetative growth, a mycelium can produce asexual or sexual reproduction structures. For instance, conidiophores form asexual conidia, while ascomata form sexual ascospores. Conidia are considered to be the main cause of food spoilage because colonies produce enormous numbers of these spores (e.g., a colony on a Petri dish can form more than one billion conidia) that are easily dispersed by wind, water droplets or other vectors such as insects.

Conidia are generally more stress-resistant than vegetative mycelium (Dijksterhuis, 2017) enabling them to survive post-harvest treatments of food. They are resistant to desiccation, UV radiation and high or low temperature. Cell wall components such as melanin protect against UV damage, while compatible solutes and heat-shock proteins reduce heat and drought sensitivity. Fungi thrive on food not only because of the availability of nutrients but also because of the favourable pH, a_w and redox potential (Garnier et al., 2017). Several preservation techniques, also called hurdles, are applied to prevent spoilage in the food industry. These can be either preventive measures to limit contamination such as air filtration or aseptic packaging, or processing methods that limit the ability of microbes to grow. Pasteurization, low storage temperature and adding antimicrobial compounds are examples of preservation techniques. From a fungal point-of-view it is of great interest to overcome

these hurdles as they will be greatly rewarded when they do (Dijksterhuis, 2017). A fungus that is capable of overcoming these hurdles is *P. roqueforti*. This can be attributed to its ability to grow at refrigeration temperatures (Kalai et al., 2017), at low O_2 levels (Nguyen Van Long et al., 2017b) and its resistance to biological and chemical preservatives, such as sorbic acid (Quattrini et al., 2019).

A single spore is sufficient to cause spoilage. Formation of heterogeneous spores is a strategy to increase the chance of successful colonization of food products. Heterogeneity can not only be found between species and strains but also between spore populations of colonies of the same strain that have been exposed to different environmental conditions. In fact, heterogeneity can even be found within a spore population of a single colony. Little is known about the mechanisms underlying these types of heterogeneity despite its importance for fungi to survive in nature and man-made conditions such as a food context. This thesis describes intra-species and intra-strain heterogeneity in the food spoilage fungi *Aspergillus niger* and *P. roqueforti* focussing on stress resistance. Results are not only of fundamental interest but also from an applied point of view to secure food from spoilage.

Intra-strain heterogeneity

Conidia dispersed to new substrates can either germinate or remain dormant waiting for more suitable conditions. Germination is often triggered by environmental factors. Prerequisites for sustained growth of germlings are water and nutrients. Yet, conidia of *Cladosporium halotolerans* and *Penicillium rubens* germinate in pure water (Segers et al., 2017) and the latter even germinates on desiccated and nutrient-depleted conditions (Ruijten et al., 2020). This strategy may be successful if high numbers of spores are dispersed to many different substrates thereby increasing the chance that one of the substrates will enable sustained growth of the germlings. **Chapters 2** and **3** describe heterogeneity in germination of *A. niger* and *P. roqueforti* conidia produced on a single Petri dish, respectively. To this end, spore germination was monitored using an oCelloScope and fitted to a microbial growth curve developed by Dantigny et al. (2011). By confluent inoculation of the plate, spores were produced in a restricted time frame. In other words, the conidia have a similar age and have been produced under similar environmental conditions. For *A. niger*, up to 6 % of these conidia were triggered to germinate in a two-component medium consisting of an inducing

carbon source and inorganic phosphate, inorganic nitrogen or magnesium sulphate (**Chapter 2**). These experiments showed that part of the conidia leave their dormant and stress-resistant state only an hour earlier than conidia in richer media (τ = 6 h instead of 5 h), even if not all required nutrients for colony sustenance are available. Such a medium-independent response could provide a competitive advantage as it allows fast germination and hence colonization of a substrate. This heterogeneity might also explain why only 20 % of conidia produces germ tubes in a minimal medium supplemented with 50 mM glucose and all other nutrients needed to support full outgrowth of the colony. Heterogenous germination is advantageous as a sudden change in environmental conditions (e.g. increasing temperature on a leaf of a plant during a sunny day) is more likely to kill germlings than conidia. An important question that remains unanswered is how the heterogeneity of conidia with respect to germination is accomplished. This could in part be explained by differences in conidia maturation, as not all conidia are produced simultaneously on a single colony, or even on a single conidiophore (**Chapter 4**; Hagiwara et al., 2017; Teertstra et al., 2017). Heterogeneity may also result from a varying number of nutrient sensors in or near the plasma membrane such as G- and Ras-proteins (Fortwendel et al., 2004, 2008; Lafon et al., 2005) and the heterogeneous composition of proteins and RNA in conidia (**Chapter 4**; Bleichrodt et al., 2013; Teertstra et al., 2017; Wang et al., 2021). These varying levels of molecules may result from stochastic processes. It is important to note that evolution may select for such stochastic processes at the moment it increases the survival of the offspring.

Germination of spores follows a three-stage process. First, conidia are activated, then spores swell, a process called isotropic growth, which is followed by germ tube formation resulting from polarized growth (d'Enfert, 1997). Hayer et al. (2013, 2014) showed that conidial swelling and hyphal outgrowth can be independently triggered in *A. niger*. Particular carbon and nitrogen sources can either activate swelling or support hyphal outgrowth, while others can do neither or both. In **Chapter 2**, high, intermediate and low inducing amino acids for *A. niger* conidia were distinguished based on the P_{max} of swelling. A P_{max} < 5 % is regarded a low inducing amino acid while intermediate and high inducing amino acids have a P_{max} of 5-25 % and >25 %, respectively. Notably, alanine, arginine and glycine were classified as highly or intermediate inducing amino acids, whereas the same amino acids has been reported not to activate spore germination (Hayer et al., 2014). We found that it could take up to 15 h to

reach half P_{max} for some amino acids, whereas Hayer et al. (2014) only assessed conidia activation after 1 h by measuring trehalose content in the conidia. The difference in measurement type, a snapshot versus online, likely explains why our results contrast those found by Hayer et al. (2014) and highlights the impact heterogeneous germination can have on results when using single time point measurements.

Proline and alanine were the most effective inducing amino acids as they activate > 80 % of the conidia to swell. The accumulation of proline and alanine in plants exposed to stress might answer why these molecules have such a strong inducing effect in the case of *A. niger* (Meena et al., 2019; Ricoult et al., 2005), as such plants may be weaker to fungal colonization (Chojak-Koźniewska et al., 2018). Indeed, proline is accumulated in onions under salt and drought stress and they are known to be infected by this fungus (Hanci & Cebeci, 2015; Romo-Pérez et al., 2020). It should be noted that the P_{max} of germ tube formation in the presence of proline and alanine was only about 50 % and 35 %, respectively. This contrasts to the 80 % or even 100 % germ tube formation in medium containing an amino acid mixture with and without glucose, respectively. This implies that spores of *A. niger* have different sensors that each contribute to germ tube formation of spores; more conidia will germinate within 24 h when the medium is rich in different amino acids.

The activation of *P. roqueforti* conidia by proteogenic amino acids or glucose was assessed in **Chapter 3**. A medium consisting of both an inorganic phosphate and nitrogen source, and magnesium sulphate was used. Potassium chloride was included in the medium, because the conidiospores of *P. roqueforti* were found to have a threefold increase in germination in the presence of potassium salts (KCl, KNO_3 or KH_2PO_4). This is in contrast with *A. niger* conidia, which germinated up to 100 % without any potassium present in the medium (**Chapter 2**). Possibly, *A. niger* conidia contain an internal storage of potassium or are better adapted to K-depleted substrates. Arginine and alanine were the strongest inducers of *P. roqueforti* germ tube formation by 21 % and 13 %, respectively. While none of the other amino acids resulted in more than 6 % germination. When glucose was used instead of an amino acid, germination reached 12 %. This is in sharp contrast with the germination rates observed by Nguyen Van Long, et al. (2017a), as they did not observe conidia unable to germinate, even in unfavourable temperature, pH or water activity. This difference could be explained by the

fact that the conidia in our experiment were submerged in liquid media, whereas they used growth on top of agar media. Even though *P. roqueforti* germinates in O_2 limited environments (Nguyen Van Long et al., 2017b), germination might be hampered due to differences in conidium adhesion. This has been observed for plant pathogens *Colletotrichum graminicola* and *Phyllosticta ampelicida*, where germination is dependent on adhesion (Chaky et al., 2001; Kuo & Hoch, 1996). However, this is a species-dependent trait because germination was not affected by surface attachment of the conidia from *Colletotrichum lagenarium*, *Magnaporthe grisea* and *Penicillium expansum* (Amiri et al., 2005; Lau & Hamer, 1998; Takano et al., 2000). Not only the germination rates (P_{max}) varied between *A. niger* and *P. roqueforti*, but their germination time (τ) also varied significantly. For example, *A. niger* conidia needed up to 12 h when germination was induced by arginine, whereas in the case of *P. roqueforti* conidia this was 25 h (**Chapter 2**; **3**). A similar difference was found in the presence of glucose: *P. roqueforti* germination time was reduced to 14 h, whereas the germination time of *A. niger* was reduced to approximately 7 h. This might indicate *P. roqueforti* conidia require a more complex medium for rapid germination. The lack of swelling in our tested conditions could also point to this. Generally, conidia diameter increases more than twofold during swelling of several *Aspergilli* (Baltussen et al., 2018; Ijadpanahsaravi et al., 2021; van Leeuwen et al., 2010; **Chapter 2**). In contrast, swelling of *P. roqueforti* conidia was limited or even absent in germinating spores in our defined medium, while swelling was observed in more complex medium such as malt extract broth (**Chapter 3**). Possibly, swelling in defined medium may be limited by nutrient availability. For instance, *Fusarium culmorum* conidia show minimal swelling in the absence of a nitrogen source (Marchant & White, 1966). Under such conditions, conidia may consume their internal compatible solute content at a higher rate, leading to a lower osmotic pressure. This would reduce the water uptake and consequently the swelling of the spores.

Intra-strain heterogeneity of conidia can also be the result of varying environmental conditions during sporulation. **Chapter 4** describes intra-strain heterogeneity of conidia caused by different maturation stages and growth conditions. *P. roqueforti* DTO377G3 conidia from three-day-old colonies had an D_{56}-value (minutes needed to reduce colony forming units by 90 % at 56 °C) of about 1.99 compared to a D_{56}-value of 4.31 found in conidia derived from colonies with an age of ten days (**Chapter 4**). Cultivation temperature also had a significant

impact as conidia from cultures produced at 15 °C had an almost fourfold lower D_{56}-value (1.12) compared to conidia from the same strain, produced at 30 °C (4.19). A similar increase in heat resistance was found for *Aspergillus fumigatus* conidia produced at elevated temperature (Hagiwara et al., 2017). Interestingly, the effect of maturation of conidia on heat resistance was not observed in *A. fumigatus* when conidia obtained from cultures between 3-14 days old were tested (Hagiwara et al., 2017). Possibly, *A. fumigatus* cultures produce mature conidia within three days, while *P. roqueforti* conidia do not fully mature in seven days. Besides heat resistance, environmental conditions also affected spore size, polyol content and transcriptomic profiles of the conidia (**Chapter 4**). For instance, *P. roqueforti* spores increase by 12 - 25 % in diameter when its cultures were either grown at 5 °C or 30 °C, which are temperatures close to the lower and upper growth boundaries of this fungus (**Chapter 4**; Kalai et al., 2017; Nguyen Van Long et al., 2017). Similar observations have been made for *A. fumigatus* (Kang et al., 2021). For *Pae. variotii* average conidia diameter has been correlated with heat resistance (van den Brule et al., 2020b), yet no such correlation was found for *P. roqueforti* conidia of different strains (**Chapter 5**). Apparently, this relation between spore size and heat resistance is species specific. Besides spore size and heat resistance, we observe a species-specific preference for different compatible solutes: arabitol is the most abundant polyol in *P. roqueforti* (**Chapter 5**, Figure 1)*,* whereas *A. niger* and *Pae. variotii* conidia contain mostly mannitol or trehalose, respectively (Novodvorska et al., 2013).

The compatible solute composition differs in more matured conidia and in conidia produced at elevated temperature. Notably, trehalose and arabitol concentration in *P. roqueforti* DTO377G3 conidia increased in time and with culture temperature (**Chapter 4**). Similarly, increased trehalose concentration as a result of higher cultivation temperature or longer spore maturation has been described for *A. fischeri* ascospores and conidia of *A. niger*, *Beauveria bassiana*, *Cordyceps farinose* and *Metarhizium anisopliae* (Hallsworth & Magan, 1995; Teertstra et al., 2017; Wyatt et al., 2015). The role of compatible solutes and specifically trehalose has been previously associated with the heat resistance of fungal conidia of filamentous fungi (Hagiwara et al., 2017; Nguyen Van Long et al., 2017a; Ruijter et al., 2003; Sakamoto et al., 2009; van den Brule et al., 2020a; Wyatt et al., 2015). We observe a similar effect; trehalose and arabitol concentrations seem to correlate with heat resistance in *P. roqueforti* DTO377G3 conidia (**Chapter 4**). However, the conditions that yielded the highest

trehalose concentrations in this strain (ten days, 30 °C) did not result in the most heat-resistant conidia (**Chapter 4**). In addition, no correlation between trehalose or arabitol concentration and heat resistance was observed when we compared 18 *P. roqueforti* strains (**Chapter 5**). This might be explained by the role trehalose has beyond heat stress mitigation. For example, trehalose serves as carbon storage molecule in fungi (Perfect et al., 2017). Furthermore, intracellular trehalose increases germination time in *P. roqueforti, B. bassiana*, *M. anisopliae* and *C. farinose* (Hallsworth & Magan, 1995). Delayed germination might have an evolutionary benefit as it could prevent premature germination at or close to sites where conidia are produced. The lack of correlation between trehalose concentration and heat resistance in 18 strains (**Chapter 5**) also implies that heat resistance in *P. roqueforti* conidia is the result of multiple factors, for instance the abundance of heat-stress mitigating proteins (HSPs), a specific compatible solute composition and thickness of the conidial cell wall.

Strikingly, compatible solute concentration and spore size, but not heat resistance, of *P. roqueforti* DTO377G3 was different in **Chapter 4** compared to **Chapter 5**. Despite the fact that these spores had been produced under the same conditions. This might be explained by differences in medium as these experiments were carried out on different batches of MEA. These results further stress the effect environmental conditions can have on conidia development. Taken together, these data show that average spore size and compatible solute concentration are not the limiting factors contributing to the total heat resistance of *P. roqueforti* conidia. Yet, trehalose and arabitol concentration are important contributors.

Gene expression profiles of *P. roqueforti* DTO377G3 conidia were analysed in **Chapter 4** and shown to be affected by maturation time and cultivation temperature. In particular, the expression profiles of genes involved in polyol biosynthesis were analysed. These included *treA*, *tpsB* and *tpsC* (involved in trehalose synthesis), *lad* (arabitol synthesis) and *err1* (erythritol synthase). In case of trehalose this pattern corresponds to the accumulation of trehalose in the spores. In contrast, the erythritol concentration does not increase, but remains relatively stable. This could be explained by *err1* acting bidirectionally or the activity of other (unknown) enzymes. Similarly, the arabitol concentration does not completely correspond to the expression profile of *lad* (**Chapter 4**).

A total of 85 genes showed a more than fourfold higher expression in conidia produced at 30 °C when compared to those produced at 15 °C. Whereas 274 genes showed over fourfold higher expression in ten-day-old conidia compared to three-day-old conida. Notably, 33 genes were shared between these two sets. These 33 genes contained the hydrophilins con-6 and con-10 and 17 predicted proteins with unknown function. Hydrophilins have been linked to increased resistance of conidia against desiccation, thermal and osmotic stress in *A. fischeri* (van Leeuwen et al., 2016) and it was shown in *A. nidulans* conidia that the absence of *con-6* and *con-10* promotes the accumulation of glycerol and erythritol (Suzuki et al., 2013). The latter is also indicated in by the results described in **Chapter 4**, as glycerol and erythritol concentrations were negatively correlated with the increased *con-6* and *con-10* expression levels. Together, it was shown that intra-strain heterogeneity can have a pronounced impact on a conidium's ability to swell, germinate and resist stress.

Heterogeneity between strains

Chapter 5 describes the variability in conidial heat resistance observed within 20 strains of *P. roqueforti*. Besides strain variability, we considered experimental variability, biological variability and total variability. Experimental, biological and strain variability of *P. roqueforti* were compared using the standard deviation of log_{10} *D*-values, quantitatively expressed in RMSE. Experimental variability had the lowest variability, followed by the biological and strain variability with values of 0.044, 0.096 and 0.179 respectively. The data obtained in **Chapter 5** were integrated with the available literature data of *P. roqueforti*. From this data a Z-value of 7.8 °C was calculated, which expresses the temperature increase needed to cause a log_{10} reduction in *D*-value. In addition, total variability of this dataset was 0.415. This demonstrates that strain variability explains 43 % of the total variability observed in literature. This is comparable what has been observed in the spoilage bacteria *Bacillus subtilis*, *Bacillus cereus*, *Listeria monocytogenes*, *Geobacillus stearothermophilus* and *Lactobacillus plantarum* where 50 - 80 % of the overall variability could be explained by strain variability (den Besten et al., 2018).

In terms of D_{56}-value an 8.6-fold difference between the most heat-resistant and heat-sensitive strain within the selection of 20 *P. roqueforti* strains was observed. This is similar to the variability in heat resistance reported in other fungal and bacterial species (**Chapter 5**).

This is remarkable considering the different mechanisms that are involved in heat resistance of different species. For instance, arabitol, trehalose and the hydrophillins Con-6 and Con-10 have been implicated in heat resistance of *P. roqueforti* conidia (**Chapter 4**, see Figure 1), while conidia of *A. niger* contain large amounts of *hsp70* transcripts (van Leeuwen et al., 2013) and mannitol (Ruijter et al., 2003). On the other hand, *Pae. variotii* conidia predominantly contain trehalose as compatible solute (van den Brule et al., 2020a) which could, at least in part, explain its remarkable high tolerance for heat stress compared to other fungal species.

It was shown that average spore diameter varied between 3.47 µm to 4.22 µm between the 18 *P. roqueforti* strains (**Chapter 5**). In addition, we observed a large variation in conidial compatible solute content in these fungi (see Figure 1 for polyol composition), out of which arabitol and mannitol were the most abundant with concentrations ranging from 82 to 535 mM and 130 to 304 mM, respectively.

It is well known that heat resistance of bacterial spores and vegetative cells differ enormously among species, and consequently the *D*-values of these cells are very different when determined at the same temperature. Interestingly, the intra-species variability of these cell types is in the same magnitude when the spore forming bacteria *B. subtilis*, *B. cereus*, *G. stearothermophilus* and the non-spore forming bacteria *L. monocytogenes* and *L. plantarum* are compared (den Besten et al., 2018). The different types of variability (strain, biological and experimental) of heat resistance of these bacteria ranges from 0.2 to 0.4, 0.05 to 0.2 and 0.02 to 0.08, respectively. These values are similar for conidia of *P. roqueforti*, *A. niger* and *Pae. variotii* (**Chapter 5**). Future studies should address whether intra-species variability is also high for other stresses than heat stress and whether strain variability is also the main contributor in total variation in these cases.

Chapter 6 discusses the heterogeneity in resistance of *P. roqueforti* strains to benzoic, propionic and, in particular, sorbic acid. The sorbic acid resistance of this fungus has been assessed in various studies (Blaszyk et al., 1998; Bullerman, 1985; Huang et al., 2010; Liewen & Marth, 1985; Quattrini et al., 2019; Razavi-Rohani & Griffiths, 1999; Suhr & Nielsen, 2004), reporting MIC values ranging from 0 to 40 mM sorbic acid (MIC_u = 0 - 20 mM). This is similar to the range (MIC_u = 4.2 - 21.3 mM) found in **Chapter 6** (Figure 1) by growing *P. roqueforti* on

malt extract. Sorbic acid resistance was lower on yoghurt (0 – 6 mM). This is probably explained by the composition of the yoghurt. During fermentation of milk various organic acids, such as lactic and acetic acid, are produced and these could limit the fungal growth. Also, the lower temperature used in this assay might act synergistically with the sorbic acid in reducing resistance.

A genome wide comparison between resistant and sensitive strains revealed a genomic region (SORBUS) containing 70 genes, of which 51 genes are unique for the resistant group. Genes homologous to sorbic acid degradation-associated genes in *A. niger* (*sdrA*, *cdcA*, *padA*) were identified in the SORBUS cluster (Lubbers et al., 2019; Plumridge et al., 2010). These genes were shown to be involved in decarboxylation and detoxification of sorbic acid (Plumridge et al., 2008; Stratford et al., 2012). Only some spoilage-related strains were found to contain the SORBUS cluster (Figure 1). This might be explained by the prevalence of *P. roqueforti* on silage. A traditional approach to prevent spoilage in silage is to treat it with lactic acid bacteria. These bacteria produce a range of small organic acids in silage such as lactic, formic and acetic acid (Broberg et al., 2007). The elevated levels of weak acids might act as a selection pressure to maintain SORBUS in *P. roqueforti* strains which grow in this niche. In contrast, this selection pressure is not present in cheese which might explain that none of *P. roqueforti* strains in the 'cheese' population contain the SORBUS cluster (Dumas et al., 2020). In addition, the presence of two genes showing homology to transposase-like proteins suggests that SORBUS may have been obtained via horizontal gene transfer. This is supported by a PFAM domain homology, where it was shown that some SORBUS genes aligned more closely to *Aspergillus* species, than to other *Penicillium* species, which suggests SORBUS originates from *Aspergillus* species.
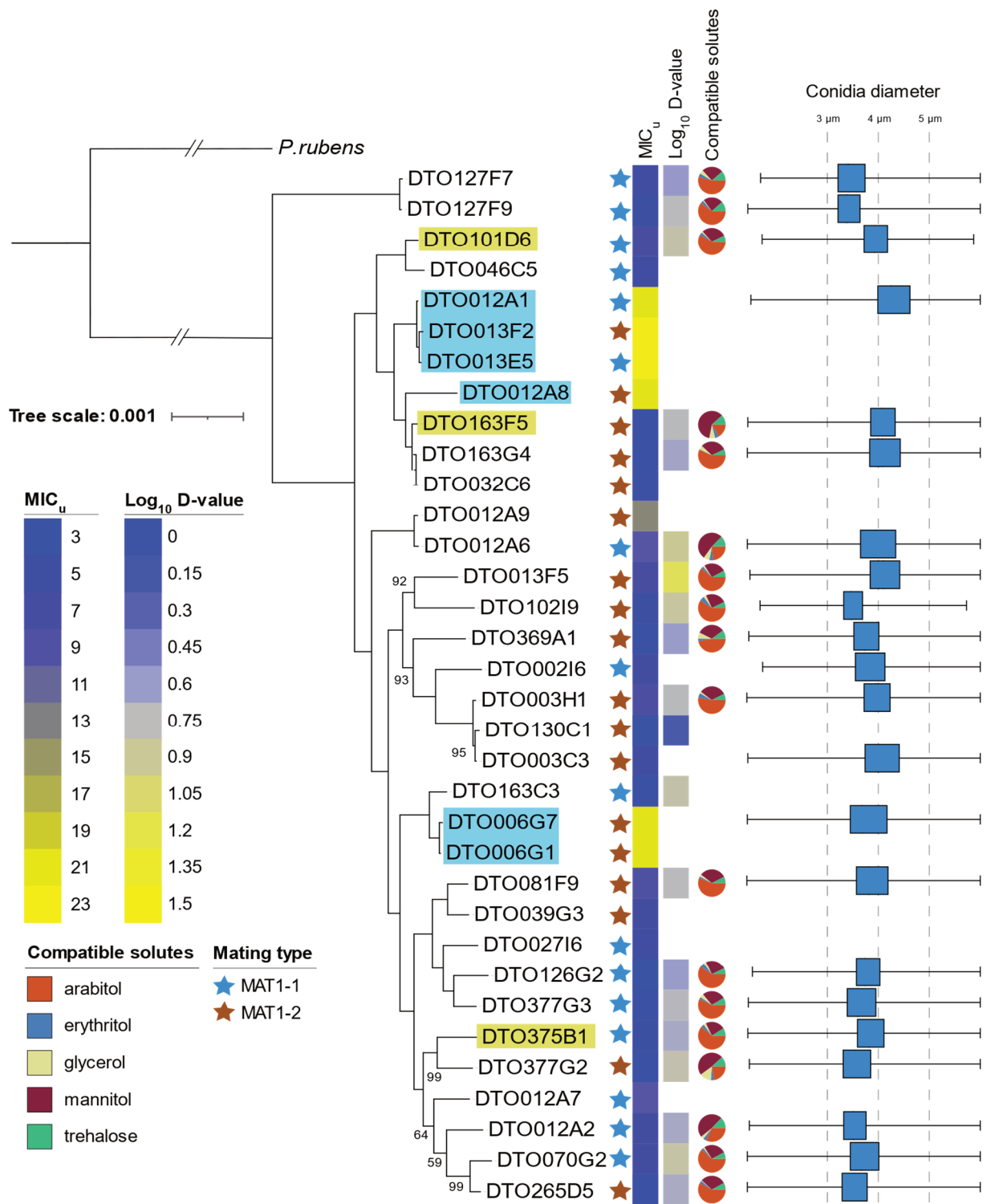
Figure 1. Phylogenetic tree of the 34 *P. roqueforti* strains used in this study. The tree is based on 6923 single-copy orthologous genes and was constructed using RAxML (Chapter 6). The genome of *P. rubens* (van den Berg et al., 2008) was used as outgroup. Bootstrap values <100 are indicated. Mating type, sorbic acid resistance (MIC$_u$), log$_{10}$ D-value and polyol composition of the conidia and spore diameter are indicated for each strain. Strains shaded blue contain the *SORBUS* cluster and those in yellow were isolated from blue-veined cheeses.

The genome-wide association study described in **Chapter 6** was also used to study genomic differences between groups of heat-resistant and heat-sensitive strains based on the data from **Chapter 5**. However this did not reveal genes or SNPs strongly correlated to thermal resistance. This might be explained by the variability in heat resistance compared to that of sorbic acid resistance. The $\log_{10}$ D-values of *P. roqueforti* are normally distributed, whereas sorbic acid resistance splits the strains in two populations (bimodal distribution). This suggests that thermal resistance is influenced by various mechanisms and is more complex than sorbic acid resistance regulation.

Transcriptome analysis of the R-type *P. roqueforti* isolate DTO006G7 revealed that the sorbic acid resistance associated genes (*cdcA*, *padA* and *sdrA*) are not higher expressed on sorbic acid. In fact, expression of *cdcA* (g12065) and *cdcC* (g12040), which show >70 % homology to the *A. niger cdcA,* was reduced (as low as -1.5 $\log_2$FC) when exposed to sorbic acid. This is in contrast with previous transcriptome and qRT-PCR studies on the expression of these genes in *A. niger* and *A. fumigatus* (Lubbers et al., 2019; Plumridge et al., 2010). With the expression analysis performed for the S-type strain, we aimed to identify genes correlated to sorbic acid resistance which have not yet been described previously. Despite the lack of the SORBUS cluster in this strain, its MIC value does not differ much from those observed in other fungal species (e.g. *A. niger* and *A. fumigatus*) (Geoghegan et al., 2020). An enrichment analysis revealed that the functional annotation 'secreted protein' was over-represented in the transcripts with a similar expression profile for R- and S-type strains.
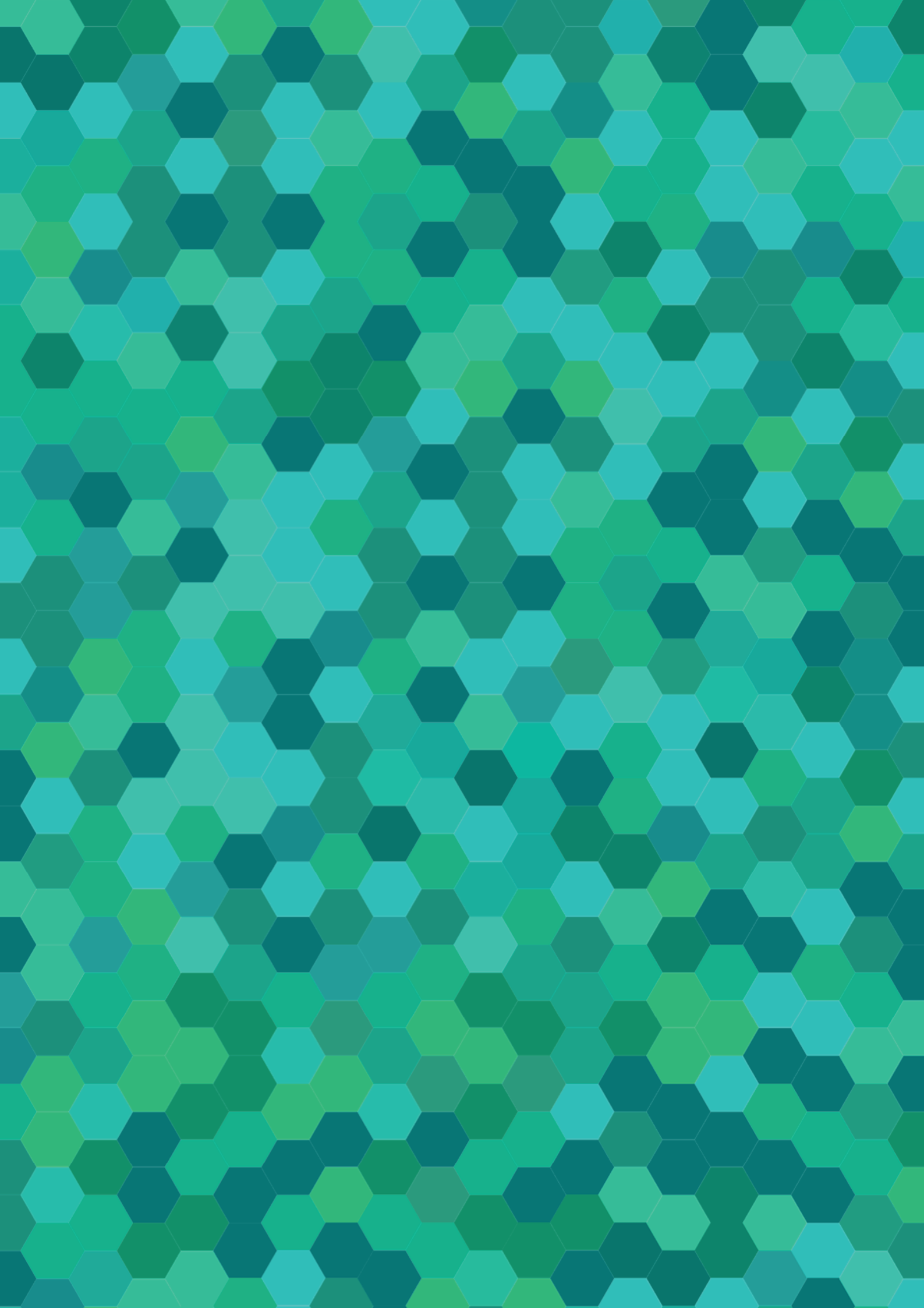
Appendix

References

Ackermann, M. (2015). A functional perspective on phenotypic heterogeneity in microorganisms. *Nature Reviews Microbiology*, *13*(8), 497–508. https://doi.org/10.1038/nrmicro3491

Aimanianda, V., Bayry, J., Bozza, S., Kniemeyer, O., Perruccio, K., Elluru, S. R., Clavaud, C., Paris, S., Brakhage, A. A., Kaveri, S. V., Romani, L., & Latgé, J. P. (2009). Surface hydrophobin prevents immune recognition of airborne fungal spores. *Nature*, *460*(7259), 1117–1121. https://doi.org/10.1038/nature08264

Alexandratos, Nikos & Bruinsma, J. (2012). WORLD AGRICULTURE TOWARDS 2030 / 2050 The 2012 Revision. *ESA Working Paper*, *12*(12), 146. www.fao.org/economic/esa

Amiri, A., Cholodowski, D., & Bompeix, G. (2005). Adhesion and germination of waterborne and airborne conidia of *Penicillium expansum* to apple and inert surfaces. *Physiological and Molecular Plant Pathology*, *67*(1), 40–48. https://doi.org/10.1016/j.pmpp.2005.07.003

Aran, N., & Eke, D. (1987). Mould mycoflora of Kaşar cheese at the stage of consumption. *Food Microbiology*, *4*(2), 101–104. https://doi.org/10.1016/0740-0020(87)90024-4

Arentshorst, M., Ram, A. F. J., & Meyer, V. (2012). Using non-homologous end-joining-deficient strains for functional gene analyses in filamentous fungi. In M. Bolton & B. Thomma (Eds.), *Plant Fungal Pathogens* (Issue 835, pp. 133–150). Humana Press. https://doi.org/https://doi.org/10.1007/978-1-61779-501-5_9

Aryani, D. C., den Besten, H. M. W., Hazeleger, W. C., & Zwietering, M. H. (2015). Quantifying variability on thermal resistance of *Listeria monocytogenes*. *International Journal of Food Microbiology*, *193*, 130–138. https://doi.org/10.1016/j.ijfoodmicro.2014.10.021

Aryani, D. C., den Besten, H. M. W., & Zwietering, M. H. (2016). Quantifying variability in growth and thermal inactivation kinetics of *Lactobacillus plantarum*. *Applied and Environmental Microbiology*, *82*(16), 4896–4908. https://doi.org/10.1128/AEM.00277-16

Baltussen, T. J. H., Coolen, J. P. M., Zoll, J., Verweij, P. E., & Melchers, W. J. G. (2018). Gene co-expression analysis identifies gene clusters associated with isotropic and polarized growth in *Aspergillus fumigatus* conidia. *Fungal Genetics and Biology*, *116*(October 2017), 62–72. https://doi.org/10.1016/j.fgb.2018.04.013

Bankevich, A., Nurk, S., Antipov, D., Gurevich, A. A., Dvorkin, M., Kulikov, A. S., Lesin, V. M., Nikolenko, S. I., Pham, S., Prjibelski, A. D., Pyshkin, A. V., Sirotkin, A. V., Vyahhi, N., Tesler, G., Alekseyev, M. A., & Pevzner, P. A. (2012). SPAdes: A new genome assembly algorithm and its applications to single-cell sequencing. *Journal of Computational Biology*, *19*(5), 455–477. https://doi.org/10.1089/cmb.2012.0021

Bao, W., Kojima, K. K., & Kohany, O. (2015). Repbase Update, a database of repetitive elements in eukaryotic genomes. *Mobile DNA*, *6*(1), 462–467. https://doi.org/10.1186/s13100-015-0041-9

Beever, R. E., & Laracy, E. P. (1986). Osmotic adjustment in the filamentous fungus *Aspergillus nidulans*. *Journal of Bacteriology*, *168*(3), 1358–1365. https://doi.org/10.1128/jb.168.3.1358-1365.1986

Benito, B., Garciadeblás, B., Schreier, P., & Rodríguez-Navarro, A. (2004). Novel P-type ATPases mediate high-affinity potassium or sodium uptake in fungi. *Eukaryotic Cell*, *3*(2), 359–368. https://doi.org/10.1128/EC.3.2.359-368.2004

Bennett, J. W. (2010). An overview of the genus *Aspergillus*, p 1--17. *Aspergillus Molecular Biology and Genomics. Caister Academic Press, Norfolk, United Kingdom*.

Beuchat, L. R. (1986). Extraordinary heat resistance of *Talaromyces flavus* and *Neosartorya fischeri* ascospores in fruit products. *Journal of Food Science*, *51*(6), 1506–1510. https://doi.org/10.1111/j.1365-2621.1986.tb13846.x

Beygelzimer, A., Kakadet, S., Langford, J., & Shengqiao, L. (2019). *Package "FNN" fast nearest neighbor search algorithms and applications*. https://cran.r-project.org/package=FNN

Blank, G., Yang, R., & Scanlon, M. G. (1998). Influence of sporulation a(w) on heat resistance and germination of *Penicillium roqueforti* spores. *Food Microbiology*, *15*(2), 151–156. https://doi.org/10.1006/fmic.1997.0154

Blaszyk, M., Blank, G., Holley, R., & Chong, J. (1998). Reduced water activity during sporogenesis in selected *penicillia*: Impact on spore quality. *Food Research International*, *31*(6–7), 503–509. https://doi.org/10.1016/S0963-9969(99)00019-8

Bleichrodt, R., Vinck, A., Krijgsheld, P., van Leeuwen, M. R., Dijksterhuis, J., & Wösten, H. A. B. (2013). Cytosolic streaming in vegetative mycelium and aerial structures of *Aspergillus niger*. *Studies in Mycology*, *74*, 31–46. https://doi.org/10.3114/sim0007

Bondi, M., Messi, P., Halami, P. M., Papadopoulou, C., & de Niederhausern, S. (2014). Emerging microbial concerns in food safety and new control measures. *BioMed Research International*, *2014*, 1–3. https://doi.org/10.1155/2014/251512

Bos, C. J., Debets, A. J. M., Swart, K., Huybers, A., Kobus, G., & Slakhorst, S. M. (1988). Genetic analysis and the construction of master strains for assignment of genes to six linkage groups in *Aspergillus niger*. *Current Genetics*, *14*(5), 437–443. https://doi.org/10.1007/BF00521266

Broberg, A., Jacobsson, K., Ström, K., & Schnürer, J. (2007). Metabolite profiles of lactic acid bacteria in grass silage. *Applied and Environmental Microbiology*, *73*(17), 5547–5552. https://doi.org/10.1128/AEM.02939-06

Bröker, U., Spicher, G., & Ahrens, E. (1987a). Zur Frage der Hitzeresistenz der Erreger der Schimmelbildung bei Backwaren. 2. Mitteilung: Einfluss endogener Faktoren auf die Hitzeresistenz von Schimmelsporen. *Getreide, Mehl Und Brot*, *41*(9), 278–284.

Bröker, U., Spicher, G., & Ahrens, E. (1987b). Zur Frage der Hitzeresistenz der Erreger der Schimmelbildung bei Backwaren. 3. Mitteilung: Einfluss exogener Faktoren auf die Hitzeresistenz von Schimmelsporen. *Getreide, Mehl Und Brot*, *41*(11), 344–355.

Brookes, G., & Barfoot, P. (2020). GM crop technology use 1996-2018: farm income and production impacts. *GM Crops and Food*, *11*(4), 242–261. https://doi.org/10.1080/21645698.2020.1779574

Bullerman, L. B. (1985). Effects of potassium sorbate on growth and ochratoxin production by *Aspergillus ochraceus* and *Penicillium* species. *Journal of Food Protection*, *48*(2), 162–165. https://doi.org/10.4315/0362-028X-48.2.162

Chaky, J., Anderson, K., Moss, M., & Vaillancourt, L. (2001). Surface hydrophobicity and surface rigidity induce spore germination in *Colletotrichum graminicola*. *Phytopathology*, *91*(6), 558–564. https://doi.org/10.1094/PHYTO.2001.91.6.558

Cheeseman, K., Ropars, J., Renault, P., Dupont, J., Gouzy, J., Branca, A., Abraham, A. L., Ceppi, M., Conseiller, E., Debuchy, R., Malagnac, F., Goarin, A., Silar, P., Lacoste, S., Sallet, E., Bensimon, A., Giraud, T., & Brygoo, Y. (2014). Multiple recent horizontal transfers of a large genomic region in cheese making fungi. *Nature Communications*, *5*. https://doi.org/10.1038/ncomms3876

Chojak-Koźniewska, J., Kuźniak, E., & Zimny, J. (2018). The effects of combined abiotic and pathogen stress in plants: Insights from salinity and pseudomonas syringae pv lachrymans interaction in cucumber. *Frontiers in Plant Science*, *871*(November), 1691. https://doi.org/10.3389/fpls.2018.01691

Collins, K. D. (1997). Charge density-dependent strength of hydration and biological structure. *Biophysical Journal*, *72*(1), 65–76. https://doi.org/10.1016/S0006-3495(97)78647-8

Coton, E., Coton, M., Hymery, N., Mounier, J., & Jany, J. L. (2020). *Penicillium roqueforti*: an overview of its genetics, physiology, metabolism and biotechnological applications. *Fungal Biology Reviews*, *34*(2), 59–73. https://doi.org/10.1016/j.fbr.2020.03.001

Cray, J. A., Russell, J. T., Timson, D. J., Singhal, R. S., & Hallsworth, J. E. (2013). A universal measure of chaotropicity and kosmotropicity. *Environmental Microbiology*, *15*(1), 287–296. https://doi.org/10.1111/1462-2920.12018

d'Enfert, C. (1997). Fungal spore germination: Insights from the molecular genetics of *Aspergillus nidulans* and *Neurospora crassa*. *Fungal Genetics and Biology*, *21*(2), 163–172. https://doi.org/10.1006/fgbi.1997.0975

Dantigny, P. (2016). Relevant issues in predictive mycology. *Current Opinion in Food Science*, *11*, 29–33. https://doi.org/10.1016/j.cofs.2016.08.011

Dantigny, P., Nanguy, S. P. M., Judet-Correia, D., & Bensoussan, M. (2011). A new model for germination of fungi. *International Journal of Food Microbiology*, *146*(2), 176–181. https://doi.org/10.1016/j.ijfoodmicro.2011.02.022

de Bekker, C., Ohm, R. A., Evans, H. C., Brachmann, A., & Hughes, D. P. (2017). Ant-infecting *Ophiocordyceps* genomes reveal a high diversity of potential behavioral manipulation genes and a possible major role for enterotoxins. *Scientific Reports*, *7*(1), 1–13. https://doi.org/10.1038/s41598-017-12863-w

den Besten, H. M. W., Berendsen, E. M., Wells-Bennik, M. H. J., Straatsma, H., & Zwietering, M. H. (2017). Two complementary approaches to quantify variability in heat resistance of spores of *Bacillus subtilis*. *International Journal of Food Microbiology*, *253*(April), 48–53. https://doi.org/10.1016/j.ijfoodmicro.2017.04.014

den Besten, H. M. W., Wells-Bennik, M. H. J., & Zwietering, M. H. (2018). Natural diversity in heat resistance of bacteria and bacterial spores: impact on food safety and quality. *Annual Review of Food Science and Technology*, *9*, 383–410. https://doi.org/10.1146/annurev-food-030117-012808

Dijksterhuis, J. (2017). The fungal spore and food spoilage. *Current Opinion in Food Science*, *17*(2), 68–74. https://doi.org/10.1016/j.cofs.2017.10.006

Dijksterhuis, J., & Teunissen, P. G. M. (2004). Dormant ascospores of *Talaromyces macrosporus* are activated to germinate after treatment with ultra high pressure. *Journal of Applied Microbiology*, *96*(1), 162–169. https://doi.org/10.1046/j.1365-2672.2003.02133.x

Dijksterhuis, J. (2019). Fungal spores: Highly variable and stress-resistant vehicles for distribution and spoilage. *Food Microbiology*, *81*(November 2018), 2–11. https://doi.org/10.1016/j.fm.2018.11.006

Dijksterhuis, J., & de Vries, R. P. (2006). Compatible solutes and fungal development. *The Biochemical Journal*, *399*(2), e3. https://doi.org/10.1042/BJ20061229

Dijksterhuis, J., Meijer, M., van Doorn, T., Samson, R., & Rico-Munoz, E. (2018). Inactivation of stress-resistant ascospores of Eurotiales by industrial sanitizers. International Journal of Food Microbiology, 285, 27–33. https://doi.org/10.1016/j.ijfoodm), 27–33. https://doi.org/10.1016/j.ijfoodmicro.2018.06.018

dos Santos, J. L. P., Silva, B. S., Furtado, M. M., Morassi, L. L. P., Vermeulen, A., & Sant'Ana, A. S. (2018). The application of growth-no growth models to directly assess the stability of wholemeal multigrain bread towards *Penicillium paneum* LMQA-002 and *Paecilomyces variotii* LMQA-001. *Lwt*, *97*(July), 231–237. https://doi.org/10.1016/j.lwt.2018.07.004

Dubey, M. K., Aamir, M., Kaushik, M. S., Khare, S., Meena, M., Singh, S., & Upadhyay, R. S. (2018). PR Toxin - biosynthesis, genetic regulation, toxicological potential, prevention and control measures: Overview and challenges. *Frontiers in Pharmacology*, *9*(MAR), 288. https://doi.org/10.3389/fphar.2018.00288

Dumas, E., Feurtey, A., Rodríguez de la Vega, R. C., Le Prieur, S., Snirc, A., Coton, M., Thierry, A., Coton, E., Le Piver, M., Roueyre, D., Ropars, J., Branca, A., & Giraud, T. (2020). Independent domestication events in the blue-cheese fungus *Penicillium roqueforti*. *Molecular Ecology*, *29*(14), 2639–2660. https://doi.org/10.1111/mec.15359

Kang, S. E., Celia, B. N., Bensasson, D., & Momany, M. (2021). Sporulation environment drives phenotypic variation in the pathogen *Aspergillus fumigatus*. *G3 Genes|Genomes|Genetics*. https://doi.org/10.1093/g3journal/jkab208

Eayre, C. G., Jaffee, B. A., & Zehr, E. I. (1990). Influence of potassium on spore germination in the nematophagous fungus, *Hirsutella rhossiliensis*. *Journal of Nematology*, *22*(4), 612–613.

El-Gebali, S., Mistry, J., Bateman, A., Eddy, S. R., Luciani, A., Potter, S. C., Qureshi, M., Richardson, L. J., Salazar, G. A., Smart, A., Sonnhammer, E. L. L., Hirsh, L., Paladin, L., Piovesan, D., Tosatto, S. C. E., & Finn, R. D. (2019). The Pfam protein families database in 2019. *Nucleic Acids Research*, *47*(D1), D427–D432. https://doi.org/10.1093/nar/gky995

Emms, D. M., & Kelly, S. (2019). OrthoFinder: Phylogenetic orthology inference for comparative genomics. *Genome Biology*, *20*(1), 1–14. https://doi.org/10.1186/s13059-019-1832-y

Fernández-Bodega, M. A., Mauriz, E., Gómez, A., & Martín, J. F. (2009). Proteolytic activity, mycotoxins and andrastin A in *Penicillium roqueforti* strains isolated from Cabrales, Valdeón and Bejes-Tresviso local varieties of blue-veined cheeses. *International Journal of Food Microbiology*, *136*(1), 18–25. https://doi.org/10.1016/j.ijfoodmicro.2009.09.014

Fillinger, S., Chaveroche, M. K., van Dijck, P., de Vries, R., Ruijter, G., Thevelein, J., & D'Enfert, C. (2001). Trehalose is required for the acquisition of tolerance to a variety of stresses in the filamentous fungus *Aspergillus nidulans*. *Microbiology*, *147*(7), 1851–1862. https://doi.org/10.1099/00221287-147-7-1851

Filtenborg, O., Frisvad, J. C., & Thrane, U. (1996). Moulds in food spoilage. *International Journal of Food Microbiology*, *33*(1), 85–102. https://doi.org/10.1016/0168-1605(96)01153-1

Fontaine, K., Hymery, N., Lacroix, M. Z., Puel, S., Puel, O., Rigalma, K., Gaydou, V., Coton, E., & Mounier, J. (2015). Influence of intraspecific variability and abiotic factors on mycotoxin production in *Penicillium roqueforti*. *International Journal of Food Microbiology*, *215*, 187–193. https://doi.org/10.1016/j.ijfoodmicro.2015.07.021

Fortwendel, J. R., Fuller, K. K., Stephens, T. J., Bacon, W. C., Askew, D. S., & Rhodes, J. C. (2008). *Aspergillus fumigatus* (RasA) regulates asexual development and cell wall integrity. *Eukaryotic Cell*, *7*(9), 1530–1539. https://doi.org/10.1128/ec.00080-08

Fortwendel, J. R., Panepinto, J. C., Seitz, A. E., Askew, D. S., & Rhodes, J. C. (2004). *Aspergillus fumigatus* rasA and rasB regulate the timing and morphology of asexual development. *Fungal Genetics and Biology*, *41*(2), 129–139. https://doi.org/10.1016/j.fgb.2003.10.004

Fredborg, M., Andersen, K. R., Jørgensen, E., Droce, A., Olesen, T., Jensen, B. B., Rosenvinge, F. S., & Sondergaard, T. E. (2013). Real-time optical antimicrobial susceptibility testing. *Journal of Clinical Microbiology*, *51*(7), 2047–2053. https://doi.org/10.1128/jcm.00440-13

Fujikawa, H., & Itoh, T. (1996). Tailing of thermal inactivation curve of *Aspergillus niger* spores. *Applied and Environmental Microbiology*, *62*(10), 3745–3749. https://doi.org/10.1128/aem.62.10.3745-3749.1996

Fujikawa, H., Morozumi, S., Smerage, G. H., & Teixeira, A. A. (2000). Comparison of capillary and test tube procedures for analysis of thermal inactivation kinetics of mold spores. *Journal of Food Protection*, *63*(10), 1404–1409. https://doi.org/10.4315/0362-028X-63.10.1404

Fung, F., & Clark, R. F. (2004). Health effects of mycotoxins: A toxicological overview. *Journal of Toxicology - Clinical Toxicology*, *42*(2), 217–234. https://doi.org/10.1081/CLT-120030947

Galagan, J. E., Calvo, S. E., Cuomo, C., Ma, L. J., Wortman, J. R., Batzoglou, S., Lee, S. I., Baştürkmen, M., Spevak, C. C., Clutterbuck, J., Kapitonov, V., Jurka, J., Scazzocchio, C., Farman, M., Butler, J., Purcell, S., Harris, S., Braus, G. H., Draht, O., … Birren, B. W. (2005). Sequencing of *Aspergillus nidulans* and comparative analysis with *A. fumigatus* and *A. oryzae*. *Nature*, *438*(7071), 1105–1115. https://doi.org/10.1038/nature04341

Gallo, A., Giuberti, G., Bertuzzi, T., Moschini, M., & Masoero, F. (2015). Study of the effects of PR toxin, mycophenolic acid and roquefortine C on in vitro gas production parameters and their stability in the rumen environment. *Journal of Agricultural Science*, *153*(1), 163–176. https://doi.org/10.1017/S0021859614000343

Garnier, L., Valence, F., & Mounier, J. (2017). Diversity and control of spoilage fungi in dairy products: an update. *Microorganisms*, *5*(3), 42. https://doi.org/10.3390/microorganisms5030042

Geoghegan, I. A., Stratford, M., Bromley, M., Archer, D. B., & Avery, S. V. (2020). Weak acid resistance a (WarA), a novel transcription factor required for regulation of weak-acid resistance and spore-spore heterogeneity in *Aspergillus niger*. *MSphere*, *5*(1), 1–39. https://doi.org/10.1101/788141

Gillot, G., Jany, J. L., Poirier, E., Maillard, M. B., Debaets, S., Thierry, A., Coton, E., & Coton, M. (2017). Functional diversity within the *Penicillium roqueforti* species. *International Journal of Food Microbiology*, *241*, 141–150. https://doi.org/10.1016/j.ijfoodmicro.2016.10.001

Gougouli, M., & Koutsoumanis, K. P. (2010). Modelling growth of *Penicillium expansum* and *Aspergillus niger* at constant and fluctuating temperature conditions. *International Journal of Food Microbiology*, *140*(2–3), 254–262. https://doi.org/10.1016/j.ijfoodmicro.2010.03.021

Gu, Z., Eils, R., & Schlesner, M. (2016). Complex heatmaps reveal patterns and correlations in multidimensional genomic data. *Bioinformatics*, *32*(18), 2847–2849. https://doi.org/10.1093/bioinformatics/btw313

Guijarro, B., Melgarejo, P., & De Cal, A. (2007). Effect of stabilizers on the shelf-life of *Penicillium frequentans* conidia and their efficacy as a biological agent against peach brown rot. *International Journal of Food Microbiology*, *113*(2), 117–124. https://doi.org/10.1016/j.ijfoodmicro.2006.06.024

Gustavsson, J., Cederberg, C., & Sonesson, U. (2010). Global food losses and food waste: Extent, causes and prevention. In *Organization* (p. 38). http://www.fao.org/fileadmin/user_upload/ags/publications/GFL_web.pdf

Hagiwara, D., Sakai, K., Suzuki, S., Umemura, M., Nogawa, T., Kato, N., Osada, H., Watanabe, A., Kawamoto, S., Gonoi, T., & Kamei, K. (2017). Temperature during conidiation affects stress tolerance, pigmentation, and trypacidin accumulation in the conidia of the airborne pathogen *Aspergillus fumigatus*. *PLoS ONE*, *12*(5), e0177050. https://doi.org/10.1371/journal.pone.0177050

Hall, B. G., Acar, H., Nandipati, A., & Barlow, M. (2014). Growth rates made easy. *Molecular Biology and Evolution*, *31*(1), 232–238. https://doi.org/10.1093/molbev/mst187

Hallsworth, J. E., & Magan, N. (1995). Manipulation of intracellular glycerol and erythritol enhances germination of conidia at low water availability. *Microbiology*, *141*(5), 1109–1115. https://doi.org/10.1099/13500872-141-5-1109

Hallsworth, J. E., & Magan, N. (1996). Culture age, temperature, and ph affect the polyol and trehalose contents of fungal propagules. *Applied and Environmental Microbiology*, *62*(7), 2435–2442. https://doi.org/10.1128/aem.62.7.2435-2442.1996

Hameed, A. A. A., Yasser, I. H., & Khoder, I. M. (2004). *Indoor air quality during renovation actions: a case study*. *6*(9), 740. https://doi.org/10.1039/b402995j

Hanci, F., & Cebeci, E. (2015). Comparison of salinity and drought stress effects on some morphological and physiological parameters in onion (*Allium cepa l.*) during early growth phase. *Bulgarian Journal of Agricultural Science*, *21*(6), 1204–1210.

Hawksworth, D. L. (2011). Naming *Aspergillus* species: progress towards one name for each species. *Medical Mycology*, *49*(SUPPL. 1), S70--S76. https://doi.org/10.3109/13693786.2010.504753

Hayer, K., Stratford, M., & Archer, D. B. (2013). Structural features of sugars that trigger or support conidial germination in the filamentous fungus *Aspergillus niger*. *Applied and Environmental Microbiology*, *79*(22), 6924–6931. https://doi.org/10.1128/AEM.02061-13

Hayer, K., Stratford, M., & Archer, D. B. (2014). Germination of *Aspergillus niger* conidia is triggered by nitrogen compounds related to L-amino acids. *Applied and Environmental Microbiology*, *80*(19), 6046–6053. https://doi.org/10.1128/AEM.01078-14

Hewitt, S. K., Foster, D. S., Dyer, P. S., & Avery, S. V. (2016). Phenotypic heterogeneity in fungi: Importance and methodology. *Fungal Biology Reviews*, *30*(4), 176–184. https://doi.org/10.1016/j.fbr.2016.09.002

Hoff, K. J., Lange, S., Lomsadze, A., Borodovsky, M., & Stanke, M. (2016). BRAKER1: Unsupervised RNA-Seq-based genome annotation with GeneMark-ET and AUGUSTUS. *Bioinformatics*, *32*(5), 767–769. https://doi.org/10.1093/bioinformatics/btv661

Hosonuma, N., Herold, M., De Sy, V., De Fries, R. S., Brockhaus, M., Verchot, L., Angelsen, A., & Romijn, E. (2012). An assessment of deforestation and forest degradation drivers in developing countries. *Environmental Research Letters*, *7*(4), 44009. https://doi.org/10.1088/1748-9326/7/4/044009

Houbraken, J., Kocsubé, S., Visagie, C. M., Yilmaz, N., Wang, X. C., Meijer, M., Kraak, B., Hubka, V., Bensch, K., Samson, R. A., & Frisvad, J. C. (2020). Classification of *Aspergillus*, *Penicillium*, *Talaromyces* and related genera (*Eurotiales*): An overview of families, genera, subgenera, sections, series and species. *Studies in Mycology*, *95*, 5–169. https://doi.org/10.1016/j.simyco.2020.05.002

Houbraken, J., Samson, R. A., & Frisvad, J. C. (2005). *Byssochlamys*: Significance of heat resistance and mycotoxin production. In *Advances in Experimental Medicine and Biology* (Vol. 571, pp. 211–224). Springer. https://doi.org/10.1007/0-387-28391-9_14

Huang, Y., Wilson, M., Chapman, B., & Hocking, A. D. (2010). Evaluation of the efficacy of four weak acids as antifungal preservatives in low-acid intermediate moisture model food systems. *Food Microbiology*, *27*(1), 33–36. https://doi.org/10.1016/j.fm.2009.07.017

Hussein, H. S., & Brasel, J. M. (2001). Toxicity, metabolism, and impact of mycotoxins on humans and animals. *Toxicology*, *167*(2), 101–134. https://doi.org/10.1016/S0300-483X(01)00471-1

Ijadpanahsaravi, M., Punt, M., Wösten, H. A. B., & Teertstra, W. R. (2021). Minimal nutrient requirements for induction of germination of *Aspergillus niger* conidia. *Fungal Biology*, *125*(3), 231–238. https://doi.org/10.1016/j.funbio.2020.11.004

Joardder, M. U. H., & Masud, M. H. (2019). Food preservation in developing countries: Challenges and solutions. In *Food Preservation in Developing Countries: Challenges and Solutions*. Springer. https://doi.org/10.1007/978-3-030-11530-2

Kaczmarek, M., Avery, S. V., & Singleton, I. (2019). Microbes associated with fresh produce: Sources, types and methods to reduce spoilage and contamination. *Advances in Applied Microbiology*, *107*, 29–82. https://doi.org/10.1016/bs.aambs.2019.02.001

Kalai, S., Anzala, L., Bensoussan, M., & Dantigny, P. (2017). Modelling the effect of temperature, pH, water activity, and organic acids on the germination time of *Penicillium camemberti* and *Penicillium roqueforti* conidia. *International Journal of Food Microbiology*, *240*, 124–130. https://doi.org/10.1016/j.ijfoodmicro.2016.03.024

Kim, D., Langmead, B., & Salzberg, S. L. (2015). HISAT: A fast spliced aligner with low memory requirements. *Nature Methods*, *12*(4), 357–360. https://doi.org/10.1038/nmeth.3317

Kim, S. X., Çamdere, G., Hu, X., Koshland, D., & Tapia, H. (2018). Synergy between the small intrinsically disordered protein Hsp12 and trehalose sustain viability after severe desiccation. *ELife*, *7*, 1–20. https://doi.org/10.7554/eLife.38337

Klassen-Fischer, M. K. (2006). Fungi as Bioweapons. *Clinics in Laboratory Medicine*, *26*(2), 387–395. https://doi.org/10.1016/j.cll.2006.03.008

Krebs, H. A., Wiggins, D., Stubbs, M., Sols, A., & Bedoya, F. (1983). Studies on the mechanism of the antifungal action of benzoate. *Biochemical Journal*, *214*(3), 657–663. https://doi.org/10.1042/bj2140657

Krijgsheld, P., Bleichrodt, R., van Veluw, G. J., Wang, F., Müller, W. H., Dijksterhuis, J., & Wösten, H. A. B. (2013). Development in *Aspergillus*. *Studies in Mycology*, *74*, 1–29. https://doi.org/10.3114/sim0006

Kumar, S., Stecher, G., & Tamura, K. (2016). MEGA7: Molecular Evolutionary Genetics Analysis version 7.0 for bigger datasets. *Molecular Biology and Evolution*, *33*(7), 1870–1874. https://doi.org/10.1093/molbev/msw054

Kunz, B. (1981). Untersuchungen über den Einfluß der Temperatur auf Konidiensuspensionen ausgewählter Penicillienspecies. *Food / Nahrung*, *25*(2), 185–191. https://doi.org/10.1002/food.19810250209

Kuo, K. C., & Hoch, H. C. (1996). Germination of *Phyllosticta ampelicida* Pycnidiospores: Prerequisite of adhesion to the substratum and the relationship of substratum wettability. *Fungal Genetics and Biology*, *20*(1), 18–29. https://doi.org/10.1006/fgbi.1996.0005

Lafon, A., Seo, J. A., Han, K. H., Yu, J. H., & D'Enfert, C. (2005). The heterotrimeric G-protein GanB(α)-SfaD(β)-GpgA(γ) is a carbon source sensor involved in early cAMP-dependent germination in *Aspergillus nidulans*. *Genetics*, *171*(1), 71–80. https://doi.org/10.1534/genetics.105.040584

Lamarre, C., Sokol, S., Debeaupuis, J. P., Henry, C., Lacroix, C., Glaser, P., Coppée, J. Y., François, J. M., & Latgé, J. P. (2008). Transcriptomic analysis of the exit from dormancy of *Aspergillus fumigatus* conidia. *BMC Genomics*, *9*(1), 417. https://doi.org/10.1186/1471-2164-9-417

Lambert, R. J., & Stratford, M. (1999). Weak-acid preservatives: Modelling microbial inhibition and response. *Journal of Applied Microbiology*, *86*(1), 157–164. https://doi.org/10.1046/j.1365-2672.1999.00646.x

Lambou, K., Pennati, A., Valsecchi, I., Tada, R., Sherman, S., Sato, H., Beau, R., Gadda, G., & Latgé, J. P. (2013). Pathway of glycine betaine biosynthesis in *Aspergillus fumigatus*. *Eukaryotic Cell*, *12*(6), 853–863. https://doi.org/10.1128/EC.00348-12

Lau, G. W., & Hamer, J. E. (1998). Acropetal: A genetic locus required for conidiophore architecture and pathogenicity in the rice blast fungus. *Fungal Genetics and Biology*, *24*(1–2), 228–239. https://doi.org/10.1006/fgbi.1998.1053

Letunic, I., & Bork, P. (2021). Interactive Tree Of Life (iTOL) v5: an online tool for phylogenetic tree display and annotation. *Nucleic Acids Research*, 1–4. https://doi.org/10.1093/nar/gkab301

Lianou, A., & Koutsoumanis, K. P. (2013). Strain variability of the behavior of foodborne bacterial pathogens: A review. *International Journal of Food Microbiology*, *167*(3), 310–321. https://doi.org/10.1016/j.ijfoodmicro.2013.09.016

Lianou, A., Nychas, G. J. E., & Koutsoumanis, K. P. (2020). Strain variability in biofilm formation: A food safety and quality perspective. *Food Research International*, *137*(February), 109424. https://doi.org/10.1016/j.foodres.2020.109424

Liewen, M. B., & Marth, E. H. (1984). Inhibition of *Penicillia* and *Aspergilli* by potassium sorbate. *Journal of Food Protection*, *47*(7), 554–556. https://doi.org/10.4315/0362-028x-47.7.554

Liewen, M. B., & Marth, E. H. (1985). Viability and ATP content of conidia of sorbic acid-sensitive and-resistant strains of *Penicillium roqueforti* after exposure to sorbic acid. *Applied Microbiology and Biotechnology*, *21*(1–2), 113–117. https://doi.org/10.1007/BF00252372

Llewellyn, D. (2018). Does global agriculture need another green revolution? *Engineering*, *4*(4), 449–451. https://doi.org/10.1016/j.eng.2018.07.017

Lopez-Delisle, L., Rabbani, L., Wolff, J., Bhardwaj, V., Backofen, R., Grüning, B., Ramírez, F., & Manke, T. (2021). pyGenomeTracks: reproducible plots for multivariate genomic datasets. *Bioinformatics (Oxford, England)*, *37*(3), 422–423. https://doi.org/10.1093/bioinformatics/btaa692

Love, M. I., Huber, W., & Anders, S. (2014). Moderated estimation of fold change and dispersion for RNA-seq data with DESeq2. *Genome Biology*, *15*(12), 1–21.

Lubbers, R. J. M., Dilokpimol, A., Navarro, J., Peng, M., Wang, M., Lipzen, A., Ng, V., Grigoriev, I. V, Visser, J., Hildén, K. S., & de Vries, R. P. (2019). Cinnamic acid and sorbic acid conversion are mediated by the same transcriptional regulator in *Aspergillus niger*. *Frontiers in Bioengineering and Biotechnology*, *7*(SEP), 249. https://doi.org/10.3389/fbioe.2019.00249

Lund, F., Filtenborg, O., & Frisvad, J. C. (1995). Associated mycoflora of cheese. *Food Microbiology*, *12*(C), 173–180. https://doi.org/10.1016/S0740-0020(95)80094-8

Lund, F., Filtenborg, O., Westall, S., & Frisvad, J. C. (1996). Associated mycoflora of rye bread. *Letters in Applied Microbiology*, *23*(4), 213–217. https://doi.org/10.1111/j.1472-765X.1996.tb00068.x

Magan, N., & Lacey, J. (1984). Effects of gas composition and water activity on growth of field and storage fungi and their interactions. *Transactions of the British Mycological Society*, *82*(2), 305–314. https://doi.org/10.1016/s0007-1536(84)80074-1

Mann, R. L., Kettlewell, P. S., & Jenkinson, P. (2004). Effect of foliar-applied potassium chloride on septoria leaf blotch of winter wheat. *Plant Pathology*, *53*(5), 653–659. https://doi.org/10.1111/j.1365-3059.2004.01063.x

Marchant, R., & White, M. F. (1966). Spore swelling and germination in *Fusarium culmorum*. *Journal of General Microbiology*, *42*(2), 237–244. https://doi.org/10.1099/00221287-42-2-237

Marth, E. H., Capp, C. M., Hasenzahl, L., Jackson, H. W., & Hussong, R. V. (1966). Degradation of potassium sorbate by *Penicillium* Species. *Journal of Dairy Science*, *49*(10), 1197–1205. https://doi.org/10.3168/jds.S0022-0302(66)88053-0

Meena, M., Divyanshu, K., Kumar, S., Swapnil, P., Zehra, A., Shukla, V., Yadav, M., & Upadhyay, R. S. (2019). Regulation of L-proline biosynthesis, signal transduction, transport, accumulation and its vital role in plants during variable environmental conditions. *Heliyon*, *5*(12), e02952. https://doi.org/10.1016/j.heliyon.2019.e02952

Melin, P., Stratford, M., Plummridge, A., & Archer, D. B. (2008). Auxotrophy for uridine increases the sensitivity of *Aspergillus niger* to weak-acid preservatives. *Microbiology*, *154*(4), 1251–1257. https://doi.org/10.1099/mic.0.2007/014332-0

Metselaar, K. I., den Besten, H. M. W., Abee, T., Moezelaar, R., & Zwietering, M. H. (2013). Isolation and quantification of highly acid resistant variants of *Listeria monocytogenes*. *International Journal of Food Microbiology*, *166*(3), 508–514. https://doi.org/10.1016/j.ijfoodmicro.2013.08.011

Mukai, N., Masaki, K., Fujii, T., Kawamukai, M., & Iefuji, H. (2010). PAD1 and FDC1 are essential for the decarboxylation of phenylacrylic acids in *Saccharomyces cerevisiae*. *Journal of Bioscience and Bioengineering*, *109*(6), 564–569. https://doi.org/10.1016/j.jbiosc.2009.11.011

Mullins, J., Hutcheson, P. S., & Slavin, R. G. (1984). *Aspergillus fumigatus* spore concentration in outside air: Cardiff and St Louis compared. *Clinical & Experimental Allergy*, *14*(4), 351–354. https://doi.org/10.1111/j.1365-2222.1984.tb02215.x

Naidu, A. S. (2000). Natural food antimicrobial systems. In *Natural Food Antimicrobial Systems*. CRC press. https://doi.org/10.1201/9781420039368

Nanguy, S. P. M., Perrier-Cornet, J. M., Bensoussan, M., & Dantigny, P. (2010). Impact of water activity of diverse media on spore germination of *Aspergillus* and *Penicillium* species. *International Journal of Food Microbiology*, *142*(1–2), 273–276. https://doi.org/10.1016/j.ijfoodmicro.2010.06.031

Nguyen Van Long, N., Vasseur, V., Coroller, L., Dantigny, P., Le Panse, S., Weill, A., Mounier, J., & Rigalma, K. (2017a). Temperature, water activity and pH during conidia production affect the physiological state and germination time of *Penicillium* species. *International Journal of Food Microbiology*, *241*, 151–160. https://doi.org/10.1016/j.ijfoodmicro.2016.10.022

Nguyen Van Long, N., Vasseur, V., Couvert, O., Coroller, L., Burlot, M., Rigalma, K., & Mounier, J. (2017b). Modeling the effect of modified atmospheres on conidial germination of fungi from dairy foods. *Frontiers in Microbiology*, *8*(OCT), 2109. https://doi.org/10.3389/fmicb.2017.02109

Nielsen, P. V., & Rios, R. (2000). Inhibition of fungal growth on bread by volatile components from spices and herbs, and the possible application in active packaging, with special emphasis on mustard essential oil. *International Journal of Food Microbiology*, *60*(2–3), 219–229. https://doi.org/10.1016/S0168-1605(00)00343-3

Nødvig, C. S., Nielsen, J. B., Kogle, M. E., & Mortensen, U. H. (2015). A CRISPR-Cas9 system for genetic engineering of filamentous fungi. *PLoS ONE*, *10*(7), 1–18. https://doi.org/10.1371/journal.pone.0133085

Novodvorska, M., Stratford, M., Blythe, M. J., Wilson, R., Beniston, R. G., & Archer, D. B. (2016). Metabolic activity in dormant conidia of *Aspergillus niger* and developmental changes during conidial outgrowth. *Fungal Genetics and Biology*, *94*, 23–31. https://doi.org/10.1016/j.fgb.2016.07.002

Osweiler, G. D. (2000). Mycotoxins. Contemporary issues of food animal health and productivity. *The Veterinary Clinics of North America. Food Animal Practice*, *16*(3), 511–530. https://doi.org/10.1016/S0749-0720(15)30084-0

Paiva, S., Devaux, F., Barbosa, S., Jacq, C., & Casal, M. (2004). Ady2p is essential for the acetate permease activity in the yeast *Saccharomyces cerevisiae*. *Yeast, 21*(3), 201–210. https://doi.org/10.1002/yea.1056

Patro, R., Duggal, G., Love, M. I., Irizarry, R. A., & Kingsford, C. (2017). Salmon provides fast and bias-aware quantification of transcript expression. *Nature Methods*, *14*(4), 417–419. https://doi.org/10.1038/nmeth.4197

Perfect, J. R., Tenor, J. L., Miao, Y., & Brennan, R. G. (2017). Trehalose pathway as an antifungal target. *Virulence*, *8*(2), 143–149. https://doi.org/10.1080/21505594.2016.1195529

Petzoldt, T. (2019). Package "growthrates" *estimate growth rates from experimental data*. https://cran.r-project.org/package=growthrates

Pitt, J. I., & Hocking, A. D. (1997). The ecology of fungal food spoilage. In *Fungi and Food Spoilage* (pp. 3–12). Springer. https://doi.org/10.1007/978-1-4615-6391-4_2

Pitt, J. I., & Hocking, A. D. (2009). Fungi and food spoilage. In *Fungi and Food Spoilage* (Vol. 519). Springer. https://doi.org/10.1007/978-0-387-92207-2

Plumridge, A., Hesse, S. J. A., Watson, A. J., Lowe, K. C., Stratford, M., & Archer, D. B. (2004). The weak acid preservative sorbic acid inhibits conidial germination and mycelial growth of *Aspergillus niger* through intracellular acidification. *Applied and Environmental Microbiology*, *70*(6), 3506–3511. https://doi.org/10.1128/AEM.70.6.3506-3511.2004

Plumridge, A., Melin, P., Stratford, M., Novodvorska, M., Shunburne, L., Dyer, P. S., Roubos, J. A., Menke, H., Stark, J., Stam, H., & Archer, D. B. (2010). The decarboxylation of the weak-acid preservative, sorbic acid, is encoded by linked genes in *Aspergillus* spp. *Fungal Genetics and Biology*, *47*(8), 683–692. https://doi.org/10.1016/j.fgb.2010.04.011

Plumridge, A., Stratford, M., Lowe, K. C., & Archer, D. B. (2008). The weak-acid preservative sorbic acid is decarboxylated and detoxified by a phenylacrylic acid decarboxylase, PadA1, in the spoilage mold *Aspergillus niger*. *Applied and Environmental Microbiology*, *74*(2), 550–552. https://doi.org/10.1128/AEM.02105-07

Popova, A. V., Hundertmark, M., Seckler, R., & Hincha, D. K. (2011). Structural transitions in the intrinsically disordered plant dehydration stress protein LEA7 upon drying are modulated by the presence of membranes. *Biochimica et Biophysica Acta - Biomembranes*, *1808*(7), 1879–1887. https://doi.org/10.1016/j.bbamem.2011.03.009

Price, A. L., Jones, N. C., & Pevzner, P. A. (2005). De novo identification of repeat families in large genomes. *Bioinformatics*, *21*(SUPPL. 1), i351--i358. https://doi.org/10.1093/bioinformatics/bti1018

Punt, M., van den Brule, T., Teertstra, W. R., Dijksterhuis, J., den Besten, H. M. W., Ohm, R. A., & Wösten, H. A. B. (2020). Impact of maturation and growth temperature on cell-size distribution, heat-resistance, compatible solute composition and transcription profiles of *Penicillium roqueforti* conidia. *Food Research International*, *136*(May), 109287. https://doi.org/10.1016/j.foodres.2020.109287

Purcell, S., Neale, B., Todd-Brown, K., Thomas, L., Ferreira, M. A. R., Bender, D., Maller, J., Sklar, P., de Bakker, P. I. W., Daly, M. J., & Sham, P. C. (2007). PLINK: A tool set for whole-genome association and population-based linkage analyses. *American Journal of Human Genetics*, *81*(3), 559–575. https://doi.org/10.1086/519795

Quattrini, M., Liang, N., Fortina, M. G., Xiang, S., Curtis, J. M., & Gänzle, M. (2019). Exploiting synergies of sourdough and antifungal organic acids to delay fungal spoilage of bread. *International Journal of Food Microbiology*, *302*(July 2018), 8–14. https://doi.org/10.1016/j.ijfoodmicro.2018.09.007

Rangel, D. E. N., Braga, G. U. L., Anderson, A. J., & Roberts, D. W. (2005). Variability in conidial thermotolerance of *Metarhizium anisopliae* isolates from different geographic origins. *Journal of Invertebrate Pathology*, *88*(2), 116–125. https://doi.org/10.1016/j.jip.2004.11.007

Rangel, D. E. N., Braga, G. U. L., Fernandes, É. K. K., Keyser, C. A., Hallsworth, J. E., & Roberts, D. W. (2015). Stress tolerance and virulence of insect-pathogenic fungi are determined by environmental conditions during conidial formation. *Current Genetics*, *61*(3), 383–404. https://doi.org/10.1007/s00294-015-0477-y

Ratkowsky, D. A. (2004). Model fitting and uncertainty. *Modeling Microbial Responses in Food*, 151–196. https://doi.org/10.1201/9780203503942.ch4

Razavi-Rohani, S. M., & Griffiths, M. W. (1999). Antifungal effects of sorbic acid and propionic acid at different pH and NaCl conditions. *Journal of Food Safety*, *19*(2), 109–120. https://doi.org/10.1111/j.1745-4565.1999.tb00238.x

Rico-Munoz, E., Samson, R. A., & Houbraken, J. (2019). Mould spoilage of foods and beverages: Using the right methodology. *Food Microbiology*, *81*, 51–62. https://doi.org/10.1016/j.fm.2018.03.016

Ricoult, C., Cliquet, J. B., & Limami, A. M. (2005). Stimulation of alanine amino transferase (AlaAT) gene expression and alanine accumulation in embryo axis of the model legume *Medicago truncatula* contribute to anoxia stress tolerance. *Physiologia Plantarum*, *123*(1), 30–39. https://doi.org/10.1111/j.1399-3054.2005.00449.x

Ritchie, H., & Roser, M. (2013). Crop yields. *Our World in Data*.

Romo-Pérez, M. L., Weinert, C. H., Häußler, M., Egert, B., Frechen, M. A., Trierweiler, B., Kulling, S. E., & Zörb, C. (2020). Metabolite profiling of onion landraces and the cold storage effect. *Plant Physiology and Biochemistry*, *146*(November 2019), 428–437. https://doi.org/10.1016/j.plaphy.2019.11.007

Ropars, J., Cruaud, C., Lacoste, S., & Dupont, J. (2012). A taxonomic and ecological overview of cheese fungi. *International Journal of Food Microbiology*, *155*(3), 199–210. https://doi.org/10.1016/j.ijfoodmicro.2012.02.005

Ropars, J., López-Villavicencio, M., Dupont, J., Snirc, A., Gillot, G., Coton, M., Jany, J. L., Coton, E., & Giraud, T. (2014). Induction of sexual reproduction and genetic diversity in the cheese fungus *Penicillium roqueforti*. *Evolutionary Applications*, *7*(4), 433–441. https://doi.org/10.1111/eva.12140

Ropars, J., Rodríguez de la Vega, R. C., López-Villavicencio, M., Gouzy, J., Sallet, E., Dumas, É., Lacoste, S., Debuchy, R., Dupont, J., Branca, A., & Giraud, T. (2015). Adaptive horizontal gene transfers between multiple cheese-associated fungi. *Current Biology*, *25*(19), 2562–2569. https://doi.org/10.1016/j.cub.2015.08.025

Ruijten, P., Huinink, H. P., & Adan, O. C. G. (2020). *Penicillium rubens* germination on desiccated and nutrient-depleted conditions depends on the water activity during sporogenesis. *Fungal Biology*, *124*(12), 1058–1067. https://doi.org/10.1016/j.funbio.2020.10.006

Ruijter, G. J. G., Bax, M., Patel, H., Flitter, S. J., van de Vondervoort, P. J. I., de Vries, R. P., VanKuyk, P. A., & Visser, J. (2003). Mannitol is required for stress tolerance in *Aspergillus niger* conidiospores. *Eukaryotic Cell*, *2*(4), 690–698. https://doi.org/10.1128/EC.2.4.690-698.2003

Sakamoto, K., Arima, T., Iwashita, K., Yamada, O., Gomi, K., & Akita, O. (2008). *Aspergillus oryzae* atfB encodes a transcription factor required for stress tolerance in conidia. *Fungal Genetics and Biology*, *45*(6), 922–932. https://doi.org/10.1016/j.fgb.2008.03.009

Sakamoto, K., Iwashita, K., Yamada, O., Kobayashi, K., Mizuno, A., Akita, O., Mikami, S., Shimoi, H., & Gomi, K. (2009). Aspergillus oryzae atfA controls conidial germination and stress tolerance. *Fungal Genetics and Biology*, *46*(12), 887–897. https://doi.org/10.1016/j.fgb.2009.09.004

Sales, K., Brandt, W., Rumbak, E., & Lindsey, G. (2000). The LEA-like protein HSP 12 in *Saccharomyces cerevisiae* has a plasma membrane location and protects membranes against desiccation and ethanol-induced stress. *Biochimica et Biophysica Acta - Biomembranes*, *1463*(2), 267–278. https://doi.org/10.1016/S0005-2736(99)00215-1

Samson, R. A., Houbraken, J., Varga, J., & Frisvad, J. C. (2009). Polyphasic taxonomy of the heat resistant ascomycete genus *Byssochlamys* and its *Paecilomyces* anamorphs. *Persoonia: Molecular Phylogeny and Evolution of Fungi*, *22*, 14–27. https://doi.org/10.3767/003158509X418925

Samson, R. A, Houbraken, J., Thrane, U., Frisvad, J. C., & Andersen, B. (2010). Food and indoor fungi. In *CBS Laboratory Manual Series 2* (2nd ed.). Westerdijk Fungal Biodiversity Institute.

Samson, R. A, Hoekstra, E. S., & Frisvad, J. C. (2004). *Introduction to food-and airborne fungi.* (Issue Ed. 7). Centraalbureau voor Schimmelcultures (CBS).

Sanchez, D. A., & Martinez, L. R. (2019). Underscoring interstrain variability and the impact of growth conditions on associated antimicrobial susceptibilities in preclinical testing of novel antimicrobial drugs. *Critical Reviews in Microbiology*, *45*(1), 51–64. https://doi.org/10.1080/1040841X.2018.1538934

Seekles, S. J., Teunisse, P. P. P., Punt, M., van den Brule, T., Dijksterhuis, J., Houbraken, J., Wösten, H. A. B., & Ram, A. F. J. (2021). Preservation stress resistance of melanin deficient conidia from *Paecilomyces variotii* and *Penicillium roqueforti* mutants generated via CRISPR/Cas9 genome editing. *Fungal Biology and Biotechnology*, *8*(1), 1–13. https://doi.org/10.1186/s40694-021-00111-w

Segers, F. J. J., van Laarhoven, K. A., Wösten, H. A. B., & Dijksterhuis, J. (2017). Growth of indoor fungi on gypsum. *Journal of Applied Microbiology*, *123*(2), 429–435. https://doi.org/10.1111/jam.13487

Shearer, A. E. H., Mazzotta, A. S., Chuyate, R., & Gombas, D. E. (2002). Heat resistance of juice spoilage microorganisms. *Journal of Food Protection*, *65*(8), 1271–1275. https://doi.org/10.4315/0362-028X-65.8.1271

Shephard, G. S. (2008). Impact of mycotoxins on human health in developing countries. *Food Additives and Contaminants - Part A Chemistry, Analysis, Control, Exposure and Risk Assessment*, *25*(2), 146–151. https://doi.org/10.1080/02652030701567442

Smit, A. F. A. (2010). Repeat-Masker Open-3.0. *Http://www.repeatmasker.org*.

Solberg, M. (1991). Mechanisms of action of food preservation procedures. In *Trends in Food Science & Technology* (Vol. 2). Elsevier Applied Science. https://doi.org/10.1016/0924-2244(91)90663-4

Stamatakis, A. (2014). RAxML version 8: A tool for phylogenetic analysis and post-analysis of large phylogenies. *Bioinformatics*, *30*(9), 1312–1313. https://doi.org/10.1093/bioinformatics/btu033

Stanke, M., Schöffmann, O., Morgenstern, B., & Waack, S. (2006). Gene prediction in eukaryotes with a generalized hidden Markov model that uses hints from external sources. *BMC Bioinformatics*, *7*, 1–11. https://doi.org/10.1186/1471-2105-7-62

Stevenson, A., Hamill, P. G., O'Kane, C. J., Kminek, G., Rummel, J. D., Voytek, M. A., Dijksterhuis, J., & Hallsworth, J. E. (2017). *Aspergillus penicillioides* differentiation and cell division at 0.585 water activity. *Environmental Microbiology*, *19*(2), 687–697. https://doi.org/10.1111/1462-2920.13597

Stovner, E. B., & Sætrom, P. (2020). PyRanges: efficient comparison of genomic intervals in Python. *Bioinformatics*, *36*(3), 918–919.

Stratford, M., & Anslow, P. A. (1998). Evidence that sorbic acid does not inhibit yeast as a classic "weak acid preservative." *Letters in Applied Microbiology*, *27*(4), 203–206. https://doi.org/10.1046/j.1472-765X.1998.00424.x

Stratford, M., Plumridge, A., Nebe-von-Caron, G., & Archer, D. B. (2009). Inhibition of spoilage mould conidia by acetic acid and sorbic acid involves different modes of action, requiring modification of the classical weak-acid theory. *International Journal of Food Microbiology*, *136*(1), 37–43. https://doi.org/10.1016/j.ijfoodmicro.2009.09.025

Stratford, M., Plumridge, A., Pleasants, M. W., Novodvorska, M., Baker-Glenn, C. A. G., Pattenden, G., & Archer, D. B. (2012). Mapping the structural requirements of inducers and substrates for decarboxylation of weak acid preservatives by the food spoilage mould *Aspergillus niger*. *International Journal of Food Microbiology*, *157*(3), 375–383. https://doi.org/10.1016/j.ijfoodmicro.2012.06.007

Stratford, M., Steels, H., Nebe-von-Caron, G., Novodvorska, M., Hayer, K., & Archer, D. B. (2013). Extreme resistance to weak-acid preservatives in the spoilage yeast *Zygosaccharomyces bailii*. *International Journal of Food Microbiology*, *166*(1), 126–134. https://doi.org/10.1016/j.ijfoodmicro.2013.06.025

Suhr, K. I., & Nielsen, P. V. (2004). Effect of weak acid preservatives on growth of bakery product spoilage fungi at different water activities and pH values. *International Journal of Food Microbiology*, *95*(1), 67–78. https://doi.org/10.1016/j.ijfoodmicro.2004.02.004

Suzuki, S., Sarikaya Bayram, Ö., Bayram, Ö., & Braus, G. H. (2013). ConF and conJ contribute to conidia germination and stress response in the filamentous fungus *Aspergillus nidulans*. *Fungal Genetics and Biology*, *56*, 42–53. https://doi.org/10.1016/j.fgb.2013.04.008

Taha, M. P. M., Pollard, S. J. T., Sarkar, U., & Longhurst, P. (2005). Estimating fugitive bioaerosol releases from static compost windrows: Feasibility of a portable wind tunnel approach. *Waste Management, 25*(4), 445–450. https://doi.org/10.1016/j.wasman.2005.02.013

Takano, Y., Kikuchi, T., Kubo, Y., Hamer, J. E., Mise, K., & Furusawa, I. (2000). The *Colletotrichum lagenarium* MAP kinase gene CMK1 regulates diverse aspects of fungal pathogenesis. *Molecular Plant-Microbe Interactions*, *13*(4), 374–383. https://doi.org/10.1094/MPMI.2000.13.4.374

Taniwaki, M. H., Hocking, A. D., Pitt, J. I., & Fleet, G. H. (2001). Growth of fungi and mycotoxin production on cheese under modified atmospheres. *International Journal of Food Microbiology*, *68*(1–2), 125–133. https://doi.org/10.1016/S0168-1605(01)00487-1

Teertstra, W. R., Tegelaar, M., Dijksterhuis, J., Golovina, E. A., Ohm, R. A., & Wösten, H. A. B. (2017). Maturation of conidia on conidiophores of *Aspergillus niger*. *Fungal Genetics and Biology*, *98*, 61–70. https://doi.org/10.1016/j.fgb.2016.12.005

Timmermans, R. A. H., Nederhoff, A. L., Nierop Groot, M. N., van Boekel, M. A. J. S., & Mastwijk, H. C. (2016). Effect of electrical field strength applied by PEF processing and storage temperature on the outgrowth of yeasts and moulds naturally present in a fresh fruit smoothie. *International Journal of Food Microbiology*, *230*, 21–30. https://doi.org/10.1016/j.ijfoodmicro.2016.04.014

Trapnell, C., Hendrickson, D. G., Sauvageau, M., Goff, L., Rinn, J. L., & Pachter, L. (2013). Differential analysis of gene regulation at transcript resolution with RNA-seq. *Nature Biotechnology*, *31*(1), 46–53. https://doi.org/10.1038/nbt.2450

Trinci, A. P. J. (1994). Evolution of the Quorn® myco-protein fungus, Fusarium graminearum A3/5. *Microbiology*, *140*(9), 2181–2188. https://doi.org/10.1099/13500872-140-9-2181

van den Berg, M. A., Albang, R., Albermann, K., Badger, J. H., Daran, J. M., M Driessen, A. J., Garcia-Estrada, C., Fedorova, N. D., Harris, D. M., Heijne, W. H. M., Joardar, V., W Kiel, J. A. K., Kovalchuk, A., Martín, J. F., Nierman, W. C., Nijland, J. G., Pronk, J. T., Roubos, J. A., van der Klei, I. J., … Bovenberg, R. A. L. (2008). Genome sequencing and analysis of the filamentous fungus *Penicillium chrysogenum*. *Nature Biotechnology*, *26*(10), 1161–1168. https://doi.org/10.1038/nbt.1498

van den Brink, J. M., Punt, P. J., Van Gorcom, R. F. M., & van den Hondel, C. A. M. J. J. (2000). Regulation of expression of the *Aspergillus niger* benzoate para-hydroxylase cytochrome P450 system. *Molecular and General Genetics*, *263*(4), 601–609. https://doi.org/10.1007/s004380051207

van den Brule, T., Punt, M., Teertstra, W., Houbraken, J., Wösten, H., & Dijksterhuis, J. (2020a). The most heat-resistant conidia observed to date are formed by distinct strains of *Paecilomyces variotii*. *Environmental Microbiology*, *22*(3), 986–999. https://doi.org/10.1111/1462-2920.14791

van den Brule, T., Lee, C. L. S., Houbraken, J., Haas, P. J., Wösten, H., & Dijksterhuis, J. (2020b). Conidial heat resistance of various strains of the food spoilage fungus *Paecilomyces variotii* correlates with mean spore size, spore shape and size distribution. *Food Research International*, *137*(February), 109514. https://doi.org/10.1016/j.foodres.2020.109514

van Dongen, P. W. J., & de Groot, A. N. J. A. (1995). History of ergot alkaloids from ergotism to ergometrine. *European Journal of Obstetrics and Gynecology and Reproductive Biology*, *60*(2), 109–116. https://doi.org/10.1016/0028-2243(95)02104-Z

van Gorcom, R. F. M., Boschloo, J. G., Kuijvenhoven, A., Lange, J., van Vark, A. J., Bos, C. J., van Balken, J. A. M., Pouwels, P. H., & van den Hondel, C. A. M. J. J. (1990). Isolation and molecular characterisation of the benzoate-para-hydroxylase gene (bphA) of *Aspergillus niger*: A member of a new gene family of the cytochrome P450 superfamily. *MGG Molecular & General Genetics*, *223*(2), 192–197. https://doi.org/10.1007/BF00265053

van Leeuwe, T. M., Arentshorst, M., Ernst, T., Alazi, E., Punt, P. J., & Ram, A. F. J. (2019). Efficient marker free CRISPR/Cas9 genome editing for functional analysis of gene families in filamentous fungi. *Fungal Biology and Biotechnology*, *6*(1), 1–13. https://doi.org/10.1186/s40694-019-0076-7

van Leeuwen, M. R., Krijgsheld, P., Bleichrodt, R., Menke, H., Stam, H., Stark, J., Wösten, H. A. B., & Dijksterhuis, J. (2013). Germination of conidia of *Aspergillus niger* is accompanied by major changes in RNA profiles. *Studies in Mycology*, *74*, 59–70. https://doi.org/10.3114/sim0009

van Leeuwen, M. R., van Doorn, T. M., Golovina, E. A., Stark, J., & Dijksterhuis, J. (2010). Water- and air-distributed conidia differ in sterol content and cytoplasmic microviscosity. *Applied and Environmental Microbiology*, *76*(1), 366–369. https://doi.org/10.1128/AEM.01632-09

van Leeuwen, M. R., Wyatt, T. T., van Doorn, T. M., Lugones, L. G., Wösten, H. A. B., & Dijksterhuis, J. (2016). Hydrophilins in the filamentous fungus *Neosartorya fischeri* (*Aspergillus fischeri*) have protective activity against several types of microbial water stress. *Environmental Microbiology Reports*, *8*(1), 45–52. https://doi.org/10.1111/1758-2229.12349

Varga, J., Frisvad, J. C., Kocsubé, S., Brankovics, B., Tóth, B., Szigeti, G., & Samson, R. A. (2011). New and revisited species in Aspergillus section Nigri. *Studies in Mycology*, *69*, 1–17. https://doi.org/10.3114/sim.2011.69.01

Vervaeke, L. (2020, August 19). Voedselpolitiek in China: grote leider Xi wil dat Chinezen hun bord leeg eten. *De Volkskrant*. https://www.volkskrant.nl/nieuws-achtergrond/voedselpolitiek-in-china-grote-leider-xi-wil-dat-chinezen-hun-bord-leeg-eten~b74d60b1/

Visagie, C. M., Houbraken, J., Frisvad, J. C., Hong, S. B., Klaassen, C. H. W., Perrone, G., Seifert, K. A., Varga, J., Yaguchi, T., & Samson, R. A. (2014). Identification and nomenclature of the genus Penicillium. *Studies in Mycology*, *78*(1), 343–371. https://doi.org/10.1016/j.simyco.2014.09.001

Vishniac, W., & Santer, M. (1957). The *thiobacilli*. *Bacteriological Reviews*, *21*(3), 195–213. https://doi.org/10.1128/mmbr.21.3.195-213.1957

Vollset, S. E., Goren, E., Yuan, C. W., Cao, J., Smith, A. E., Hsiao, T., Bisignano, C., Azhar, G. S., Castro, E., Chalek, J., Dolgert, A. J., Frank, T., Fukutaki, K., Hay, S. I., Lozano, R., Mokdad, A. H., Nandakumar, V., Pierce, M., Pletcher, M., … Murray, C. J. L. (2020). Fertility, mortality, migration, and population scenarios for 195 countries and territories from 2017 to 2100: a forecasting analysis for the Global Burden of Disease Study. *The Lancet*, *396*(10258), 1285–1306. https://doi.org/10.1016/S0140-6736(20)30677-2

Wang, F., Sethiya, P., Hu, X., Guo, S., Chen, Y., Li, A., Tan, K., & Wong, K. H. (2021). Transcription in fungal conidia before dormancy produces phenotypically variable conidia that maximize survival in different environments. *Nature Microbiology*. https://doi.org/10.1038/s41564-021-00922-y

Washabaugh, M. W., & Collins, K. D. (1986). The systematic characterization by aqueous column chromatography of solutes which affect protein stability. *Journal of Biological Chemistry*, *261*(27), 12477–12485. https://doi.org/10.1016/s0021-9258(18)67112-1

Welker, S., Rudolph, B., Frenzel, E., Hagn, F., Liebisch, G., Schmitz, G., Scheuring, J., Kerth, A., Blume, A., Weinkauf, S., Haslbeck, M., Kessler, H., & Buchner, J. (2010). Hsp12 is an intrinsically unstructured stress protein that folds upon membrane association and modulates membrane function. *Molecular Cell*, *39*(4), 507–520. https://doi.org/10.1016/j.molcel.2010.08.001

Wells-Bennik, M. H. J., Janssen, P. W. M., Klaus, V., Yang, C., Zwietering, M. H., & den Besten, H. M. W. (2019). Heat resistance of spores of 18 strains of *Geobacillus stearothermophilus* and impact of culturing conditions. *International Journal of Food Microbiology*, *291*(November 2018), 161–172. https://doi.org/10.1016/j.ijfoodmicro.2018.11.005

Williams, J. H., Phillips, T. D., Jolly, P. E., Stiles, J. K., Jolly, C. M., & Aggarwal, D. (2004). Human aflatoxicosis in developing countries: A review of toxicology, exposure, potential health consequences, and interventions. *American Journal of Clinical Nutrition*, *80*(5), 1106–1122. https://doi.org/10.1093/ajcn/80.5.1106

Wolschek, M. F., & Kubicek, C. P. (1997). The filamentous fungus *Aspergillus niger* contains two "differentially regulated" trehalose-6-phosphate synthase-encoding genes, tpsA and tpsB. *Journal of Biological Chemistry*, *272*(5), 2729–2735. https://doi.org/10.1074/jbc.272.5.2729

Wyatt, T. T., Golovina, E. A., van Leeuwen, R., Hallsworth, J. E., Wösten, H. A. B., & Dijksterhuis, J. (2015). A decrease in bulk water and mannitol and accumulation of trehalose and trehalose-based oligosaccharides define a two-stage maturation process towards extreme stress resistance in ascospores of *Neosartorya fischeri* (*Aspergillus fischeri*). *Environmental Microbiology*, *17*(2), 383–394. https://doi.org/10.1111/1462-2920.12557

Wyatt, T. T., Wösten, H. A. B., & Dijksterhuis, J. (2013). Fungal spores for dispersion in space and time. In *Advances in Applied Microbiology* (Vol. 85). https://doi.org/10.1016/B978-0-12-407672-3.00002-2

Yanai, S., Ishitani, T., & Kojo, T. (1980). The effects of low-oxygen atmospheres on the growth of fungi. *Nippon Shokuhin Kogyo Gakkaishi*, *27*(1), 20–24. https://doi.org/10.3136/nskkk1962.27.20

Appendix

Nederlandse samenvatting

De wereldbevolking zal deze eeuw naar verwachting oplopen tot 11 miljard. Hierdoor zal de vraag naar voedsel stijgen tot 70 % in 2050. Eén van de methoden om aan deze vraag te voldoen is het beperken van de jaarlijkse voedselverspilling, wat momenteel ongeveer een derde van al het geproduceerde voedsel betreft. De belangrijkste oorzaak van deze verspilling komt door voedselbederf, wat een fysische, chemische of microbiologische oorzaak kan hebben. Micro-organismen zoals schimmels veroorzaken microbiologisch bederf en dit maakt producten oneetbaar. In sommige gevallen kan dit zelfs tot voedselvergiftiging leiden.

Schimmelbederf wordt voornamelijk veroorzaakt door gistachtige of filamenteuze schimmels die behoren tot de Ascomycota. In dat laatste geval vormen deze schimmels een netwerk van vegetatieve schimmeldraden dat mycelium wordt genoemd. Na een periode van vegetatieve groei kan een mycelium aseksuele of seksuele voortplantingsstructuren voortbrengen. Deze seksuele en aseksuele sporen worden respectievelijk ascosporen en conidia genoemd. Deze laatste sporen worden beschouwd als de belangrijkste oorzaak van voedselbederf, omdat er enorme aantallen van deze sporen geproduceerd worden (zo kan een kolonie op een Petrischaal meer dan een miljard conidia vormen), die gemakkelijk worden verspreid door wind, waterdruppels of via andere vectoren, zoals insecten. Daarnaast zijn conidia over het algemeen beter bestand tegen stress dan het mycelium. Zo zijn ze resistent tegen uitdroging, UV-straling en hoge en lage temperaturen. Celwandcomponenten zoals melanine beschermen tegen UV-schade, terwijl interne suikers, polyolen en hitteschok-eiwitten de hitte- en droogteresistentie kunnen verhogen.

Schimmels gedijen op voedsel door de grote hoeveelheid aan voedingsstoffen en de gunstige pH, wateractiviteit en redoxpotentiaal. Om bederf te voorkomen, worden er in de voedingsmiddelenindustrie verschillende conserveringstechnieken toegepast. Dit kunnen zowel preventieve maatregelen zijn om besmetting te beperken, zoals luchtfiltratie of steriel verpakken, maar ook verwerkingsmethoden die microbiële groei beperken. Pasteurisatie, gekoeld bewaren en de toevoeging van antimicrobiële zuren zijn hier voorbeelden van. Een schimmel die in staat is om deze hindernissen te overwinnen is *Penicillium roqueforti*. Dit kan

worden toegeschreven aan zijn vermogen om te groeien op lage temperatuur, bij lage zuurstofgehaltes en zijn resistentie tegen biologische en chemische conserveringsmiddelen, zoals sorbinezuur.

Eén enkele spore is voldoende om bederf te veroorzaken. Daarom kan het vormen van een heterogene sporenpopulatie de kans vergroten om te overleven op voedsel. Heterogeniteit komt niet alleen voor tussen soorten en stammen, maar ook binnen de sporenpopulatie van een enkele schimmelkolonie. Over de mechanismen die aan deze types heterogeniteit ten grondslag liggen is weinig bekend. Dit proefschrift beschrijft de heterogeniteit die zichtbaar is binnen en tussen stammen van *Penicillium roqueforti* en *Aspergillus niger*, met de nadruk op stressresistentie. De resultaten zijn niet alleen van fundamenteel belang, maar ook vanuit een toegepast oogpunt om voedselbederf te voorkomen.

Intraspecifieke heterogeniteit

Ontkieming van conidia is één van de processen waar variabiliteit tussen sporen zichtbaar is. Meestal wordt kieming in gang gezet door omgevingsfactoren, maar zelfs in droge en nutriëntarme condities ontkiemen sommige schimmelsoorten (zoals *Penicillium rubens*). In **Hoofdstuk 2** en **3** wordt de heterogeniteit in kieming van respectievelijk *A. niger* en *P. roqueforti* conidia onderzocht door gebruik te maken van een wiskundig groeimodel. In een relatief arm medium bestaande uit een koolstofbron en anorganisch fosfaat of magnesiumsulfaat ontkiemde 6 % van de *A. niger* conidia (**Hoofdstuk 2**). Deze experimenten toonden aan dat een deel van de conidia zelfs ontkiemd als niet alle vereiste nutriënten voor koloniegroei beschikbaar zijn. Een dergelijke mediumonafhankelijke respons zou een concurrentievoordeel kunnen opleveren, aangezien daardoor een snelle kieming en dus kolonisatie van een substraat mogelijk wordt. Heterogene kieming kan ook een evolutionair voordeel geven in het geval van wisselende omgevingsfactoren, want conidia zijn een stuk resistenter tegen stress dan kiembuizen. Dit zou kunnen verklaren waarom slechts 20 % van de conidia kiembuizen produceert in een gedefinieerd medium waarin alle nutrienten aanwezig zijn die nodig zijn voor de volledige uitgroei. Het is nog onbekend hoe de heterogeniteit van conidia met betrekking tot kieming wordt bewerkstelligd. Deels zou dit verklaard kunnen worden door verschil in rijping, aangezien niet alle conidia tegelijkertijd worden geproduceerd op een enkele kolonie. Heterogeniteit in ontkieming zou ook het

gevolg kunnen zijn van een variërend aantal nutriëntsensoren in het plasmamembraan of de heterogene samenstelling van eiwitten en RNA in conidia.

De kieming van sporen verloopt in drie fasen. Eerst worden conidia geactiveerd, vervolgens zwellen sporen op, een proces dat isotrope groei wordt genoemd, wat wordt gevolgd door kiembuisvorming als gevolg van gepolariseerde groei. De zwelling en kiembuis uitgroei kunnen onafhankelijk van elkaar worden geïnduceerd. Sommige koolstof- en stikstofbronnen kunnen alleen zwelling activeren of alleen hyfe-groei ondersteunen, terwijl andere geen van beide of beide kunnen doen. In **Hoofdstuk 2** werden aminozuren onderverdeeld op basis van hun inducerende effect op de kieming van *A. niger* conidia. Dit wordt uitgedrukt in een percentage (gedefinieerd als P_{max}). Aminozuren met een P_{max} < 5 % worden beschouwd als laag-inducerend, terwijl gemiddeld- en hoog-inducerende aminozuren een P_{max} hebben van respectievelijk 5 - 25 % en > 25 %. Proline en alanine bleken hoog inducerende aminozuren met het grootste effect in *A. niger*, aangezien ze > 80 % van de conidia activeerden om te zwellen. De accumulatie van proline en alanine in aan stress blootgestelde planten zou een antwoord kunnen zijn op de vraag waarom deze moleculen zo'n sterk inducerend effect hebben op *A. niger* conidia, aangezien dergelijke planten mogelijk vatbaarder zijn voor schimmelkolonisatie. In het tijdsbestek waarin kieming kon worden gevolgd in de aanwezigheid van alalnine en proline (op een gegeven moment wordt de culture overgroeid) was kiembuisvorming tot 30 % minder dan de zwelling. In het geval van een mix van verschillende aminozuren werd echter tot wel 100 % kiembuisvorming waargenomen, wat er op duidt dat *A. niger* conidia meerdere sensoren bevatten die elk bijdragen aan de vorming van kiembuizen.

De activering van *P. roqueforti* conidia door aminozuren of glucose werd bestudeerd in **Hoofdstuk 3**. Hiervoor werd gebruik gemaakt van een medium bestaande uit anorganisch fosfaat, anorganisch stikstof en magnesiumsulfaat. Daarnaast werd er kaliumchloride in het medium toegevoegd, omdat de conidia van *P. roqueforti* een drievoudige toename in kieming vertoonden in aanwezigheid van kaliumzouten (KCl, KNO_3 of KH_2PO_4). Dit in tegenstelling tot de conidia van *A. niger* die tot 100 % kiemden zonder de aanwezigheid van kalium in het medium (**Hoofdstuk 2**). Mogelijk bevatten *A. niger* conidia een interne opslag van kalium of zijn ze beter aangepast aan K-arme substraten. Arginine en alanine waren met respectievelijk

21 % en 13 % de sterkst inducerende aminozuren voor *P. roqueforti* kieming. Geen van de andere aminozuren resulteerde in meer dan 6 % kieming. Wanneer glucose werd gebruikt in plaats van een aminozuur, ontkiemde 12 % van de conidia. Niet alleen het kiemingspercentage (P_{max}) verschilde tussen *A. niger* en *P. roqueforti* conidia, maar ook de kiemtijd (τ). Zo hadden *A. niger* conidia 12 uur nodig voor kieming in de aanwezigheid van arginine, terwijl dit 25 uur was in het geval van *P. roqueforti* (**Hoofdstuk 2** en **3**). Een soortgelijk verschil werd gevonden in de aanwezigheid van glucose, waar kieming plaatsvond na respectievelijk 7 en 14 uur. Dit wijst erop dat *P. roqueforti* conidia een complexer medium nodig hebben voor snelle kieming.

In een rijk medium verdubbelde de diameter van *P. roqueforti* conidia tijdens de zwelling, maar dit was niet het geval in de gedefinieerde media die in **Hoofdstuk 3** werden gebruikt. Mogelijk was het gedefinieerde medium te beperkt en worden interne voedingsstoffen zoals suikers en polyolen eerder aangesproken. Dit zou dan de wateropname en als gevolg daarvan de zwelling van de sporen kunnen verminderen. Daarnaast is het van belang dat kieming plaats kan vinden zonder waarneembare zwelling en dat het drie stadia programma van kieming (activatie, zwellen, kiembuisvorming) niet altijd plaatsvindt.

Intraspecifieke stamvariabiliteit kan ook het gevolg zijn van variërende milieuomstandigheden tijdens de sporevorming. **Hoofdstuk 4** beschrijft wat het effect is van verschillende rijpingsstadia en groeiomstandigheden op de hitteresistentie van *P. roqueforti* conidia. De hitteresistentie wordt uitgedrukt in een 'D_{56}-waarde', deze maat geeft het aantal minuten aan dat nodig is om 90 % van de populatie te inactiveren bij een temperatuur van 56 °C. Conidia van drie dagen oude kolonies hadden een D_{56}-waarde van ongeveer 1.99 vergeleken met een D_{56}-waarde van 4.31 voor conidia van tien dagen oude kolonies (**Hoofdstuk 4**). De opgroeitemperatuur had ook een significante invloed; conidia gegroeid bij 15 °C hadden bijna een viermaal lagere D_{56}-waarde (1.12) dan conidia van dezelfde stam die bij 30 °C waren geproduceerd (4.19). Mogelijkerwijs rijpen *P. roqueforti* conidia niet volledig in zeven dagen wat dit verschil zou kunnen verklaren. Naast hittebestendigheid hadden de omgevingscondities invloed op de sporengrootte, het polyolgehalte en het transcriptoom van deze conidia (**Hoofdstuk 4**). Zo nam de diameter van de conidia tot wel 12 % toe wanneer ze bij 30 °C in plaats van 25 °C werden geproduceerd. De polyol samenstelling verschilt in meer

gerijpte conidia en in conidia die bij verhoogde temperatuur zijn geproduceerd. Met name de trehalose- en arabitolconcentratie nemen toe in *P. roqueforti* conidia bij een langere incubatie tijd of hogere temperatuur (**Hoofdstuk 4**). De rol van polyolen en daarvan specifiek trehalose is in eerder onderzoek in verband gebracht met de hitteresistentie van conidia van filamenteuze schimmels. Een soortgelijk effect zien we in *P. roqueforti* conidia, waar trehalose- en arabitolconcentraties lijken te correleren met hitteresistentie (**Hoofdstuk 4**). Echter, de condities die de hoogste trehalose concentraties opleverden (10 dagen, 30 °C) resulteerden niet in de meest hitteresistente conidia (**Hoofdstuk 4**). Bovendien werd er geen correlatie tussen trehalose- of arabitolconcentratie en hitteresistentie waargenomen toen we 18 *P. roqueforti*-stammen vergeleken (**Hoofdstuk 5**). Dit zou verklaard kunnen worden door de rol die trehalose heeft buiten het beperken van hittestress. Trehalose dient bijvoorbeeld als koolstofopslag in schimmels en bovendien verhoogt intracellulaire trehalose de kiemtijd in *P. roqueforti*. Vertraagde kieming kan een evolutionair voordeel hebben, omdat het voortijdige kieming zou kunnen voorkomen op of dicht bij plaatsen waar conidia worden geproduceerd. Het gebrek aan correlatie tussen trehalose concentratie en hitteresistentie in 18 *P. roqueforti* stammen (**Hoofdstuk 5**) impliceert ook dat de hitteresistentie in *P. roqueforti* conidia het resultaat is van meerdere factoren, bijvoorbeeld de aanwezigheid van heat-shock proteins (HSPs), de totale polyol samenstelling en de dikte van de celwand.

Rijpingstijd en temperatuur hebben invloed op genexpressie van *P. roqueforti* conidia (**Hoofdstuk 4**). De expressieprofielen van genen die betrokken zijn bij de polyolbiosynthese werden bekeken, waaronder *treA*, *tpsB* en *tpsC* (betrokken bij trehalose synthese), *lad* (arabitol synthese) en *err1* (erythritol synthese). In het geval van trehalose komt het expressiepatroon overeen met de accumulatie van trehalose in de sporen. Dit was niet het geval voor *err1* en *lad*. In totaal lieten 85 genen een meer dan viervoudige expressie zien in conidia geproduceerd bij 30 °C vergeleken met die geproduceerd bij 15 °C. Terwijl 274 genen een meer dan viervoudige expressie vertoonden in tien dagen oude conidia vergeleken met drie dagen oude conidia. Opmerkelijk was dat er 33 genen waren die in beide groepen voorkwamen. Deze 33 genen bevatten de hydrophilines *con-6* en *con-10* en 17 voorspelde eiwitten met onbekende functie. Samengevat werd aangetoond dat intra-stam heterogeniteit een uitgesproken invloed kan hebben op het vermogen van een conidium om te zwellen, te ontkiemen en stress te weerstaan.

Heterogeniteit tussen stammen

Hoofdstuk 5 beschrijft de variabiliteit in hitteresistentie tussen 20 *P. roqueforti* stammen. Naast stamvariabiliteit wordt ook de experimentele variabiliteit, biologische variabiliteit en totale variabiliteit beschreven. Experimentele, biologische en stamvariabiliteit van *P. roqueforti* werden vergeleken met behulp van de standaardafwijking van $\log_{10} D$-waarden, kwantitatief uitgedrukt in RMSE. De experimentele variabiliteit had de laagste variabiliteit, gevolgd door de biologische en stamvariabiliteit met waarden van respectievelijk 0.044, 0.096 en 0.179. Door de data uit dit hoofdstuk samen te voegen met die uit de literatuur kon de Z-waarde worden bepaald. De Z-waarde (7.8) drukt het aantal graden uit dat nodig is om een 1 $\log_{10}$-verlaging van de D-waarde te veroorzaken. De totale variabiliteit van deze dataset was 0.415, waarvan 43 % verklaard kan worden door de stamvariabiliteit. Toekomstige studies moeten nagaan of stamvariabiliteit ook bij andere stressoren de belangrijkste bijdrage levert aan de totale variatie.

In termen van D_{56}-waarde werd een 8.6-voudig verschil tussen de meest hittebestendige en hittegevoelige stam waargenomen. Dit is vergelijkbaar met de variabiliteit in hittebestendigheid die is gerapporteerd bij andere schimmel- en bacteriesoorten. Daarnaast werd er aangetoond dat de gemiddelde sporendiameter varieerde van 3.47 µm tot 4.22 µm tussen de 18 *P. roqueforti* stammen (**Hoofdstuk 5**). Bovendien zagen we bij deze schimmels een grote variatie in polyol samenstelling, waarvan arabitol en mannitol met respectievelijke concentraties van 82 tot 535 mM en 130 tot 304 mM het meest voorkomend waren.

In **Hoofdstuk 6** werd de heterogeniteit in resistentie van *P. roqueforti* stammen tegen benzoëzuur, propionzuur en, in het bijzonder, sorbinezuur bestudeerd. De resistentie die werd gevonden bij groei op mout extract (MIC_u = 4.2 - 21.3 mM) bleek overeenkomstig de waarden uit de literatuur. In yoghurt bleek de resistentie lager, wat mogelijk verklaard wordt door de organische zuren die in dit melkproduct aanwezig zijn en de lagere temperatuur waarop werd gegroeid. Deze factoren kunnen ook een invloed hebben op het afdoden van de conidia. Door de genomen van resistente en gevoelige stammen te vergelijken werd een genomische cluster (SORBUS) geïdentificeerd dat uniek is voor de resistente stammen. Sommige van de genen (*padA*, *sdrA* en *cdcA*) die op SORBUS gelokaliseerd zijn, spelen een belangrijke rol bij de decarboxylering en detoxificatie van sorbinezuur in *A. niger*. De

aanwezigheid van twee genen die homologie vertonen met transposase-achtige eiwitten duiden erop dat SORBUS mogelijk is verkregen via 'horizontale gene transfer'. Door het maken van een gedeeltelijke SORBUS-deficiënte stam kon worden aangetoond dat SORBUS een belangrijke rol speelt bij de sorbinezuur resistentie.

Appendix

Curriculum Vitae

Maarten Punt was born the 18th of April 1993 in Pijnacker, The Netherlands. He followed his secondary education at the Koningin Wilhelmina College in Culemborg and enrolled in the BSc Biology at Utrecht University in September 2011. After his graduation, he enrolled in the Environmental Biology master's program at Utrecht University in September 2014. During the master's program, Maarten completed two research internships. The first internship took place at the Microbiology group (Department of Biology, Utrecht University). Under the supervision of Prof. Han Wösten and Dr. Aurin Vos, he studied the ligninolytic activity of *Schizophyllum commune*. Maarten performed his second internship at the Estación Experimental del Zaidín (CSIC, Granada, Spain), supervised by Dr. María José Pozo Jiménez and Dr. Javier Rivero Bravo, where he studied the role of arbuscular mycorrhiza symbiosis on the resistance of tomato plants. Maarten obtained his MSc degree in January 2017 and started his PhD project the same month at the Microbiology group (Department of Biology, Utrecht University) under the supervision of Prof. Han Wösten, Dr. Robin Ohm and Dr. Wieke Teertstra. This project was part of a consortium of knowledge institutes (Utrecht University, Leiden University and the Westerdijk Institute) and industrial partners (Unilever, Heineken, DuPont and PepsiCo). During his PhD project he investigated the heterogeneity within and between strains of the food spoilage fungi *Aspergillus niger* and *Penicillium roqueforti*. The results of his research are described in this thesis.

Appendix

List of publications

van den Brule, T., **Punt, M.**, Seekles, S. J., Segers F. J. J. , Houbraken, J., Hazeleger, W. C., Ram, A. F. J., Wösten, H. A. B., Zwietering, M. H., Dijksterhuis, J., den Besten, H. M. W. (2021). Interkingdom microbial variability in heat resistance. *In review*

Punt, M., Teertstra, W. R., & Wösten, H. A. (2021). *Penicillium roqueforti* conidia induced by L-amino acids can germinate without detectable swelling. *Antonie van Leeuwenhoek*, 1-8. https://doi.org/10.1007/s10482-021-01686-5

Seekles, S. J., Teunisse, P. P. P., **Punt, M.**, van den Brule, T., Dijksterhuis, J., Houbraken, J., Wösten, H. A. B., & Ram, A. F. J. (2021). Preservation stress resistance of melanin deficient conidia from *Paecilomyces variotii* and *Penicillium roqueforti* mutants generated via CRISPR/Cas9 genome editing. *Fungal Biology and Biotechnology*, *8*(1), 1–13. https://doi.org/10.1186/s40694-021-00111-w

Ijadpanahsaravi, M., **Punt, M.**, Wösten, H. A. B., & Teertstra, W. R. (2021). Minimal nutrient requirements for induction of germination of *Aspergillus niger* conidia. *Fungal Biology*, *125*(3), 231–238. https://doi.org/10.1016/j.funbio.2020.11.004

Punt, M., van den Brule, T., Teertstra, W. R., Dijksterhuis, J., den Besten, H. M. W., Ohm, R. A., & Wösten, H. A. B. (2020). Impact of maturation and growth temperature on cell-size distribution, heat-resistance, compatible solute composition and transcription profiles of *Penicillium roqueforti* conidia. *Food Research International*, *136*(May), 109287. https://doi.org/10.1016/j.foodres.2020.109287

van den Brule, T., **Punt, M.**, Teertstra, W., Houbraken, J., Wösten, H., & Dijksterhuis, J. (2020). The most heat-resistant conidia observed to date are formed by distinct strains of *Paecilomyces variotii*. *Environmental Microbiology*, *22*(3), 986–999. https://doi.org/10.1111/1462-2920.14791

Vele handen maken licht werk. Dat geldt ook zeker voor mijn proefschrift, en wat was het een genot om met zoveel mensen deze vier jaar door te maken.

Allereerst Han, bedankt voor de kans die jij me gaf om als laatste PhD bij het TiFN project aan te sluiten. Dank voor je haast onuitputbare enthousiasme, interesse en motivatie. Die hebben mij veel geholpen, zeker op momenten dat ik het zelf wat minder leuk vond. Je had eigenlijk altijd tijd voor wat vragen en was bliksemsnel met commentaar op de verschillende hoofdstukken, dit was zeker op het eind erg fijn!

Robin en Wieke, op jullie kon ik altijd rekenen. Wieke, jouw creatieve blik en oog voor mens en detail heb ik erg gewaardeerd. Robin, jouw professionaliteit en thuisgebrouwen bier waren meer dan welkom. Daarnaast ben ik erg blij dat jij me wegwijs hebt gemaakt in de wereld van de bio-informatica!

Kamergenoten van O404. Ik heb genoten van de gezellige sfeer en al onze gesprekken. Zo denk ik aan de talloze snoepjes van jou, Inge, en wat was ook het heerlijk samen te zeuren over de timesheets en koffie te halen op de 7de. Monsieur Pommes, ook jij bedankt voor de mooie jaren, je betrokkenheid en je Brabantse gezelligheid. Mijn mede-bioinformaticus, Peter Jan, altijd maakte jij tijd om te helpen met dingen die ik niet binnen 1 minuut op StackOverflow kon vinden en ook je scherp wetenschappelijke blik kwam meer dan eens van pas. Ioana, what to say, you were always strong spirited and I admire your truth-to-power mentality, I hope our paths cross in the future, but for now *la revedere*! Koen, al deelden wij maar een klein jaar het kantoor, ik weet wel dat ik alle koffiemomenten en pakketbezorgerimitaties ga missen.

Tom, Sjoerd en Inge, het TiFN-dreamteam. Het is al vaak tijdens het project genoemd, maar ik vond onze onderlinge samenwerkingen echt ontzettend prettig. Tom, natuurlijk dank voor hoe jij de weg baande door hele delen van het project met al die protocollen en HPLC metingen. Sjoerd, sommige weken hadden wij bijna dagelijks discussies over polyolen en RNAseq methodes, ik heb genoten van jouw eindeloze drang op zoek naar antwoorden en uiteraard kwam je hulp met transformaties goed van pas. Ik denk niet dat dit project zo geslaagd was zonder jullie input!

Arthur, Heidy, Jan en Jos. Jullie waren onmisbaar in het project en verzorgden een enorme wetenschappelijke 'breedte'. Dank voor alle tijd die jullie erin hebben gestoken!